EPAC Isoform Specificity; Drug Development, Subcellular Targeting and Relevance to Cell Morphology

Euan Parnell, B.Sc. (Hons)

Submitted in fulfilment of the requirements for the degree
Doctor of Philosophy

Institute of Molecular Cell and Systems Biology,
College of Medical Veterinary and Life Sciences,
University of Glasgow

April 2015

Abstract

Cyclic adenosine monophosphate (cAMP) is a second messenger signalling molecule that has been reported to exert beneficial effects within the vasculature and other physiological systems. cAMP produces its effects within the cell through two key downstream effector molecules: exchange protein activated by cAMP (EPAC) and protein kinase A (PKA). Many of the effects of cAMP have been attributed to PKA, however there is a growing appreciation of the potential of EPAC, particularly isoform 1 (EPAC1), based therapies for the regulation of inflammatory responses within the vasculature, thereby promoting cardiovascular health. Furthermore, side effects associated with global cAMP elevating agents may be avoided by isoform selective EPAC regulation. To date no small molecule agonists have been discovered to effectively or selectively promote EPAC1 activity. In order to address this, we have developed a fluorescence based competition assay able to identify compounds which interact with the cyclic nucleotide binding domains (CNBs) of both EPAC1 and EPAC2. Rigorous testing of the assay has confirmed that it is able to reliably and reproducibly identify EPAC interacting compounds within high throughput screening (HTS) of small molecule libraries. Furthermore, dual screening of EPAC1 and EPAC2 has allowed isoform selective compounds to be identified from a small compound library, confirming the suitability of this assay for HTS. This HTS assay is likely to facilitate the discovery of EPAC1-selective interacting molecules with the potential to be effective, small molecule regulators of EPAC1.

In order to classify small molecules isolated by HTS as either agonists or antagonists of EPAC1, we developed a secondary screen that is able to detect EPAC1 activation *in vivo*. This assay is based on the ability of EPAC1 to produce a rapid, cell spreading response in HEK293T cells stably transfected with EPAC1. However, the precise signalling pathways which produce these changes in cell shape are unknown. Therefore, we have attempted to identify pathways involved in EPAC1-mediated morphological change by assessing the effects of various inhibitors on cell spreading. Interestingly, we found that EPAC1 and PKA synergise to produce maximal cell spreading in HEK293T cells. Recent reports suggest that the cortical actin-membrane linker protein ezrin is required for the cell spreading effects of EPAC1. Here, we demonstrate that ezrin responds to elevations in intracellular cAMP in HEK293T cells in a PKA-dependent manner. Indeed, PKA

activation promotes the post translational modification of ezrin and alters the response of EPAC1-expressing cells to cAMP. These results suggests that the PKA pathway is able to regulate ezrin by post translational modification and that this is required for PKA and EPAC1 to synergise and produce maximal cell spreading.

In addition to agents which directly activate the catalytic activity of EPAC1, there is a body of evidence that supports the idea that compartmentalisation of cAMP effectors is an important mechanism for the determination of downstream signalling events leading to cellular responses, such as cell spreading. As such, we have attempted to identify the regions within EPAC proteins that determine their subcellular distribution. This was done through a combination of subcellular fractionation and the immunofluorescent detection of the localisation of EPAC isoforms. In particular, mutational analysis of EPAC1 revealed a carboxy terminal (C-terminal) nuclear localisation domain that is required for the perinuclear distribution of EPAC1 alongside the nuclear pore protein, RANBP2. Structural analyses suggest that this domain appears to be conserved within EPAC2 despite EPAC2 adopting a distinct cytoplasmic distribution. One explanation for this observation is steric interference within EPAC2 which blocks access to the conserved nuclear localisation domain. We have observed that the additional amino-terminal (N-terminal) CNB of EPAC2 appears to disrupt nuclear localisation and promote a cytoplasmic distribution within the cell. Indeed, the absence of the CNB1 promotes nuclear accumulation of EPAC2, with a pattern similar to that of EPAC1. The presence of this domain within EPAC2, absent in EPAC1, may represent a mechanism which regulates the subcellular distribution, and therefore function, of EPACs within the cellular environment.

In summary, we have developed a screening cascade to identify small molecules which may form the basis of therapeutic agents able to selectively target EPAC1 to promote the beneficial effects of EPAC1. In addition, a secondary screen involving EPAC1 induced morphological change was developed and characterised as an effective assay in which to test the agonist properties of compounds identified by primary HTS screening. We have confirmed that HEK293T cell spreading in response to cAMP elevation requires the expression of EPAC1, but that a secondary pathway involving interactions between PKA and ezrin is able to supplement the primary cell spreading effects of EPAC1. Finally, we have identified a potential mechanism for the different subcellular localisation of

EPAC1 and EPAC2: EPAC1 is targeted to the perinuclear compartment via a previously undiscovered C-terminal nuclear localisation domain.

Table of Contents

List of Tables

Chapter 1

Chapter 2

Chapter 3

List of Figures

Chapter 1

Chapter 3

Chapter 4

Chapter 5

List of Equations

Chapter 3

Preface

This PhD Thesis contains the result of research conducted in the laboratory of Dr Stephen Yarwood within the Department of Molecular, Cell and Systems Biology, University of Glasgow. This work was funded by a Biotechnology and Biological Sciences Research Council (BBSRC, UK) doctoral training partnership studentship. Drug development and screening was carried out in the laboratory of Dr Stuart McElroy within the European Screening Centre, Newhouse. This placement was funded by the technology and knowledge transfer internship fund. Biophysical and structural analyses were carried out in the laboratory of Dr Brian Smith, University of Glasgow.

Acknowledgements

I would like to thank my supervisor, Stephen Yarwood, for his continual support throughout my studies. Stephen has been an invaluable source of guidance, attention and supervision.

I would also like to thank Brian Smith, Tim Palmer and Stuart McElroy for their support during my time in their labs and their excellent teaching. I would like to thank Nia Bryant and Iain Johnstone for their advice throughout my PhD studies.

I would also like extend my gratitude to the people who gave me technical support throughout my four years. In particular, Julia Dunlop who was always willing to help out in the lab and go out of her way to give me assistance. Everyone in Lab 241; Jess, Dimi, Phil Hazel, Laura, Helen, Sarah, Alistair, Iain, Anna, Sylvia, Jolanta, Alex, Cassie, Claire, Scott, Musab, Gwyn and Louise. They were responsible for the day to day success of my experiments thanks to their eagerness to help out and friendliness. I would like to thank the Biology Department at the European Screening Centre for their welcome and tutelage and Sharon Kelly for her assistance with CD measurements.

I would also like to extend my gratitude to all the members of the GTTI lab meetings that gave regular advice on my research. In particular Ian Salt, George Baillie and Tom van Agtmael, for their attention and advice.

I would also like to thank my family and Barbara for support during my studies.

Authors Declaration

I declare that, except where explicit reference is made to the contribution of others, that this dissertation is the result of my own work and has not been submitted for any other degree at the University of Glasgow or any other institution.

Signature _____

Printed name _____

List of Abbreviations

007	- 8-pCPT-2'-O-Me-cAMP (8- (4- Chlorophenylthio)- 2'- O-methyladenosine- 3', 5'- cyclic monophosphate
007-AM	- 8-pCPT-2'-O-Me-cAMP-AM (8- (4- Chlorophenylthio)- 2'- O-methyladenosine- 3', 5'- cyclic monophosphate acetoxymethyl ester
2'-O-Me-cAMP	- 8- (4- Chlorophenylthio)- 2'- O- methyladenosine- 3', 5'- cyclic monophosphate
2'	- Second carbon (2') of the ribose moiety of cAMP
^{3}H-cAMP	- Tritiated cAMP
^{15}N	- A heavy isotope of nitrogen
5'-AMP	- 5'-adenosine monophosphate
3P-A	- EPAC1, amino acids P818, P820 and P823
8-CPT	- 8-CPT-cAMP (8-(4-chlorophenylthio) adenosine- 3', 5'-cyclic monophosphate)
8-NBD-cAMP	-8- (2- [7-nitro- 4- benzofurazanyl] aminoethylthio) adenosine- 3', 5'- cyclic monophosphate
$(^{15}NH_4)_2SO_4$	- ^{15}N labelled ammonium sulphate
%CV	- Coefficient of variance
A_{280}	- Absorbance at 280 nm
A_{600}	- Absorbance at 600 nm
AC	- Adenylate cyclase

ATCC	- American type culture collection
ATP	- Adenosine-5’-triphosphate
AJ	- Adherens junction
AKAP	- PKA anchoring protein
AREA1	- Amino acids R805, A806 and M809 within EPAC1
AREA2	- Amino acids 831-851 within EPAC1
AZD	- AZD6244
BCA	- Bicinchoninic acid assay
BIS	- Bisindolymaleimide
BRET	- Bioluminescence resonance energy transfer
C-terminal	- Carboxy-terminal
C-terminus	- Carboxy-terminus
cAMP	- Adenosine- 3', 5'- cyclic monophosphate
CDC25-HD	- CDC25 homology domain
CIC	- Cyclic nucleotide gated ion channel
CNB	- Cyclic nucleotide binding domain
CNB1	- The additional, amino-terminal CNB present in EPAC2
Co-IP	- Co-immunoprecipitation
COPD	- Chronic obstructive pulmonary disease

CVD	- Cardiovascular disease
D_20	- Deuterium
dH_2O	- Distilled water
DEP	- Dishevelled, EGL, pleckstrin homology domain
DMR	- Dynamic mass redistribution
DMSO	- Dimethyl sulfoxide
DMF	- Dimethyl formamide
DOPE	- Discrete optimised protein energy
E.Coli	- *Escherichia Coli*
EBF	- Endothelial barrier function
EPAC	- Exchange protein activated by cAMP
EPAC1	- Exchange protein activated by cAMP isoform 1
EPAC2/EPAC2A	- Exchange protein activated by cAMP isoform 2/2A
EPAC2B	- Exchange protein activated by cAMP isoform 2B
ERM	- Ezrin, radixin and moesin family protein
ESI	- EPAC specific inhibitor
FDA	- United States food and drug administration
F/R	- A combination of forskolin and rolipram
F-actin	- Filamentous actin

FERM	- Four point one, ezrin, radixin, moesin domain
FRET	- Fluorescence/forster resonance energy transfer
GAP	- GTPase activating protein
GDP	- Guanosine-5'-diphosphate
GEF	- Guanine nucleotide exchange factor
GIR	- Glucose stimulated insulin release
GLP	- Glucagon like peptide
GO	- Gö-6983
GPCR	- G-protein coupled receptor
Gs/Gi protein	- Adenylate cyclase stimulatory/inhibitory G-protein
GST	- Glutathione-s-transferase
GTP	- Guanosine-5'-triphosphate
HCNs	- Hyperpolarization activated cyclic nucleotide-gated channels
HEK293T	- Human embryonic kidney cells
HTS	- High throughput screening
HSQC	- Heteronuclear single quantum coherence
IP	- Immunoprecipitation
IP3	- Inositol triphosphate

IPTG	- Isopropyl ß-D-1-thiogalactopyranoside
K^{ATP} channel	- ATP-dependant potassium channel
kbp	- kilobasepair
K_D	- Dissociation constant
LB	- Luria-Bertani
LTD	- Long term depression
LTP	- Long term potentiation
LY29	- Ly294002
MAPK/ERK	- Mitogen activated protein kinase/extracellular regulated protein kinase
MLC	- Myosin Light Chain
N8	- 8^{th} residue of the adenosine moiety of cAMP
N-terminal	- Amino-terminal
N-terminus	- Amino-terminus
NCC	- NIH clinical collection
NIH	- National institute of health
NLD	- Nuclear localisation domain
PBC	- Phosphate binding cassette
pCPT	- Parachlorophenylthio
PDE	- Phosphodiesterase

PD1	- PD184352
PGE2	- Prostaglandin E2
PGI2	- Prostaglandin I1
PMA	- Phorbol 12-myristate 13-acetate
PI3K	- Phosphoinositide 3-kinase
PIP2	- Phosphatidylinositol 4,5-bisphosphate
PKA	- Protein kinase A
PKB/AKT	- Protein kinase B
PKC	- Protein kinase C
Popdc	- Popeye domain containing proteins
RA	- Ras association domain
RANBP2	- Ran binding protein 2
RCF	- Relative centrifugal force
REM	- Ras exchange motif
RIM2/3	- Rab interacting molecule isoform 2/3
ROCK	- RhoA-activated protein kinase
RT	- Room temperature
RWG	- Resonant waveguide grating
SAR	- Structure activity relationship

SEM	- Standard error of the mean
sMAD	- Scaled median absolute deviation
SOCS-3	- Suppressor of cytokine 3
StDev	- Standard deviation
SU	- Sulfonylurea
SUR1	- Sulfonylurea receptor
TJ	- Tight junction
TREK-1	- Two-pore domain potassium channel
VDCC	- Voltage dependent calcium channel
VE-Cadherin	- Vascular endothelial specific cadherin
VECs	- Vascular endothelial cells
VSMC	- Vascular smooth muscle cells
Y27	- Y27632

Chapter 1 : Introduction

1.1 cAMP signalling

Cyclic adenosine monophosphate (cAMP) has been the target of intensive study since its discovery in the 1950s. Its study was prompted by the observation that stimulation of liver homogenates with glucagon and epinephrine induced phosphorylation of glycogen phosphorylase (Sutherland and Wosilait 1956). By separating homogenates into membrane and cytosolic fractions, this effect was lost (Berthet et al. 1957), however, a heat stable molecule was produced which, when incubated with the cytosolic fraction, was able to induce enzyme phosphorylation independent of hormonal stimulation. This was the first observation of second messenger action; namely, a molecule which is produced in response to hormonal signalling at the membrane and is then able to activate intracellular signalling pathways. The structure of the heat stable molecule was identified as cAMP (Rall and Sutherland 1958; Sutherland and Rall 1958), and glycogen phosphorylase was shown to be regulated by a signalling cascade initiated by the cAMP dependent protein kinase (PKA) (Berg et al. 2002). This elegant model of extra- to intra- cellular signalling formed the basis of over 50 years of subsequent scientific study that has been vital in the understanding of the molecular mechanisms of cell signalling within the body.

The study of cAMP signalling has revealed that the action of hormones, such as incretins (Baggio and Drucker 2007), dopamine (Tamaki et al. 1989), prostaglandins (Kida et al. 2014) and adrenaline (Rall and Sutherland 1958; Sutherland and Rall 1958), is through the activation of transmembrane receptors called G-protein coupled receptors (GPCRs). GPCRs convert ligand binding into intracellular signals by virtue of conformational changes within the receptor that are able to span the membrane. These structural effects result in the release within the cell of the plasma membrane bound heterotrimeric G-protein subunits; alpha, beta and gamma (Levitzki 1987). The alpha subunit is specifically involved in the synthesis of cAMP, as it can either activate (Gs alpha subunit) or inhibit (Gi/o alpha subunit) adenylate cyclase (AC). AC activation catalyses the conversion of adenosine-5'-triphosphate (ATP) into cAMP and pyrophosphate. This process can be reversed by the cAMP phosphodiesterase (PDE) family, which hydrolyse cAMP to 5'-adenosine monophosphate (5'-AMP) (Maurice et al. 2014). This action ensures cAMP signalling is transient, allowing precise control over the

intensity and duration of the cAMP signal. Elevated cAMP levels are able to activate a select range of intracellular signalling pathways via proteins which contain cyclic nucleotide binding domains (CNB), including exchange proteins activated by cAMP (EPACs) (de Rooij et al. 1998; Kawasaki et al. 1998), protein kinase A (PKA) (Walsh et al. 1968) as well as Popeye domain containing proteins (e.g. Popdcs) (Schindler et al. 2012) and cAMP responsive ion channels (CIC) (Matulef and Zagotta 2003). cAMP second messenger signalling via these proteins controls many aspects of cell function, including cell differentiation (Gabrielli et al. 2014), secretion (Shibasaki et al. 2007), cell morphology (Ross et al. 2011), inflammatory pathways (Parnell et al. 2012), contractility (Pereira et al. 2013) and synapse formation (Penzes et al. 2011). As such, cAMP signalling has become an attractive target in drug development for the treatment of a variety of disease states.

1.1.1 cAMP Responsive Proteins

PKA was the first cAMP responsive protein to be identified and has subsequently been implicated in a huge range of cellular effects (Tasken and Aandahl 2004; Pidoux and Tasken 2010), such as insulin secretion (Seino and Shibasaki 2005), transcriptional control (Mayr and Montminy 2001), and cell growth (Stork and Schmitt 2002) and differentiation (Yamamizu et al. 2012). PKA is made up four individual subunits which form an inactive complex; two regulatory subunits, which each contain a CNB, that bind to and inactivate two catalytic subunits by masking their kinase domains (Taylor et al. 2005). cAMP binding to the regulatory subunits results in their dissociation from the catalytic elements facilitating the interaction and phosphorylation of a plethora of downstream signalling proteins (Krebs and Beavo 1979).

Following the discovery of cAMP, cyclic nucleotide gated ion channels (CICs) were found to bind cyclic nucleotides in photoreceptor cells. Detection of light in these cells induces the activation of phosphodiesterases which degrade cAMP resulting in channel closure, the inhibition of charged ion influx/efflux and photoreceptor depolarisation (Kaupp and Seifert 2002). In addition to photoreceptor cells, CICs are also found within olfactory sensory neurons, brain, kidneys and the heart. Indeed, cAMP gated CICs within the heart play a vital role in maintaining cardiac

rhythm and are called hyperpolarization-activated cyclic nucleotide-gated channels (HCNs) due to their ability to respond to both hyperpolarisation and cAMP (Matulef and Zagotta 2003). Indeed, HCNs are responsible for inducing the diastolic phase of cardiac contraction as repolarisation takes place following systolic depolarisation of cardiomyocytes. cAMP plays a key role in regulating the membrane voltage at which HCN mediated depolarisation occurs. At high cAMP levels, HCN opening is promoted and, as a result, a lower voltage is required to induce depolarisation. High cAMP levels therefore promote tachycardia as diastolic cardiomyocyte contraction occurs closer to the systolic event.

Although PKA was thought to be the dominant effector of the cAMP second messenger signal in the majority of cell types, the ability of cAMP to promote Rap1 GTPase activation in the presence of PKA inhibitors prompted the search for other cAMP responsive proteins. As a result of this, EPAC was identified during an *in silico* search for genes exhibiting the characteristic CNB (de Rooij et al. 1998; Kawasaki et al. 1998). EPACs were the first class of PKA independent signalling proteins identified and activated by cAMP binding, though activation and catalytic mechanisms were found to be strikingly different. Indeed, as opposed to PKA, the regulatory and catalytic regions of EPACs are contained within a single gene product, and regulation is imparted by an interaction between the amino-terminus (N-terminus) regulatory domain and C-terminal catalytic domain. Furthermore, whereas as PKA is able to induce phosphorylation events upon a plethora of target proteins (Walsh et al. 1968), EPAC was observed to act as a guanine nucleotide exchange factor (GEF), stimulating the activity of Rap1 and Rap2 GTPases and, therefore, represented the cAMP responsive molecule responsible for the PKA independent activation of Rap (de Rooij et al. 2000).

The most recently discovered cAMP signalling molecules are the Popdcs. Popdcs were identified by cDNA library screening for proteins specifically enriched within cardiomyocytes (Reese et al. 1999), although expression is also observed within skeletal muscle (Andree et al. 2000). Interestingly, the CNB of Popdcs display low sequence homology compared to those of other cAMP binding proteins, suggesting convergent evolution of the phosphate binding cassette (PBC) (Froese et al. 2012). Popdcs are membrane bound, where they have been reported to interact with the two-pore domain potassium channel (TREK-1) (Froese et al. 2012) and Caveolin-3

(Alcalay et al. 2013) to regulate cardiac pacemaker activity. Indeed, deletion of Popdcs produced pronounced cardiac arrhythmia, suggesting that they have a vital role in cardiac function, consistent with their targeted expression within cardiomyocytes (Schindler et al. 2012).

1.1.2 Compartmentalisation of cAMP Signalling

In addition to the production of cAMP, the distribution of AC, PDEs and effector molecules within the cell provides an additional layer of regulation. Indeed, by limiting cAMP elevation to distinct subcellular locales, cAMP is able to activate specific subsets of effector molecules (Zaccolo and Pozzan 2002). The archetypal example of compartmentalisation arose from the different effects of isoprenaline and prostaglandin-I1 (PGI1) in rat cardiomyocytes (Buxton and Brunton 1983). Although both isoprenaline and PGI2 were observed to act through membrane receptors to induce cAMP elevation, isoprenaline achieved cAMP increases in both the particulate and soluble cellular fractions, whereas cAMP was synthesised in the soluble fraction alone following PGI1 stimulation (Buxton and Brunton 1983). Indeed, isoprenaline treatment has been shown to produce cardiomyocyte contractility, whereas PGI1 is unable to induce this effect (Keely 1979) despite both compounds acting to increase cAMP levels. Thus, the subcellular compartment in which cAMP synthesis occurs is vitally important in determining the cellular response to elevation in intracellular cAMP.

Compartmentalisation of cAMP signalling is underscored by the action of anchoring proteins which interact with PDEs and cAMP effector proteins to spatially control the response to the cAMP signal (Mongillo et al. 2004; Zaccolo 2006). Indeed, if a compartment is rich in PDEs, the cAMP signal will be limited within the local region, and conversely if PDEs are absent, the cAMP signal will be more intense and sustained (Zaccolo and Pozzan 2002). In addition, both PKA and EPAC are regulated by sequestration to distinct subcellular compartments. This is brought about by a range of anchoring proteins which regulate the distribution of EPAC and PKA, including PKA anchoring proteins (AKAPs) (Scott et al. 2013) and EPAC anchors (E.g. RANBP2) (Gloerich et al. 2011). Through this mechanism, elevation of cAMP may fail to activate one effector, whilst producing strong effects through another. Indeed, signalling through EPAC and PKA has been shown to be intricately

controlled by their subcellular distribution (Newhall et al. 2006; Niimura et al. 2009) and manipulating distribution may provide a potential mechanism in regulating the signalling pathways activated by EPAC and PKA.

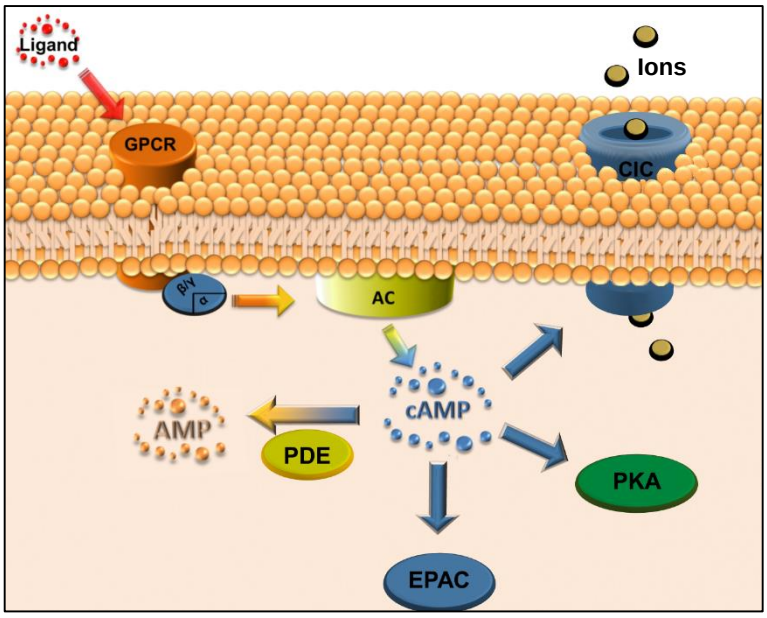

Figure 1-1 : Schematic of cAMP signalling in response to G-protein coupled receptor (GPCR) activation at the membrane.
cAMP signalling is induced when a hormone or drug binds to GPCRs. The activation of the GPCR results in the release of the G-protein αβγ subunits, which are able to regulate various intracellular signalling molecules. The α subunit of a Gs-coupled GPCR is able to stimulate adenylate cyclase and provoke the conversion of ATP into cAMP. Following elevations in intracellular cAMP levels, CIC, PKA and EPACs are activated to produce various cAMP-dependent effects. The intensity and duration of the cAMP signal is regulated by the action of cAMP phosphodiesterases which degrade cAMP into 5'-AMP. αβγ – G-protein subunits, AC – Adenylate cyclase, PKA – Protein kinase A, EPAC – exchange protein activated by cAMP, CIC –cyclic nucleotide gated Ion channel, PDEs – cAMP phosphodiesterases, AMP – 5'-adenosine monophosphate.

1.1.3 EPAC Structure

Two main isoforms of EPAC exist within mammals; EPAC1 and EPAC2 (de Rooij et al. 1998; Kawasaki et al. 1998). Whereas EPAC1 is widely expressed in almost every mammalian tissue, EPAC2 exhibits far more restricted expression patterns, limited to the heart, brain, pancreas, testes and other secretory cells (Kawasaki et al. 1998). The major difference between EPAC1 and EPAC2 is the presence of an additional CNB (CNB1) within the N-terminus of EPAC2 (de Rooij et al. 2000). The presence of this extra CNB underlies the difference in molecular weight observed between EPAC1 (100 kDa) and EPAC2 (110 kDa). Despite homology to CNB conserved in both isoforms, CNB1 exhibits a reduced affinity for cAMP and is unable to induce EPAC2 activation in response to cAMP binding. As a result, CNB1 has been described as non-functional; however it has recently been implicated in controlling the subcellular localisation of EPAC2, thereby regulating insulin secretory effects in pancreatic beta cells (Niimura et al. 2009). Despite this difference, EPAC1 and EPAC2 share structural motifs throughout the regulatory and catalytic domains (Figure 1-2). Indeed, the dishevelled-EGL-pleckstrin homology domain (DEP), CNB, Ras exchange motif (REM), Ras association domain (RA) and CDC25 homology domain (CDC25-HD) are conserved between isoforms (Li et al. 2006; Borland et al. 2009; Liu et al. 2010).

In the absence of cAMP, EPACs are held in an inactive conformation due to intermolecular interactions between the regulatory and catalytic domains. These interactions inhibit EPAC GEF activity by limiting substrate access to the catalytic CDC25-HD domain (Rehmann et al. 2006; Rehmann et al. 2008). The common CNB of EPAC1 and EPAC2 is vital in the activation of this auto-inhibited form. cAMP binding to the phosphate binding cassette results in a local tightening within the CNB and the closure of the “lid” region over the cAMP binding pocket (Rehmann et al. 2003). These changes are transmitted to several key sites within the molecule (Figure 1-2) altering the stability of the “hinge helix”, disrupting the beta sandwich “switchboard” and breaking the key linkage between the regulatory and catalytic domains, dubbed the “ionic latch” (Rehmann et al. 2006; Rehmann et al. 2008). Together these cAMP binding promoted structural changes promote the open form of EPAC, revealing the catalytic CDC25-HD for Rap1 binding and GEF activity (Figure 1-2).

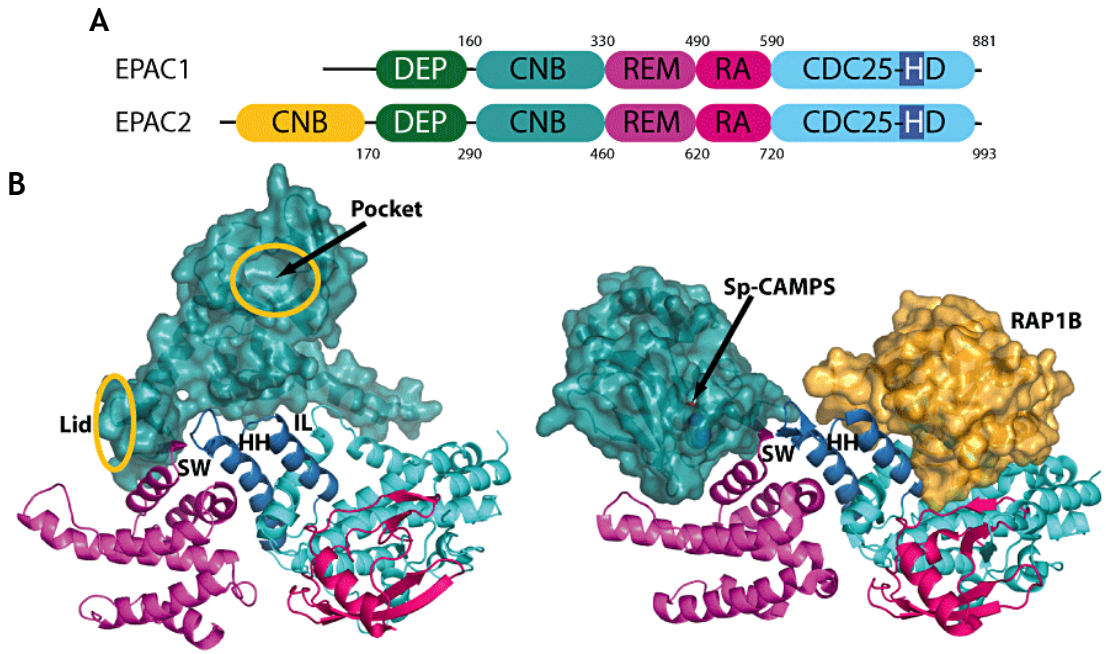

Figure 1-2 : Structure and mode of activation of EPAC proteins.
A - Schematic representation of the primary structure EPAC protein. **B** - The crystal structure of EPAC2 is shown in the closed conformation (left, 2BYV) (Rehmann et al. 2006) as cartoon, with the CNB displayed in spacefill. The open conformation (right, 3CF6) (Rehmann et al. 2008) is promoted as the lid region closes over the cAMP analogue Sp-cAMP within the cAMP binding pocket (pocket). As the IL, HH and SW become disrupted Rap1B is able to bind to the catalytic region of EPAC2. CDC25-HD - CDC25 homology domain, CNB - cyclic nucleotide binding domain; DEP - Dishevelled-Egl-10-Pleckstrin, EPAC - exchange protein activated by cAMP, HH - helix hairpin, IL - ionic latch, RA - Ras association domain, REM - Ras exchange motif, SW - Switchboard, Sp-CAMPs - Sp isomer of cAMP. Modified from (Borland et al. 2009).

Whereas the REM domain is involved in maintaining the overall structure and activity of the catalytic domain, the DEP domain and RA motifs provide more subtle regulation of EPAC activity within the cell. Indeed, these structural motifs have been implicated in regulating the subcellular distribution and protein-protein interactions outside of Rap binding (de Rooij et al. 2000). The DEP motif is involved in targeting proteins to the plasma membrane via an interaction with the membrane component phosphatidic acid (Consonni et al. 2012). The RA has also been linked to the subcellular localisation of EPAC2 through interactions with Ras (Li et al. 2006). Deletion of residues 650-689 within the RA inhibits the interaction with Ras at the plasma membrane, limiting the activation of a specific plasma membrane pool of Rap in response to EPAC2 activation (Li et al. 2006). Although unable to bind to Ras, the RA of EPAC1 was found to interact with Ran GTPase at the nuclear membrane (Liu et al. 2010). This forms part of a multi-protein complex with the nuclear pore protein, RANBP2, which is involved in tethering EPAC1 to

the nuclear membrane and limiting its catalytic activity (Gloerich et al. 2011). EPAC proteins are therefore under intricate control based on their distribution within the cell in conjunction with cAMP binding.

1.1.4 EPAC Signalling through Rap GTPases

The family of small GTPases consists of five related subgroups; Ras, Rho, Ran, Rab and Arf. Each is associated with specific aspects of cell function, for example vesicle trafficking (Rab) (Harris and Littleton 2011) and cytoskeletal dynamics (Rho) (Shi and Wei 2013). Rap is a member of the Ras family, but is largely involved in the control of cell morphology, adhesion and cohesion (Gloerich and Bos 2010), functions that underlie the ability of EPAC1 to regulate cell adhesion (Rangarajan et al. 2003), cell-cell contact stability within the vascular endothelium (Kooistra et al. 2005), as well as cell spreading (Ross et al. 2011).

Rap cycles between an inactive, guanosine-5'-diphosphate- (GDP) bound form and the active guanosine-5'-triphosphate- (GTP) bound conformation. The cycling of activation status is regulated by the stimulatory effects of GEFs which induce GTP binding, or GTPase activating proteins (GAPs) which promote GTP hydrolysis and the GDP-bound state (Gloerich and Bos 2011). Two main isoforms of Rap exist which differ in their subcellular targeting, and their level of activity. Rap2 maintains a low GTPase activity, is relatively insensitive to the action of regulatory GEFs/GAPs, compared to Rap1, and therefore has a higher basal activity (Ohba et al. 2000). Rap1 is responsive to a variety of signalling cues and GEF activities, and is rapidly turned over ensuring rapid responses (Gloerich and Bos 2011).

1.2 EPAC and Cell Spreading

One of the most striking roles for cAMP in the control of cell morphology is the ability of EPAC1, through Rap1, to induce a distinct spread cell phenotype in a variety of cell types (Ross et al. 2011). This morphological change arises from uniform, isotropic membrane projection resulting in large increases in cell area. Interestingly, this response appears to be independent of classical cAMP mediated focal adhesion and integrin stabilisation (Enserink et al. 2004; Bernardi et al. 2006; Duchniewicz et al. 2006). Recently, the actin- cytoskeletal linker protein ezrin was found to be required for EPAC mediated cell spreading (Ross et al. 2011). However, the manner in which cAMP is able to regulate ezrin to produce cell spreading is currently unknown.

1.2.1 Ezrin

Ezrin was the first member of the highly homologous ERM (ezrin, radixin and moesin) family to be identified (Mangeat et al. 1999), all of which share a characteristic amino-terminal (N-terminal) 4.1, ezrin, radixin and moesin (FERM) membrane binding domain (Gould et al. 1989). Ezrin plays a key role in connecting the cortical actin cytoskeleton to the cell membrane through direct interaction with phosphatidylinositol 4,5-bisphosphate (PIP_2) and actin (Bosk et al. 2011). These linkages allow ezrin to acts as a regulator of membrane dynamics, including the formation of cell protrusions (Mangeat et al. 1999).

Ezrin is regulated by a complex interplay of post translational modifications, protein-protein interactions and lipid binding. The protein exists in an auto-inhibited form in the cytosol and becomes active when it interacts with phosphotidylinositol 4,5-bisphosphate (PIP_2) at the plasma membrane (Niggli et al. 1995; Bosk et al. 2011). Two sites were found to be required for ERM-lipid interaction, termed by Ben-Aissa as the lipid binding patch and pocket (Ben-Aissa et al. 2012). Indeed, crystal structure analysis of the related protein, radixin, revealed inositol triphoshate bound within the pocket (Hamada et al. 2000). However, mutational studies highlighted a central role for the patch, supported by the observation that the pocket is hidden by the carboxy terminus (C-terminus) in the auto-inhibited conformation. A two-step model was therefore hypothesised whereby lipid binding at the patch induces conformational changes, revealing the

pocket and allowing the lipid molecule to bind stably within this deeper cleft (Ben-Aissa et al. 2012). Lipid binding disturbs the head to tail conformation of ezrin and the C-terminal actin-binding domain is released to interact with the cytoskeleton (Figure 1-3) (Gary and Bretscher 1995; Saleh et al. 2009). In addition to its importance in cAMP mediated cell spreading, a direct link between cAMP signalling and ezrin has been observed. Indeed, phosphorylation of a key activation phospho-site (Thr567) within ezrin has been observed to involve PKA in response to cAMP elevation (Zhu et al. 2007). Importantly, Thr567 phosphorylation has been shown to increase the ability of ezrin to interact with actin and inhibits the return to the auto-inhibited state (Pearson et al. 2000; Bosk et al. 2011). Despite evidence strongly supporting PIP_2 binding as the activation step (Bosk et al. 2011), reports of Thr567 phosphorylation as an activation signal (Simons et al. 1998) underlie its ability to induce considerable alterations to ezrin function. However, phospho-mimetic Thr567Asp mutants can display aberrant results, suggesting that the continual action of kinases and phosphatases to regulate the protein appears to be required for normal ezrin function (Zhu et al. 2007; Liu et al. 2012). Despite this complexity, phosphorylation of Thr567 of ezrin has been observed to occur in conjunction with the activation of signalling proteins involved in cell

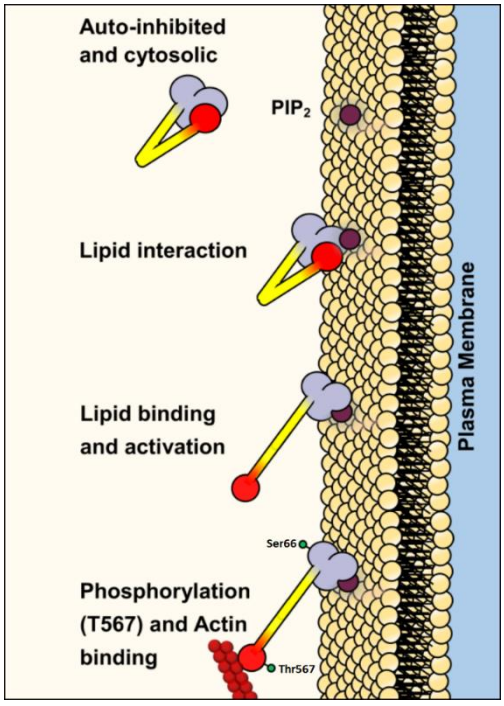

Figure 1-3 : Mechanisms of Ezrin activation.
Ezrin remains inactive within the cytosol. Interaction with the plasma membrane component PIP2 activates Ezrin. Furthermore, once active phospho-regulation at Thr567 and Ser66 can promote stability and actin binding.

morphological change, such as the RhoA-activated kinase, ROCK (Matsui et al. 1998; Haas et al. 2007), and cAMP elevation itself (Figure 1-4) (Zhu et al. 2007). Along with Thr567 phosphorylation, cAMP has been implicated in promoting the post translational modification of Ser66 by PKA (Zhou et al. 2003; Wang et al. 2005). This residue has been shown to be a direct substrate of PKA using *in vitro* kinase assays, and furthermore, mutation of this serine into alanine is able to block PKA-mediated phosphorylation *in vivo* (Zhou et al. 2003). These phospho-inhibitory and -mimetic mutants were shown to either block or promote, respectively, acid secretion provoked by ezrin in gastric parietal cells (Zhou et al. 2003). This may be linked to the observation that PKA mediated phosphorylation prevented the proteolytic action of calpain-I on ezrin, suggesting that ezrin protein stability may be altered by cAMP mediated modification of Ser66 (Wang et al. 2005). The cellular effects of PKA mediated ezrin regulation have, as yet, to be shown outside of the gastric epithelium, though the widespread expression of both proteins suggests an important regulatory mechanism in a wide range of cell backgrounds (Fehon et al. 2010). In addition to Ser66 modification, ezrin has also been shown to linked to cAMP signalling by acting as a scaffold for PKA (Dransfield et al. 1997) and the regulation of the subcellular distribution of EPAC1

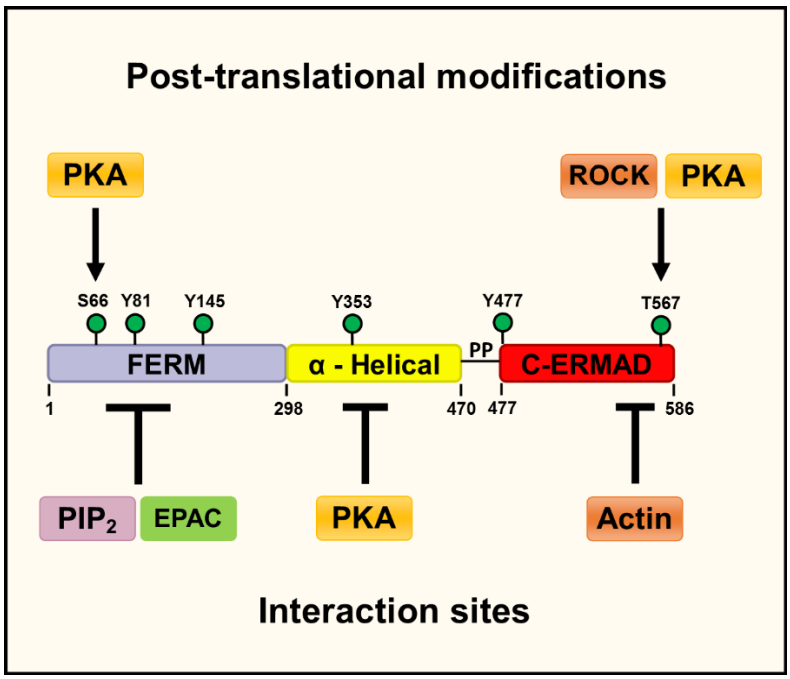

Figure 1-4 : Ezrin is regulated by post-translational modification and protein-protein interaction.
cAMP can regulate ezrin by phosphorylation of Ser66 and Thr567. ROCK can also phosphorylate Thr567. Activation is mediated by interaction with PIP2 through the FERM domain, which relieves an autoinhibitory interaction between the FERM and C-ERMAD domains, thereby revealing the actin binding domain. Furthermore,ezrin acts as an anchor for both EPAC1 and PKA through interactions with the FERM and alpha-helical domains respectively.

within cells (Figure 1-4) (Gloerich et al. 2010). Clearly cAMP signalling via PKA and EPAC1 are intimately linked to ezrin function and alterations in cellular morphology. However, it remains to be discovered how EPAC1 and Rap1 are able to regulate ezrin activity to produce cell spreading.

1.3 The Role of EPAC and Rap1 in Disease

EPAC proteins have been shown to play both positive and negative roles in various disease states (Gloerich and Bos 2010). Indeed, the expansion of research into EPAC-targeted therapeutics in recent years (Chen et al. 2014) may provide tools to activate or inactivate EPAC specifically, allowing EPAC to be regulated independently of PKA within the body. As such, the role of EPAC isoforms in various disease states will be discussed, with emphasis on the benefits of targeted EPAC regulation.

1.3.1 EPAC-Rap1 Signalling in Insulin Secretion

Pancreatic ß-cells are responsible for insulin secretion into the blood stream. The exocytosis of insulin from ß-cells occurs as a result of elevated glucose levels within the blood and is termed glucose induced insulin release (GIR) (Baggio and Drucker 2007). As glucose enters the pancreatic ß-cell, alterations in the ratio of cellular AMP to ATP promotes closure of the ATP-dependant potassium (K^{ATP}) channel and a build-up of charged ions which results in membrane depolarisation. Depolarisation induces voltage dependant calcium channel (VDCC) opening, which produces an influx of calcium into the cell. This increase in cellular calcium levels promotes insulin exocytosis. Indeed, as calcium levels rise, synaptotagmin/SNARE complexes are able to insert into the plasma membrane (Iezzi et al. 2005), allowing fusion of the insulin-containing vesicles and release of their contents outside of the cell. Calcium elevation can also produce calcium release from intracellular stores, an effect described as calcium induced calcium release (CICR). This process can further potentiate exocytotic processes and upregulate insulin secretion (Kang and Holz 2003; Kang et al. 2003).

In addition to elevated blood glucose, feeding induces gut K and L cells to release the incretin hormones, glucagon-like peptide (GLP) and gastric inhibitory peptide (GIP) (Baggio and Drucker 2007). These hormones bind to and activate their respective Gs-coupled GPCRs present on the pancreatic ß-cells and thereby provoke an increase in cAMP levels. cAMP elevation is a major factor in determining the intensity of the GIR response (Shibasaki et al. 2007). Both EPAC1 and EPAC2 are found within in pancreatic ß-cells, and cAMP has been shown to potentiate insulin secretion in a PKA dependent (Ding and Gromada 1997) and

independent manner (Seino and Shibasaki 2005). Interestingly, cAMP is able to upregulate GIR, CICR and exocytotic processes through EPAC2 (Figure 1-5), supporting EPAC2 as an important regulatory player in the control of insulin secretion and, potentially, as a drug target for the treatment of type 2 diabetes.

Various mechanisms have been identified which underlie the ability of cAMP and EPAC2 to regulate insulin secretory pathways within pancreatic ß-cells. The first reports of EPAC2 in ß-cell function stemmed from the ability of EPAC2 to regulate the sensitivity of the K^{ATP} channel through direct interaction with the sulfonylurea receptor (SUR1) subunit of this complex (Kang et al. 2006). This effect is able to lower the cellular ATP content required to provoke potassium channel closure, resulting in membrane depolarisation in response to lower blood glucose and cell metabolism.

EPAC2 has also been linked to the effects of incretins in pancreatic ß-cells by upregulating basal and stimulated calcium levels, independently of a glucose stimulus (Seino et al. 2009). Indeed, EPAC2 is intimately involved in calcium flux via CICR. By regulating ryanodine receptors (Kang et al. 2003), activating phospholipase C-epsilon (Dzhura et al. 2010) and the inositol-3-phosphate (IP3) receptor (Kang et al. 2006), EPAC2 is able to regulate the release of calcium from intracellular stores. Thus, EPAC2 is involved in increasing the sensitivity of the ß-cell to glucose and thereby potentiates secretory responsiveness to elevated blood glucose (Seino et al. 2009).

Finally, EPAC2 knockout mice have been shown to be deficient in vesicle-membrane docking, a process which increases the pool of insulin-containing vesicles available for exocytosis (Shibasaki et al. 2007; Dzhura et al. 2010). Indeed, by directly regulating the vesicular population in contact with the membrane, EPAC2 can regulate vesicle fusion events and thus insulin release. These effects stem from the regulation of vesicular trafficking, as EPAC2 can directly interact and activate Rab interacting molecules, isoforms two and three (Rim2 and Rim3) (Ozaki et al. 2000; Yasuda et al. 2010; Park et al. 2012) and Piccolo (Fujimoto et al. 2002). Rim/Piccolo complexes are key regulators of insulin vesicle trafficking via Rab GTPases and their activation can promote vesicle fusion

to the cell membrane and insulin secretion from the pancreatic cell (Kasai et al. 2005; Park et al. 2012).

Although EPAC1 is present at low levels within pancreatic ß-cells (Chepurny et al. 2010), it has also been implicated in insulin secretion, ß-cell function and metabolism (Yang et al. 2012; Kai et al. 2013). Indeed, EPAC1 null mice show blunted GIR when injected with glucose to circumvent incretin mediated cAMP elevation within ß-cell (Kai et al. 2013), suggesting a specific role for EPAC1 in GIR at basal cAMP levels. However, when glucose was introduced by feeding no deficiencies in GIR were observed in EPAC1$^{-/-}$ mice, suggesting that EPAC2 may be dominant in incretin potentiated GIR (Yan et al. 2013). However, EPAC1$^{-/-}$ knockout mice displayed deregulated energy metabolism, altered islet of Langherhan development (Kai et al. 2013) and increased sensitivity to leptin (Yan et al. 2013). Indeed, EPAC1 appears to play a role in energy metabolism that may facilitate drug development for the treatment of diet-induced obesity, as well as insulin resistance.

Given the importance of EPAC2 in insulin vesicle priming a small molecule EPAC2 agonist may be an effective tool in promoting insulin secretion in type two diabetic patients. Furthermore, although the effects of EPAC1 may be limited, activation of this EPAC isoform may also upregulate insulin secretion, supporting either an EPAC1 or dual action small molecular activator as a viable option in drug development for insulin resistance.

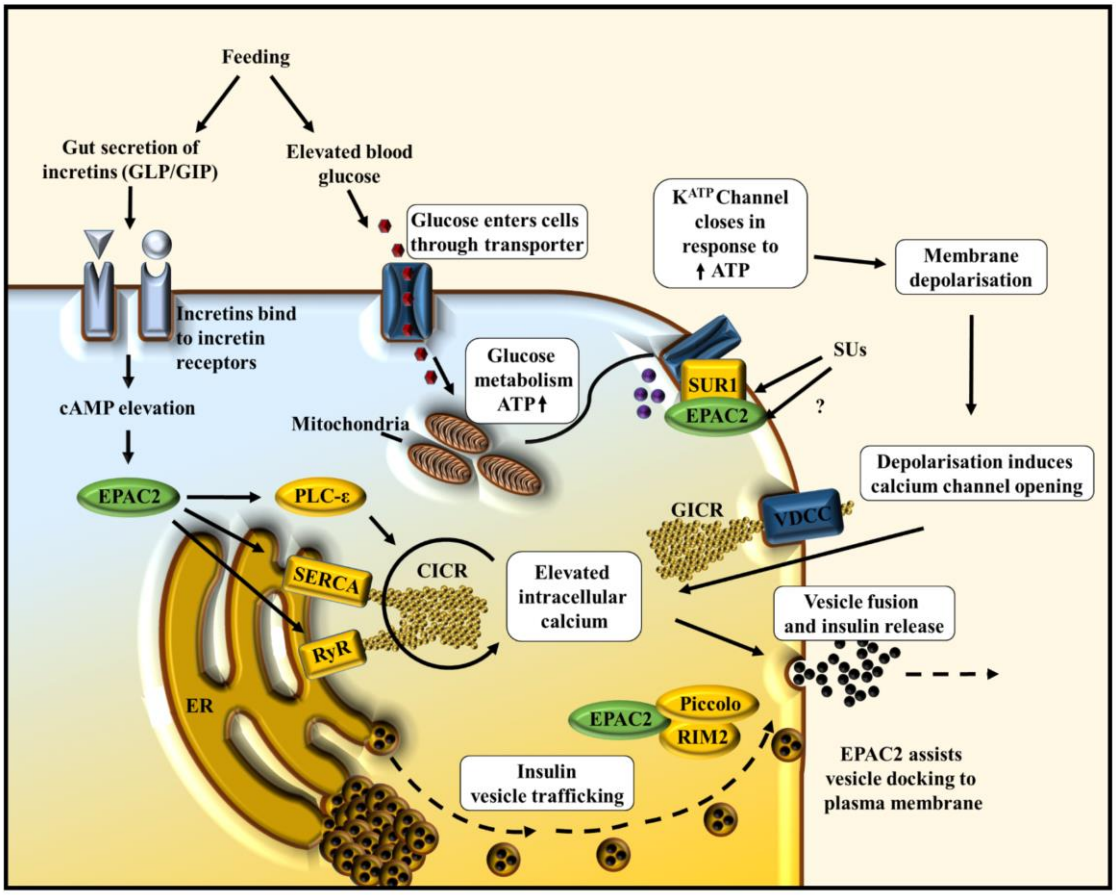

Figure 1-5 : EPAC2 is involved in potentiating insulin release from the pancreatic β-cell through multiple mechanisms.
This schematic of the pancreatic β-cell shows the manner in which EPAC2 can regulate the insulin secretory pathway. Two pathways are activated by feeding. First, secretion of GLP and GIP is stimulated within the gut, activating GPCRs on the pancreatic β-cell (Baggio and Drucker 2007). This in turn activates adenylate cyclase and cAMP production is stimulated, activating EPAC2. Simultaneously, elevation in blood glucose signals to glucose transporters on the β-cell, which import glucose. Metabolism of glucose within the mitochondria yields an increase in ATP within the cell, closing ATP sensitive potassium channels (K^{ATP} channel) and therefore promoting depolarisation. Depolarisation causes glucose stimulated calcium influx (GICR), which in turn stimulates calcium induced calcium release (CICR), and promotes vesicle fusion (Holz 2004). EPAC2 is able to regulate insulin secretion through three pathways, with proteins shown to be regulated by EPAC2 shown in yellow. Direct interaction with the SUR1 (sulfonylurea receptor) increases the sensitivity of the K^{ATP} channel to ATP and thus stimulates GICR (Holz et al. 2006). Sulfonylureas (SU) are able to produce similar effects by targeting SUR1, however, this effect has been attributed in part to EPAC2 as a secondary drug target within β-cells (Zhang et al. 2009). Additionally, EPAC1-Rap1 signalling can regulate endoplasmic reticulum (ER) calcium store release (CICR) through stimulation of phospholipase C epsilon (PLCε) (Oestreich et al. 2007; Dzhura et al. 2011), the ryanodine receptor (RyR) (Pereira et al. 2007) and the sarcoendoplasmic calcium transport ATPase (SERCA) (Lacabaratz-Porret et al. 1998). Furthermore, EPAC2 can interact directly with the docking proteins RIM2 (Rab interacting molecule-2) and piccolo and facilitate insulin vesicle docking to the plasma membrane (Kwan et al. 2007), increasing the pool of insulin available for release. ER – Endoplasmic reticulum, VDCC – Voltage dependent calcium channel, ATP – Adenosine triphosphate, GLP – Glucagon like peptide, GIP – Gastric inhibitory peptide.

1.3.2 EPAC-Rap1 Signalling in Brain and Neuronal Function

Both EPAC1 and EPAC2 are expressed within the brain (Kawasaki et al. 1998). Knockout of either EPAC1 or EPAC2 from the mouse forebrain has no effect on phenotype, however double knockout results in impaired social interaction and memory, suggesting functional redundancy between neuronal EPACs (Yang et al. 2012). Indeed, an important role for EPACs within the prefrontal cortex has been confirmed, as knockout mice display altered learning and social capacity (Yang et al. 2012). However, recent studies have also reported phenotypic alterations in response to isoform specific knockout, suggesting that EPACs may have independent functions in specific neuronal cell types, such as in the cortex (Srivastava et al. 2012) and hypothalamus (Yang et al. 2012).

A major feature of EPAC dual knockout mouse models is the down-regulation of EPAC mediated transcription linked to neuronal function (Suzuki et al. 2010; Yang et al. 2012). Indeed, EPAC1/2 knockout blocks the expression of the neuro-regulatory miRNA-124 which inhibits its downregulation of Zif-268 protein translation, which has been implicated in neural plasticity and memory formation (Hall et al. 2001). Although EPACs provide cAMP responsive control over gene expression, the precise molecular mechanisms are unknown.

One potential mechanism for EPAC2 in regulating brain function is linked to the observation that EPAC2 has been implicated in regulating dendritic size and stability. These effects have been correlated to the formation of EPAC2 complexes with key dendritic regulatory proteins, PSD-95 and NR-1, within the post-synaptic density (Woolfrey et al. 2009). In particular, EPAC2 activation has been linked to smaller, more motile dendrites, which correlate with synaptic plasticity in social behaviour and memory (Gelinas et al. 2008). Indeed, EPAC1/2 knockout mice display impaired social behaviour linked to impaired dendritic development (Srivastava et al. 2012). These data suggest a functional role for EPACs in the regulation of synaptic function.

cAMP elevation has been proposed as an effective avenue in regulating neuronal function (Kanes et al. 2007). For example, D2 dopamine receptor antagonists have previously be employed to treat brain disorders via inhibition of postsynaptic

receptors and increases in cAMP levels (Kapur and Mamo 2003). In addition, the PDE-inhibitor, rolipram, has also been proposed to be a potential regulator of depression and psychosis by producing similar increases in postsynaptic cAMP levels (Kanes et al. 2007). cAMP has been shown to activate both PKA and EPAC to alter brain function (Otmakhov and Lisman 2002), however recent studies have shown EPACs plays a vital role in promoting long term potentiation (LTP) and memory formation in the prefrontal cortex (Yang et al. 2012). Furthermore, hypothalamic sensitivity to leptin is regulated by EPAC1 (Yan et al. 2013), perhaps linked to EPAC1-mediated long term depression (LTD) within this tissue (Ster et al. 2009).

Interestingly, EPAC1 becomes upregulated in neurodegenerative disease (Suzuki et al. 2010) and the expression of an inactive EPAC2 mutant is observed in patients suffering from autism spectrum disease (Woolfrey et al. 2009; Srivastava et al. 2012). Thus, a specific role for cAMP signalling in neuronal function has been proposed where EPACs may regulate learning and memory. Furthermore, cAMP elevating agents have proven to be effective in the treatment of various neurological defects, such as PDE inhibition in Parkinsons (Laddha and Bhatnagar 2009), schizophrenia (Siuciak 2008) and depression (Scott et al. 1991) and resveratrol in Alzheimers (Park et al. 2012). As EPAC1 and EPAC2 appear to display some redundancy and beneficial effects have been attributed to both EPAC1 and EPAC2, non-selective small molecule agonists of EPAC may be an effective therapeutic avenue in the treatment of neurological disorders. Indeed, promoting cAMP production within the brain forms the biochemical basis of many anti-psychotic drugs, and targeting EPACs may achieve similar benefit with fewer off target effects.

1.3.3 EPAC-Rap1 Signalling within the Heart

cAMP elevation occurs within the heart in response to ß-adrenergic receptor activation within cardiac tissue and has been linked to cardio-myopathy (Sears 2001). Furthermore, the application of an EPAC-specific activator to langendorff perfused hearts revealed a central role for EPAC proteins in the development of ventricular arrhythmia (Hothi et al. 2008). The role for EPAC1 in cardiac hypertrophy was hypothesised as EPAC1 expression is up regulated in response to

thoracic aortic constriction in rats (Metrich et al. 2008). Furthermore, characteristic hypertrophic markers such as increased cell size and hypertrophy-associated gene expression (e.g. atrial naturetic factor) were limited by knockdown of EPAC1 (Metrich et al. 2008). These factors supported a role for EPAC1 within the heart; however recent data suggests that these factors may be a response to, rather than causative of cardiomyopathy (Pereira et al. 2013).

Despite the evidence supporting a role for EPAC1 in the development of hypertrophic cardiac cells, recent work suggests that EPAC2 is directly responsible for many of the deleterious cardiac effects associated with non-selective EPAC activation (Pereira et al. 2013). Generation of EPAC1 and EPAC2 knockout mice has allowed the isoform-specific roles of EPACs within the heart to be directly assessed for the first time (Pereira et al. 2013). Importantly, $EPAC1^{-/-}$ ventricular myocytes responded to EPAC activation with Ca2+ release from the sarcoplasmic reticulum in a similar manner to wild type cells. However, this response was completely ablated in $EPAC2^{-/-}$ cells, supporting the idea that EPAC2 is the isoform involved in cardiacmyocyte calcium release and the subsequent cardio-myopathy observed (Pereira et al. 2013). Similarly to calcium flux within the pancreatic ß-cell, cAMP signalling through EPAC2 and Rap1 is a major of regulator of calcium signalling leading to cardiomyocyte contractility (Pereira et al. 2012; Pereira et al. 2013). Indeed, EPAC activation in cardiomyocytes has been linked to the activation of key calcium signalling proteins calcinuerin and CaMKII (Metrich et al. 2008) which are able to promote calcium release from cardiomyocyte intracellular stores by inducing phosphorylation and activation of the ryanodine receptor (Pereira et al. 2013). It is this deregulated stimulus that is involved in the pro-hypertrophic and arrhythmic signalling that contributes to cardio-myopathy. Thus, EPAC2 and dysregulation of calcium signalling play a major role in cardiac remodelling (Metrich et al. 2008) and ventricular arrhythmia (Pereira et al. 2013).

As EPAC2 is responsible for cardiac arrhythmia (Pereira et al. 2013), acute application of an EPAC2-selective agonist may allow precise control over contractility. Indeed, such an approach may be of use in the treatment of diseases associated with deregulated contractility. Conversely, EPAC2 antagonism within cardiomyocytes may provide an excellent mechanism to limit cardiac hypertrophy and arrhythmia in chronic heart disease.

1.3.4 EPAC-Rap1 Signalling and Vascular Function

One particular action of cAMP is to alter endothelial barrier function (EBF); the ability of the vascular endothelium to act as a semi-permeable barrier to inflammatory agents within the circulatory system (Parnell et al. 2012). Under normal conditions, the vascular endothelium limits the passage of liquid, chemokines, cytokines and leukocytes into the underlying tissue, preventing oedema and inflammation. However, in response to physical damage or the accumulation of lipid, endothelial barrier function can become deregulated (Figure 1-6-A), leading to the accumulation of inflammatory agents within blood vessels (Calabro et al. 2008). De-regulated inflammatory signalling has been shown to play a major role in the progression of CVD. Indeed, blood vessel thickening can be largely attributed to chronic inflammatory stimuli, which can progress into hypertension, stroke and cardiac arrest (Calabro et al. 2008). The maintenance of vascular endothelial permeability by cAMP is a tightly regulated process, incorporating cell-cell interactions and cytoskeletal rearrangement (Figure 1-6-A). In addition, the vascular endothelium and EPAC1 signalling can limit proliferative and migratory effects of vascular smooth muscle cells (VSMCs) in response to inflammatory cues (Figure 1-6-C). However, EPAC1 may play a role in promoting VSMC migration (Yokoyama et al. 2008), a causative factor in thickening of the vascular *tunica intima* following stent insertion, suggesting that EPAC1 function within the vasculature is complex and varies according to the cellular environment and the intensity of the cAMP signal.

Various mechanisms converge to regulate barrier function in vascular endothelial cells (VECs). Key regulators of barrier function are adherens junctions (AJ) and tight junction (TJ), which have been shown to be vital in forming linkages between VECs and limiting trans-endothelial permeability (Gulino et al. 1998; Zhadanov et al. 1999; Kooistra et al. 2005). One vital function ascribed to EPAC1-Rap1 signalling is the stabilisation of vascular endothelial cadherin (VE-Cadherin) complexes between VECs (Kooistra et al. 2005). Indeed, EPAC1-Rap1 signalling to VE-Cadherin is able to enhance barrier function in a PKA independent manner (Cullere et al. 2005).

Increased cytoskeletal contractility also plays a large part in the deregulation of cell-cell junctions by producing tension laterally across VECs that can disrupt interactions between adjacent cells, thereby increasing trans-endothelial permeability (Wojciak-Stothard and Ridley 2002). EPAC-Rap1 barrier protective effects have been shown to involve two Rho GTPase family members; RAC and RhoA. These key regulators of the cytoskeleton are able to induce opposing effects on endothelial barrier function. RAC activation induces the formation of cortical actin bundles, which through promote junction stability (Beckers et al. 2010). Conversely, RhoA activation in response to inflammatory agents such as thrombin promote the formation of actin stress fibres, myosin contraction and the disruption of endothelial cell shape (Bogatcheva et al. 2002). EPAC1 contributes to the regulation of these macromolecular structures through the activation of

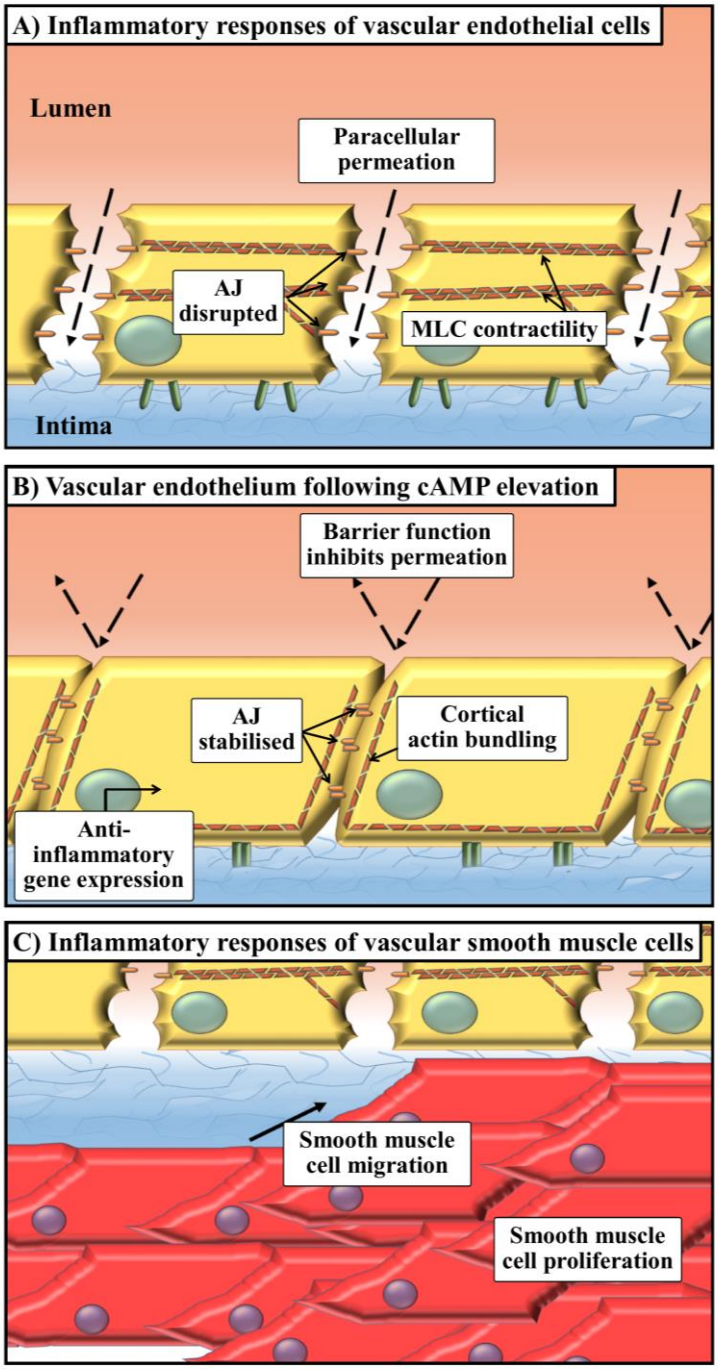

Figure 1-6 : Protective effects of EPAC1 signalling within the vasculature.
A – Inflammatory signalling promotes endothelial permeability to liquid, cytokines, chemokines and leukocytes into the underlying tissue, exacerbating vascular inflammation. This occurs due to the interrelated effects on cell-cell contact produced by impaired adherens junction stability (AJ) and increased cell contractility produced by myosin light chain (MLC) (Bogatcheva et al. 2002). **B** – The effects of cAMP signalling on vascular endothelial permeability. cAMP activation can promote, cortical actin bundling and adherens junction stability (Cullere et al. 2005; Fukuhara et al. 2005; Kooistra et al. 2005), tightening cell-cell contacts and limiting paracellular permeation. In addition, EPAC1 can induce anti-inflammatory gene expression (Sands et al. 2006). **C** – In response to inflammatory stimuli, vascular smooth muscle cells undergo proliferation and migration which can promote neo-intima hyperplasia, effects which can be countered by upregulated EPAC1 activity (Hewer et al. 2011).

RAC (Birukova et al. 2007; Birukova et al. 2008; Baumer et al. 2009; Birukova et al. 2010) and, additionally, through inhibition of RhoA (Stockton et al. 2010; Post et al. 2013). Thus, EPAC1-Rap1 signalling maintains the balance of activation between Rho GTPase family members by promoting the beneficial effects of RAC and suppressing the negative effects of RhoA on barrier integrity (Figure 1-7-A).

1.3.4.1 Rho GTPases

The molecular mechanisms underlying the regulation of Rho-family GTPases by EPAC1-Rap1 are now beginning to be understood. Birukova et al identified a correlation between elevations in cAMP, increased levels of active, GTP-bound RAC, improved barrier function (Birukova et al. 2007) and cell spreading (Arthur et al. 2004). Additionally, upon cAMP elevation with prostaglandin E2, the RAC-specific GEFS, VAV and TIAM, were observed to become phosphorylated and translocate to the membrane, coincident with their activation (Birukova et al. 2007). Inhibition of PKA, as well as knockdown of EPAC1, inhibited activation of RAC and co-activation of PKA and EPAC1 failed to produce an enhanced response (Birukova et al. 2010), suggesting that RAC is downstream of both cAMP inducible pathways.

RhoA inhibition is vital for Rap1 mediated barrier protective effects and various mechanisms have been proposed for this. The ability of Rap1 to relocalise the Rap1-binding protein, Krit1, to cell-cell junctions in the vascular endothelium has been observed, where it inhibits both the formation of stress fibres and the associated disruption of barrier function (Glading et al. 2007). Furthermore, down-regulation of Krit1 inhibits Rap1-dependent responses effects in VECs (Glading et al. 2007). The role of RhoA in Krit1 signalling was established after loss of Krit1 led to increased permeability of VECs, an effect reversed by treatment with a RhoA inhibitor (Stockton et al. 2010). In addition, Post et al identified a role for the Ras interacting proteins, Rasip1 and Radil, in regulating the activity of ArhGAP29, a Rho-GAP, and subsequently inhibition of RhoA (Post et al. 2013). Accordingly, siRNA mediated depletion of ArhGAP29, or Rasip1 and Radil in combination, was able to inhibit the beneficial barrier effects of Rap1 in VECs.

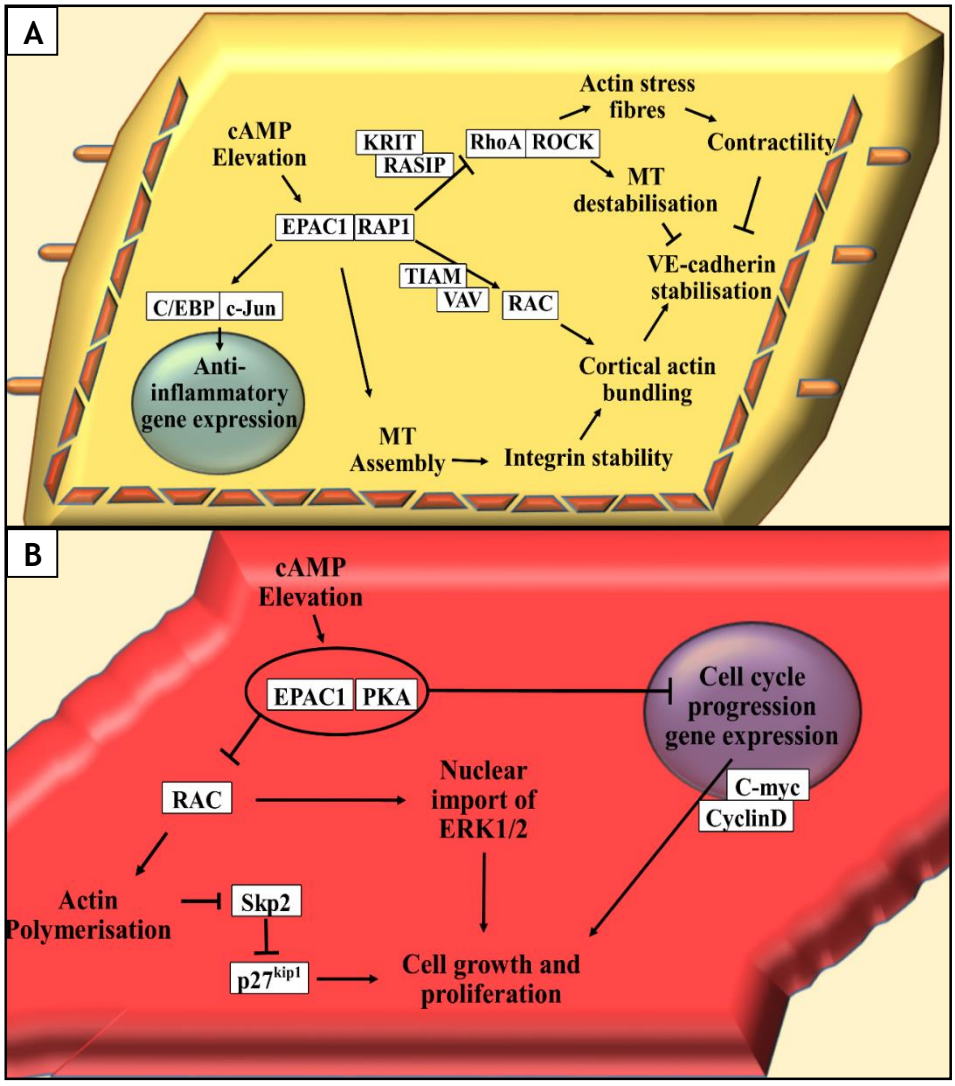

Figure 1-7 : EPAC1-Rap1 signalling within the vasculature has various protective effects. **A** – EPAC1 activation within vascular endothelial cells is responsible for the induction of suppressor of cytokine 3 (SOCS-3) expression by C/EBP and c-Jun transcription factors (Yarwood et al. 2008; Wiejak et al. 2014). Furthermore, regulation of microtubule assembly is able to stabilise integrin binding at cell-cell contacts, to promote barrier function (Sehrawat et al. 2011). The regulation of Rho-GTPases RAC and RhoA are central to EPAC1s effects on the cytoskeleton and adherens junction stability. EPAC1 has been shown to downregulate RhoA activity through both KRIT (Glading et al. 2007; Stockton et al. 2010) and RASIP (Ras interacting protein)(Post et al. 2013), which decrease cell contractility and inhibit the disruption of VE-cadherins by microtubules. Conversely, RAC has been shown to be activated in response to EPAC1-Rap1 signalling by the RAC-GEFs VAV and TIAM (Birukova et al. 2010). RAC is able to promote cortical actin structures which stabilise VE-cadherin at cell-cell contacts (Kooistra et al. 2005). **B** – Vascular smooth muscle cell proliferation can be inhibited by cAMP signalling through EPAC1 and PKA synergy (Hewer et al. 2011). In contrast to the vascular endothelium, PKA/EPAC1 signalling inhibits RAC activity and actin polymerisation. However, this in turn results in an up-regulation of the ubiquitin ligase components, Skp2, which inhibits cell growth and proliferation through degradation of $p27^{kip1}$ (Bond et al. 2008). Additionally, cAMP signalling is able to inhibit cell growth markers, such as c-myc and cyclin D, and inhibit the nuclear export and activation of ERK1/2 (Kimura et al. 2014).

Indeed, Rasip1 was observed by fluorescence resonance energy transfer (FRET) analysis to interact directly with Rap1, suggesting a direct link between EPAC1-Rap1 signalling, regulation of a RhoA GAP and the control of vascular endothelial barrier function (Post et al. 2013).

Clearly EPAC1-Rap1 signalling has a profound effect on the cell cytoskeletal and cohesive pathways of VECs. In addition, EPAC1 is vitally important in the regulation of VSMC migration and proliferation in response to inflammatory stimuli. Intriguingly, alterations in cytoskeletal stability are also thought to underlie the effects of EPAC1 in VSMCs, where EPAC1 has been shown to synergise with PKA to suppress VSMC proliferation, which is normally associated with neo-intima formation (Hewer et al. 2011). As opposed to the action of EPAC1 in VECs, EPAC1 is thought to suppress RAC activity within VSMCs (Figure 1-7-B), leading to cytoskeletal remodelling, nuclear export of ERK1/2 and inhibition of the transcription factor, Egr1 (Kimura et al. 2014). RAC activation normally promotes VSMC proliferation and neo-intima formation, whereas inhibition of RAC by PKA and EPAC1 leads to up-regulation of the cell-cycle inhibitor, $p27^{kip1}$ through suppression of Skp2, an F-box protein component of the Skp-Cullin-F-box ubiquitin-ligase, which normally targets $p27^{kip1}$ for proteolytic degradation during S-phase (Bond et al. 2008).

As such, an EPAC activator may exert positive effects on both barrier function and smooth muscle integrity, thereby limiting the damaging effects of inflammatory stimuli and the progression of CVD. Furthermore, EPAC1 selective activation may allow these positive effects within the vasculature endothelium whilst avoiding off-target activation of EPAC2 in other cell types. As such an EPAC1 agonist may be an effective tool in regulating the inflammatory response of VECs and VSMCs, thereby promoting cardiovascular health.

1.4 cAMP Signalling as a Therapeutic Target

The cAMP signalling pathway is a key target in drug development. However, various pitfalls have been identified relating to effects produced as a result of global cAMP elevation throughout the body. Here I will discuss new efforts to target the cAMP system therapeutically to produce beneficial effects whilst avoiding the common side effects associated with global cAMP elevation.

The first cAMP elevating agents available were ß-adrenergic receptor agonists, which form the basis of bronchodilators for the treatment of asthma such as isoproterenol and salbutamol (Sears 2001; Sears and Lotvall 2005). Additionally, cAMP elevating agents, such as chlorpromazine and haloperidol, have been used in the treatment of psychosis and schizophrenia through Gi-coupled D2 Dopamine receptor antagonism within the post-synaptic neuron (Kapur and Mamo 2003). These applications show the value of membrane protein stimulation in producing cAMP elevation intracellularly. Finally, cAMP signalling can be stimulated by intervention with cAMP-PDE inhibitors (Beavo 1995). In particular, isoform specific PDE4-inhibitors, such as rolipram and rofumilast, have shown promise in the treatment of inflammatory disease due to the localised expression of PDE4 isoforms within smooth muscle and immune cells (Burnouf and Pruniaux 2002).

cAMP signalling has a wide range of protective effects, however, pharmaceutical agents that globally elevate cAMP levels have been associated with severe side effects. As such, much research has focussed on developing greater tissue specificity by targeted application. For example, salbutamol inhalation avoids activation of cardiac beta receptors (Sears and Lotvall 2005), and the PDE isoform specificity of rofumilast results in fewer off target effects (Rabe 2011). However, EPACs are responsible for many of the protective effects of cAMP observed in various disease states and as such recent research has attempted to produce beneficial effects through direct regulation of EPAC (Chen et al. 2014). Indeed, by bypassing the effects of PKA, many benefits may be observed independently of the side effects associated with global cAMP elevation and dual PKA/EPAC activation. Furthermore, tissue specific expression of EPAC isoforms may allow a targeted approach to therapeutic intervention in disease states. This will no doubt

be facilitated by new high throughput screening methods for identifying small molecule regulators of EPACs (Chen et al. 2014).

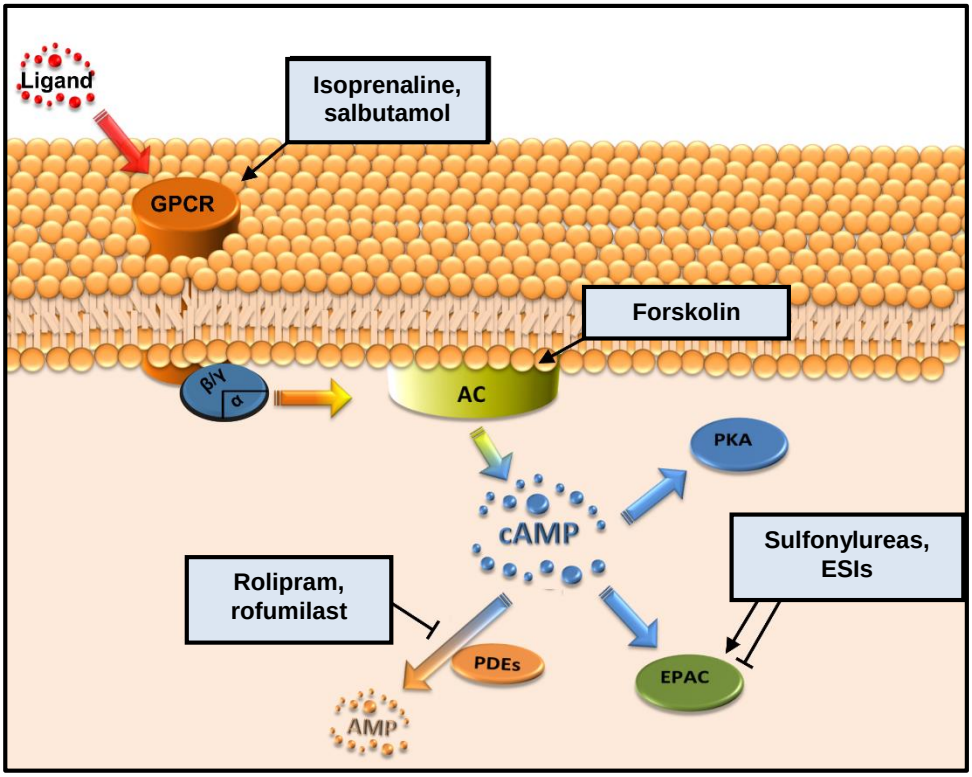

Figure 1-8 : Targets of cAMP regulatory drugs.
Membrane G-protein coupled receptor activation by isoprenaline and salbutamol, AC activation by forskolin and cAMP-phosphodiesterase inhibition by rofumilast and rolipram are all able to stimulate cAMP elevation within the cell to activate PKA and EPAC. Novel EPAC targeted small molecules, such as sulfonylureas and EPAC specific inhibitors (ESIs) have been proposed to activate and inhibit EPAC respectively.

1.5 EPAC as a Drug Target

EPAC has been implicated in the control of a number of disease states as detailed earlier. In order to effectively target EPAC medicinally it will be necessary to develop small molecule regulators that selectively activate EPAC over PKA, avoid inhibition of PDEs and are able to enter target tissues effectively. The following sections describe some of the recent work that has attempted to address these issues.

1.5.1 Development of EPAC Specific Cyclic Nucleotide Analogues.

The first attempt to selectively regulate EPAC centred on the development of a cAMP analogue that was able to activate EPACs independently of PKA (Enserink et al. 2002). This work was aided by the determination of the three dimensional structure of EPAC2 (Rehmann et al. 2006; Rehmann et al. 2008) and the development of a range of cAMP analogues with varying kinetic properties (Kraemer et al. 2001). In particular, the addition of a methyl group to the oxygen of the second carbon (2') of the ribose moiety of cAMP was observed to promote EPAC activation whilst greatly reducing the affinity of cAMP for PKA (Figure 1-9-B) (Enserink et al. 2002). This specificity is due to a single amino acid deviation between PKA and EPACs within the cAMP binding pocket of the otherwise highly conserved CNB. The substitution of a glutamic acid residue within PKA for glutamine or lysine (Figure 1-9-E), in EPAC1 and EPAC2 respectively, was found to be the key structural difference which allows EPACs, but not PKA, to accept the 2'O-methylated cAMP analogue (Enserink et al. 2002). This modification to the ribose moiety of EPAC1 decreased the affinity of cAMP for EPAC. However, coupling a parachlorophenylthio group (pCPT) to the eigth position of the adenosine ring (N8) stabilised a favourable trans base conformation, which is efficient in binding and activating EPACs and PKA (Kraemer et al. 2001). The combination of these cAMP modifications produced 8-pCPT-2'-O-Me-cAMP (007) which displays the dual properties of enhanced selectivity towards EPAC coupled to high affinity binding (Figure 1-9-C).

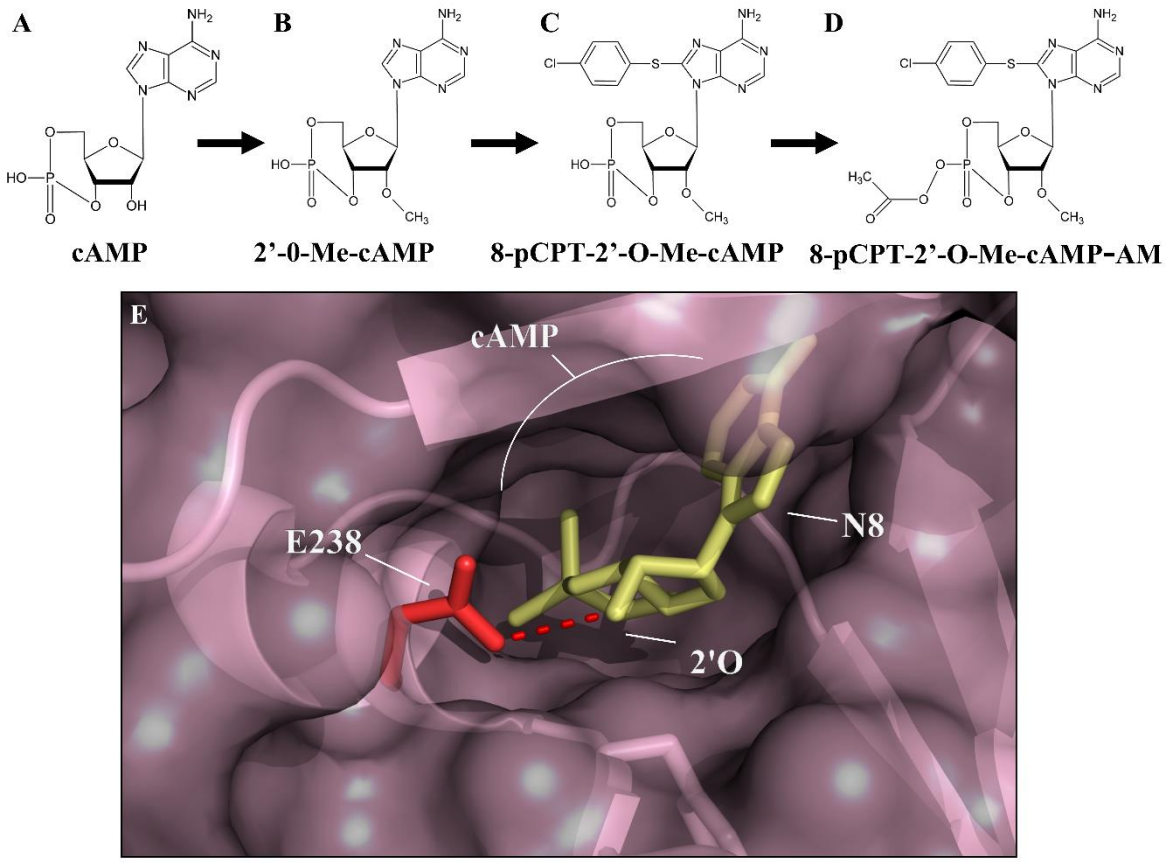

Figure 1-9 : Development of EPAC specific cAMP analogues.
The structure of cyclic adenosine monophosphate (cAMP) is shown (**A**). Methylation of cAMP at the ribose 2' oxygen (2'-O-Me-cAMP) results in greatly improved EPAC specificity, but affinity is lowered (Enserink et al. 2002) (**B**). The subsequent modification of the 8th carbon of adenosine with parachlorophenylthio (pCPT) produces 8-pCPT-2'-O-Me-cAMP (007) and greatly increases the affinity for EPACS, whilst maintaining selectivity over PKA (Enserink et al. 2002) (**C**). Finally, the addition of an acetoxymethyl ester (8-pCPT-2'-O-Me-cAMP-AM / 007-AM) masks the phosphate group, facilitating prodrug membrane permeability (Vliem et al. 2008) (**D**). Subsequent intracellular esterase activity removes this group allowing interaction with EPAC. **E** – The cAMP binding site of EPAC2 (pink, crystal structure 3CF6) (Rehmann et al. 2008) is shown. The highly conserved CNB of the PKA regulatory subunit (1RGS) (Su et al. 1995) has been aligned to the EPAC2 CNB. The position of glutamic acid 238 (E238, red) of the PKA regulatory subunit is shown with a red dashed line indicating hydrogen bonding between PKA E238 and cAMP (yellow) at the ribose 2' oxygen moiety. Substitution of this conserved glutamic acid within EPAC1 and EPAC2, to glutamine and lysine respectively, is the key structural difference within the CNB which accommodates the 2' oxygen-methylated cAMP analogue and imparts EPAC specificity to 007. Position 8 of the base (N8) is shown, which can be modified (e.g. with pCPT in 007) to increase the affinity of cAMP for CNBs.

007, along with its improved, cell permeable analogue (007-AM, Figure 1-9-D) (Vliem et al. 2008) have greatly facilitated the study of the cellular actions of EPAC by allowing the PKA independent effects of cAMP signalling to be observed directly (Enserink et al. 2002; Fukuhara et al. 2005; Kooistra et al. 2005).

However, *in vivo* use has been limited by its high effective dose, low cell permeability and the induction of cardiac arrhythmia, fibrosis and hypertrophy (Metrich et al. 2009). Furthermore, various off-target effects limit its specificity, such as its inhibitory effect over PDEs (Poppe et al. 2008) and off-target activation of P2Y12 platelet receptors (Herfindal et al. 2013). In order to effectively regulate disease through the EPAC family, small molecule regulators of EPACs are required. As a results of these caveats, a number of groups have adopted novel high-throughput screening approaches to identify small molecule regulators of EPAC activity (Chen et al. 2014).

1.5.2 High Throughput Screening For EPAC Inhibitors

In order to identify chemically distinct, small molecule regulators of EPAC activity, a number of groups have adapted existing assays of EPAC function for high throughput screening (HTS) and some progress has been made, particularly in the development of EPAC inhibitors. Moreover, in addition to selectivity over PKA, a number of compounds have been developed with the ability to selectively interact with EPAC1 or EPAC2 (Chen et al. 2013). These compounds show promise in forming the basis of future therapeutic agents designed to combat disease states where specific EPAC isoforms play an important regulatory role.

1.5.3 Discovery of Inhibitors of EPAC Activity

Recently, an isoform-specific EPAC1 inhibitor has been identified through HTS approaches. The assay was based on the priming of recombinant Rap1 with a fluorescent GDP analogue. This allowed the GEF activity of EPAC1 to be monitored as Rap-bound fluorescent GDP is exchanged for unlabelled GTP, producing a measurable decrease in fluorescence (de Rooij et al. 1998; Kraemer et al. 2001). By developing this assay for 384-well format it was possible to screen for small molecules capable of preventing this drop in fluorescence associated with Rap1 activation, and thus the GEF activity of EPAC1. The tetrahydroquinoline, 3ECF4,

was the first EPAC1 small molecule regulator to be isolated and is able to produce significant decreases in EPAC1 activity (Courilleau et al. 2012). Importantly, 3ECF4 was shown to act without directly disrupting EPAC1-Rap interaction or cAMP binding. Although the mode of action was not disclosed, 3ECF4 was observed to preferentially bind to the cAMP-bound, open conformation of EPAC1, supporting an inhibitory allosteric mechanism (Courilleau et al. 2012).

In addition to high throughput GEF assays, a bioluminescence assay has recently been developed to identify EPAC1 antagonists that are able to bind and stabilise the hinge region found within the CNB (Brown et al. 2014). EPAC1 protein was fused to citrine and Renilla luciferase, allowing conformational change to be visualised by a change in the emission wavelength as bioluminescent resonance energy transfer (BRET) occurs between the citrine and Renilla tags. Thus, EPAC activity can be assayed in response to compound binding. Indeed, an allosteric inhibitor was identified that was able to induce BRET, block EPAC1 activity *in vitro* and in cells by interacting with the key hinge region within the CNB that is involved in regulating enzyme activation (Brown et al. 2014).

The fluorescent properties of 8-[2-[(7-nitro-4-Benzofurazanyl)aminoethyl]thio]-cAMP (8-NBD-cAMP) have also been harnessed for the identification of compounds able to compete for binding to the CNB of EPACs. 8-NBD-cAMP has been modified at the eighth carbon of the adenosine ring to include the fluorescent benzofurazanyl moiety which is excited at 471 nm and exhibits a Stokes shift of 70 nm, producing emission wavelengths at 540 nm (Kraemer et al. 2001). Interestingly, binding to the hydrophobic environment of the CNB promotes a highly fluorescent conformation. Tsalkova et al, 2012, tested the ability of cAMP analogues and other small molecules to compete with 8-NBD-cAMP for binding to EPAC2 (Tsalkova et al. 2012). The appropriateness of this competition assay for HTS was demonstrated through extensive screening which has yielded various compounds with the ability to specifically inhibit EPAC2 activity *in vitro* and *in vivo* (Tsalkova et al. 2012; Almahariq et al. 2013; Chen et al. 2013). Importantly, these compounds did not alter PKA activity during *in vitro* counter screening, leading to their designation as EPAC specific inhibitors (ESIs).

1.5.3.1 Non-Selective ESIs

ESI-08 was the first EPAC inhibitor to be characterised using an 8-NBD-cAMP competition assay and was observed to inhibit both EPAC1 and EPAC2 to similar degrees (Chen et al. 2013). In order to define structure-affinity relationship (SAR) and to maximise affinity for the EPAC CNB, chemical modification of the R2 cyclohexyl group to cyclopropyl and cyclopentyl yielded the analogues HJC0198 and HJC0197 respectively. Each displayed improved IC_{50} values in 8-NBD-cAMP competition assays compared to the unmodified ESI-08 (Chen et al. 2013). Furthermore, both analogues were able to inhibit 007 induced protein kinase B (PKB/AKT) phosphorylation in HEK293T cells expressing EPAC1 or EPAC2, indicating non-selective EPAC inhibition (Chen et al. 2013). Confusingly, despite the ability of HJC0198 to block EPAC2 mediated PKB/AKT phosphorylation *in vivo* it was unable to affect GEF activity *in vitro* suggesting potential off-target effects (Rehmann 2013).

ESI-09 was also identified as a compound capable of down-regulating both EPAC1 and EPAC2 GEF activity (Almahariq et al. 2013). Lorenz et al. 2008, observed that EPAC1 expression levels were higher in cancerous pancreatic cells (Lorenz et al. 2008). Consistent with this, targeted knockdown of EPAC1 within these cells inhibited both their transwell migration and their ability to adhere in response to 007-AM stimulation, suggesting that EPAC1 may play an important role in the invasive character of pancreatic cancer (Lorenz et al. 2008). Interestingly, pre-incubation of cells with ESI-09 was able to mimic the effects of targeted knockdown of EPAC1 on cell migration, wound healing and adhesion, supporting a *bona fide* effect of ESI-09 on EPAC function and a potential avenue for the future treatment of pancreatic cancer (Almahariq et al. 2013). However, care must be taken, as HTS assays can be liable to detect denaturing agents, and indeed, ESI-09 has been suggested to act through denaturation of EPAC *in vitro* (Rehmann 2013).

Table 1-1 : Table of EPAC antagonists identified by high throughput screening.
ESI – EPAC specific inhibitor, FRET – Fluorescence resonance energy transfer, BRET - Bioluminescence resonance energy transfer.

Antagonists	Chemical name	Isoform targeted	In vitro data	In vivo data	Additional Information	References
3ECF4	5,7-dibromo-6-fluoro-2-methyl-1,2,3,4-tetrahydroquinoline-1-carbaldehyde	EPAC1	Inhibits recombinant EPAC1 GEF activity	Inhibits EPAC1 GEF activity towards Rap1 in HEK293T cells Inhibits autophagy in cardiomyocytes	Preferentially binds open, cAMP bound EPAC1. Allosteric	(Courilleau et al. 2012), (Laurent et al. 2014)
ESI-05	4-Methyl-2,4,6-trimethylphenylsulfone	EPAC2	Inhibits recombinant EPAC2 GEF activity	Inhibits EPAC2-FRET reporters and Rap1-GTP pulldown	CNBD1 required for EPAC2 inhibition	(Tsalkova et al. 2012), (Rehmann 2013)
ESI-07	Undisclosed	EPAC2	Inhibits recombinant EPAC2 GEF activity	Inhibit EPAC2-FRET Reporters and Rap1–GTP pulldown	Allosteric binding site at interface between CNBDs	(Tsalkova et al. 2012)
ESI-08 and analogues HJC0197/HJC0198	5-cyano-6-oxo-1,6-dihydro-pyamidine* (* pyramidine = cyclohexyl (ESI-08), cyclopentyl (HJC0197) and cyclopropyl (HJC0198)).	EPAC1 & EPAC2	Competes with 8-NBD-cAMP for binding to EPAC2	Inhibits EPAC1/EPAC2 induced phosphorylation of AKT S304/T574 in HEK293T cells	HJC0197 identified as denaturing agent	(Chen et al. 2012; Rehmann 2013)
ESI-09	3-(5-tert-butyl-isoxazol-3-yl)-2-[(3-chloro-phenyl)-hydrazno]-3-oxo-propionitrile	EPAC1 & EPAC2	Competes with 8-NBD-cAMP for binding to EPAC2	Inhibits T cell proliferation and cytokine production Inhibits pancreatic cell migration line and insulin secretion	Identified as denaturing agent	(Almahariq et al. 2013; Chen et al. 2013; Rehmann 2013; Almahariq et al. 2014),(Almahariq et al. 2014)
5225554 and 5376753	Undisclosed (barbituric/thiobarbituric acid)	EPAC1	Inhibits a BRET-based EPAC1 construct	Inhibits migration of cardiac fibroblasts	Allosteric inhibitors targeting CNBD hinge region	(Brown et al. 2014; Brown et al. 2014)

Table 1-2 : Table of EPAC agonists identified by high throughput screening.
GEF – Guanine exchange factor, FRET – Fluorescence resonance energy transfer, ITC - Isothermal titration calorimetry

Agonists	Chemical name	Isoform targeted	In vitro data	In vivo data	Additional Information	
8-$_p$CPT-2'-O-ME-CAMP (007)	8- (4-pChlorophenylthio)- 2'- O-methyladenosine- 3', 5'- cyclic monophosphate	EPAC1 & EPAC2	Activates recombinant EPAC1	Widely used in numerous cell systems	Super activator of EPAC1	(Enserink et al. 2002; Rehmann et al. 2003)
Sulfonylureas	Tolbutamide Glibenclamide Gliaclazide	EPAC2	Unable to stimulate GEF activity in vitro. Binding is not detectable by ITC.	Able to activate EPAC2 FRET-sensors. Able to induce EPAC2-dependent insulin secretion in mouse beta cells.	Proposed to bind to the CNBD1 of EPAC2 and synergise with cAMP to up-regulate cellular effects.	(Zhang et al. 2009; Herbst et al. 2011; Rehmann 2012; Takahashi et al. 2013)
SB compounds	Undisclosed	EPAC1 & EPAC2	Able to compete for ^{3}H cAMP-binding to CNBDs			(McPhee et al. 2005)

1.5.3.2 Isoform Selective ESIs

Due to the limited tissue distribution of EPAC2 and its association with various disease states, including type two diabetes, inhibition of EPAC2 may be an effective mechanism for the treatment of disease. Indeed, a range of small molecules have been identified that display selectivity towards EPAC2 (Chen et al. 2014). Of these, ESI-05 and ESI-07 were identified as compounds that specifically antagonise EPAC2 (Tsalkova et al. 2012). Both compounds were found to be effective in reducing EPAC2 GEF activity towards Rap1 both *in vitro*, and in HEK293T cell lines. The mechanisms of antagonist selectivity has been ascribed to the presence of the second inactive CNB of EPAC2, CNB1. Deuterium exchange mass spectrometry revealed a decrease in solvent exposure upon ESI-07 binding at two sites within EPAC2 (Tsalkova et al. 2012). The regions identified encompass a potential binding site found at the interface between the first and second CNBs of EPAC2. Tsalkova et al, hypothesised that ESI-07 binding may therefore lock EPAC2 in the closed, inactive form by inhibiting cAMP binding and GEF activity (Tsalkova et al. 2012). The requirement for the CNB1 of EPAC2 may explain the selectivity of ESI-07 for EPAC2, since EPAC1 lacks this additional domain (de Rooij et al. 2000). Consequently, both ESI-07 and ESI-05 are unable to inhibit EPAC1 activation in response to 007. Moreover, EPAC2 lacking the CNB1 is insensitive to ESI-05 inhibition, further supporting the idea that the CNB1 of EPAC2 is important for inhibitor binding (Rehmann 2013).

1.5.3.3 Caveats in the use of HTS for the Identification of Small Molecule Regulators of EPAC Isoforms

Despite the successful identification of ESIs as EPAC antagonists, doubts concerning the modes of action of these compounds have been raised due to the denaturing properties of HJC0197 observed *in vitro* experiments (Rehmann 2013). The increased exposure of hydrophobic residues is indicative of a reduction in protein stability and a thermal shift assay has been employed to detect the effects of the ESI compounds on EPAC and reference protein stability. Indeed, Sypro orange fluorescence was observed to increase dramatically as EPAC and other reference proteins became denatured in the presence of 50-100 μM ESI-09 and the ESI-08 analogue, HJC0197 (Rehmann 2013). Furthermore, the temperature at which these proteins become denatured drops in the presence of both ESIs. These

observations suggest that the inhibitory effects of ESI-09, ESI-08 and its derivatives are potentially nonspecific and may be linked to protein denaturation. However, docking experiments and *in vivo* data support a specific interaction between ESI-09 and ESI-08 with EPACs (Tsalkova et al. 2012; Almahariq et al. 2013; Chen et al. 2013). The denaturing properties of these compounds may therefore be exacerbated by *in vitro* analysis, or may be concentration dependent. These observations highlight an inherent danger when using HTS to detect ligand-protein interactions; namely, the detection of non-specific denaturing agents. As such it is important, wherever possible, to reduce the hit rate associated with non-specific denaturing agents and to confirm *in vivo* activity of isolated hits. Despite the concerns raised over the mechanism of action of ESI-08 and ESI-09, ESI-05 was confirmed to inhibit EPAC2 activity specifically without altering protein stability (Rehmann 2013).

1.5.4 EPAC2 Agonist Discovery

Few studies have led to the development of EPAC selective agonists. The most studied and controversial group of small molecule EPAC agonists are the sulfonylurea family. Sulfonylureas (SU) were originally characterised as anti-diabetic drugs capable of regulating SUR1 – a regulatory component of the k^{ATP} channel (Babenko et al. 1998). Activation of SUR1 is able to potentiate the opening of the k^{ATP} channel, causing potassium regulated calcium release and increased insulin exocytosis. The majority of SUs effects within the pancreatic ß-cell are attributed to regulation of this pathway, however, various low affinity SU receptors have also been postulated (Nelson et al. 1992).

In order to confirm that EPAC2 is a *bone fide* SU receptor, a range of SUs were screened for their ability to produce changes in the conformation of EPAC2 protein associated with the “open”, active form of the enzyme. The screening strategy was based on the dramatic structural changes undergone by EPAC proteins following cAMP binding (Rehmann et al. 2008). By fusing CFP and YFP to the N and C-termini respectively, fluorescence resonance energy transfer (FRET) is produced in the inactive form of the enzyme. Following cAMP binding and subsequent enzyme activation, the open conformation separates the two fluorescent proteins, resulting in a detectable decrease in FRET activity (Ponsioen et al. 2004). Using

this protocol, Zhang et al discovered that various sulfonylureas decreased the FRET signal detected in MIN6 ß-cells expressing the EPAC2 sensor. Furthermore, EPAC2$^{-/-}$ mice display impaired insulin release response to SU treatment (Zhang et al. 2009). The ability of SUs to promote the active conformation of EPAC2 combined with the decreased responsiveness of EPAC2$^{-/-}$ cells to SUs supports the hypothesis that EPAC2 is a low affinity SU receptor. However, Tsalkova et al. 2012, observes that SUs are able to induce elevations in intracellular cAMP, which may explain the positive effects of SUs on the activation EPAC2-FRET sensors and why insulin secretion is impaired in EPAC2 knockout mice (Tsalkova et al. 2011). This particular possibility remains to be assessed.

Herbst et al (2011) confirmed the ability of SUs to induce FRET changes in EPAC sensors in cellular systems and, importantly, reproduced these effects *in vitro*, after immuno-purification of these EPAC sensors from transfected cells (Herbst et al. 2011). Interestingly, although the full length EPAC2-FRET sensor responded to sulfonylureas with a decrease in FRET, neither EPAC1-FRET (which lacks CNB-1), nor the isolated EPAC2-CNB2-FRET sensor were able to reproduce this. It was therefore postulated that SUs are isoform selective, and able to bind to EPAC2 via an allosteric mechanism involving the low affinity CNB1 of EPAC2 (Herbst et al. 2011). Despite this evidence, the role of SUs as isoform specific EPAC2 agonists remains controversial. Indeed, the widely used SU, glibenclamide, was unable to induce GEF activity during i*n vitro* EPAC2 activation assays (Tsalkova et al. 2011). In agreement with Herbst et al, SUs were also unable to displace 8-NBD-cAMP from the CNB of EPAC2, which points towards the existence of an allosteric interaction site (Tsalkova et al. 2011). However, isothermal titration calorimetry failed to detect any heat changes following incubation with GLB, strong evidence against direct interaction between SUs and EPAC2. These issues may be explained by the required synergy between cAMP and SUs in the activation EPAC2 (Takahashi et al. 2013). It was observed that neither 100 nM GLB nor 1 µM 007 were able to produce a decrease in FRET alone. However, when applied in combination, a robust decrease in FRET of the EPAC2-FRET sensor was observed. Furthermore, residues vital to SU binding are masked in the closed conformation suggesting that SU binding may not occur in the closed state and, indeed, the proposed SU binding site is only exposed after cAMP binding (Takahashi et al. 2013). Although this may explain the inability to detect EPAC/SU binding via ITC, it fails to explain the

inability of GLB to upregulate EPAC2 GEF activity when applied alongside cAMP *in vitro* (Tsalkova et al. 2011). It appears, therefore, that although SUs can bind to the EPAC2-CNB1 when cAMP is present to produce a decrease in FRET, this binding does not directly relate to EPAC2 GEF activity. One explanation may relate to limitations of a FRET based activation assay. A drop in FRET is correlated to conformational change only and may not represent an increase in GEF activity. It is therefore possible that SUs bind to cAMP-bound EPAC2 to produce FRET without appreciable increases in GEF activity. Indeed, 3ECF4 has been shown to also target the cAMP bound form of EPAC1, stabilising the open form whilst inhibiting GEF activity (Courilleau et al. 2012). It would therefore be interesting to assess the effects of this compound on an EPAC1-FRET sensor. However, it is clear that a proportion of SU activity can be attributed to EPAC2 *in vivo* (Herbst et al. 2011), suggesting SUs may act through a distinct mechanism, perhaps altering EPAC2 subcellular distribution within the pancreatic ß-cell. Despite the considerable body of work regarding SUs, definitive evidence for EPAC2 agonism is yet to be shown.

1.5.5 EPAC1 Agonism has Therapeutic Potential in a Range of Disease States

Experiments using EPAC1 and EPAC2 knockout models have demonstrated the importance of EPACs in maintaining health, suggesting that EPAC agonism, rather than antagonism, is likely to produce the greatest therapeutic benefit. Greater selectivity of compounds for EPAC would likely reduce off target effects produced by activation of PKA, resulting in fewer side effects and drugs better suited to the treatment of chronic disease. Moreover, cardio-myopathy associated with EPAC2 activation (Pereira et al. 2013) and global cAMP elevation (Sears 2001) has limited the use of non-selective EPAC activators (Hothi et al. 2008). Despite this, no small molecule agonists for EPAC1 have been developed to date.

1.6 Aims

As no isoform-selective EPAC1 agonists exist, my objectives are to;

1. Develop a HTS platform that is able to identify isoform-selective EPAC1-interacting small molecules.

2. Develop a secondary, cell spreading screen that will allow classification of hits as either EPAC1 agonists or antagonists.

3. Elucidate the molecular mechanisms by which of EPAC1 promotes cell spreading in the secondary screen.

4. Identify the structural differences that underlie the differential intracellular targeting of EPAC1 and EPAC2 isoforms.

Chapter 2 : Materials and Methods

2.1 Suppliers

Abcam, Cambridge, UK

American Type Culture Collection (ATCC), Teddington, Middlesex, UK

Agilent, Stockport, Cheshire, UK

BD-Transduction laboratories, Oxford, UK

Bibby Scientific Ltd, Stone, Staffordshire, UK

Biolog Life Sciences, Bremen, Germany

Cambridge Bioscience, Cambridge, UK

Dundee Cell Products, Dundee, UK

Dundee Sequencing and Services, Dundee, UK

Evotech (UK) Ltd, 114 Innovation Drive, Milton Park, Abingdon, UK

Formedium, Hunstanton, Norfolk, UK

GE-Healthcare, Chalfont, St Giles, Buckinghamshire, UK

Greiner Bio-One, Stonehouse, UK

Invitrogen Ltd, Paisley, UK

Labcyte, Sunnyvale, California, USA

Life Technologies Ltd, Paisley, UK

Li-Cor Biosciences, Lincoln, Nebraska, USA

Melford Laboratories Ltd, Ipswich, Suffolk, U.K.

Millipore (UK) Ltd, Watford, Hertfordshire, UK

New England Biolabs Ltd (NEB), Hitchin, Hertfordshire, UK

Premier International Foods Ltd, Lincs, UK

Promocell, Heidlberg, Germany

Qiagen, Manchester, UK

Roche, Burgess Hill, UK

Santa-Cruz Technologies, Wembley, Middlesex, UK

Selleckchem, Newmarket, Suffolk, UK

Sigma-Aldrich Ltd, Gillingham, Dorset, UK

Thermo Fisher Scientific (UK) Ltd, Loughborough, Leicestershire, UK

Thistle Scientific Ltd, Glasgow, UK

VWR International, Lutterworth, Leicestershire, UK

Yorkshire Biosciences Ltd, York, UK

Zeiss, Cambridge, UK

2.2 Materials

Table 2-1 : Reagents.

Compound	Order number	Diluent/Stock Concentration	Supplier
3xFLAG-myc-CMV-26 vector	#E6401	Solid	Sigma-Aldrich
96 well plate, black	#655079	N/A	Greiner
384 well plate, black, low volume	#784076	N/A	Greiner
5-Bromo-4-chloro-3-indolyl-□-D-galactopyranoside (X-Gal)	#B4252	20 mg/ml DMF	Sigma-Aldrich
8- (4- Chlorophenylthio) adenosine- 3', 5'- cyclic monophosphate (8-CPT-cAMP)	#C-010	10 mM DMSO	Biolog Life Sciences
8- (4- Chlorophenylthio)- 2'- O-methyladenosine- 3', 5'- cyclic monophosphate (8-pCPT-2'-O-Me-cAMP/007)	#C-041	10 mM DMSO	Biolog Life Sciences
8-(2-[7-Nitro-4-benzofurazanyl] aminoethylthio)adenosine-3',5'- cyclic monophosphate (8-NBD-cAMP)	#N-002	6 mM dH_2O	Biolog Life Sciences
15N enriched ammonium sulfate	#299286	solid	Sigma-Aldrich
α-FLAG M2 Sepharose Beads	#A2220	Stored as 20% (w/v) ethanol slurry	Sigma-Aldrich
Adenosine-3',5'- cyclic monophosphate	#A9501	50 mM DMSO	Sigma-Aldrich
Acetic Acid Glacial	#0714	100% (w/v)	VWR
30% Acrylamide, 1% Bis-Acrylamide	#20-2100-10	As supplied	Thistle Scientific
Agar	#AGA02	Solid	Formedium^{Tm}

Ammonium Persulfate	#7727-54-0	Solid	Thermo Fisher
AZD6244	#S1008	1 mM DMSO	Selleckchem
Bisindolemaleide	#203290	10 mM DMSO	Millipore
BL-21 cells	#C2527I	As supplied	New England Biolabs
Brilliant blue	#B7920	Solid	Sigma-Aldrich
Bromophenol blue	#130126	Solid	Sigma-Aldrich
Bugbuster protein extraction reagent	#70584-4	10x	Millipore
Calcium chloride	#223506	1 M	Sigma-Aldrich
Deuterium oxide	#151882	Solid	Sigma-Aldrich
Dimethylformamide (DMF)	#D8654	0.944 g/ml	Sigma-Aldrich
Dimethylsulphoxide (DMSO),	#472301	1.1 g/ml	Sigma-Aldrich
Dithiothreitol	#M1505	Solid	Melford Laboratories
Echo 384 well plate	#LP-0200	N/A	Labcyte
EcoR1 Restriction Endonuclease	#15202-013	10x to be diluted in the supplied buffer reagents	Invitrogen
Ethylenediaminetetraacetic acid (EDTA)	#E9984	Solid	Sigma-Aldrich
FDA-approved Drug Library	#L1300	10 mM DMSO	Selleckchem
Fish Skin Gelatin	#G7765	40-50% (w/v) dH_2O	Sigma-Aldrich
Forskolin	#344270	10 mM DMSO	Millipore
Gö6983	#365251	1 mM DMSO	Millipore
Goat Serum	#G9023	As supplied	Sigma Aldrich

Glucose	#G0350500	20% (w/v) stock solution dH_2O	Sigma-Aldrich
Glutathione sepharose 4B	#GE17075601	Stored as 20% (w/v) ethanol slurry	Sigma Aldrich
Glycerol	#G5516	100% (w/v)	Sigma-Aldrich
Glycine	#BP381-1	Solid	Thermo Fisher
H-89 dihydrochloride	#371963	10 mM DMSO	Millipore
HEPEs	#4414855H	Solid	Sigma-Aldrich
Insulin from porcine pancreas	#I5523	1 mM dH_2O	Sigma-Aldrich
Isopropyl-ß-D-thio-galactopyranoside (IPTG)	#MB1008	1 M dH_2O	Melford Laboratories
L-Glutathione (Reduced)	#G6013	Solid	Sigma Aldrich
LY294002	#1130	10 mM DMSO	Tocris Biosciences
“Marvel” milk powder	198 g tin	Solid	Premier International Foods
Magnesium sulfate	#M7506	Solid	Sigma-Aldrich
NIH clinical collection (NCC)	#NCC1	10 mM DMSO	Evotech
Not1 restriction endonuclease	#15202-013	10x to be diluted in supplied buffer reagents	Invitrogen
One shot® TOP10 chemically competent *Escherichia Coli*	#C4040-10	As supplied	Invitrogen
PD184352	#S1020	1 mM DMSO	Selleckchem
pGEX-6P-1	#28-9546-48	Solid	GE-Healthcare

Prestained protein marker, broad range (7-175 kDa)	#P7708	0.1 mg/ml	New England Biolabs
Prestained protein marker, broad range (2-212 kDa)	#P7702	0.1 mg/ml	New England Biolabs
Phorbol 12-myristate 13-acetate	#524400	1 mM DMSO	Millipore
Prostoglandin E2	#P5640	10 mM DMSO	Sigma-Aldrich
Protease inhibitor cocktail	#11697498001	Solid	Roche
Protein A Sepharose Beads	#17-5280-01	Stored as 20% (w/v) ethanol slurry	Thermo Fisher
Protein G Sepharose Beads	#17-0618-01	Stored as 20% (w/v) ethanol slurry	Thermo Fisher
Ponceau S dye	#P3504	Solid	Sigma-Aldrich
Prescission protease	#27-0843-01	2000 units/ml (where one unit cleaves 100 µg gst-protein)	GE Healthcare
REDDOT nuclear stain	#40061	200x solution, dH_2O	Cambridge Bioscience
Rhodamine Phalloidin	#R415	6.6 µM Methanol	Invitrogen
Rolipram	#557330	10 mM DMSO	Millipore
Shandon Immu-mount	#9990402	Ready to use	Thermo Fisher
Sodium phosphate dibasic (Na_2HPO_4)	# 255793	Solid	Sigma-Aldrich
Sodium chloride	#7647-14-5	Solid	Thermo Fisher
Sodium deoxycholate	#D6750	Solid	Sigma-Aldrich
Sodium dodecyl sulfate	#442444	Solid	VWR

Sodium fluoride	#S1504	Solid	Sigma-Aldrich
Sodium phosphate	#102-494	Solid	VWR
Sodium azide	#S2002	Solid	Sigma-Aldrich
T4 DNA Ligase	#D2886	10x solution to be prepared in the supplied 10x buffer	Sigma-Aldrich
Triton X-100	#T9284	1.7 M	Sigma-Aldrich
Tris-Hcl	#RES3098T	Solid	Sigma-Aldrich
Tryptone	#TRP02	Solid	Formedium^{Tm}
Tween-20	#P1379	100% (w/v)	Sigma-Aldrich
Y27632	#L5288	10 mM dH_2O	Sigma-Aldrich
Yeast Extract	#YEA02	Solid	Formedium^{Tm}
Unstained protein marker, broad range (2-212 kDa)	#P7702	As supplied	New England Biolabs

2.3 Kits

Table 2-2 : Kits.

Kit	Order number	Supplier
BCA kit	#23227	Thermo Fisher
Miniprep kit	#12163	Qiagen
Nuclear fractionation kit	#40010	Active Motif
Quikchange mutagenesis kit	#210518	Agilent

2.4 Cell Culture Reagents

Table 2-3 : Table of reagents and equipment used in cell culture applications.

Reagent	Order number	Supplier
0.2 μm Nalgene vacuum filter	#Z358207	Sigma-Aldrich
Corning® 100 mm x 20 mm dish	#CLS430591	Sigma-Aldrich
Corning® 12 well cell culture cluster	#CLS3512	Sigma-Aldrich
Corning® 75 cm^2 flasks, canted neck, vented	#CLS430641	Sigma-Aldrich
Opti-MEM	#31985070	Life Technologies Ltd
DMEM	#41965-039	Life Technologies Ltd
HEK293T cell line	#CRL-3216	ATCC
COS1 cell line	#CRL-1650	ATCC
Penicillin/Streptomycin (10,000 μg/ml)	#15140-122	Life Technologies Ltd
G418 (powder)	#A1720	Sigma-Aldrich
Glutamine (200 mM)	#25030-081	Life Technologies Ltd
Trypsin-EDTA	#25200-056	Life Technologies Ltd
Foetal bovine serum	#16000-044	Life Technologies Ltd
Endothelial Cell Growth Medium MV2	#C-22022	Promocell
HUVEC (pooled)	#C-12203	Promocell

2.5 Equipment

Table 2-4 : Experimental equipment.

Equipment	Supplier
Axiovert 135 + Axiocam MRm	Zeiss
AVANCE 600 MHz spectrometer equipped with cryoprobe	Bruker
Biomek Fx Laboratory automation workstation with 96 multichannel pippeting head	Beckman Coulter
Echo® Liquid Handler	Labcyte
Envision Plate Reader	Perkin-Elmer
Jenway 6300 Visible Spectrophotometer	Bibby Scientific Ltd
J810 Spectropolarimeter	Jasco
LSM5 Pascal Axiovert 200M laser scanning confocal microscope LSM5 pascal instrument and AOTF Laser module	Zeiss
Mini-protean gel electrophoresis and Mini Trans-Blot® electrophoretic transfer cell	Biorad
Odyssey Sa Infrared Imaging System	Li-Cor
Optima Fluostar Plate reader	BMG Labtech
Wellmate Automated Pipette	Matrix

2.6 Antibodies

2.6.1 Primary antibodies

Table 2-5 : Primary antibodies.
WB – antibody/concentration used for Western blotting. IF – antibody/concentration used for Immunofluorescence.

Name	Order number	Epitope	Species	Working Dilution	Supplier
α-AKT	#9272	Polyclonal	Rabbit	WB-1:1000	New England Biolabs
α-beta-Tubulin (9F3)	#2128	Monoclonal	Rabbit	WB-1:1000	New England Biolabs
α-EPAC1 (5D3)	#4155	Monoclonal	Mouse	WB-1:1000 IF-1:500	New England Biolabs
α-EPAC2 (5B1)	#4156	Monoclonal	Mouse	WB-1:1000	New England Biolabs
α-ERK	#9102	Polyclonal	Rabbit	WB-1:2000	New England Biolabs
α-ERM (41A3)	#3142	Polyclonal	Rabbit	IF-1:500	New England Biolabs
α-ezrin (H276)	#SC-20773	Polyclonal	Rabbit	WB-1:1000 IF -1:500	Santa Cruz
α-FLAG (M2)	#F3165	Monoclonal	Mouse	WB-1:1000 IF-1:200	Sigma-Aldrich
α-HA	#H9658	Monoclonal	Mouse	WB-1:1000 IF-1:200	Sigma-Aldrich
α-Moesin	#3146	Polyclonal	Rabbit	IF-1:100	New England Biolabs
α-Myc	#C3956	Polyclonal	Rabbit	WB-1:1000	Sigma-Aldrich
α-phospho AKT (Ser473)	#4051	Monoclonal	Mouse	WB-1:1000	New England Biolabs
α-phospho CREB (Ser133)	#9196	Monoclonal	Mouse	WB-1:500	New England Biolabs

α-phospho ERK (Thr202/Tyr204)	#9106	Monoclonal	Mouse	WB-1:1000	New England Biolabs
α-Radixin	#2636	Polyclonal	Rabbit	IF-1:100	New England Biolabs
α-RAN	#610341	Monoclonal	Mouse	WB-1:2000	BD Transduction
α-RANBP (IF)	#64276	Polyclonal	rabbit	WB-1:200	Abcam
α-RANBP2 (WB)	#2938	Polyclonal	Rabbit	WB-1:500	Abcam
Normal Rabbit IgG	#2729	Polyclonal	Rabbit	1:100	New England Biolabs
Normal Mouse IgG	#37355	Polyclonal	Mouse	1:100	Abcam

2.6.2 Secondary antibodies

Table 2-6 : Western blotting secondary antibodies.

Western Blotting Antibodies	Order number	Species	Working Dilution	Supplier
IRDye® anti-Rabbit 680nm	#926-32223	Donkey	1:10,000	Li-Cor Biosciences
IRDye® anti-Rabbit 700nm	#926-32213	Donkey	1:10,000	Li-Cor Biosciences
IRDye® anti-mouse 680nm	#926-32222	Donkey	1:10,000	Li-Cor Biosciences
IRDye® anti-mouse 700nm	#926-32212	Donkey	1:10,000	Li-Cor Biosciences

Table 2-7 : Immunofluoresence secondary antibodies.

Immunofluorescence Antibodies	Order number	Species	Working Dilution	Supplier
Alexafluor anti-rabbit 488nm	#A-11008	Goat	1:400	Invitrogen
Alexafluor anti-mouse 488nm	#A-11001	Goat	1:400	Invitrogen
Alexafluor anti-rabbit 568nm	#A-11036	Goat	1:400	Invitrogen
Alexafluor anti-mouse 568nm	#A-11004	Goat	1:400	Invitrogen

2.7 Constructs

Table 2-8 : Constructs.
N/A – not available

Construct Name	Source	Institution	Reference
3xFLAG-myc-CMV-26-EPAC1	Insert-PCR amplified from human EPAC1 gene Backbone, Sigma-Aldrich	Ligation performed by Dundee Cell Products,UK	(Gupta and Yarwood 2005)
3xFLAG-myc-CMV-26-Vector	Backbone, Sigma-Aldrich	Ligation performed by Dundee Cell Products, UK	(Gupta and Yarwood 2005)
GST-EPAC1-CNB	In House	University of Glasgow, UK	(Magiera et al. 2004)
GST-EPAC2-CNB2	In House	University of Glasgow, UK	N/A
pFLAG-CMV2-EPAC2A	Professor Susumu Seino	Kobe University, Japan	(Niimura et al. 2009)
pFLAG-CMV2-EPAC2B	Professor Susumu Seino	Kobe University, Japan	(Niimura et al. 2009)
pCAsalFLAG-GFP	Professor Gwyn Gould,	University of Glasgow, UK	N/A
pLV-CMV-ezrin-GFP	Professor Johannes Bos	University of Utrecht, Netherlands	(Ross et al. 2011)
pLV-CMV-ezrinThr567Asp-GFP	Professor Johannes Bos	University of Utrecht, Netherlands	(Ross et al. 2011)
pMT2-HA-EPAC1	Professor Johannes Bos	University of Utrecht, Netherlands	(de Rooij et al. 1998)
pMT2-HA-EPAC2	Professor Johannes Bos	University of Utrecht, Netherlands	(de Rooij et al. 1998)
p-eGFP-ezrin Thr567Ala	Professor Sabrina Marion,	Institut Cochin, Paris, France	(Marion et al. 2011)

p-eGFP-ezrin Arg579Ala	Professor Helen Morrison,	Fritz Lipmann Institute, Leibniz, Germany	(Saleh et al. 2009)
pFLAG-CMV2-EPAC1	In House	University of Glasgow, UK	(Borland et al. 2006)
pFLAG-CMV2-EPAC1-620-881	In House	University of Glasgow, UK	(Borland et al. 2006)
pFLAG-CMV2-EPAC1-691-881	In House	University of Glasgow, UK	(Borland et al. 2006)
pFLAG-CMV2-EPAC1-764-881	In House	University of Glasgow, UK	(Borland et al. 2006)
pFLAG-CMV2-EPAC1-838-881	In House	University of Glasgow, UK	(Borland et al. 2006)
pFLAG-CMV2-EPAC1-Arg279Glu	Professor George G. Holz	New York University School of Medicine, US	(Kang et al. 2006)

2.8 Methods

2.8.1 Transformation

Plasmid DNA (1 µg) was incubated on ice with 30 µl One Shot® TOP10 Chemically Competent *Escherichia Coli (E. Coli)* for 30 minutes. *E. Coli* were heat shocked at 42 °C for 30 seconds and immediately cooled on ice. 250 µl SOCS medium (component of One Shot® TOP10 pack) was added to *E. Coli* and incubated shaking at 37 °C for 60 minutes. Bacteria were then plated onto L-Agar plates (0.5% (w/v) NaCl, 1% (w/v) tryptone, 0.5% (w/v) yeast extract powder, 1% (w/v) agar) supplemented with the appropriate antibiotic. *E. Coli* were then grown overnight (37 °C) and plates were subsequently stored at 4 °C for up to two weeks. Single colonies were then picked and grown overnight in Luria-Bertani (LB) broth (0.5% (w/v) NaCl, 1% (w/v) tryptone, 0.5% (w/v) yeast extract powder, pH7.4) supplemented with appropriate antibiotic selection. These overnights were then used to isolate plasmid DNA, inoculate large scale protein cultures or long term storage at -80 °C.

2.8.2 DNA Quantification

DNA was quantification was performed by spectrophotometry in a Jenway 6300 Visible Spectrophotometer (Bibby Scientific Ltd), by measuring the absorbance at 260 nm (A_{260}). Where A_{260} is equal to one, the double stranded DNA concentration is equal to 50 µg/ml.

2.8.3 DNA sequencing

All mutants produced in house were sequenced to ensure successful mutagenesis. For mutagenesis of N-terminal amino acids, plasmid or tag primers were used (e.g. GFP forward primer for S66D mutagenesis). Otherwise sequencing primers were designed based on proximity (e.g. 50 base pairs before the mutated base pair). All sequencing and primers were provided and performed by Dundee Sequencing and Services.

2.8.4 Glycerol stock storage

E. Coli were prepared for long term storage by adding 680 µl of transformed One Shot® TOP10 Chemically Competent *E. Coli* overnight cultures to 320 µl glycerol (4.4 M) and frozen at -80 °C.

2.8.5 Plasmid DNA Preparation

Plasmids were isolated from overnight cultures (see transformation) using provided maxiprep kit reagents. 100 mls of overnight culture was used for DNA preparation. Cells were pelleted at 3000 x g for 30 minutes at 4 °C. The supernatant was removed and the pellet resuspended in P1 (10 mls). Subsequently, resuspended bacterial cells were lysed by the addition of detergent P2 (10 mls) and gently mixed by inverting the tube six to eight times with subsequent incubation for five minutes at 15-25 °C. Precipitation of DNA using 10 mls buffer P3, followed by incubation on ice for 20 minutes allows centrifugation to pellet chromosomal DNA (20,000 x g, 30 minutes, 4 °C). The supernatant was then centrifuged again (20,000 x g, 30 minutes, 4 °C) with the supernatant applied to a Qiagen-tip gravity flow column. Following washing with 2x30 ml buffer QC, plasmid DNA was eluted with 15 ml Buffer QF, followed by precipitation with 10.5 ml isopropanol and centrifugation at 15,000 x g (30 minutes, 4 °C). The supernatant is then removed and washed with 5 mls 70% ethanol to facilitate resusupension, followed by further centrifugation (15,000 x g, 10 minutes, 4 °C). After removing alcohol, the pellet was air-dryed (10 minutes) and resuspended in the desired volume of distilled water (dH_2O). DNA concentration was calculated by measuring absorbance at 260 nm as described above.

2.8.6 Mutagenesis

Constructs were mutated using the QuikChange Lightning Site-Directed Mutagenesis Kit according to manufacturer's instructions. Template plasmid was mutated using mutagenesis primers (purchased from Yorkshire Biosciences) containing a codon mismatch, introducing single or multiple amino acid changes, or for deletions, mutagenesis primers were designed to anneal to the regions flanking the deletion. PCR amplification incorporates either a specific mismatch,

or fails to amplify the deleted region. PCR amplification with a high fidelity polymerase (Pfu Fusion-based DNA polymerase, included in kit) allows amplification of the insert-plasmid DNA, replicating the plasmid alongside the insert and introducing a single mutated site. Incubation of DNA with Dpn-1 results in the breakdown of the original, unaltered plasmid DNA only. This occurs as the source DNA, subcloned within *Escherichia Coli* contains methylated DNA. Dpn-1 restriction endonuclease targets only the methylated/hemimethylated source plasmid DNA at the target sequence: 5'Gm^6ATC-3'.

Source plasmid DNA was obtained by maxiprep and PCR with mutageneisis primers yielded mutagenized plasmid DNA. Mutagenesis primers were designed based on provided guidelines (QuickChange Lightning Site-Directed Mutagenesis Kit manual) In brief, 25 ng plasmid DNA was incubated with 125 ng of both forward and reverse mutagenesis primers alongside the provided buffer components, dNTPs and QuickChange Lightning polymerase. PCR was carried out using the following thermal cycling protocol;

Table 2-9 : Thermal cycling employed for mutagenesis.

Stage	Number of cycles	Temperature	Time
1	1	95 °C	30 seconds
2	18	95 °C 55 °C 68 °C	30 seconds 1 minute 1 minute/kilobasepair (kbp)
3	hold	4 °C	Forever

Original methylated DNA was digested by incubation of PCR product with Lightning Dpn1 (37 °C, 15 minutes). TOP10 chemically competent cells were subsequently transformed with the mutagenized plasmid DNA (see transformation). 37 µl of X-Gal (20 mg/ml) and 100 µl isopropyl-ß-D-thio-galactopyranoside (IPTG, 10 mM) was added to L-Agar plates (supplemented with appropriate antibiotic) prior to bacterial plating. *E.Coli* were allowed to grow overnight. Five to ten colonies were picked and plasmid DNA isolated (see plasmid DNA preparation) for sequencing to confirm mutagenesis.

Table 2-10 : Mutagenesis primers.
Emboldened codon indicates mismatched base pairs within mutated codon (separated). Square brackets indicate position of deletions.

Mutant construct	pLV-CMV-ezrinS66D-GFP
Source	pLV-CMV-ezrin-GFP
Forward primer	5'- GCTGGATAAGAAGGTG **GAT** GCCCAGGAGCTCAGG –3'
Reverse Primer	5'- CCTGACCTCCTGGGC **ATC** CACCTTCTTCTTATCCAGC –3'
	Codon AGT (Ser66) – GAT (Asp66).

Mutant construct	pFLAG-CMV2-EPAC1-R806N-A807T-M810T (Area1)
Source	pFLAG-CMV2-EPAC1
Forward primer	5'- GATGAGAATGATGGCC **AAC A**CC GCGCGG A**CC** CTGCAC CACTGCCG –3'
Reverse Primer	5'- CGGCAGTGGTGCAG **GG**T CCGCGC GG**T GTT** GGCC ATCATTCTCATC –3'
	Codon AGA (Arg806) to AAC (Asn806), GCC (Ala807) – ACC (Thr807), ATG (Met810) – ACC (Thr810).

Mutant construct	pFLAG-CMV2-EPAC1-Δ824-844 (Area2)
Source	pFLAG-CMV2-EPAC1
Forward primer	5'- CGAGTTTCCCACCTC**][**CCAGCCAGCACCTGGGC –3'
Reverse Primer	5'- GCCCAGGTGCTGGCTGG**][**GAGGTGGGAAACTCG –3'
	Region "CGAGTTTCCCACCTC" binds to flanking region 5' of H825 codon. Region "CCAGCCAGCACCTGGGC" binds to flanking region 3' of S844 codon. Plasmid amplification results in deletion of amino acids 825-844.

Mutant construct	pFLAG-CMV2-EPAC1-P819A-P821A-P824A (3P-A)
Source	pFLAG-CMV2-EPAC1
Forward primer	5'- GCCGAAGCCACAAC **GCG** GTG **GCG** CTCTCA **GCG** CTCA GAAGCCGAGTTTCC –3'
Reverse Primer	5'- GGAAACTCGGCTTCTGAG **CGC** TGAGAG **CGC** CA

	C **CGC** GTT GTGGCTTCGGC –3’
	Codon CCT (Pro819) – GCG (Ala819), CCT (Pro821) – CCG (Ala821), CCA (Pro824)- CGC (Ala824).

Mutant construct	pFLAG-CMV2-EPAC1Δ764-838
Source	pFLAG-CMV2-EPAC1
Forward primer	5’- CGACTGGCCAGG**][**ATTTCCACATGC –3’
Reverse Primer	5’- GCATGTGGAAAT**][**CCTGGCGAGGGCCAGTCG –3’
	Region “CGACTGGCCAGG” binds to flanking region 5’ of K764 codon. Region “ATTTCCACATGC” binds to flanking region 3’ of R838 codon. Plasmid amplification results in deletion of amino acids 764-838.

Mutant construct	pFLAG-CMV2-EPAC1 Δ1-50
Source	pFLAG-CMV2-EPAC1
Forward primer	5’- GCTTGCGGCCGCGATG**][**GCCTCCACAGAGC –3’
Reverse Primer	5’- GCTCTGTGGAGGC**][**CATCGCGGCCGCAAGC –3’
	Region “GCTTGCGGCCGCG” binds to flanking region 5’ of M2 codon Region “ATGGCCTCCACAGAGC” binds to flanking region 3’ of A50 codon Plasmid amplification results in deletion of amino acids 1-50.

2.8.7 Cell Culture

Human Embryonic Kidney HEK293T (ATCC), HUVEC (Promocell) and COS1 (ATCC) cells were cultured aseptically and stored long term in liquid nitrogen. Cells pelleted at 500 x g (relative centrifugal force (RCF)) for five minutes at room temperature (RT) and were then resuspended in freezing medium (3 mls, foetal

bovine serum (FBS) supplemented with 1.28 M DMSO as cryopreservant) per confluent 10 cm^2 flask (approx. $3x10^6$ cells) and frozen overnight by incubation at -80 °C followed by storage in liquid nitrogen.

To revive, COS1, HEK293T and HUVEC cells were pelleted in a 15 ml centrifugation tube (500 x g, five minutes, room temperature (RT)) and freezing medium was removed. COS1 and HEK293T cell pellets were resuspended in 10 ml growth medium (DMEM supplemented with, FBS 10% (v/v), Glutamine 2 mM, Penicillin/Streptomycin 100 µg/ml) and incubated at 37 °C, 5% CO_2 in 25 cm^2 flasks. Human umbilical cord endothelial cells (HUVEC) were resuspended in endothelial growth medium MV2 with penicillin/streptomycin (100 µg/ml). MV2 supplement contains epidermal growth factor, 5 ng/ml; basic fibroblast growth factor, 10 ng/ml; insulin-like growth factor (long R3 IGF), 20 ng/ml; vascular endothelial growth factor 165, 0.5 ng/ml; ascorbic acid, 1 µg/ml and hydrocortisone, 0.2 µg/ml which promote cell growth whilst inhibiting differentiation into fibroblast. Experiments on HUVEC were performed between passages three and six.

EPAC1, PCR amplified from the human EPAC1 gene, or a vector construct were ligated into the 3xFLAG-myc-CMV-26 vector yielding 3xFLAG-myc-CMV-26-vector and 3xFLAG-myc-CMV-26-EPAC1. Stable transfection of HEK293T cells was performed by Dundee Cell Products, involving transfection, selection of 25-50 clones and gene stability testing. Final clone selected was shown to express fusion tagged EPAC1 by both western blot analyses (Figure 3-12) and immunofluorescence (Figure 5-1). For stably transfected HEK293T cells, selection was maintained by the addition of 400 µg/ml G418.

COS1, HEK293T and HUVE cells were grown to 80% confluence and then passaged to maintain growth. Cell lines were passaged by removing growth medium and washing 2x with 10 mls (per 25 cm^2 flask) filter sterilised PBS (37 mM NaCl, 2.7 mM KCl, 8 mM Na_2HPO_4, 1.46 mM KH_2PO_4, pH 7.4) in order to remove residual FBS and calcium. Incubation with 2.5 mls Trypsin/EDTA per 25 cm^2 flask (five minutes, 37 °C, 5% CO_2) induces the dissociation of HEK293T and COS1 adherent cells from the flask base. Trypsination was then blocked by the addition of 2.5 mls growth medium followed by collection of cells and centrifugation at 500 x g (RCF).

Trypsin/medium was removed and cell pellets were then resuspended in growth medium and diluted to 1/5 concentration and plated for experiments, maintained in 25 cm^2 flasks or discarded.

2.8.8 Cell Transfection

Cells were seeded and allowed to grow to 50% confluency on ethanol sterilised 13 mm glass coverslips. DNA constructs were then transfected into cells using Lipfectamine 2000 according to the manufacturer's instructions. Briefly, 40 μl Optimem medium, containing 2.5 μl Lipofectamine 2000 reagent, was combined with 40 μl Optimem containing 2.4 μg DNA constructs for each well of a 12 well culture plate and allowed to form DNA-Liposomal complexes for 20 minutes (RT). Cells were then washed twice with PBS at 37 °C and incubated in 0.5 ml Optimem Medium. Following this DNA/Lipofectamine 2000 complexes were added to wells and incubated for a further two hours at 37 °C, whereupon medium was replaced with complete medium and cells were grown overnight. Cells were treated as described in figure legend and fixed for western blotting, confocal microscopy, acquisition and analysis. Successful transfection of GFP constructs was assessed using a Zeiss Axiovert 135 immunofluorescent microscope using a 20x objective lens (excitation and emission at 488 nm and 535 nm respectively).

2.8.9 Immunoprecipitation

Cells were grown to 90% confluency and treated as described in figure legend. Cells were lysed in 10 μl per cm^2 well/plate area (~1 x 10^6 cells) with immunoprecipitation (IP) buffer (Hepes pH 7.4, 150 mM NaCl, 5 mM EDTA, 1 mM NaF, 10 mM $NaPO_4$, 1% (v/v) Triton X-100 and one tablet protease inhibitor cocktail (Roche) per 50 mls lysis buffer). Following lysis, the cell debris was removed by centrifugation (8000 x g, 10 minutes). Lysates were then pre-cleared with non-specific antibodies (2 μg/ml) from the species matching the final precipitating antibody (e.g. normal mouse IgG for subsequent anti-EPAC1 (5D3) IP) and the relevant protein A/G sepharose beads (protein G beads for mouse, protein A for rabbit antibodies) at 20 μl of beads/ml for 60 minutes (4 °C, rotating). Lysate was then centrifuged to remove beads and lysates were incubated (60 minutes, 4 °C, rotating) with relevant antibody or nonspecific control antibodies (2 μg/ml). The

relevant FLAG or protein A/G conjugated beads were added and complexes allowed to form overnight (4 °C, rotating). Beads were pelleted at 100 x g (one minute) and lysate removed followed by washing with IP buffer. Beads were pelleted and washed three times before removing the supernatant and boiling bead/antibody complexes in electrophoresis sample loading buffer (63 mM Tris-HCl, 1 M Glycerol, 104 µM SDS, 37 µM Bromophenol Blue) at 95 °C for five minutes. Cell lysate and IP samples were analysed by western blotting.

2.8.10 Immunofluorescent Confocal Microscopy

Cells were seeded at a density of $0.25x10^5$ cells/cm^2 on ethanol sterilised 13 mm glass coverslips and allowed to adhere overnight in growth medium (37°C, 5% CO_2). Cells were then stimulated with indicated treatments prior to fixation with fixing buffer (3% (w/v) paraformaldehyde, 1% (w/v) sucrose, 1 mM $CaCl_2$, 1 mM $MgCl_2$ in PBS). Coverslips were then quenched for 10 minutes in 50 mM NH_4Cl, in PBS, permeabilised for four minutes with 0.1% (v/v) Triton X-100 in PBS. Cells were then blocked with 0.02% (v/v) goat serum and 0.02% (w/v) fish skin gelatine in PBS, filtered (0.2 µm Nalgene vacuum filter). Primary and secondary antibodies (anti-mouse/anti-rabbit FITC/rhodamine conjugates or rhodamine-phalloidin (33 nM) in actin stained cells) were incubated for one hour (RT) sequentially before incubation with 4',6-diamidino-2-phenylindole (DAPI, 10 µg/ml) for 20 minutes at RT or REDDOT (1 in 200, five minutes). Coverslips were then washed 3x in block buffer between incubations. Coverslips were mounted onto glass slides using Shandon Immu-Mount and analysed using a 63x Zeiss oil immersion objective, on a Zeiss LSM5 Pascal Axiovert 200M laser scanning confocal microscope (Carl Zeiss, Germany) equipped with a Zeiss LSM5 Pascal instrument and AOTF Laser module. Alexa Fluor® Dyes (488nm) and GFP fusion proteins were excited with an argon laser whereas 568 nm Alexa Fluor® Dyes and rhodamine phalloidin were excited with a helium neon laser. Zeiss Pascal software was used to collect images, which were saved in the LSM file format and analysed using ImageJ software (http://rsbweb.nih.gov/ij/). For morphology assessments ImageJ wand tool was used to select cells from thresholded images. For comparisons of HEK293T-Vector and –EPAC1 cells, EPAC1 protein was immunostained with anti-EPAC1 (5D3) to ensure the cells observed maintained EPAC1 expression. Threshold was set to encompass greyscale data above background signal and cell perimeters were

verified against transmission images. These were then measured for various variables, including area and perimeter which were collected and processed using Excel (Microsoft).

2.8.11 Statistical Analyses

For data sets with two or more sets of means, with a minimum of three biological repeats, analysis of variance (ANOVA) was employed. This retains the strength of a Students T-Test, but limits the widening confidence intervals associated with multiple data set comparisons. Where two or more factors were assessed (for example cell type and treatment) two way ANOVA was employed. P values were obtained from ANOVAs using the Dunnets Post-test, which was used to compare each data set to a known control, where a known control was available (for example mock stimulated vs stimulated). For comparisons of variable responses without a defined control (for example between different, non-basal stimulations), Tukeys post-test was employed. All statistical tests were carried out using Graphpad Prism version 6.00 for Windows (GraphPad Software). Where statistical tests comprised part of assay development process, more in depth information is given within the text (see Equation 3-1 – Signal to background, Equation 3-2 – Z'Factor, Equation 3-3 – Coefficient of variance and Equation 3-4 - Scaled mean absolute deviation).

2.8.12 Western Blotting

Cells were washed twice with ice cold PBS (0.5 ml/cm^2 culture dish area), lysed in 10 µl per cm^2 well/plate area (~1 x 10^6 cells) ice cold lysis buffer (50 mM HEPEs pH 7.5, 150 mM NaCl, 1% (v/v) Triton x-100, 12 mM sodium deoxycholate, 3.5 mM SDS, 10 mM NaF, 5mM EDTA, 10 mM Sodium Phosphate with protease inhibitor cocktail (Roche) and then cell debris was removed by centrifugation 13,000 x g for 20 minutes. The bicinchoninic acid assay (BCA) (Smith et al. 1985) was then used to assess protein concentration of cleared lysates using prepared BCA kit reagents.

Equal amounts of lysate protein were separated on made in house Tris/Glycine SDS PA gels (with polyacrylamide concentration varied 5-15% depending on protein size). Electrophoresis was carried out using the Biorad Mini-Protean

electrophoresis kits with running buffer (25 mM tris, 192 mM glycine, 0.35 mM SDS).

Protein was wet transferred from gel to nitrocellulose membrane using the Mini Trans-Blot® electrophoretic transfer cell and transfer buffer (25 mM tris, 192 mM glycine, 10% (v/v) Methanol). Equal protein loading was verified by Ponceau Staining (2.6 mM Ponceau S, 3% (v/v) Acetic acid in dH_2O) for one minute, followed by two washes in TBST (50 mM Tris, 150 mM NaCl, 0.05% (v/v) Tween 20). Prestained molecular weight marker (p7708) was used for all blots unless otherwise indicated. Membranes were then incubated shaking for 60 minutes in block buffer (TBST with 5% (w/v) Marvel skimmed milk powder). Primary antibodies were incubated at 4 °C overnight at given concentrations (Table 2-5 : Primary antibodies) followed by incubation with IRDye® secondary conjugated antibodies at given concentrations (Table 2-6 : Western blotting secondary antibodies), one hour at RT. Secondary antibodies were visualised using the ODYSSEY® Sa Infrared Imaging System.

2.8.13 Fractionation

Cells were fractionated using nuclear fractionation kit proprietary reagents (Active Motif) as per manufacturer's instructions into cytoplasmic and nuclear components. Briefly, cells were grown on 10 cm^2 cell culture dishes to 90% confluency (~8 x 10^6 cells), followed by washing in ice cold PBS (5 ml) + phosphatase inhibitors (supplied as kit reagent). PBS + phosphatase inhibitors were removed and replaced with a further 3ml PBS + phosphatase inhibitors. Cells were scraped down with a cell lifter and transferred to a 15ml centrifugation tube. Cells were pelleted (500 x g, five minutes), buffer was then removed and cell membranes were incubated in 500 µl hypotonic buffer (kit reagent) at 4 °C to swell the cells, and promote membrane fragility. Detergent (kit reagent) was added and samples were vortexed to allow leakage of cytoplasmic proteins into the buffer. The nuclear fraction was pelleted at 12,000 x G and the supernatant containing the cytoplasmic component was removed and retained. The nuclear component was obtained by disruption of the pellet in 25 µl detergent free complete lysis buffer (kit reagent) with protease inhibitor (shaking, 4 °C, 30 minutes). Samples were vortexed 30 seconds before removing the pellet. Protein concentration was

calculated by BCA assay and samples were run on SDS-PA gels. For ezrin molecular weight increase analysis (band shift), the nuclear fraction (retaining the particulate fraction) was probed by western blotting for total-ezrin.

2.8.14 Recombinant Protein Purification

EPAC1-CNB (amino acids 169-318 of EPAC1), and EPAC2-CNB (amino acids 304-453 of EPAC2) were PCR amplified from human sources. Adenine overhangs were added to facilitate insertion into TOPO vectors and transformation using taq polymerase and subcloned into One Shot® TOP10 Chemically Competent E. coli cells (Invitrogen). Both plasmid and insert were prepared by cleavage using EcoR1 and BamH1 restriction endonucleases. The insert was ligated into the multiple cloning site of the pGEX-6P-1 (GE-Healthcare) expression vector using T4 DNA Ligase (Sigma).

E.Coli BL-21 (Invitrogen) cells were transformed (see Transformation) with pGEX-6P-1-GST-EPAC1-CNB/ pGEX-6P-1-GST-EPAC2-CNB/ pGEX-6P-1-GST and cultured shaking overnight in LB (with 100 µg/ml ampicillin selection) at 37 °C. This culture was used to inoculate a large culture of one litre in a 2 litre conical flask (1:50 dilution, 20 mls into one litre) which was grown 60 minutes (shaking, 37 °C) or until optical density readings at 600 nm (OD_{600}) reached 0.7. At this point EPAC1/EPAC2-CNB GST-fusion protein or GST expression was induced by the addition of Isopropyl-ß-D-thio-galactopyranoside (ITPG, final concentration 1 mM achieved by a 1:1000 dilution from 1 M stock solution). Bacteria were allowed to grow four hours (or until OD_{600} reached 1.4-1.6) when cells were collected by centrifugation 2250 x g, 20 minutes at 4 °C. Broth was removed, and cells were frozen overnight at -80 °C. Pellets were thawed and resuspended in 10 mls 1x Bugbuster Lysis Reagent (Invitrogen) per litre of *E.Coli* broth. Incubation on ice for 20 minutes preceeded centrifugation at 8500 x g, 10 minutes, 4 °C in a centrifugation tube. supernatant (S/N) was decanted into fresh centrifuge tube and centrifuged again at 8500 x g, 10 minutes, 4 °C. S/N was to transferred to 50 mls centrifugation tube(s) containing 0.1 ml glutathione sepharose per ml of S/N (5 mls beads), pre-equilibrated in wash buffer (50 mM Tris-HCl, 50 mM NaCl, 1 mM EDTA, 1 mM DTT pH 7.8). S/N was incubated with glutathione beads with gentle rocking (4 °C, 60 minutes). Beads were pelleted at 500 x g (4 °C, five minutes)

followed by removal of buffer and washing in 25 mls wash buffer. Pelleting and washing was repeated 5x, at which point the buffer was removed and pellets were incubated with two mls elution buffer (150 mM Glutathione, 50 mM Tris-HCl, 50 mM NaCl, 1 mM EDTA, 1 mM DTT pH 7.8.) per one ml of beads for 30 minutes at 4 °C. Beads were pelleted at 500 x g (4 °C, five minutes) and eluate was gently removed and retained. Elution with two mls elution buffer, incubation and centrifugation was removed and eluate sample two was retained. Protein samples were dialysed against three changes of wash buffer (one litre, 60 minutes, 4 °C). Protein concentration was assessed by BCA and eluates were pooled where appropriate. All protein was assessed to be 80% minimum pure, judged by SDS-PAGE analysis. Protein was stored in aliquots as required and stored at -80 °C.

2.8.15 Circular Dichroism

The Jasco J810 spectropolarimeter was used to record the spectra in both the near and far UV, giving spectral data for submission to the online database Dichroweb for analysis and comparison to known secondary structure elements. For far UV samples, a 0.02 cm cell cuvette was used and for near UV, a 0.5 cm cell cuvette (Greenfield 2006).

2.8.16 NMR

EPAC1-CNB-GST was recombinantly expressed and purified as described above. However, E.Coli were grown in M9 minimal medium (97 mM Na_2PO_4, 44 mM KH_2PO_4, 17 mM NaCl with 2 mM $MgSO_4$, 0.1 mM CaCl, 16.6 mM glucose and 100 µg/ml ampicillin added on day of use, pH 7.2) supplemented with 7 mM ^{15}N enriched $(^{15}NH_4)_2SO_4$ (ammonium sulphate) on day of use, as a sole nitrogen source. The GST tag present upon EPAC1-CNB-GST was removed using Prescission protease (GE Healthcare) for 30 minutes. Protein was dialysed into NMR buffer (20 mM Na_2PO_4, 0.01% (w/v) NaN_3, pH 7.2) and diluted to 107 nmoles in 600 µl , with a 5% final concentration (v/v) of D_2O (deuterium oxide) to lock. Nuclear magnetic resonance [1H,15N] heteronuclear single quantum coherence (HSQC) spectra were recorded using a Bruker AVANCE 600MHz spectrometer with cryoprobe (Harper et al. 2007).

2.8.17 Competition assay validation

Optimisation of 8- (2- [7-nitro- 4- benzofurazanyl] aminoethylthio) adenosine- 3', 5'- cyclic monophosphate (8-NBD-cAMP) competition assay was performed using purified EPAC1 and EPAC2 CNBs plus GST (see recombinant protein purification) using modified assay conditions previously described (Tsalkova et al. 2012). Briefly, EPAC1-CNB-GST/EPAC2-CNB-GST protein sample was incubated in a 96 well black assay plate (Greiner) in order to reduce autofluorescence associated with white or clear plates. These protein samples each were made up to a 3x stock solution (2.4 µM) of which 33 µl was added to a 96 well assay plate (Greiner). To this, 33 µl of the fluorescent cAMP analogue 8-NBD-cAMP 3x stock solution (300 nM) was added. In order to ascertain the maximum and minimum signals in the assay, DMSO and cAMP was incubated with the protein/8-NBD-cAMP sample. cAMP dissolved in DMSO (10 mM stock) was made up as a 3x stock solution (150 µM) in assay buffer and 33 µl added to the relevant wells in the 96 well plate (final DMSO concentration – 0.5 % / 64 mM). For every other well, DMSO was added to match the concentration present in the cAMP negative control. Protein (0.8 µM) / probe (100 nM) / controls (cAMP at 50 µM) at 99 µl per well were spun at 800 x g in a plate centrifuge. The fluorescence intensity was measured after four hours using the Optima Fluostar plate reader (BMG Labtech), (excitation wavelength 480 nm and detection wavelength 535 nm).

2.8.18 8-NBD-cAMP competition assay development

In order to optimise the assay for high throughput screening, various variables were varied. The assay was first scaled down into black, low volume (to maximise the signal produced by low volume assays) 384 assay plates (Greiner) with a maximum volume of 30 µl. In order to maximise plate reproducibility, EPAC1-CNB /EPAC2-CNB protein, 8-NBD-cAMP, DMSO and cAMP analogue titrations were performed using the Biomek Fx laboratory automation workstation with 96-multichannel pipetting head (Beckman Coulter). Briefly, a 2x stock solution of the given probe, protein or control/compound concentrations in assay buffer was incubated in a black, 96 well assay plate (Greiner). A 384 well assay plate was prepared with the required wells filled with assay buffer to 10 µl. 10 µl of the protein/probe was then added and mixed to the first row/column. 10 µl of this diluted stock was then added to the subsequent row/column and mixed. This

process was repeated as required to give a dilution curve. The final row/column was prefilled with assay buffer to the required volume to give the final 0% concentration. To this plate, the remaining required assay components were added to give a final 30 µl working volume (e.g. if protein concentration was being varied, 10 µl 8-NBD-cAMP and 10 µl DSMO/cAMP controls would subsequently be added), span at 800 x g (10 seconds) and incubated for four hours (or as indicated in figure legend) before 8-NBD-cAMP fluorescence intensity was measured using the Envision plate reader (Perkin-Elmer, excitation wavelength 480 nm, detection wavelength 535 nm).

2.8.19 Pilot Screening

Compounds from the National Institute of Health (NIH) Clinical Collection (NCC) Library and the Selleckchem Food and Drug Administration (FDA) approved drug library (L1300) were incubated with EPAC1-CNB and EPAC2-CNB to test their ability to compete with 8-NBD-cAMP for the cyclic nucleotide binding domain. This was performed using the optimised assay conditions ascertained, with EPAC1-CNB and EPAC2-CNB probed simultaneously. Briefly, DMSO (12.8 mM final assay concentration) and cAMP (50 µM) controls and library compounds (10 µM final concentration, in DMSO) were seeded in black, low volume 384 assay plates (Greiner) at 25 nl volumes from preprepared Echo source plates (Labcyte, compounds and controls stored within plates at 1000x stock concentration, 100 µl) using the Echo® Liquid Handler (Labcyte). Control concentrations were ascertained by performing a dose curve to ensure the concentration of cAMP was at sufficient conditions to ensure maximal fluorescence signal inhibition. Library compound concentrations were high enough to ensure even low affinity compounds were isolated, though concentration was limited by supply and cost. 12 µl of EPAC1-CNB/EPAC2-CNB (of 2x (1.6 µM) stock concentration giving a 0.8 µM final concentration) was immediately added to each well using the Wellmate automated dispenser (Matrix) before 30 minutes pre-incubation to promote compound-protein complex formation. 12 µl of 8-NBD-cAMP (of 2x (125 nM) stock concentration to give a 62.5 nM final concentration) was added to every well using the Wellmate dispenser and plates were briefly centrifuged (800 x g, 10 seconds) to mix reagents. The assay was incubated (RT) until fluorescence intensity was measured at 4 hours and 15 hours (within demonstrated window of stability and

consistent with times associated with high and ultra high throughput assays) using the Envision plate reader (Perkin-Elmer) with excitation at 480 nm and detection at 535 nm. 15 hours measurements were compared to 4 hours results to ensure sample stability. For all experiments no significant deviation was observed between 4 and 15 hours, and as such all results given are 4 hour time point values. For follow up hit confirmation, a serial dilution of each compound was performed from a starting concentration of 30 µM under assay conditions as described above with the exception of DMSO concentration which was maintained at 36.8 mM (0.3% (v/v)) throughout due to the initial seeding of 75 µl for 30 µM compound concentrations.

2.8.20 Computational analysis

Sequence analysis of EPAC1 and EPAC2A and EPAC2B (UniProt accession numbers, 095398, Q8WZA2 and A2ASW8, respectively) was carried out using Jalview (Waterhouse et al. 2009). Additionally, the fast and reliable online alignment server "Muscle" (Edgar 2004) was employed in order to compare sequence homology between isoforms. Structural alignment and analysis of protein physical features, such as solvent exposure and secondary structure, was carried out using PyMol (Schrödinger) and PDB files 3CF6 (EPAC2 open form) (Rehmann et al. 2008) 1RGS (PKA CNB) (Su et al. 1995) and 2byv (EPAC2 closed form) (Rehmann et al. 2006). NMR spectral analysis was carried out using CCPN analysis software, to assign peaks and compare spectra (Vranken et al. 2005). Many thanks to Hans Wienk for his generous gift of spectral data and amino acid peak positions, which together with in house data provided greater than~70% amino acid coverage.

In order to assess the structure of EPAC1, for which no crystal structure is available, a homology model was made using the program "Modeller" (Sali and Blundell 1993) to model the EPAC1 or EPAC2B primary sequence (UniProt accession number, 095398 and A2ASW8 respectively) on the closed form of EPAC2 (2BYV). This program uses spatial constraints to construct the models and regions of known structure and homology are combined with energetically favourable conformations of regions with low or no sequence homology. Specifically, the "align2D" command was used to produce a sequence alignment based on both primary and structural features, followed by the "model-single" command. Up to

20 models were exported and the most energetically favourable models (as determined by the output discrete optimised protein energy score (DOPE) score) were selected for imaging and analysis. For flexible loops the “loop-model” command was employed to identify the most favourable and likely conformation adopted. Linear regression and line plotting was performed using XLfit (XLfit Software) using a model assuming single site binding. Chemical structures of cAMP and analogues were drawn using ChemSketch (ACD Labs).

Chapter 3 : Development of High Throughput EPAC1 Agonist Screening Methods

3.1 Introduction

cAMP signalling exerts beneficial effects in a range of disease states, including cardiovascular disease (CVD) (Parnell et al. 2012). Indeed, elevated cAMP levels are able to counter vascular endothelial hyper-permeability by limiting the secretion of chemokines and the recruitment of inflammatory leukocytes (Fukuhara et al. 2005). Unresolved, chronic inflammation in the vascular endothelium is a common feature in the progression of CVD, and is linked to atherosclerosis, hypertension, congestive heart failure, primary pulmonary hypertension, and other inflammatory syndromes (Bruunsgaard et al. 2001; Calabro et al. 2008).

Due to the ability of cAMP to suppress inflammatory signalling, various drugs targeting cAMP signalling pathways have been tested for their ability to treat CVD. These drugs act to either promote cAMP production through activation of AC (Ammon and Muller 1985), or inhibit its breakdown by phosphodiesterases (Maurice et al. 2014). However, both classes of drugs suffer from serious limitations. For example, cAMP phosphodiesterase inhibitors, such as pentoxifylline, ibudilast, drotaverine and rofumilast produce nausea, emesis, diarrhoea and cardiac arrhythmia which limits their usefulness. The use of forskolin, to activate adenylate cyclase, has also been linked to various side effects, including flush syndrome and hypotension (Schlepper et al. 1989). These caveats demonstrate that the strategy of promoting elevation in intracellular cAMP may be unsuitable for the treatment of chronic inflammatory disease. It is therefore important to develop novel drugs that are able to combat CVD with reduced side effects. Although many of the cellular effects of cAMP have been attributed to PKA, EPAC is increasingly understood to be an important mediator of cAMP signalling. Indeed, synergy between EPACs and PKA, or EPAC activity alone have been shown to produce a range of beneficial effects originally attributed to PKA alone (Cheng et al. 2008). Therefore, it may be possible to exert protective effects against disease by selectively activating EPACs, while avoiding many of the side effects associated with global cAMP elevation and activation of PKA.

To date, only one EPAC specific agonist has been identified; the cAMP analogue, 8-pCPT-2'-O-Me-cAMP (007), which is able to selectively activate both EPAC1 and

EPAC2 isoforms independently of PKA (Enserink et al. 2002). Indeed, 007, along with its improved, cell permeable orthologue 8-pCPT-2'-O-Me-cAMP-acetomethyl ester (007-AM) (Vliem et al. 2008) have greatly facilitated the study of EPAC function by allowing the PKA-independent effects of cAMP signalling to be directly observed (Enserink et al. 2002; Enserink et al. 2004; Fukuhara et al. 2005; Kooistra et al. 2005). However, *in vivo* use of 007 has been limited by low cell permeability and, importantly, the induction of cardiac arrhythmia, fibrosis and cardiac hypertrophy (Hothi et al. 2008; Metrich et al. 2010). Furthermore, various off-target effects limit its specificity, such as its inhibitory effect towards cAMP phosphodiesterases (Poppe et al. 2008). However, recent studies have revealed that the EPAC2 isoform is solely responsible for disturbed cardiac calcium signalling and cardiomyopathy in response to 007 stimulation (Pereira et al. 2013). Therefore, the development of EPAC1-selective agonists may facilitate the treatment of vascular inflammation and CVD, without the side effects associated with global cAMP elevation (nausea, vomiting) and EPAC2 activation (cardiac arrhythmia).

3.1.1 HTS for Isoform Specific Agonists

Various assays have been developed to identify compounds capable of binding to EPAC and regulating its activity (McPhee et al. 2005; Courilleau et al. 2012; Tsalkova et al. 2012). Of these high throughput screening assays (HTS) assays, only one has successfully identified molecules with the potential to activate EPAC1 (McPhee et al. 2005). In this case, the screening platform was based on the ability of compounds to displace tritiated cAMP (^{3}H-cAMP) from the CNB of EPAC1 and EPAC2. Displacement of ^{3}H-cAMP resulted in a demonstrable drop in radioactivity, allowing the characterisation of interacting molecules. This HTS assay allowed screening of 10,000 compounds from the Scottish Biomedical Lead Generation Library, with multiple competitors identified (McPhee et al. 2005). Of these, 15 small molecules demonstrated selectivity for EPAC over PKA, and several displayed isoform selectivity for EPAC1 or EPAC2. However, further research on these compounds has not been forthcoming.

Recently a fluorescence-based competition assay has been employed to identify EPAC inhibitors (Tsalkova et al. 2011; Chen et al. 2012; Tsalkova et al. 2012;

Tsalkova et al. 2012; Almahariq et al. 2013). This assay utilises the properties of the cAMP analogue 8-[2-[(7-nitro-4-benzofurazanyl) aminoethyl]thio]-cAMP (8-NBD-cAMP), which fluoresces strongly within the hydrophobic environment of the cAMP binding pocket (Kraemer et al. 2001). Displacement of 8-NBD-cAMP by competitor compounds leads to a reduction in fluorescence, allowing the identification of interacting molecules. The 8-NBD-cAMP competition is equally sensitive to EPAC agonists as antagonists and represents a powerful, high throughput mechanism for the identification of EPAC interacting molecules. Despite the considerable therapeutic potential of isoform specific agonists, this HTS method has not yet been harnessed to discover EPAC activators. Indeed, 8-NBD-cAMP competition is equally sensitive to EPAC agonists as antagonists and represents a powerful, high throughput mechanism for the identification of EPAC interacting molecules. To date, isoform specific screening has been limited due to the inability to probe isoform specificity within the primary screen. Indeed many identified hits to bind both EPAC1 and EPAC2, or required further analysis to confirm specificity (Tsalkova et al. 2012). Here, we aim to develop a competition assay able to confirm isoform selectivity during primary screening. Indeed, a robust primary screen would allow the identification of isoform specific binding molecules, facilitating follow up analysis and drug development.

To date, the 8-NBD-cAMP competition assay has only been used to identify EPAC2 interacting molecules. This is likely due to the stability of recombinant EPAC2 in the screening assay and the reported therapeutic benefits of EPAC2 regulation, including potentiation of insulin secretion (Holz et al. 2006). Indeed, the low stability of full length recombinant EPAC1 *in vitro* has limited its study in HTS and structural assays (Kraemer et al. 2001). Although full-length EPAC1 is unstable *in vitro*, the isolated EPAC1-CNB displays superior stability. Furthermore, initial characterisation of 8-NBD-cAMP revealed its ability to bind and fluoresce within the isolated CNB of EPAC1 (Kraemer et al. 2001). As 8-NBD-cAMP forms molecular interactions within the cAMP binding pocket it may be possible to perform a HTS utilising the isolated CNB of EPACs. Indeed, the only confirmed EPAC agonist, 007, acts competitively with cAMP to target the CNB of EPACs, highlighting the importance of this region for EPAC activation and the suitability of this region for agonist screening (Christensen et al. 2003). The CNB of cAMP binding proteins are not only vital for activation, but display considerable structural differences which

have facilitated the development of isoform selective regulators (Rehmann 2005; Dao et al. 2006; Rehmann et al. 2007). By screening both EPAC1 and EPAC2 simultaneously it will be possible to disregard compounds that bind non-selectively, greatly facilitating isoform specific compound discovery. As full length EPAC1 is unstable, screening will be facilitated through the use of the isolated CNBs of EPAC1 and EPAC2. However, the suitability of EPAC-CNBs for HTS within an 8-NBD-cAMP HTS assay has not been previously demonstrated.

We aim to:

- Develop a primary HTS assay with the ability to identify EPAC isoform selective small molecules

- Confirm the suitability of a primary HTS through a small pilot screen

- Develop a secondary, in vivo screen for the follow up characterisation of hit compounds, in terms of agonist or antagonist mode of action.

3.2 Results

3.2.1 Expression and Purification of EPAC1-CNB and EPAC2-CNB

Previous studies have shown that the interaction with the CNB of EPAC1 is sufficient to increase the fluorescence intensity of 8-NBD-cAMP. However, interaction of 8-NBD-cAMP with EPAC1 produced significantly lower levels of fluorescence intensity compared to than those brought about through interaction with EPAC2 (Tsalkova et al. 2012). Low fluorescence levels produced by interaction of 8-NBD-cAMP with the EPAC1-CNB may reduce the ability to detect competitor compounds in HTS. Furthermore, the ability of 8-NBD-cAMP to fluoresce when bound to the isolated CNB of EPAC2 has not been previously shown. In order to test this and develop an EPAC1-CNB and EPAC2-CNB-based competition assay it was first necessary to carry out large scale recombinant protein purification of the two CNBs.

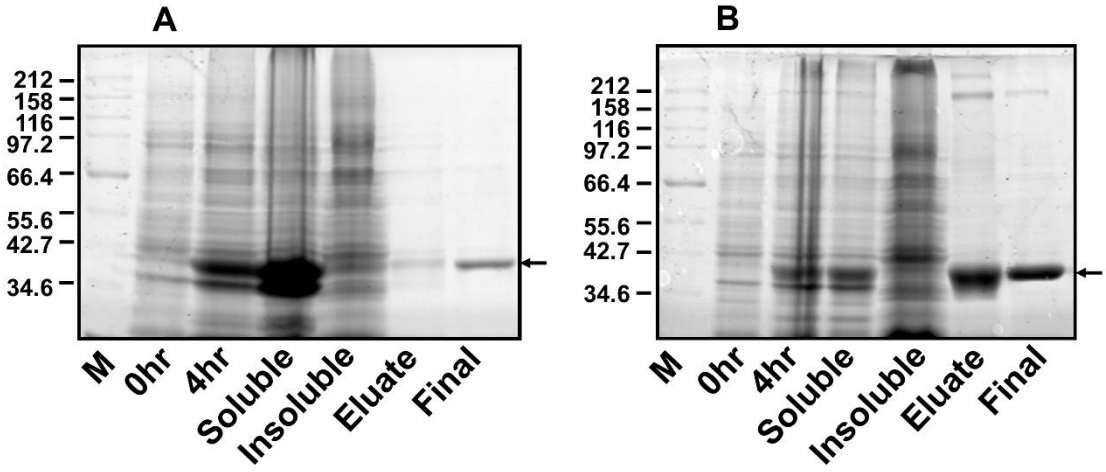

Figure 3-1 : Purification of GST-EPAC1-CNB and GST-EPAC2-CNB.
Protein samples were taken during the purification of GST-EPAC1-CNB (**A**) and GST-EPAC2-CNB (**B**) and loaded onto 12% (w/v) SDS polyacrylamide gels and separated by electrophoresis. Separated protein was visualised on each gel using coomassie blue dye solution, followed by washing with de-stain solution. The molecular weights (kDa) of protein standards are shown (M, unstained protein marker, broad range, 2-212 kDa). Protein expression was induced by incubation of bacterial cultures with 1 mM IPTG. This induced expression of a distinct ~40 kDa protein product after four hours. This is consistent with the production of GST-EPAC1-CNB and GST-EPAC2-CNB. Most of the induce protein was present in the soluble fraction of bacterial extract. Elution with glutathione and subsequent dialysis produced a single, 40 kDa protein product (Final). Arrows indicate induced GST-fusion proteins.

Tagging of EPAC isoforms with glutathione-S-transferase (GST), by subcloning into the pGEX-6p-1 plasmid, has been used extensively to assist the purification of recombinant EPAC proteins (Yarwood 2005; Harper et al. 2007). EPAC1-CNB (amino acids 169-318) and EPAC2-CNB (amino acids 304-453) DNA was amplified from cDNAs encoding full-length EPAC1 and EPAC2, and then ligated into the multiple cloning site of the pGEX-6p-1 plasmid (Yarwood 2005). After transformation of BL-21 *Escherichia Coli* (*E.Coli)*, expression of GST-EPAC-CNB protein was induced by the addition of isopropyl ß-D-1-thiogalactopyranoside (IPTG, 1 mM). This non-hydrolysable lactose analogue stably relieves repression of the lac operon, inducing protein expression from the pGEX-6P-1 vector. Indeed, IPTG treatment was found to induce expression of a strong 40 kDa protein product consistent with GST-EPAC1-CNB or GST-EPAC2-CNB (Figure 3-1). The GST-fusion proteins were found to be stable as the protein was observed within the soluble fraction following lysis and fractionation into soluble and insoluble components. The recombinant proteins were also present after column washing, elution and subsequent dialysis of the final protein sample. The final protein yield was calculated at 0.5 mg (GST-EPAC1-CNB) and 0.8 mg (GST-EPAC2-CNB) per litre of starting culture grown. All protein was subsequently analysed by circular dichroism (CD) to confirm that the ratio of helical and sheet secondary structure matched expected values (data not shown).

3.2.2 Protein Analysis of GST-EPAC1-CNB

EPAC2-CNB has been shown to be amenable to HTS (Tsalkova et al. 2012; Tsalkova et al. 2012). However, the EPAC1-CNB has not yet been employed within HTS. In order to confirm that the GST-EPAC1-CNB is able to bind to cAMP, and other small molecules, recombinant GST-EPAC1-CNB protein was expressed in minimal medium where ammonium sulfate enriched in the heavy nitrogen isotope (^{15}N), was the sole source of nitrogen. As a result, the heavy isotope was incorporated into recombinant GST-EPAC1-CNB, thereby facilitating structural analyses using nuclear magnetic resonance (NMR). Incorporation of ^{15}N with atomic spin into each backbone amide facilitates heteronuclear quantum coherence (HSQC) analyses. This method of NMR analyses yields a single spectral peak for each amino acid in the peptide backbone (barring glutamine and asparagine with side chain amides, which produce doublets, and proline which lacks a backbone amide) the frequency

of which relates to the surrounding chemical environment. The manner in which the amino acid spectral peak position changes due to its environment is referred to as chemical shift, and this can be influenced by local shielding or deshielding events produced by secondary structure, nearby residues, or, pertinent for this study, drug/ligand binding.

For HSQC, ^{15}N-labelled GST-EPAC1-CNB was purified as described above, however, prior to dialysis, the GST tag was cleaved using precision protease to remove the GST-tag. This reduces the number of backbone peaks produced, thereby simplifying spectral analyses. In order to test whether cAMP was able to bind to recombinant EPAC1-CNB, saturating concentrations of cAMP (1 mM) were incubated with ^{15}N-labelled protein. Spectra were then recorded in the presence, or absence, of cAMP. Comparison of apo and cAMP bound NMR spectra indicated that the presence of cAMP induces large chemical shift changes, as observed by the positional changes of key CNB residue spectral peaks (Figure 3-2-A). This indicates that cAMP either binds to, or produces conformational changes in the EPAC1-CNB. Previous triple labelling NMR analyses both in house, and data provided as a gift from Hans Wienk (Harper et al. 2007), allowed each spectral peak to be correlated to its corresponding amino acid, allowing over 70% coverage of the CNB. Interestingly, many of the residues identified as undergoing chemical shift (Figure 3-2-B) have previously been identified as important in cAMP binding and the structural changes which promote the active form of EPAC1 (Harper et al. 2007). This provides strong evidence that cAMP is able to bind to purified, recombinant EPAC1-CNB. In addition, the well dispersed peaks observed within the spectra indicate a well folded protein.

In addition to testing the binding potential of cAMP, it was also possible to ascertain whether the recently identified EPAC2 agonist, tolbutamide (Zhang et al. 2009), was able to interact with and produce chemical shift changes within the EPAC1-CNB. Despite being described as an EPAC2 selective agonist (Herbst et al. 2011), tolbutamide was found to produce large changes in the structure of the EPAC1-CNB (Figure 3-2-A). Indeed, many of the residues undergoing chemical shift changes were shared between tolbutamide and cAMP bound protein, suggesting that tolbutamide may also bind and produce structural changes within the CNB of EPAC1. This provides evidence that the CNB of EPAC1 is able to bind to compounds

with structures varying from that of cAMP, and that the EPAC1-CNB is appropriate for identifying CNB-interacting molecules during HTS.

3.2.3 HTS

The availability of compound libraries combined with the need for targeted therapeutics has necessitated the development of HTS technologies. HTS involves probing a library of chemical compounds within an industrial scale biochemical assay. As most lab-based assays are unsuitable for HTS, novel assay development is required for appropriate screening methods. Importantly, the costs associated with HTS screening necessitates low reagent consumption and high throughput, plate-based screening that is suitable for industrial scale compound library screening (Table 3-1) (Iversen et al. 2004). In addition to the scale required for screening methods, the assay itself must be robust enough to identify active compounds (hits) reliably and reproducibly. This is particularly important considering that most screening platforms assess each compound singly in libraries of up to a hundred thousand compounds (Mayr and Bojanic 2009). As such, prior to HTS, each assay must be characterised in terms of the quality of the assay and its appropriateness for HTS. Furthermore, each descriptor is calculated for every experiment to ensure no sources of error are introduced throughout the screening process.

3.2.3.1 Signal to Background Ratio

The first assay measure that is widely used to assess an HTS assay is the signal to background ratio (S/B, Equation 3-1) (Sittampalam et al. 1997). This parameter describes the assay response in terms of the fold change upon activation/inhibition. In terms of screening, mean signal describes a condition in which the output of the assay is altered maximally (i.e. by a known regulator of the assay system). Mean background describes the signal produced in the absence of stimulation (i.e. the basal, minimal output). Although this measurement is useful in describing the magnitude of the assay response, it does not take into account assay variability, and, as such, cannot reflect assay quality alone.

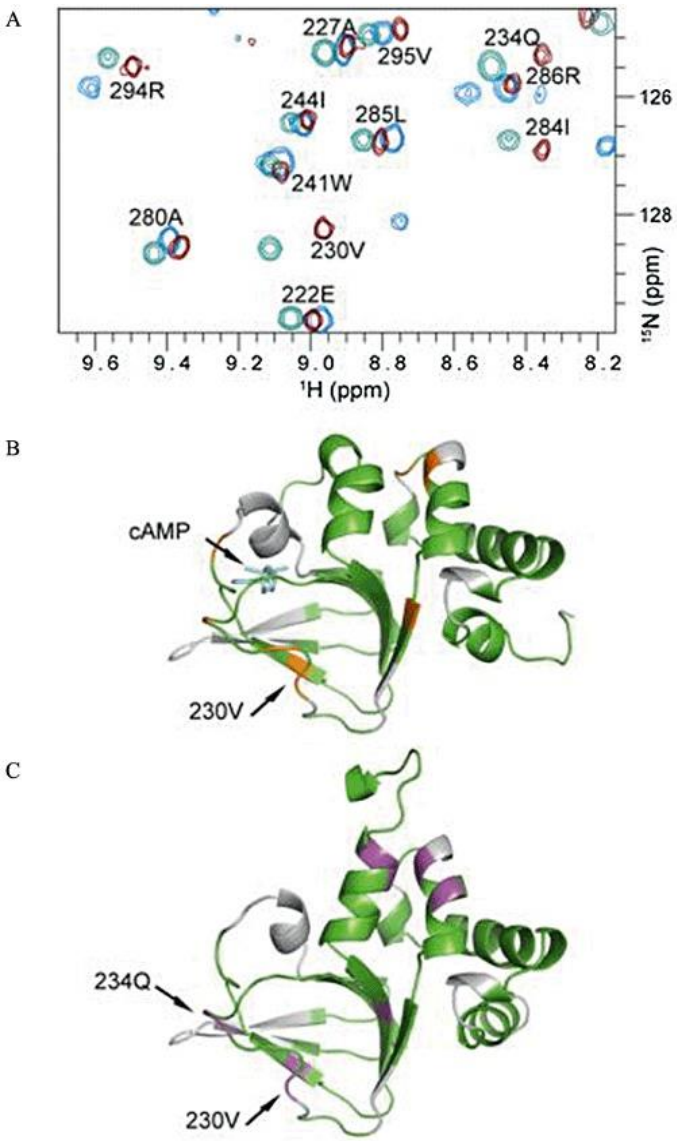

Figure 3-2 : Tolbutamide interacts with EPAC1 and appears to bind to, or produce conformational changes in, several residues important for cyclic AMP binding.
(**A**) A region of the heteronuclear single quantum coherence spectra of EPAC1 cyclic nucleotide binding (CNB) domain (residues 169–318) alone (green), in the presence of 1 mM cyclic AMP (blue) or 2 mM tolbutamide (red). Labelled amino acids undergo a change in chemical shift as a result of cAMP and tolbutamide binding, indicative of direct interaction with the ligand or induced conformational change. (**B**) Homology model of EPAC1 in its open, cAMP bound state (based on PBD file 3CF6). The residues that undergo a significant chemical shift change upon cAMP binding are coloured orange. The locations of valine 230 is indicated, along with cAMP bound in the phosphate binding cassette (**C**) Homology model of EPAC1 in its autoinhibited state (based on PBD file 2BYV). The residues that undergo a significant chemical shift upon tolbutamide binding are coloured magenta. Unassigned residues are coloured grey. The locations of Valine 230 and Glutamine 234 are indicated.

$$S/B = \frac{\mu\, signal}{\mu\, Background}$$

Equation 3-1 : Signal to background ratio (S/B).
The signal to background ration is a useful tool with which to gauge the amplitude of signal change. By dividing the maximum signal (e.g. DMSO diluent control) by the minimum signal (e.g. saturating cAMP concentrations) the magnitude of the fluorescence change can be identified. This is particularly important for assays utilising enzymatic reactions, where signal measurement may be limited to very large changes in substrate concentration. Although changes in fluorescence are very readily measured using plate readers, it is a useful descriptive tool to indicate the dynamic nature of an assay. μ - mean value, S – signal, B – background.

3.2.3.2 Z' Factor

In order to fully characterise the suitability of an assay for HTS, the intrinsic assay variability must be included. Indeed, an assay with large S/B may exhibit large standard deviation not represented by the mean max/min values. In order to accurately identify hits, the variability at both basal and stimulated levels must be incorporated. If the signal and background values overlap due to assay variability it would be difficult to accurately identify hit molecules within a screening program. Thus, the Z factor incorporates the variability associated with the maximum and minimum mean values. For assessing the suitability of an assay for HTS the Z' factor (Equation 3-2) is used (Zhang et al. 1999), which incorporates only the control data, disregarding the values associated with experimental responses. Therefore, only the mean of maximal stimulation (positive control) and basal output (negative control) along with their standard deviations are used to calculate the Z' of an assay, giving a value between negative one and one. A value approaching one describes an assay with large dynamic range coupled with small variability which would facilitate hit identification and a value exceeding 0.6 indicates an assay appropriate for HTS.

$$Z' = 1 - \frac{(3\sigma p + 3\sigma n)}{(\mu p - \mu n)}$$

Equation 3-2 : Z' factor (Z').
The Z' factor of an assay makes use of both the sample standard deviation, which indicates the variability, and the signal change fold change, which indicates the magnitude of the response. By combining these two factors a dimensionless value which represents the ability of the assay to be used in high throughput screening is returned, i.e. the ability of a hit compound to produce a large, reproducible change in signal intensity. The Z' factor utilises the control values from minimum (n, cAMP) and maximum (p, DMSO) control values of an assay. σ – Standard deviation, μ - mean value.

3.2.3.3 Plate variability

In addition to the strength of the assay in reliably identifying hits, it is also necessary to assess signal reproducibility. HTS screening involves plate format biochemical analysis and as such variations across a single plate, or across multiple plates within a single screen are likley to greatly limit the ability to detect hit compounds. It is therefore necessary to test assay reproducability prior to screening. Indeed, a major factor in succesful hit identification is identifying and removing systematic error. As random error affects single wells it has little effect on the assay parameters or hit identification. However, systematic error is often associated with row/column effects, edge effects or reader errors which can result in large variability across large regions of a plate and losses in hit identification. Systematic error can be correlated to time and heat effects, such as evaporation, which is often associated with large variations at the plate periphery. Automation error can result in rows or columns exhibiting variability which produce spikes in data, particularly evident in dose response curves. Finally, reader error is often associated with a gradient effect across the plate as reader positioning errors accumulate laterally. By identifying and reducing the sources systematic error prior to screening, variability can be kept at an acceptable level and hits effectively identified.

$$\%\boldsymbol{CV} = \frac{\boldsymbol{\sigma}}{\boldsymbol{\mu}}\ \boldsymbol{x}\ \mathbf{100}$$

Equation 3-3 : Coefficient of variance (%CV).
The coefficient of variance is the standard deviation of a given response, normalised to the mean signal intensity. %CV is able to give the variability of the signal in relation to the signal strength. For example, a standard deviation of one may be low if the average signal intensity is 100, however it is very high if the average signal intensity is 0.5. These two values would give a %CV of one and 50 respectively, and may indicate that the latter has an unacceptable source of error. $\boldsymbol{\sigma}$ – Standard deviation, $\boldsymbol{\mu}$ - mean value.

Table 3-1 : Summary of assay criteria for high throughput screening.
HTS requires the ability to accurately and reproducibility detect hit compounds. The thresholds which describe a suitable assay are shown below with a description of why the threshold has been set at the given level. %CV – Coefficient of variance, S/B – Signal to background ratio, Z' – Z prime factor.

CRITERIA	THRESHOLD	DESCRIPTION
%CV	<10% intra/interplate	Avoids false or missed hits associated with high plate variability
S/B	≥3	Demonstrates a reasonable change in signal to allow hit identification
Z'	≥0.6	Inherent assay variability is low compared to the change in signal
FORMAT	384 well, homogenous, mix and measure	Must be amenable to high throughput machine analysis
DMSO TOLERANCE	≥1%	Assay must be stable in the presence of compound diluent
ASSAY/REAGENT STABILITY	≥4 hours	Reagents must be stable within time frames associated with HTS

In order to confirm reproducibility, the coefficient of variance (%CV) is employed as a statistical measure of the signal deviation as a product of the average signal intensity (Equation 3-3). In order to demonstrate that identical assay conditions produce similar outputs, the %CV of matching wells within a plate are calculated. A low %CV indicates that each matching condition produces the same signal within the assay, regardless of well position, sample preparation or measurement limitations. As screening occurs over multiple plates, the %CV of matching wells between plates will also be assessed.

3.2.4 Validation of an 8-NBD-cAMP Competition Assay

Of the assays developed for HTS of EPAC modulators, the fluorescence assay based on 8-NBD-cAMP provides a robust high throughput assay for screening full length EPAC2 (Tsalkova et al. 2012). However, the ability of 8-NBD-cAMP to bind and undergo fluorescence change within the isolated EPAC2-CNB has not been assessed. Furthermore, the suitability of EPAC1 and EPAC2 CNBs for 8-NBD-cAMP competition HTS has not been demonstrated. In order to isolate EPAC specific agonists during primary screening, both EPAC1-CNB and EPAC2-CNB must be suitable for HTS.

In order to validate EPAC-CNBs within a competition assay, it was necessary to test the ability of each CNB to bind 8-NBD-cAMP and promote fluorescence. Therefore, to provide proof of principle and to begin validation of an EPAC1-CNB/EPAC2-CNB competition assay, GST, GST-EPAC1-CNB, GST-EPAC2-CNB (0.8 µM) and a “no protein” control were incubated with 8-NBD-cAMP (0.1 µM, Figure 3-3). In agreement with published results, 8-NBD-cAMP fluorescence was significantly greater in the presence of GST-EPAC1-CNB than in the absence of protein (Kraemer et al. 2001). The EPAC2-CNB-GST, similarly to full length protein (Tsalkova et al. 2012), displayed a greater increase in fluorescence compared to EPAC1-CNB (Figure 3-3). Incubation of the fluorescent probe with recombinant GST produced fluorescence values comparable to the no protein control. Therefore, 8-NBD-cAMP fluorescence change occurs as a direct result of interaction with each EPAC-CNB, independently of the GST-tag (Figure 3-3). As such, removal of the GST tag is not required and CNB-GSTs will henceforth be referred to as EPAC1-CNB and EPAC2-CNB only.

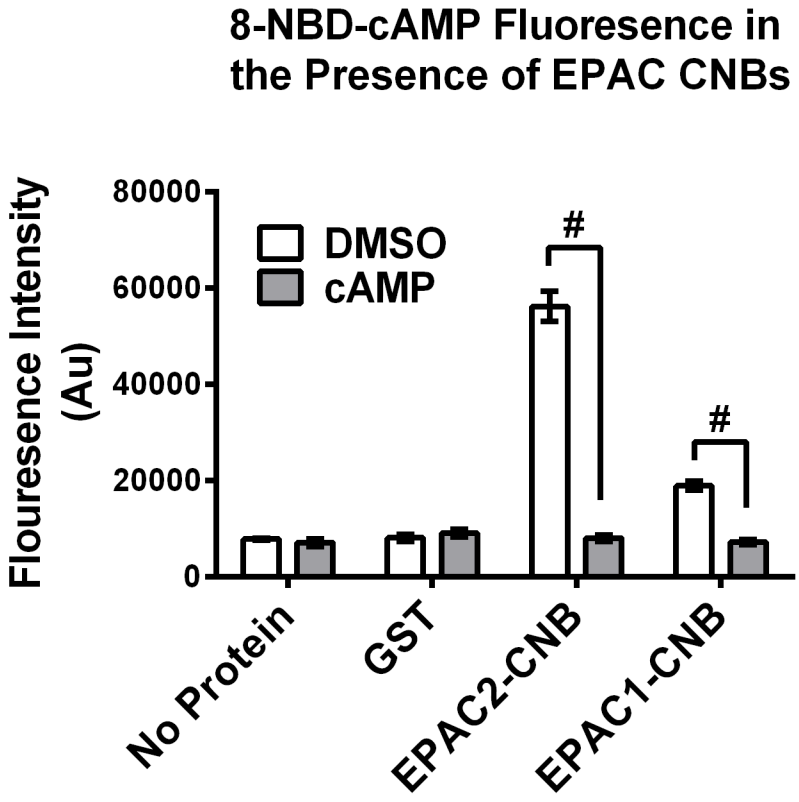

Figure 3-3 : 8-NBD-cAMP fluorescence increases following binding to EPAC-CNBs.
The 8-NBD-cAMP fluorescence assay was carried out in quadruplicate, in black 96 well plates (final volume - 100 µl). Stock solutions for each reagent were prepared as follows; protein stock was prepared as a 3x solution (2.4 µM) in assay buffer. cAMP was prepared as a 150 µM solution (50 mM stock solution in DMSO and was diluted in assay buffer to 150 µM). 8-NBD-cAMP was prepared as a 0.3 µM solution. 33 µl purified protein (GST, EPAC2-CNB or EPAC1-CNB, final concentration - 0.8 µM) or assay buffer (no protein) was incubated with 33 µl cAMP (final concentration - 50 µM) or vehicle control (DMSO, final concentration - 12.8 mM). 8-NBD-cAMP (final concentration - 0.1 µM) was subsequently added to every well (33 µl). Fluorescence intensity was measured after four hours using the Optima Fluostar plate reader (BMG Labtech). # - $P<0.0001$, two way ANOVA using Tukeys post test, n-3.

Next, fluorescence intensity was assessed in the presence and absence of saturating concentrations of cAMP in order to confirm competitive binding. Incubation with cAMP (50 µM) reduced 8-NBD-cAMP fluorescence to levels similar to the no protein control, suggesting maximal inhibition. EPAC2 provoked a 6.94 fold change in 8-NBD-cAMP fluorescence over maximal inhibition; however, EPAC1 provoked only a 2.62 fold increase. Despite the low signal to background ratio of EPAC1-CNB, both EPAC1 and EPAC2 produced robust Z' values of 0.64 and 0.77 respectively. The statistical parameters for each protein are given (Table 3-2). Z' values exceeding the minimum threshold outlined indicate that the isolated CNBs are viable for an 8-NBD-cAMP competition assay. However, optimisation is required to meet the stringent signal to background criterion required for HTS (Table 3-1).

Table 3-2 : Summary of assay statistical parameters.
Parameters obtained from data in Figure 3-3 using the averages and stadard deviations acquired from the minimum and maximum control wells for each protein assayed. GST – Glutathione-S-transferase tag alone, EPAC1-CNB – GST tagged, purified EPAC1 cyclic nucleotide binding domain, EPAC2-CNB - GST tagged, purified EPAC2 cyclic nucleotide binding domain. Min signal – the florescence intensity of 8-NBD-cAMP in the presence of saturating cAMP. Max signal – fluorescence intensity in the absence of competing cAMP. S/B – ratio of maximum signal (DMSO) to signal in the presence of cAMP (50 µM), Z' score as previously described.

PROTEIN	MIN SIGNAL	MAX SIGNAL	S/B	Z'
GST	9134	8136	0.89	-
EPAC1-CNB	7245	18987	2.62	0.63
EPAC2-CNB	8109	56262	6.94	0.77

3.2.5 Assay Development

3.2.5.1 Buffer Optimisation

In order to effectively screen small molecule libraries, a HTS requires the sensitivity to detect sub-maximal fluorescence inhibition associated with low affinity partners. EPAC1-CNB displayed a sub-optimal S/B which in turn resulted in a reduced Z' value. Improving the S/B is likely to improve the assay accuracy and reliability in the detection of hit compounds. In order to produce the maximal signal possible, the buffer components were varied to assess their impact on 8-NBD-cAMP fluorescence in the presence of EPAC1.

In order to achieve optimal S/B, buffer pH and ionic strength were varied within the assay. Indeed both pH and ionic strength are known to affect protein-ligand interactions (Hulme and Trevethick 2010) and optimal conditions may improve sensitivity. Varying sodium chloride concentrations from 10 mM to 150 mM (x-axis) whilst simultaneously altering buffer pH (z-axis) allowed the ideal conditions to be ascertained (Figure 3-4). The highest signal to background ratio was observed at 50 mM sodium chloride, pH 7.8 with a 50% increase in the fluorescence intensity over starting conditions (150 mM, pH 7.5).

3.2.5.2 Probe-Protein Titration

The concentration of both 8-NBD-cAMP (probe) and EPAC1-CNB (protein) within the assay is likely to affect the fluorescence intensities obtained. In order to calculate the optimal concentrations of both protein and probe, the concentration of each were varied simultaneously (Figure 3-5) using optimised buffer conditions of sodium chloride, 50 mM, pH 7.8 (see section 3.2.5.1). The fluorescence signal produced in the presence of protein was normalised to the background intensity to calculate the S/B at each probe/protein concentration. Although S/B values greater than three were observed for many of the conditions, large adjustments in either probe or protein concentration are likely to negatively affect the sensitivity of the assay. Indeed, high protein concentrations combined with limited ligand concentrations can lead to ligand depletion which will limit the identification of low affinity competitors (Hulme and Trevethick 2010). Similarly to protein concentration, an excess of probe increases the concentration of

competitor required to effectively compete within the CNB and may mask low affinity hits within HTS. Accordingly, the minimal protein concentration of EPAC1-CNB (0.08 µM) was selected which meets the required three fold signal to background criterion (Figure 3-5). In addition, a concentration range of 8-NBD-cAMP (0.5 - 0.0625 µM) was identified as suitable for producing signal change. However, further characterisation is required to select the optimal concentration of 8-NBD-cAMP for assay quality and hit detection.

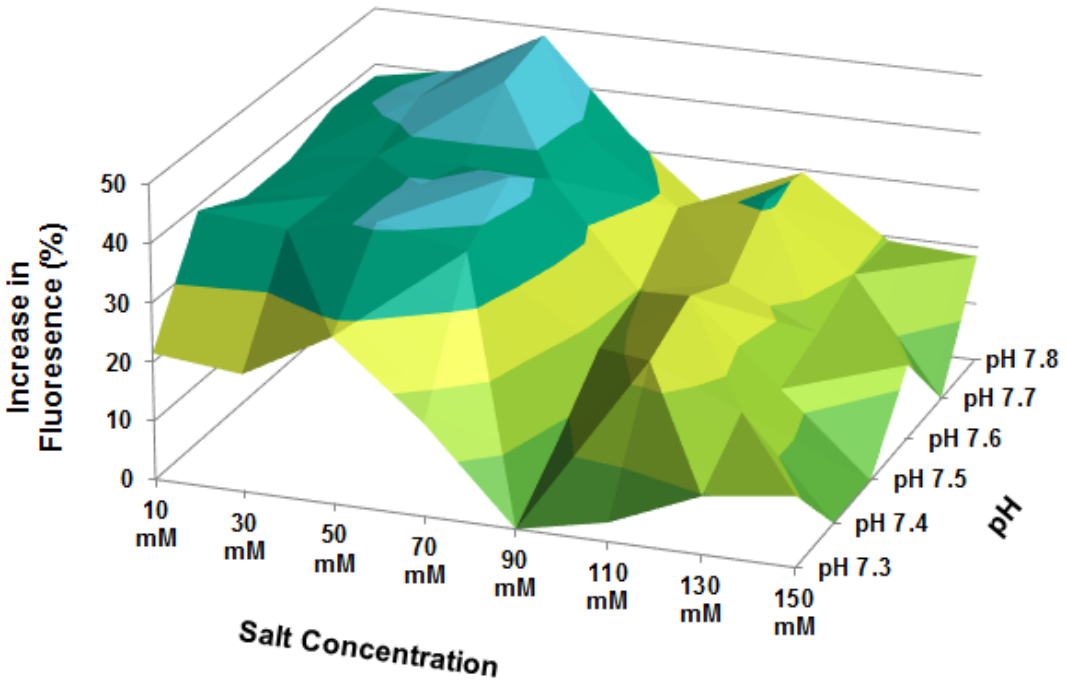

Figure 3-4 : Increase in 8-NBD-cAMP fluorescence under varying salt and pH conditions. The optimal conditions for 8-NBD-cAMP fluorescence was calculated by incubating the fluorescent 8-NBD-cAMP probe (0.1 µM) with EPAC1-CNB (0.8 µM) and altering the salt and pH of the assay buffer to each of the conditions shown. The assay was prepared in black 96 well plates. 2x stock solutions of EPAC1-CNB (1.6 µM) protein and 8-NBD-cAMP (0.2 µM) were prepared in assay buffer of the given salt concentration and pH, and then equal volumes were combined and incubated for four hours (100 µl volume). The fluorescence intensity was recorded and normalised to fluorescence in the absence of protein. Fluorescent intensity is expressed as the percentage increase in signal strength compared to fluorescence intensity under initial buffer conditions (150 mM NaCl, pH 7.5). Shading scale proceeds green to yellow to blue with percentage increase in fluorescence intensity. Conditions given represent quadruplicate wells, n-2.

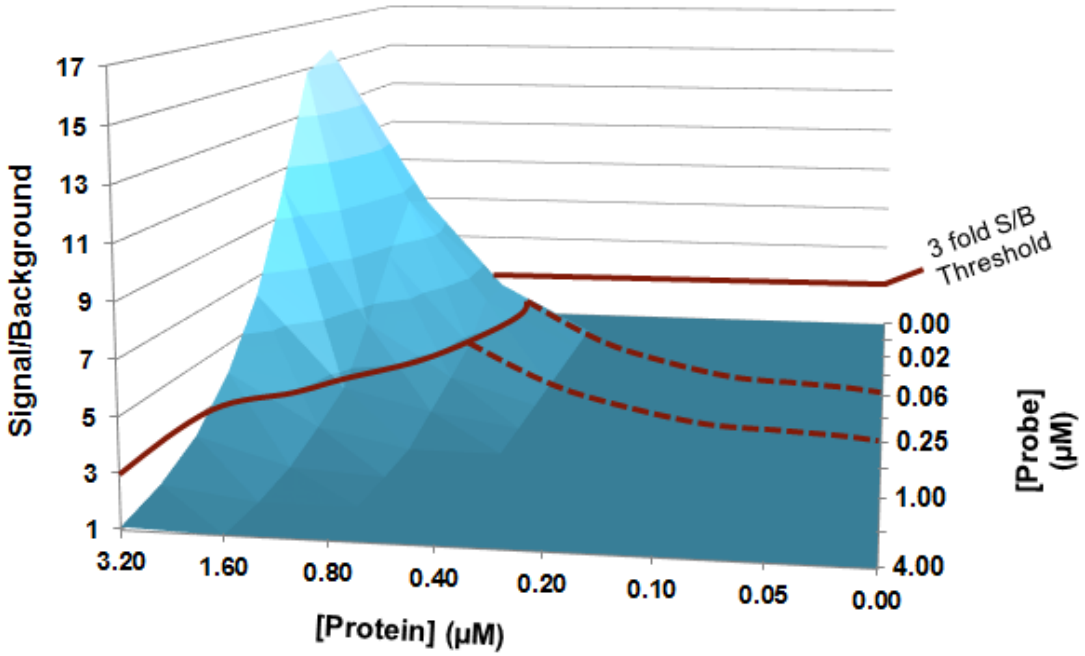

Figure 3-5 : The effect of varying probe/protein concentration on the S/B ratio.
The S/B ratio was calculated using optimised buffer conditions (50 mM Tris, pH 7.8, 10 mM NaCl, 1 mM EDTA, 1 mM DTT,) under the varying concentrations of EPAC1-CNB and 8-NBD-cAMP given. EPAC1-CNB-GST was prepared as a 12.8 µM stock solution and 200 µl was seeded into the top row of a black 96 well plate. 100 µl assay buffer was seeded into all wells of a plate and the Biomek automated pipetting station was used to transfer 100 µl from the first row into the second. This was mixed and then 100 µl was transferred from row two into row three, producing a serial dilution. This was repeated until a final concentration of 0.01 µM was achieved. In a separate 96 well plate an 8-NBD-cAMP stock solution (8 µM) was added to the first column (100 µl), and 100 µl buffer was added to all wells. Again a serial dilution was performed by transferring 100 µl of buffer from column to column sequentially. For both protein and probe the final row/column was not altered in order to give a background reading. These two stock plates were used to seed a final, black, 384 well, low volume assay plate with equal volumes (15 µl) of protein and probe, in quadruplicate. Fluorescence intensity was recorded after four hours, and the S/B ratio was calculated by normalising the signal at each concentration to the background signal (no probe/protein). The dotted line indicates the desired three fold S/B threshold. Shading scale proceeds dark blue to light blue as S/B ratio increases. The three fold signal to background ratio required is shown by a solid red line. The minimal protein concentration (0.8 µM) and probe concentration (0.6 µM – 0.25 µM) at which the three fold signal to background ratio is indicated by a dashed red line. S/B – Signal to background, probe – 8-NBD-cAMP, protein – GST-EPAC1-CNB.

3.2.5.3 Optimal Probe concentration

In order to determine the 8-NBD-cAMP concentration with maximal sensitivity for low affinity compounds, two concentrations of probe were assessed for their ability to respond to competition with reference compounds. Both 8-(4- Chlorophenylthio)-cAMP (8-CPT) and 8-pCPT-2'-0-Me-cAMP (007) bind to EPAC1 within the CNB with known affinities relatable to the IC_{50} values obtained within the competition assay (Table 3-3). Indeed, titration of these reference molecules

with EPAC1-CNB displayed competition with the fluorescent probe for the cAMP binding site (Figure 3-6). Furthermore, the degree of fluorescence inhibition was consistent with their affinities for EPAC. As expected, the high affinity cAMP analogue, 8-CPT, is able to inhibit fluorescence at lower concentrations than 007. Although 8-CPT binding at both concentrations of 8-NBD-cAMP produces a linear decrease in IC_{50}, the ability to accurately describe 007 competition is limited at high probe concentrations. This suggests that although the S/B intensity is greater at higher probe concentrations, the ability to detect low affinity binding partners is greatly reduced. This effect would likely lead to numerous compounds being overlooked during HTS despite an improvement in signal to background. The probe concentration of 0.0625 µM was identified as the lowest value able to produce above-threshold S/B whilst maintaining sensitivity to low affinity compounds.

The inhibitory profiles of cAMP, 007 and 8-CPT reveal that the conditions identified allow the identification of competitor compounds with a range of affinities (Figure 3-7). The resulting IC_{50} of cAMP and 007 are linear, in terms of their published dissociation constants (Dao et al. 2006). However, although it is possible to produce inhibition in the presence of 8-CPT-cAMP, the IC_{50} produced does not correlate to the hundred fold greater affinity over cAMP reported (Dao et al. 2006). This suggests that the inhibitory effect of high affinity compounds and further structure activity relationship (SAR) characterisation may be limited within this assay. However despite these limitations, this assay displays excellent detection of competitive compounds.

Table 3-3 : IC_{50} values of reference compounds under varying probe concentrations.
The IC_{50} values of 8-CPT-O'-2-Me-cAMP (007) and 8-CPT-cAMP (8-CPT) obtained from Figure 3-6 are shown alongside published affinities (Dao et al. 2006).

COMPOUND	0.5 µM PROBE IC_{50} (µM)	0.0625 µM PROBE IC_{50} (µM)	PUBLISHED K_D (µM)
007	5.88	1.68	0.63
8-CPT	3.563	0.5335	0.04

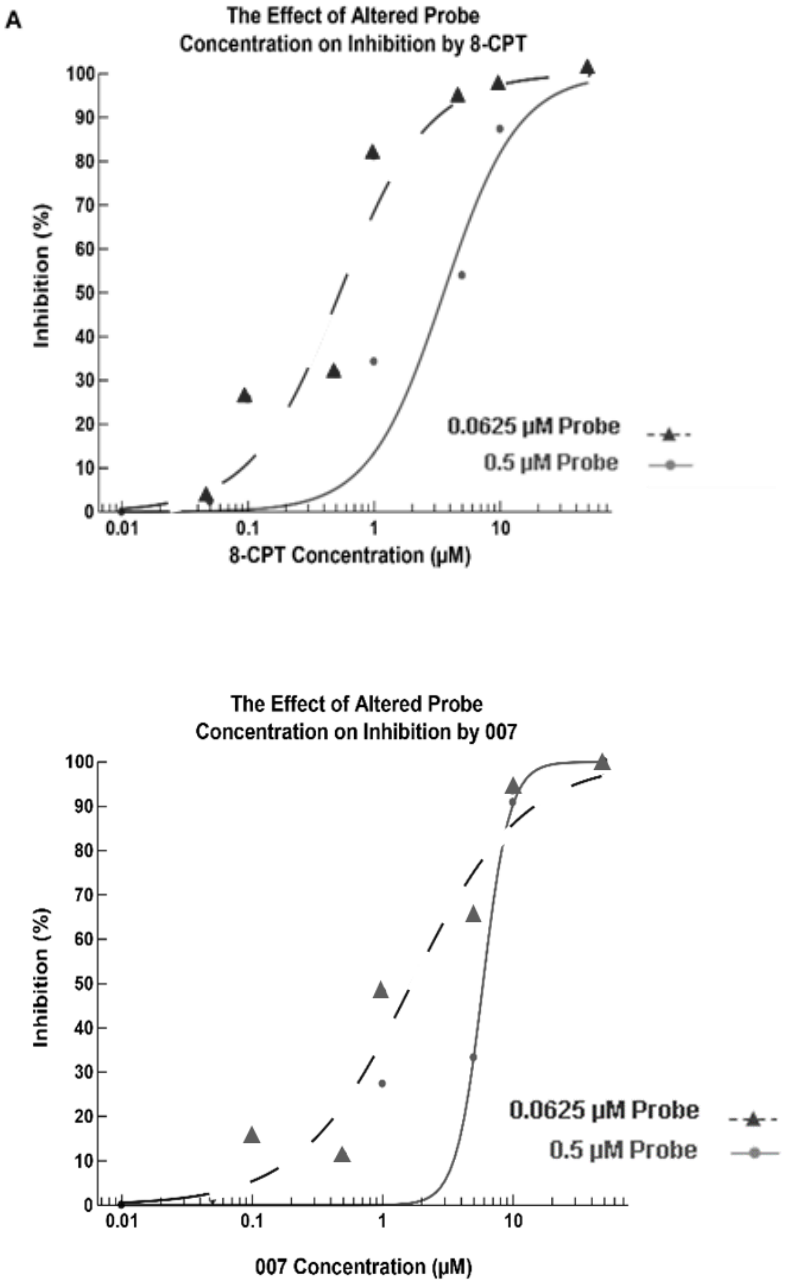

Figure 3-6 : The effects of varied probe concentration on reference molecule inhibition. Titrations of two reference molecules known to interact with the CNB of EPAC1 with different affinities were performed using the Biomek automated laboratory. The titration was carried out in the presence of the probe concentrations found to produce maximal signal to noise ratio, namely 0.0625 µM (dashed line with data points shown as circles) or 0.5 µM 8-NBD-cAMP (solid line with data points shown as triangles) at 0.8 µM EPAC1-CNB. Reagents were prepared as three fold stock solutions in 96 well plates which were then combined in a black, 384 well, low volume assay plate (final volume 30 µl) alongside wells containing only 8-NBD-cAMP and reference compounds as a background control (no EPAC1-CNB). EPAC1-CNB (0.8 µM), reference compounds and probe were incubated for four hours before fluorescence intensity was measured. Data are displayed as percentage inhibition calculated from max signal (DMSO vehicle control, 70 mM) and min signal (no protein). **A -** The ability of 8-CPT-cAMP (8-CPT) to compete with 8-NBD-cAMP for EPAC1-CNB binding and inhibit fluorescence is shown. **B** – The ability of 8-CPT-O'-2-Me-cAMP (007) to compete with 8-NBD-cAMP for EPAC1-CNB binding and inhibit fluorescence is shown. Curve fits and graphs plotted using XLFit (XLfit Software). Samples were recorded in quadruplicate, n-1.

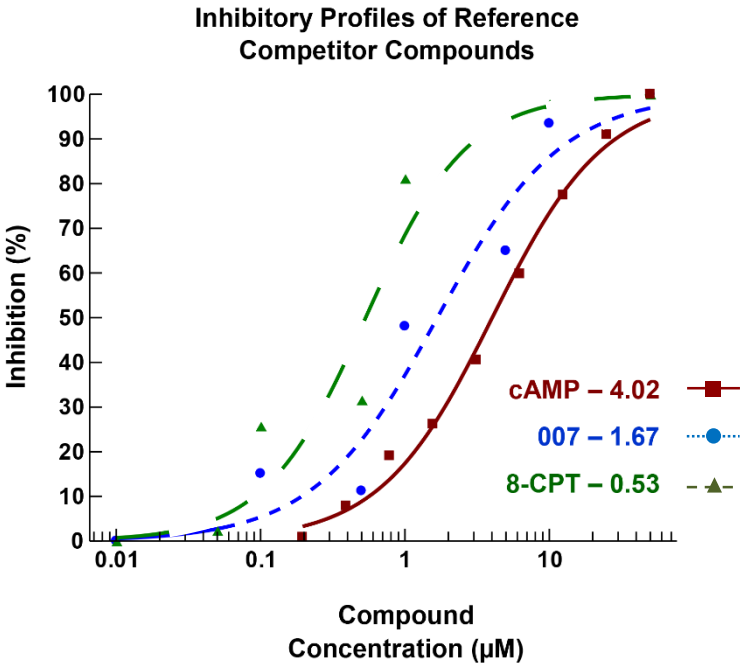

Figure 3-7 : The inhibitory profiles of reference competitor compounds.
Titration of three reference compounds were prepared. EPAC1-CNB (0.8 µM) was incubated with cAMP (solid line, points marked by squares), 007 (dotted line, points marked by circles) or 8-CPT (dashed line, points marked by triangles) in the presence of 0.0625 µM 8-NBD-cAMP. 3x stock solutions were prepared for reagents, which were then combined and incubated four hours in a black, low volume, 384 well assay plate before recording fluorescence intensity. Percentage inhibition was calculated as the drop in 8-NBD-cAMP fluorescence produced by incubation with each concentration of reference compounds compared to a DMSO (12.8 mM) vehicle control. IC_{50} values of each compound are given (µM). Curve fits and graphs plotted using XLFit (XLfit Software). Samples recorded in quadruplicate, n-1.

3.2.5.4 Optimal Incubation Time

HTS is typically performed in large batches and, as such, significant turnover times occur during the screening process. In order to confirm that both protein and probe are stable within the time frames associated with HTS, fluorescence intensity was measured over time. Under these conditions the assay was found to display excellent stability, with no significant decrease in fluorescence up to 72 hours after initialising the reaction (Figure 3-8). Although initial fluorescence was variable, the assay signal was observed to stabilise after 60 minutes and remain constant and reproducible up to four hours (Figure 3-8). Therefore a minimum incubation period of four hours was utilised to ensure maximal reproducibility between wells. However, the assay displayed excellent stability up to 72 hours and turnover times are likely to be well tolerated during the screening process.

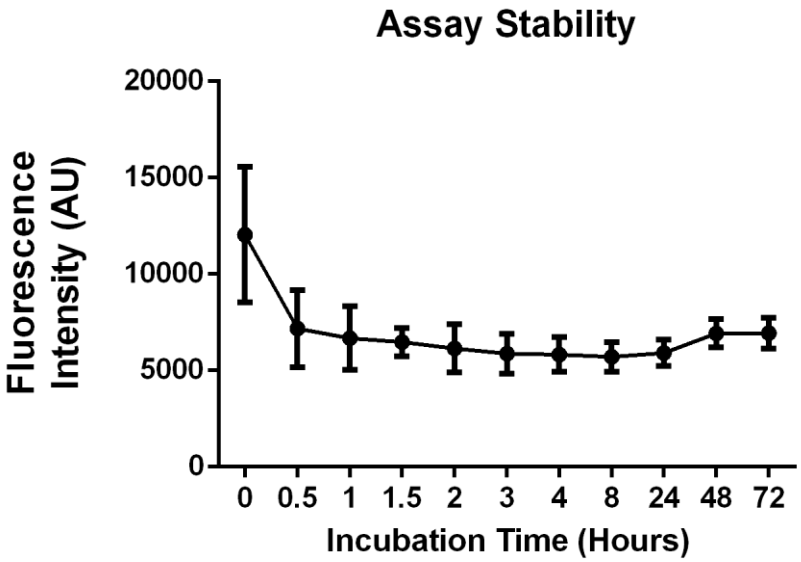

Figure 3-8 : Assessing optimal assay incubation time.
8-NBD-cAMP (0.0625 µM) and EPAC1-CNB (0.8 µM) were prepared as 2x stock concentrations and equal volumes were combined in black, low volume, 384 well assay plates in quadruplicate (final volume 30 µl). Fluorescent intensity was recorded hourly over a 72 hour period and is presented at the various time points here (Mean +/- SEM of four wells, n-1).

3.2.6 EPAC1-CNB Competition Assay Evaluation

3.2.6.1 DMSO Tolerance

Compounds in large chemical libraries are often dissolved in the diluent dimethylsulfoxide (DMSO). As such, any assay developed for HTS requires a DMSO tolerance of up to one per cent final DMSO concentration. In order to ensure the presence of DMSO does not affect 8-NBD-cAMP fluorescence intensity, the competition assay was carried out in the presence of increasing concentrations of DMSO and fluorescence was measured at each DMSO concentration (Figure 3-9). 8-NBD-cAMP displayed a trend of signal loss with increasing DMSO concentration. However, the signal was well tolerated at concentrations under one percent in line with the required parameters (Table 3-1). Furthermore, novel compound seeding technologies, such as acoustic liquid handling (Ellson et al. 2003), allow very low final DMSO concentrations. Indeed, the use of nanolitre dispensing techniques (Echo® Liquid Handler) ensures the final concentration of DMSO is well below one per cent.

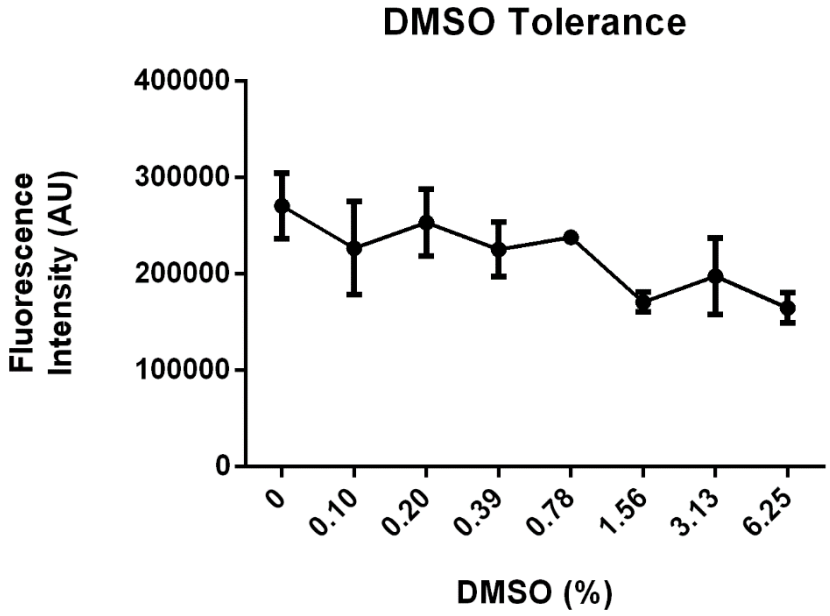

Figure 3-9 : Effect of DMSO on 8-NBD-cAMP flourescence.
8-NBD-cAMP (0.0625 µM) and EPAC1-CNB (0.8 µM) were prepared as 3x stock solutions and combined in the presence of increasing concentrations of DMSO, in black, low volume, 384 well assay plates. DMSO was prepared as a 3x stock solution of the final percentage (v/v) concentration and incubated for four hours. The effect of DMSO on fluorescence intensity was observed. Data are presented as the average of quadruplicate values (+/- SEM, n-1).

3.2.6.2 Intraplate Variability

In order to accurately identify hit compounds, it is necessary for there to be a high level of reproducibility within a single assay plate. Indeed, significant intra-plate variability can result from measurement error, inaccurate well seeding or differential temperature effects across a plate all of which can seriously limit the success of HTS (Iversen et al. 2004). The signal reproducibility within each 384 well assay plate was tested by two means. The first was calculated from the the maximum (DMSO vector control) and minimum (cAMP, 50 µM) signals obtained from distinct quadrants within the same plate (Table 3-4). In addition, cAMP titrations within the top left and bottom right quadrants of a 384 well plate were used to ensure that intermediate values within an inhibitory curve were not affected by their position within an individual plate. The results obtained demonstrated that there was no large difference in fluorescence intensity observed at different locations within a single plate (Figure 3-10).

Table 3-4: Intraplate variability across quadrants.
8-NBD-cAMP (0.0625 µM) and EPAC1-CNB (0.8 µM) were prepared as 3x stock solutions and combined in black, low volume, 384 well assay plates. Wells A1-H12 (Max 1) and I13-P24 (Max 2) were seeded with DMSO (vehicle control, 12.8 mM) to produce the maximal assay signal. Wells A13-H24 (Min 1) and I1-P12 (Min 2) were seeded with cAMP (50 µM) to compete with 8-NBD-cAMP binding to EPAC1-CNB and produce the minimal fluorescence signal. Plates were incubated four hours before measuring fluorescent intensities. The mean and standard deviation (StDev) of fluorescence intensity was calculated for each quadrant (Quadrant) and for all matching conditions within the plate (intraplate). From these parameters the coefficient of variance (%CV) was calculated.

QUADRANT	MEAN	STDEV	%CV	INTRAPLATE	MEAN	STDEV	%CV
MAX 1	203940	12608	6.2	Max 1 vs Max 2	206804	4051	1.9
MAX 2	209669	16884	8.1				
MIN 1	43206	4345	10.1	Min 1 vs Min 2	42949	363	0.9
MIN 2	42693	2918	6.8				

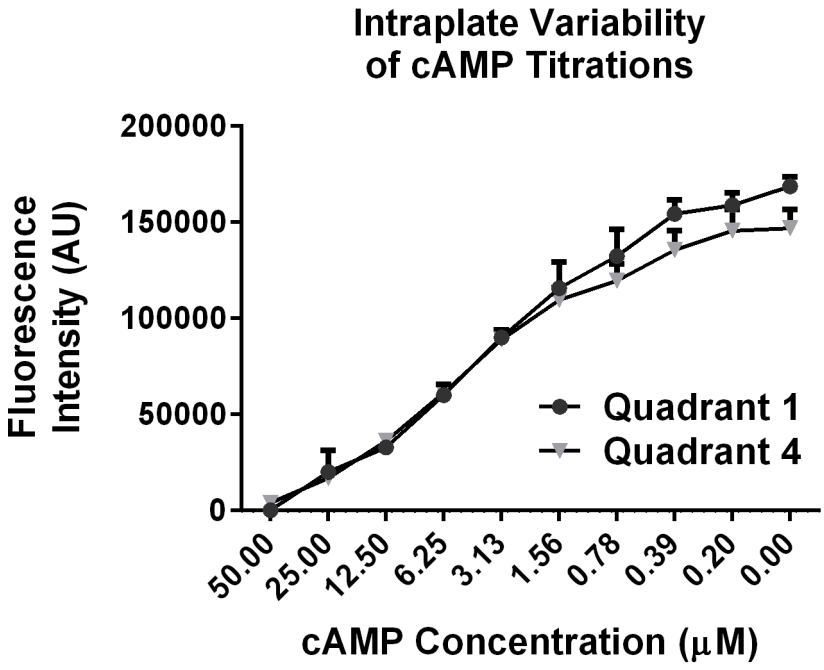

Figure 3-10 : Intraplate variability of intermediate fluorescence values.
3x stock solutions of each cAMP concentration were obtained by serial dilution of a 150 µM stock (in assay buffer), with DMSO concentration maintained throughout (12.8 mM). EPAC1-CNB (0.8 µM), 8-NBD-cAMP (0.0625 µM) and cAMP (at given concentrations) in quadruplicate (final volume 30 µl) were incubated in black, low volume, 384 well assay plates. Varying cAMP concentrations were seeded into wells A4/D4-A14/D14 (Quadrant 1) and wells M14/P14-M24/P24 (Quadrant 4) in order to compare the fluorescent intensity at various positions within the plate at varying levels of 8-NBD-cAMP fluorescence. Quadruplicate fluorescence intensity values were measured after a four hour incubation and plotted against cAMP concentration (mean +/-StDev, n-1).

3.2.6.3 Plate to Plate Variability

In addition to intraplate homogeneity, the signal variation between plates must be low as hit identification will be based on data obtained from multiple plates. In order to ensure that the fluorescent signal is accurate between plates, reproducibility was assessed in a manner similar to that for intraplate variability. The variability between each quadrant of two separate plates (Table 3-5), alongside the intermediate values within a dose response curve (Figure 3-11) were assessed. The variability between plates was shown to be remarkably low for both the maximum, minimum and intermediate values tested.

Table 3-5 : Interplate variability across quadrants.
8-NBD-cAMP (0.0625 µM) and EPAC1-CNB (0.8 µM) were prepared as 3x stock solutions and combined in black, low volume, 384 well assay plate wells. Wells A1-H12 (Max 1) and I13-P24 (Max 2) were seeded with DMSO (vehicle control, 12.8 mM) to produce the maximal assay signal. Wells A13-H24 (Min 1) and I1-P12 (Min 2) were seeded with cAMP (50 µM) to compete with 8-NBD-cAMP binding to EPAC1-CNB and produce the minimal fluorescence signal. Plates were incubated four hours before measuring fluorescent intensities. The mean and standard deviation (StDev) were calculated and the intraplate variation between quadrants within each plate is shown (Intraplate). The variation between maximum and minimum signals between plates is shown (Interplate). From these parameters the Coefficient of Variance (%CV) was calculated.

INTRAPLATE	MEAN	STDEV	%CV	INTERPLATE	MEAN	STDEV	%CV
MAX (PLATE 1)	199791	5866	2.9	**Plate 1 vs Plate 2**	199492	424	0.2
MAX (PLATE 2)	199192	14817	7.4				
MIN (PLATE 1)	43704	703	1.6	**Plate 2 vs Plate 2**	43200	713	1.7
MIN (PLATE 2)	42696	4	0.1				

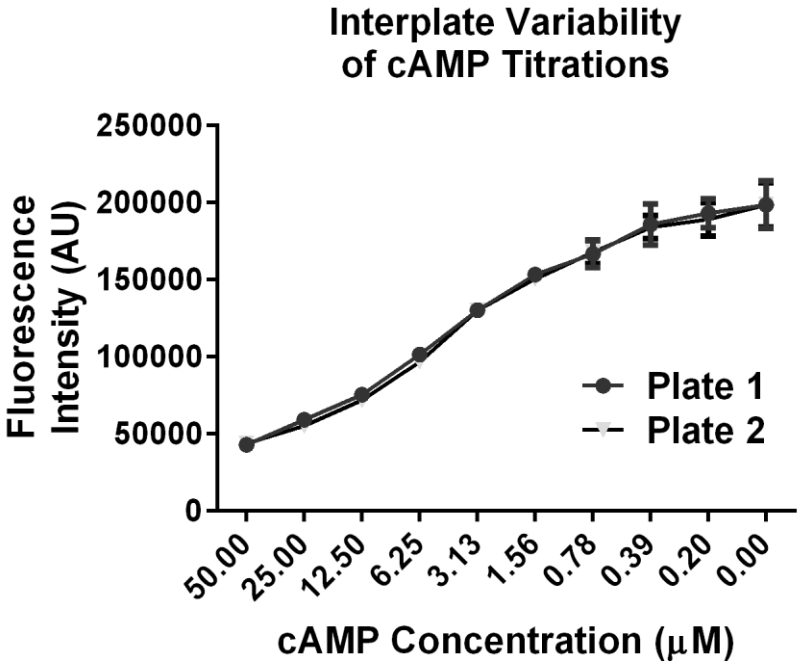

Figure 3-11 : Interplate variability of intermediate fluorescence values.
3x stock solutions of each cAMP concentration were obtained by serial dilution of a 150 µM stock (in assay buffer), with DMSO concentration maintained throughout (12.8 mM). Black, low volume, 384 well assay plates were seeded with EPAC1-CNB (0.8 µM), 8-NBD-cAMP (0.0625 µM) and cAMP (at given concentrations) in quadruplicate (final volume 30 µl). Varying concentrations of cAMP were seeded into wells A4/D4-A14/D14 (Quadrant 1) and wells M14/P14-M24/P24 (Quadrant 4) of two different plates in order to compare the fluorescent intensity at various positions within multiple plates at varying levels of 8-NBD-cAMP fluorescence. Quadruplicate fluorescence intensity values were measured after a four hour incubation and plotted against cAMP concentration (mean +/-StDev, n-1).

Table 3-6 : Summary of EPAC1-CNB competition assay statistical parameters.
The parameters recorded for the EPAC1-CNB competition assay after optimisation are summarised alongside the required thresholds for efficient high throughput screening. %CV – coefficient of variance, S/B – signal to background ratio, Z' – Z primer factor.

CRITERIA	THRESHOLD	EPAC1-CNB PARAMETERS
%CV	<20% intra/interplate	Max 1.9% / 1.8%
S/B	≥3	4.8
Z'	≥0.6	0.66
FORMAT	384 well, homogenous, mix and measure	Performed in 384 plate, no wash steps, single assay step
DMSO TOLERANCE	≥1%	1% tolerated
ASSAY/REAGENT STABILITY	≥4 hours	Up to 72 hours

3.2.7 EPAC1-CNB Competition Assay Validation

In order to validate the EPAC1-CNB based competition assay for HTS, a pilot screen was performed using the final conditions characterised (assay buffer – 50 mM Tris-HCl, pH 7.8, 10 mM NaCl, 1 mM EDTA, 1 mM DTT; minimum incubation time – four hours; 8-NBD-cAMP concentration – 0.0625 µM; protein concentration – 0.8 µM). Two commercially available compound libraries of bioactive molecules were screened; the National Institute of Health (NIH) Clinical Collection Library (NCC) and the Selleckchem FDA approved drug library (L1300). Each library contains US FDA approved bioactive molecules with drug-like structures and known safety profiles.

Both EPAC1-CNB and EPAC2-CNB were used to screen the NCC and L1300 compound libraries. The statistical parameters from these screens are given and suggest assay optimisation dramatically improved the power of the assay (Table 3-7). For example, the revised signal to background value for EPAC1-CNB was almost double the pre-optimised value (Table 3-2, 1.83 fold increase). Both EPAC1-CNB and EPAC2-CNB based HTS assays identified numerous hits able to inhibit 8-NBD-cAMP fluorescence below the significance threshold. The inhibitory cut-off for each protein was calculated using robust statistics (three scaled median absolute deviations (sMAD) from the median inhibitory effect) (Asli 2013). As a result of screening, 11 hit compounds were identified for both EPAC1-CNB and EPAC2-CNB.

$$\boldsymbol{sMAD = K\ x\ (median\sqrt{(X_i - \ median(X_j)^2})}$$

Equation 3-4 : Scaled median absolute deviation.
The scaled median absolute deviation (sMAD) is a useful method to reduce the effects of outliers in large data sets. The median absolute deviation calculates the median value of the absolute deviations ($\sqrt{deviation\ from\ median^2}$) of each value within the data set (X_i) from the data set median (X_j). The absolute value of the deviations simply negates negative values and returns the difference from the median value (deviation) as a positive integer (for example the absolute of -4 is 4). The MAD is preferred for large data sets as the standard deviation weights large outliers very strongly by squaring the deviation from the mean. Robust statistics using the median value reduces these effects. However, a data set with a normal distribution (lacking large outliers) produces a median absolute deviation smaller than the standard deviation, producing bias. The constant ($\boldsymbol{K}$), representing the relationship between the MAD and standard deviation within a normal distribution, is employed to remove this bias. $\boldsymbol{K}$ – 1.4826

Table 3-7 : Statistical parameters of pilot screen.
The signal to background ration (S/B) and Z' values were calculated from the maximum and minimum signal controls from the EPAC1-CNB and EPAC2-CNB pilot screen data. The hit rate is calculated as the percentage of compounds above the cut-off threshold (median inhibitory effect + 3* scaled median average deviation) from the entire screen.

	EPAC1-CNB	EPAC2-CNB
S/B	4.82	9.85
Z'	0.79	0.75
HIT RATE	0.69%	0.69%

3.2.8 Hit Confirmation

Of the 22 hits returned, a total of 15 isoform selective compounds were identified. Indeed, seven compounds competed with 8-NBD-cAMP for binding to both EPAC1-CNB and EPAC2-CNB. Hits were further validated by identifying the IC_{50} values and the specificity of each compound for EPAC1-CNB or EPAC2-CNB (Table 3-8). This was achieved by serial dilution of each hit compound from a maximum concentration of 30 µM. In addition to isolating several compounds able to compete within the CNB of EPAC1 and EPAC2, compounds exhibiting specificity for either EPAC1 or EPAC2 were observed (Table 3-8). Indeed, one compound was observed to specifically target EPAC1-CNB; conjugated oestrogen. Although the observed IC_{50} for this compound was low (16 µM) the specificity over EPAC2-CNB suggests it may be suitable for development as an EPAC1 selective agonist. Conversely, multiple compounds were observed to compete for EPAC2-CNB binding specifically; e.g. tamoxifen and dronedarone. As such, the benefits of screening both EPAC1-CNB and EPAC2-CNB simultaneously have been demonstrated.

Table 3-8 : Validated hits identified in a pilot screen.
Compounds identified in the pilot screen were validated by titration of each compound into the assay against EPAC1-CNB and EPAC2-CNB. IC_{50} values were calculated for both EPAC1-CNB and EPAC2-CNB (IC_{50}). Where the IC_{50} value was greater than the highest compound concentration tested the maximum inhibitory effect at 30 µM is given (%Inhibition). In addition the hill slope, which can inform on the mechanism of inhibition, is given for each compound (Hill slope).

Hit		EPAC1			EPAC2		
Name	ID	IC_{50}	%Inhibition	Hill slope	IC_{50}	%Inhibition	Hill slope
HEXACHLOROPHINE	SAM002554903	5		2.2	6.3		2.2
THYROXINE	SAM002264651	>30	30	2.3	20		3.2
RALOXIFENE	SAM002548975	>30	38	2.5	20		0.8
HMS3259A19	SAM002554902	>30	34	2.5	>30	21	3.4
5-NONYLOXYTRYPTAMINE	SAM001247103	>30	13	1.9	12.6		2.8
OESTROGENS, CONJUGATED	SAM001246904	25		2.0	>30	16	1.9
AMIODARONE	SAM001246646	>30	4	3.5	15.8		2.3
SGI-1776	s1776	>30	16	2.4	20		1.7
CRYSTAL VIOLET	s1917	>30	23	1.5	12.6		2.4
MOMETASONE FUROATE	s1987	>30	1	0.8	>30	1	3.7
TAMOXIFEN CITRATE	s1972	>30	5	0.2	15.8		1.8
DRONEDARONE-HCL	s2114	>30	7	3.8	12.6		1.3
OLSALAZINE	S4041	>30	17	1.3	20		0.8

3.2.9 Characterisation of a Cell Based Screen for EPAC1 Agonists

The EPAC1-CNB competition assay, although effective at identifying compounds that interact with the cAMP-binding pocket, is unable to discriminate between potential agonist or antagonist properties of the isolated compounds. Give that EPAC1 agonists have the potential as novel therapeutics for the treatment of a range of disorders, as described above, it is therefore necessary to confirm that hits identified via HTS are able to effectively activate EPAC1. Indeed, many cAMP analogues have been observed to bind EPAC but not induce GEF activity (Kraemer et al. 2001). In order to confirm EPAC1 agonism, a secondary screen is required to confirm binding and activation of full length EPAC. Recently, EPAC1 activation has been linked to rapid changes in cell morphology (Ross et al. 2011). In particular cells were observed to undergo cell spreading; a uniform extension of the cell periphery. These effects were directly attributed to EPAC1, independently of conventional cell adhesion pathways (Ross et al. 2012). Therefore cell spreading may represent a cell based assay to report EPAC1 activation *in vivo*.

3.2.9.1 EPAC1 is required for cAMP induced morphological change

To test whether EPAC1 activation is sufficient to promote cell spreading in response to elevations in intracellular cAMP, the EPAC-null human embryonic kidney (HEK293T) cell line was stably transfected to express FLAG-tagged EPAC1 or an empty vector construct (Figure 3-12-A). To assess the ability of transfected EPAC1 to control cell spreading, EPAC1 signalling was activated by the addition of a combination of forskolin and rolipram (F/R, 10 μM) to elevate cAMP levels by simultaneously activating AC and inhibiting PDEs. In addition, the EPAC-selective agonist, 007 (10 μM), was used to directly activate transfected EPAC1. After 60 minute treatment cells were fixed and cell area determined (Figure 3-12). The results obtained established that cells transfected with an empty vector were completely non-responsive to the applied treatments in terms of cell spreading (Figure 3-12). In contrast, cells transfected with EPAC1 demonstrated a marked increase in cell area following treatment with either F/R or 007 (Figure 3-12). This confirms that cell spreading in response to increases in intracellular cAMP is dependent on EPAC1 expression in this cell line.

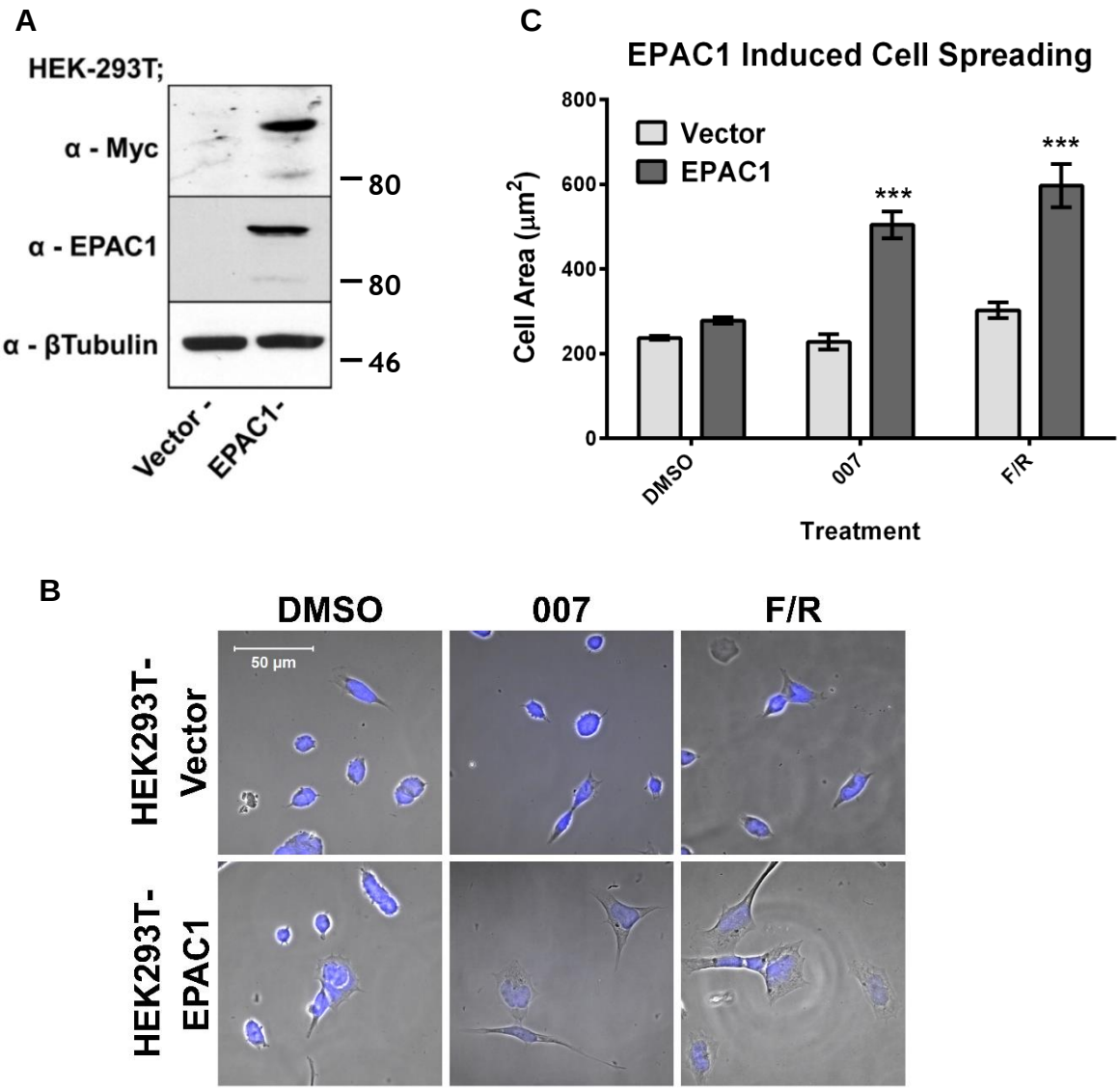

Figure 3-12 : Cell spreading is dependent on EPAC1 expression in HEK293T.
A; HEK293T cells were stably transfected with vector or Myc-EPAC1-FLAG construct. Cell extracts were western blotted with anti-EPAC1, anti-Myc or anti-β-Tubulin antibodies as indicated. **B;** Vector- and EPAC1-expressing HEK293T cells were incubated for 60 minutes with a DMSO vehicle control (final concentration 12.8 mM), 10 μM 007 or 10 μM forskolin and 10 μM rolipram (F/R). Cells were fixed and immunostained with anti-EPAC1 antibodies to confirm EPAC1 expression (not shown). Representative transmission images with DAPI stained nuclei (blue) are shown. **C**; HEK293T-vector and HEK293T-EPAC1 cell spreading was assessed using ImageJ analysis software to measure cell area (mean +/- s.e.m.). Data were collected from 10 randomly acquired images per experiment. Significant difference of 007 and F/R stimulated HEK293T-EPAC1 to DMSO stimulated HEK293T-EPAC1 is indicated; ** - p <0.01 and *** - P<0.001, two way ANOVA using Dunnets post test, n-3.

3.2.10 Cell Spreading is a Specific Response to EPAC1 activation in HEK293T cells

Cell morphological change can be induced through a range of signalling pathways. In order to ensure that HEK293T-EPAC1 cell spreading is a feature of EPAC1 signalling, a range of related signalling pathways were tested for their ability to induce cell spreading independently of EPAC1 activation. Indeed, a number of signalling pathways are known to regulate cell morphology and may produce a spread phenotype independent of EPAC1 activation, and as such, may produce false positives in a cell based EPAC1 activation assay.

3.2.10.1 Phosphatidyl-Inositol-3 Kinase

EPAC1 has been shown to activate phosphatidyl-inositol-3 kinase (PI3K) and regulate proteins directly implicated in cytoskeletal reorganisation and cell adhesion (Cass et al. 1999; Tang et al. 2012). Regulation of the cell cytoskeleton suggests a possible mechanism for EPAC1 mediated cell spreading, through PI3K in HEK293T cells. To test the role of PI3K signalling in the control of HEK293T-EPAC1 cell spreading, cells were incubated with the selective PI3K inhibitor, LY294002 (LY29) and the known PI3K activator, insulin. Insulin was found to activate PI3K, indicated by phosphorylation of the downstream PI3K target, AKT (Serine 473, Figure 3-13-B), and yet was unable to promote cell spreading (Figure 3-13-C). Furthermore, LY29 was found to be effective at inhibiting Ser472 phosphorylation of AKT in response to insulin, however it was unable to reduce cell spreading in response to F/R (Figure 3-13). Therefore regulation of PI3K activity is unable to affect the response of HEK293T-EPAC1 cells to elevated cAMP levels, suggesting that the PI3K signalling cascade is not involved in EPAC1 mediated changes in cell morphology.

3.2.10.2 Protein Kinase C

It has recently been reported that protein kinase C (PKC) isoforms can be activated in response to EPAC activation in COS1 cells and HUVEC (Borland et al. 2009; Wiejak et al. 2012). Furthermore, PKC has been shown to regulate Rho family GTPases, actin structure and cell morphology (Downey et al. 1992; Slater et al. 2001; Estevez et al. 2014). In order to test the involvement of PKC signalling in the

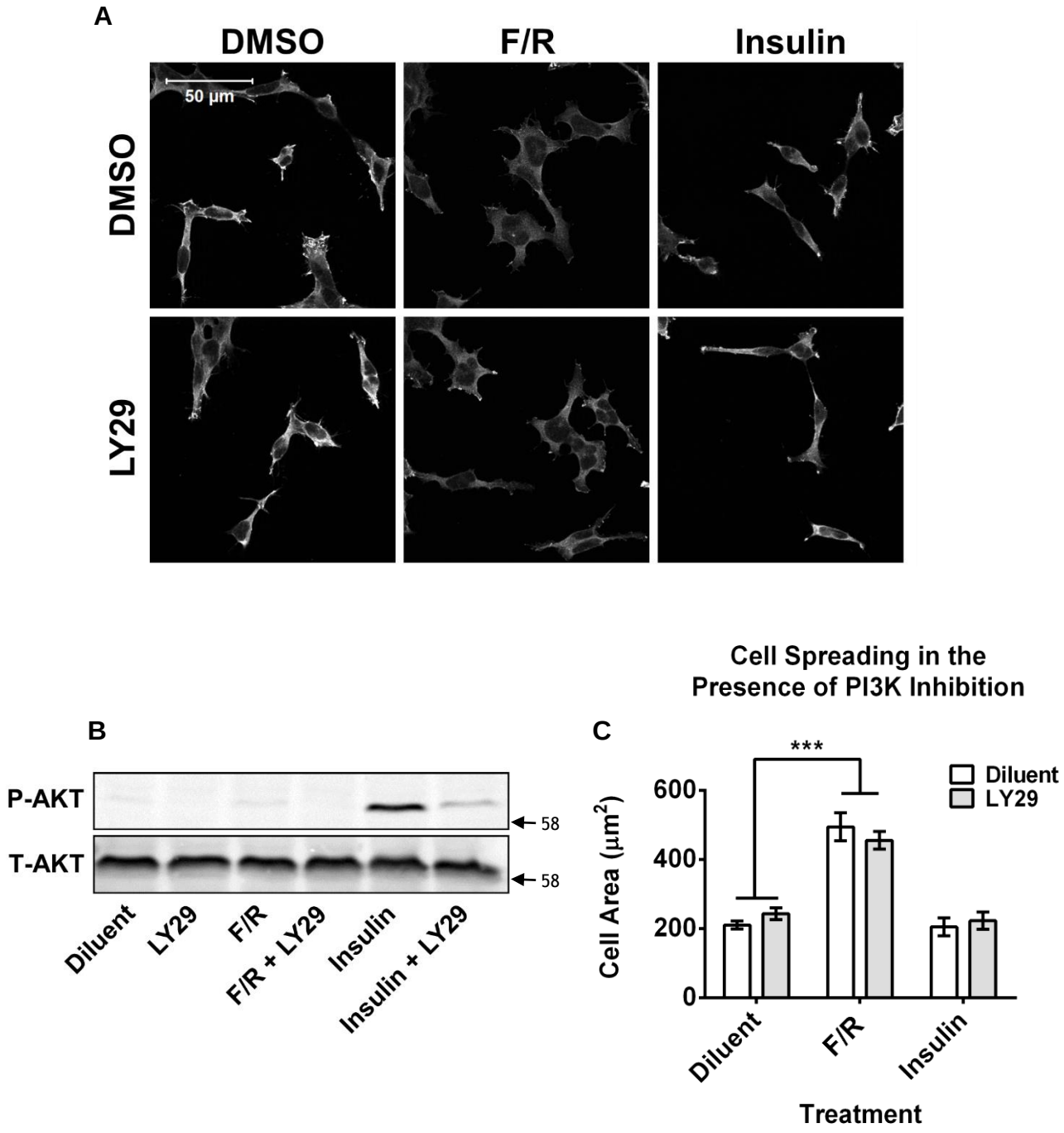

Figure 3-13 : PI3K inhibition is unable to affect EPAC1 mediated cell spreading.
A – Representative images of HEK293T-EPAC1 cells were stimulated for one hour with the indicated treatments, DMSO vehicle control (12.8 mM) F/R (10 µM), insulin (1 µM) and ly294002 (LY29, 10 µM). Cells were then fixed and immunostained with antibodies to detect T-ezrin to stain the cell periphery and allow visualisation of the cell periphery (white). **B** – Western blot of AKT Ser473 phosphorylation (P-AKT) in response to stimulation with insulin (1 µM) and Ly29 (10 µM) for 60 minutes. Positions of molecular weight markers is shown (kDa). **C** –. Cell area was determined from five randomly acquired images (minimum 30 cells) per experiment using the ImageJ wand tool on cells from thresholded images. Data are presented as a histogram (mean +/- s.e.m). *** - $p<0.001$, two way ANOVA using Dunnets post test, n-3.

control of cell morphology, the phorbol ester phorbol 12-myristate 13-acetate (PMA), was incubated with cells to activate PKC.

Interestingly, stimulation of cells with PMA resulted in a significantly reduced basal cell area, which correlated with an increase in cell rounding. Thus, PKC activity is observed to oppose the effects of EPAC1 signalling on cell morphology (Figure 3-14). In order to assess whether EPAC1 may induce cell spreading by negatively regulating the effects of PKC, the small molecule inhibitors Gö-6983 (Go) and Bisindolymaleimide (Bis) were employed to directly inhibit PKC isoform activity. Both inhibitors were observed to reverse the cell rounding associated with PMA stimulation. However, PKC inhibition failed to affect basal cell spreading or modify the effects of cAMP elevation (Figure 3-14). Although PKC is able to produce contrasting effects in HEK293T-EPAC1 cells, this does not appear to be linked to the cAMP spreading response *per se*. PKC does therefore not appear to be involved in the morphological response to cAMP elevation in these cells.

3.2.10.3 ERK

Elevations in intracellular cAMP have been linked to the regulation of the mitogen activated protein kinase/extracellular regulated protein kinase (MAPK/ERK) family (Gerits et al. 2008). In particular, EPAC1 activation has been reported to directly activate ERK (Keiper et al. 2004; Borland et al. 2009; Woolson et al. 2009). The ability of EPAC1 to activate ERK therefore presents itself as a mechanism for the regulation of cell morphology. We found that stimulation of HEK293T-EPAC1 cells with F/R led to a robust activation of ERK, as detected by ERK phosphorylation on Thr202/Tyr204, using phospho-specific antibodies, which was coincident with an induction of cell spreading (Figure 3-15-B), suggesting that cell spreading may be linked to ERK activity. The role of ERK activity in cell spreading was assessed by inhibition of ERK activity with the MEK1/2 inhibitors, AZD6244 (AZD) and PD184352 (PD1). Each inhibitor effectively inhibited both basal and F/R-induced phospho-ERK levels (Thr202/Tyr204) (Figure 3-15-B). However, neither AZD nor PD1 were able to reverse EPAC1 mediated cell spreading (Figure 3-15), suggesting that ERK phosphorylation in response to cAMP elevation is not directly involved in EPAC1-mediated changes in cell morphology.

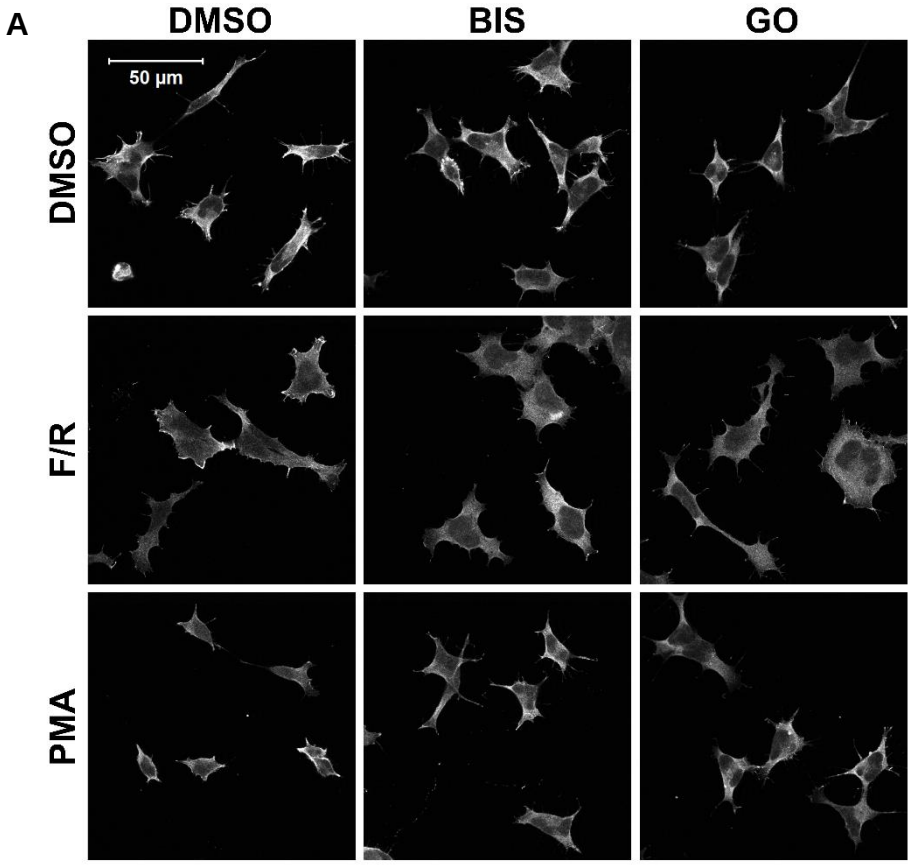

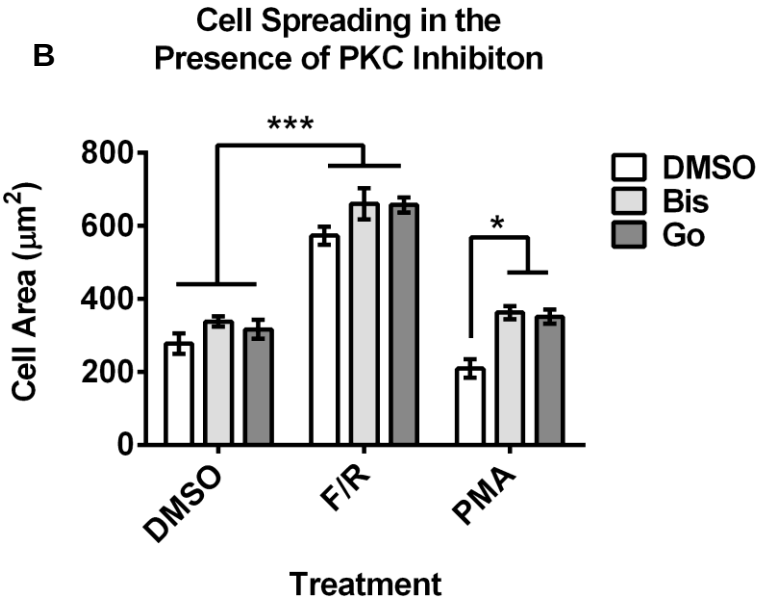

Figure 3-14 : EPAC1 induced cell spreading is insensitive to PKC activation.
A – Representative images of HEK293T-EPAC1 cells stimulated for 60 minutes with a DMSO vehicle control (12.8 mM), forskolin (10 µM) and rolipram (10 µM) in combination (F/R), the PKC agonist phorbol 12-myristate 13-acetate (PMA, 10 nM) and the PKC inhibitors Go6983 (GO; 10 µM) or Bisindolymaleimide (Bis, 10 µM) as indicated. **B** - Changes in cell area from five randomly acquired images (minimum 30 cells) were determined and presented as a histogram (mean +/- s.e.m). ** - P<0.001, *** - P<0.01, two way ANOVA using Tukeys post test, n-3.

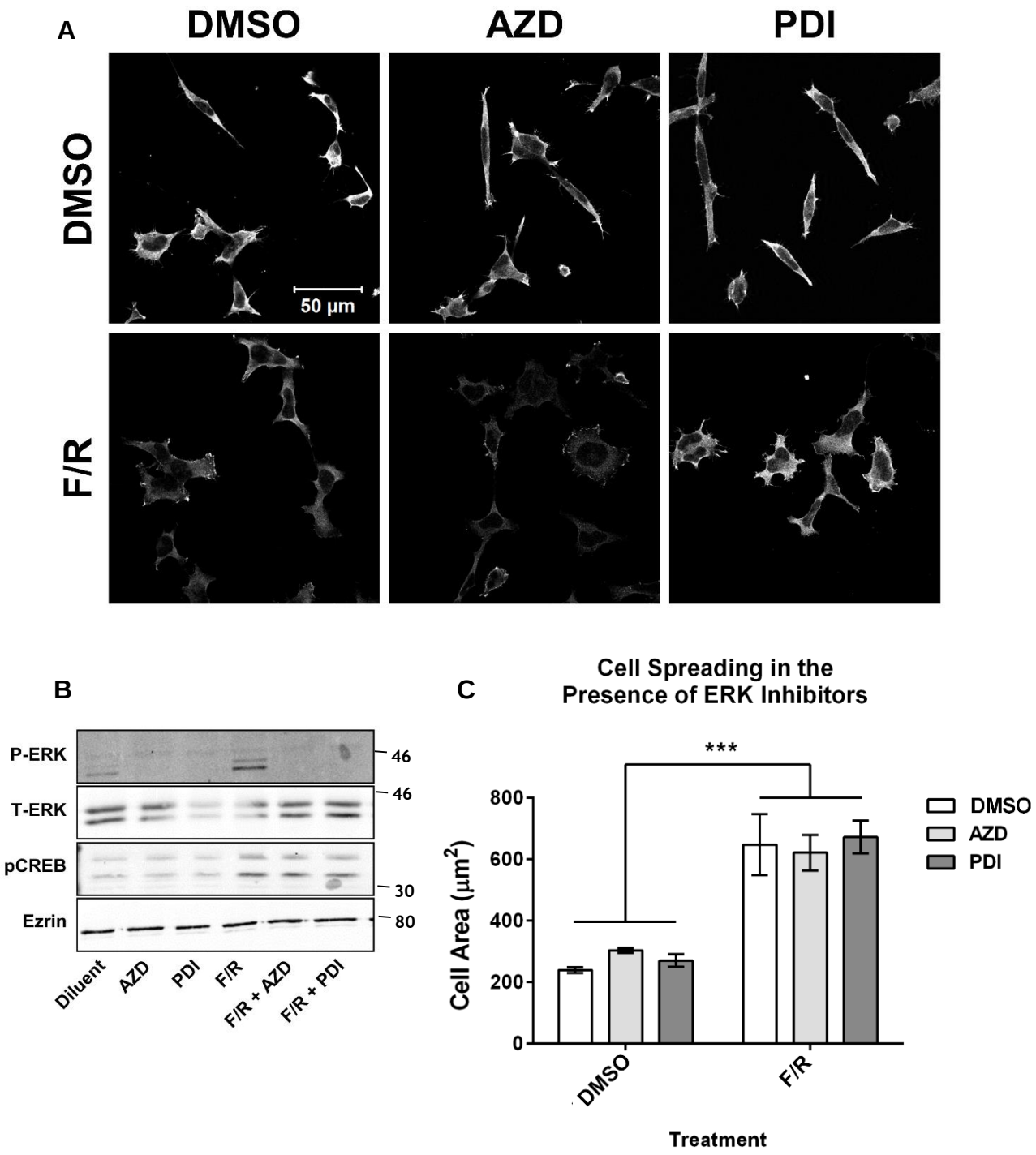

Figure 3-15 : EPAC1 Induced Cell Spreading is Insensitive to ERK Inhibition.
A – Representative images of HEK293T-EPAC cells stimulated for 60 minutes with a DMSO vehicle control (12.8 mM) or F/R (10 µM) in the presence or absence of the MEK1/2 inhibitors AZD6244 (AZD, 1 µM) and PD184352 (PD1, 1 µM) for 60 minutes and imaged by immunofluorescent confocal microscopy. **B** - Western blot analysis of ERK phosphorylation (Thr202/Tyr204) in the absence or presence of the ERK inhibitors AZD and PD1. T-ezrin indicates equal loading and P-Creb (Ser133) indicates PKA activation and phosphorylation of Creb. Positions of molecular weight markers is shown (kDa). **C** – Changes in cell area from five randomly acquired images (minimum 30 cells) were determined and presented as a histogram (mean +/- s.e.m.; n=3).

3.3 Discussion

3.3.1 Assay Development

We have demonstrated that an 8-NBD-cAMP competition assay can be performed using the isolated, recombinant CNBs of EPAC1 and EPAC2. Both EPAC1-CNB and EPAC2-CNB were observed to bind to 8-NBD-cAMP to promote its fluorescence (Figure 3-3). Furthermore, NMR analysis revealed that EPAC1-CNB retained its ability to bind to cAMP following removal of the GST fusion (Figure 3-2), ruling out any possible interference from the GST-tag. EPAC1-CNB used in the 8-NBD-cAMP fluorescence assay produced sub-optimal signal strength, limiting its usefulness in HTS. However, the optimisation of buffer conditions (Figure 3-4), effective concentrations of EPAC1-CNB (Figure 3-5), 8-NBD-cAMP (Figure 3-6) and incubation times (Figure 3-8) dramatically improved the sensitivity and power of the EPAC1-CNB based competition assay. Indeed, all statistical parameters required for efficient HTS were met for both EPAC1-CNB and EPAC2-CNB, allowing dual HTS of a small compound library within a pilot screen.

By adapting existing protocols to simultaneously screen EPAC1-CNB and EPAC2-CNB, it was possible to identify 8-NBD-cAMP competing compounds within pilot screens of two compound libraries with known drug-like qualities (Table 3-8). Indeed, the ability of this assay to identify compounds that are able to discriminate between EPAC1-CNB and EPAC2-CNB has been shown. Such a screening platform, greatly reduces the number of nonspecific hits requiring further characterisation. Furthermore, as well as identifying isoform selective hits, denaturing agents can also be identified. For example, hexachlorophine was found to inhibit 8-NBD-cAMP fluorescence in the presence of EPAC1-CNB and EPAC2-CNB to similar degrees and the steep Hill slope and strong inhibitory effect suggested denaturation, rather than non-selective 8-NBD-cAMP competition. A steep Hill slope suggests that the rate of fluorescence inhibition increases at a rate greater than competitive inhibition and that the pool of protein was reduced as compound concentration increased. Indeed, as the concentration of a denaturing agent increases, the rate of denaturation, and therefore fluorescence inhibition, can increase as protein aggregates form. Care must also be taken during follow up analysis of hit compounds, with regards to the use of GST tagged

CNBs. Although 8-NBD-cAMP failed to show any change in flouresence in the presence of GST alone, it is possible that hits identified may denature the EPAC-CNBs by interaction with the GST-tag. It would therefore be wise to carry out subsequent SAR analyses on protein lacking the GST tag.

3.3.2 Analysis of Isolated Hits

3.3.2.1 Common Features of Hit Compounds

Analysis of each of the compounds isolated from the pilot screen revealed a number of common features. For example, many of the hit molecules contained an acidic phenol group flanked by halogens and a diaryl motif separated by a spacer unit (e.g. hexachlorophene, thyroxine, raloxifene and HMS3259A19). Interestingly, many of the structures identified are reminiscent of previously characterised EPAC inhibitors (Chen et al. 2013). For example hexachlorophene and ESI-05 show similar structure and chemistry (Figure 3-16). These may represent previously uncharacterised motifs shared by compounds that are able to interact with the EPAC CNB. Whether these represent *bona fide* competitor compounds or mimic the denaturing properties identified for similar compounds (Rehmann 2013) is yet to be seen. Interestingly, although hexachlorophene displays a steep Hill slope, its structure is similar to the confirmed EPAC inhibitor ESI-05 (Chen et al. 2013; Rehmann 2013), suggesting that diaryl motifs may be involved in interaction with the CNB. In addition three oestrogen receptor modulators were identified (tamoxifen citrate, raloxifene and conjugated oestrogen), suggesting potential similarity between the cAMP and oestrogen receptor ligand binding sites.

3.3.2.2 EPAC1-Specific Competitor Compounds

Of the 15 hit compounds identified, only one displayed a higher IC_{50} value for EPAC1 over EPAC2 in follow up hit confirmation; conjugated oestrogen (Table 3-8). Despite the potential for agonism, steroids, such as conjugated oestrogen, display low flexibility in terms of the development of structural analogues. Furthermore, pharmacological intervention with hormone based drugs can produce significant off-target effects, due to interaction with the endogenous hormone system. As such, conjugated oestrogen is unlikely to be amenable to modification and further

development. However, recurring structures, such as acidic phenol groups, exposed halogens and diaryl motifs of the compounds identified (Figure 3-16) may elucidate features that convey EPAC or isoform specificity. Subsequently, the structure of conjugated oestrogen may inform on modifications accepted within the CNB of EPAC1 facilitating modification of hit compounds identified in further large scale HTS. It would therefore be of interest to ascertain the ability of this compound to activate EPAC1 within cell based agonist screening.

3.3.2.3 EPAC2-Specific Competitor Compounds

Interestingly, many compounds were observed to compete with high affinity for binding to the EPAC2-CNB (Table 3-8). This may indicate the existence of structural features that favour molecular interaction with the CNB of EPAC2 over EPAC1-CNB. Indeed, despite the outlined value of novel EPAC1 agonists, EPAC2 agonists may also be of therapeutic interest for the treatment of type two diabetes (Kang et al. 2003; Shibasaki et al. 2007; Kelley et al. 2009) and cardiac function (Pereira et al. 2013). One of the isolated hits, SGI-1776, displayed excellent potential for development into an EPAC2 selective competitor compound (Figure 3-16-B). Indeed, SGI1776 has few reported targets from previous studies and the molecule is suitable for chemical modification in order to achieve high affinity binding.

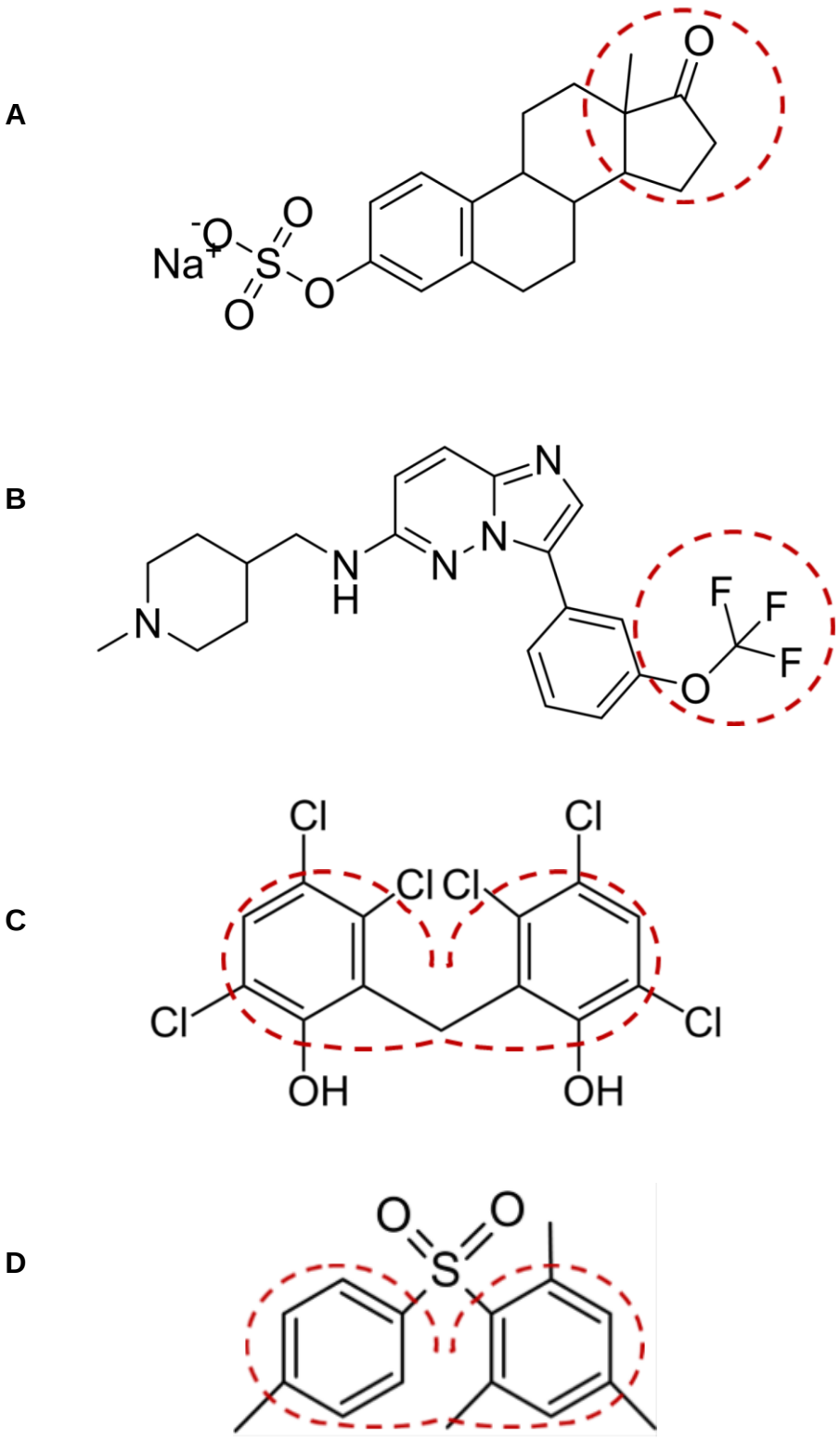

Figure 3-16 : Structures of hit compounds displaying recurring features.
Recurring features (dashed red lines) in the above compounds were found in multiple hits and may represent motifs involved in EPAC1-CNB or EPAC2-CNB binding. **A** - Conjugated oestrogen is shown with an acidic phenol group highlighted (red dotted line). **B** – The exposed halogens (dotted red line) of SGI-1776 are indicated. **C** – Hexachlorophene highlights the diaryl motif (dotted red line) identified in various structures, including (**D**) ESI-05 with red dotted line showing diaryl motif (Chen et al. 2013).

3.3.3 Cell Based Screening

In addition to the novel primary HTS screen described, a secondary screen was developed based on the cell spreading response of HEK293T cells stably transfected with EPAC1. The secondary screen can be used to classify hits from the primary screen as being agonists or antagonists of EPAC1 activity in cells and also for follow up structure activity relationship (SAR) analysis. EPAC1 activation was shown to be required for cell spreading in this system, producing a rapid reorganisation of the actin cytoskeleton and flattened, extended cells (Figure 3-12). The cell spreading response appears to rely on EPAC1 activation in isolation, as cell spreading appeared to occur independently of PKC (Figure 3-14), PI3K (Figure 3-13) and ERK (Figure 3-15) signalling pathways. Therefore, it is likely that hits that exert a positive spreading response will likely be acting through EPAC1 specifically, and not associated down-stream signalling. To make the cell spreading assay truly useful for screening for EPAC1 agonists it will be necessary to adapt it for rapid, single step analysis that is amenable to HTS. One possible approach to scaling up the assay is to measure cellular mass redistribution with resonant waveguide grating (RWG), used by corning EPIC technologies. By correlating the effects of cell shape to the refractive index of light across a RWG, dynamic mass redistribution (DMR), indicating morphological change, can be measured (Gitschier et al. 2014). This method would allow a label free, real-time, live cell measurement of EPAC1 activity in 384 well format.

In conclusion, we have developed a HTS assay for isoform selective EPAC competitor compounds. Additionally, a potential secondary agonist screen has been characterised, allowing a preliminary screening cascade to be developed (Figure 3-17). Use of this screening cascade is likely to facilitate the discovery of EPAC1 selective agonists and contribute to the development of EPAC1 targeted therapeutics.

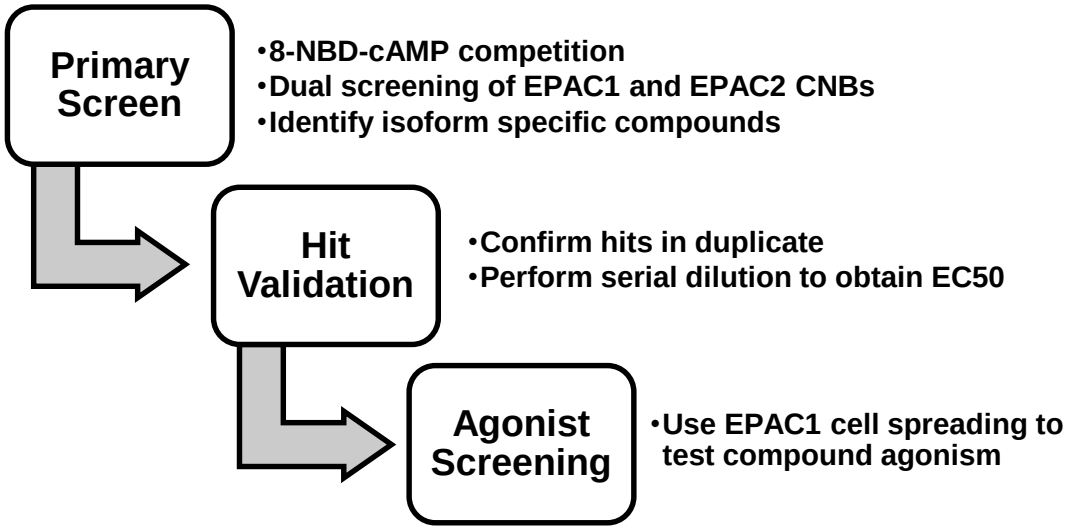

Figure 3-17 : EPAC1 Lead Identification Screening Cascade.
The screening cascade highlighted above shows the steps that could be carried out in order to identify EPAC1 selective agonists through HTS. Both primary screening and hit validation have been shown to be valuable approaches for hit identification as outlined within this chapter. Further work is required to confirm that a cell spreading assay is appropriate for follow up agonist screening.

Chapter 4 : The Role of EPAC1 in cAMP Mediated Morphological Change

4.1 Introduction

A large body of evidence points toward a role for EPAC1-Rap1 signalling in governing cAMP-regulated cell shape, spreading and morphology (Borland et al. 2009; Parnell et al. 2012). Furthermore, EPAC1/Rap1 signalling has been linked to the promotion of barrier protective functions in the vascular endothelium through the regulation of adhesive and cohesive pathways connected by the dynamic cytoskeleton (Bos 2005; Boettner and Van Aelst 2009). These effects are largely attributed to the relocalisation of vascular endothelial-specific VE-cadherin (Arthur et al. 2004) and the regulation of cytoskeletal elements (Moy et al. 1996; Bogatcheva et al. 2002). In particular, cytoskeletal reorganisation occurs through Rap1-mediated regulation of the Rho GTPase family of cytoskeletal regulators (Bogacheva et al. 2001; Arthur et al. 2004; Post et al. 2013). However, many of the protective pathways of EPAC1 synergise with PKA for maximal effect (Hochbaum et al. 2007; Lorenowicz et al. 2008; Aslam et al. 2010; Birukova et al. 2010; Hewer et al. 2011). We have found that cell spreading is promoted by EPAC1 activation in stably transfected HEK293T cells (Figure 3-12). Such a platform may therefore allow the characterisation of the cAMP signalling pathways involved in morphological changes in response to activation of both PKA and EPAC1.

A novel mediator of EPAC1-dependent morphological changes is the ezrin-radixin-moesin (ERM) protein family member, ezrin (Ross et al. 2011). ERM proteins are a homologous group of actin binding proteins, with a characteristic N-terminal 4.1-ezrin-radixin-moesin (FERM) domain (Gould et al. 1989), that control of a wide range of cellular processes through their role as scaffold proteins linking the actin cytoskeleton and the plasma membrane component phosphoinositol-4,5-bisphosphate (PIP2) (Bosk et al. 2011). Recent studies have identified cooperation between EPAC1 and ezrin in cAMP-mediated cell spreading. Indeed, siRNA-mediated knockdown of ezrin was able to produce a significant reduction in cell spreading (Ross et al. 2011). Multiple kinases have been reported to regulate ezrin function, notably through phosphorylation of Ser66 (Zhou et al. 2003), Tyr81 (Bretscher 1989), Tyr145, Tyr353 (Krieg and Hunter 1992) and Tyr477 (Heiska and Carpen 2005). However, it is Thr567 phosphorylation that has been identified as being key in relieving an auto-inhibitory head to tail conformation within ERM proteins, thereby facilitating activation (Pearson et al. 2000; Bosk et al. 2011).

Interestingly, phosphorylation of ezrin (Thr567) has been observed to occur in response to cAMP elevation, through PKA (Zhu et al. 2007). In addition to Thr567, phosphorylation of ezrin Ser66 in response to cAMP elevation has also been reported (Zhou et al. 2003). We therefore intend to identify whether either of these sites are involved in the control of cell spreading and the manner by which this is linked to ezrin activity.

In the present study we investigate the roles of PKA, EPAC1 and ezrin in controlling the morphological response to cAMP elevation in a cell model of EPAC1-dependent cell spreading. In addition, the signalling pathways involved will be assessed, with particular emphasis on ezrin, the Rho GTPase family and the actin cytoskeleton. This will provide a greater understanding of the role of cAMP in the control of cell morphology.

In this chapter I aim to;

- Determine whether synergy between EPAC1 and PKA signalling pathways can produce alterations in cell morphology.
- Determine whether phosphorylation of ezrin and interactions with the actin cytoskeleton are required for cAMP mediated spreading.

4.2 Results

4.2.1 EPAC Activation Promotes Cell Spreading in Different Cell Types

Activation of endogenous EPAC is able to induce cell spreading in A549 lung cancer cells and HUVEC (Arthur et al. 2004; Enserink et al. 2004; Ross et al. 2011; Ross et al. 2012). In order to confirm this effect in our hands, the EPAC1-expressing COS1 and human umbilical vein endothelial cell (HUVEC) lines were stimulated with a combination of the adenylate cyclase (AC) activator, forskolin, and the type four PDE inhibitor, rolipram (F/R), to elevate intracellular levels of cAMP. As both cell lines express both EPAC and PKA, the EPAC specific cAMP analogue 007 (8-pCPT-2'-O-Me-cAMP) (Enserink et al. 2002) was also used in order to assess the relative roles of EPACs and PKA.

Treatment of COS1 (one hour) and HUVEC (two hours) with either F/R or 007 led to a significant increase in cell size (Figure 4-1, Figure 4-2). The ability of 007 to induce spreading indicates that endogenous EPAC activation is sufficient to promote cell spreading in both cell lines. However, in contrast with COS1 cells, there was a significant difference in HUVEC spreading observed between targeted EPAC1 activation with 007 and global cAMP elevation with F/R (Figure 4-2-B). Furthermore, there was a redistribution of actin into cortical actin bundles in response to cAMP elevation with F/R, an effect absent when EPAC was activated alone with 007 (Figure 4-2-C). This suggests that EPAC1 activation is not sufficient to promote maximal levels of cell spreading or cortical actin bundling in HUVEC. Therefore, synergy between cAMP responsive pathways may occur within HUVEC to produce the cytoskeletal reorganisations that are linked to maximal cell spreading.

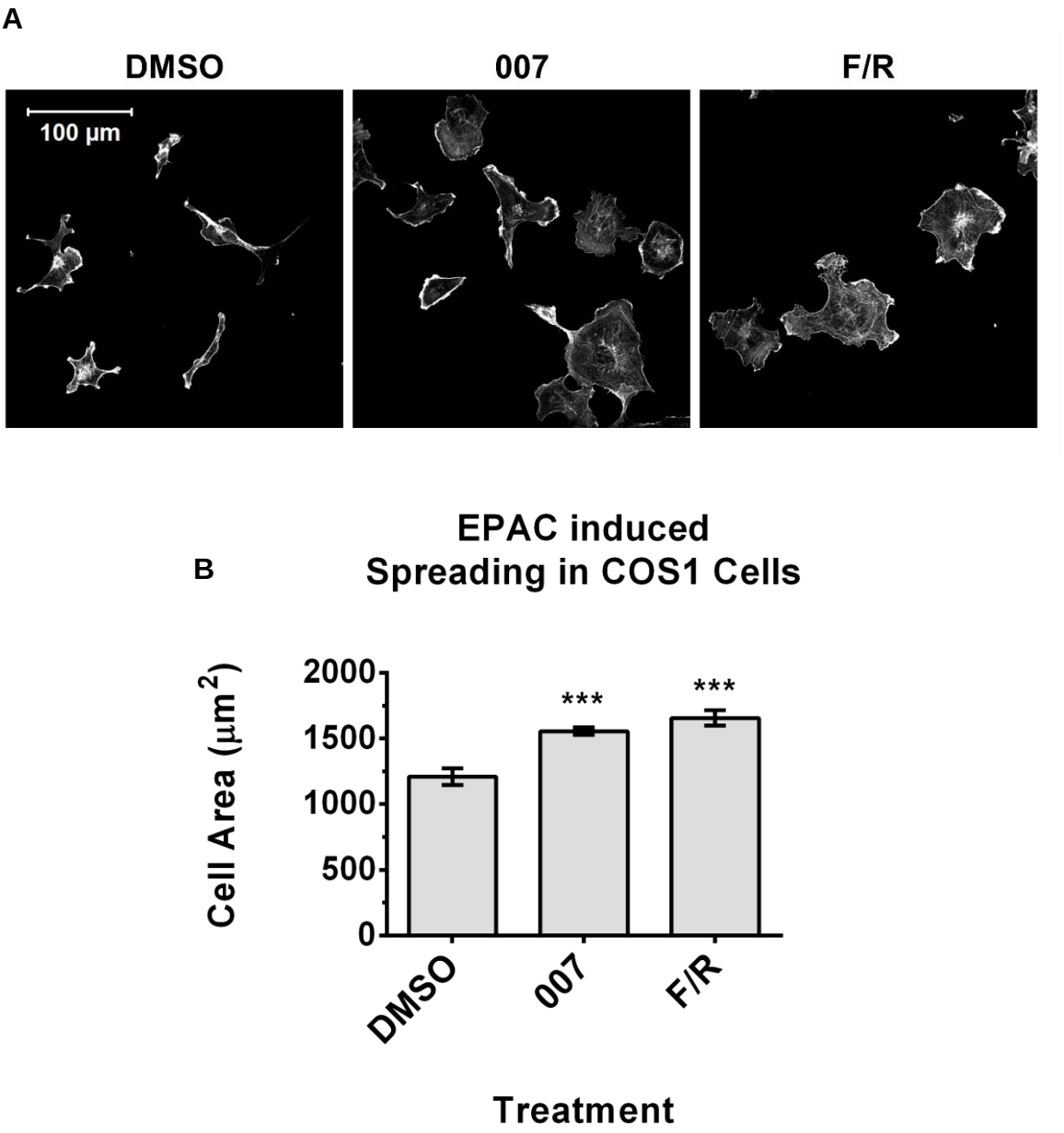

Figure 4-1 : EPAC activation produces cell spreading in COS1 cells.
A -COS1 cells were treated with either a DMSO vehicle control (12.8 mM, 60 minutes), 007 (8-pCPT-2'-O-Me-cAMP , 10 µM, 60 minutes) or F/R (10 µM forskolin plus 10 µM rolipram, 60 minutes) and then stained with rhodamine phalloidin in order to visualise F-actin. **B** - Mean cell areas were measured from ten randomly acquired images (minimum 50 cells). Cell areas from three separate experiments are shown (mean +/- s.e.m.). Statistical significance is indicated; *** P<0.001 ANOVA using Dunnets post test, n-3.

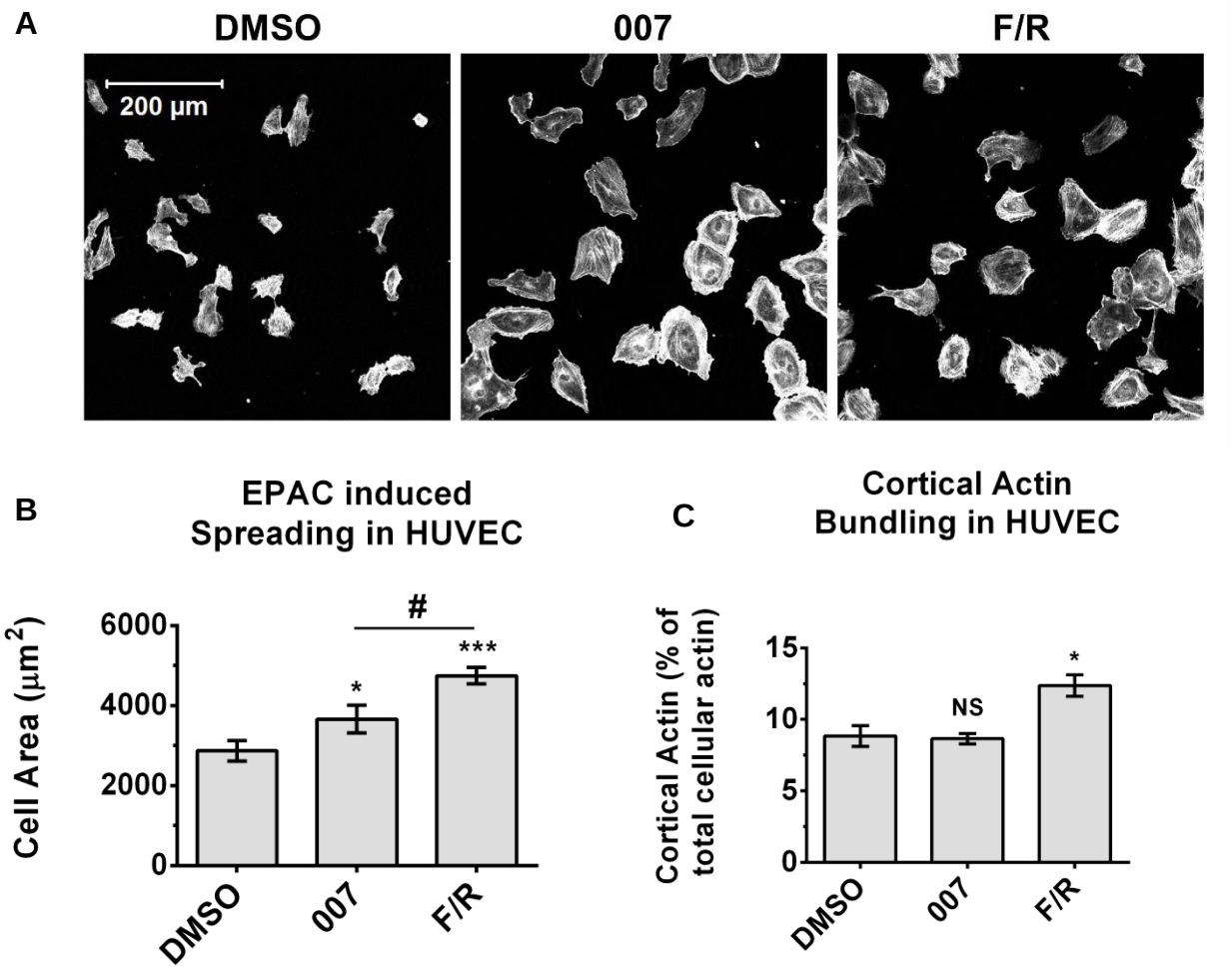

Figure 4-2 : EPAC activation is sufficient to induce HUVEC spreading, however cAMP elevation is required for maximal spreading and cortical actin bundling.
A - HUVEC were treated with a DMSO vehicle control (12.8 mM), 007 (10 µM) or F/R (10 µM) for 120 minutes, fixed and then stained with rhodamine phalloidin to visualise F-actin. **B** - Cell areas were calculated from ten randomly acquired images (minimum 50 cells) from three separate experiments (mean +/- s.e.m.). **C** - Cortical actin bundling was calculated from line scans taken across the longest cell axis. The percentage of actin found in the outermost 10% at both sides of 10 cells were normalised to total cell fluorescence to give the percentage of cortical actin (mean +/- s.e.m.). Statistical significance is indicated; * - $p<0.05$, # - $p<0.01$, *** - $P<0.001$, ANOVA using Tukeys post test, n-3.

4.2.2 cAMP Induced Cell Spreading Coincides with Cytoskeletal Reorganisation

In order to test whether cooperativity between the cAMP effectors EPAC1 and PKA contributes to cell spreading, HEK293T cells were stably transfected with either FLAG- and myc-tagged EPAC1 or a vector construct (Figure 3-12). This allowed us to assess whether changes in cell shape in response to EPAC1-activation are linked to reorganisation of the actin cytoskeleton (Gerasimenko et al. 2001; Bogatcheva et al. 2002).

We found that increases in cell area coincided with rearrangements of the actin cytoskeleton following cAMP stimulation of EPAC1-transfected cells, but not vector-transfected cells (Figure 4-3). In unstimulated cells, both cell lines demonstrated low levels of F-actin, largely localised to the cell periphery (Figure 4-3). However, F/R stimulation induced the formation of cortical actin bundles in EPAC1-expressing cells only. Although, cAMP elevation induced the formation of a strong cortical actin network at the cell periphery in EPAC1-expressing cells, direct activation of EPAC1 with 007 failed to reproduce this effect and F-actin was observed throughout the cell body (Figure 4-3).

In order to test the cell spreading response at more physiological levels of cAMP, prostaglandin E2 (PGE2) was used to activate endogenous PGE2 receptors and promote cAMP elevation. Indeed, HEK293T-EPAC1 cells responded to PGE2 and exhibited increased cell spreading, demonstrating that cAMP elevation in response to Gs-protein coupled receptor (GsPCR) activation is sufficient for cell spreading. Interestingly, cortical actin bundling occurred in response to PGE2 but not 007, despite the observation of similar spread areas, suggesting that EPAC1 activation alone is insufficient to promote cortical actin bundling. Thus, it may be concluded that PKA may promote supplemental cell spreading effects that are dependent on EPAC1 activation, and that PKA facilitates further cell spreading and cortical actin bundling than that achieved through EPAC1 activation alone.

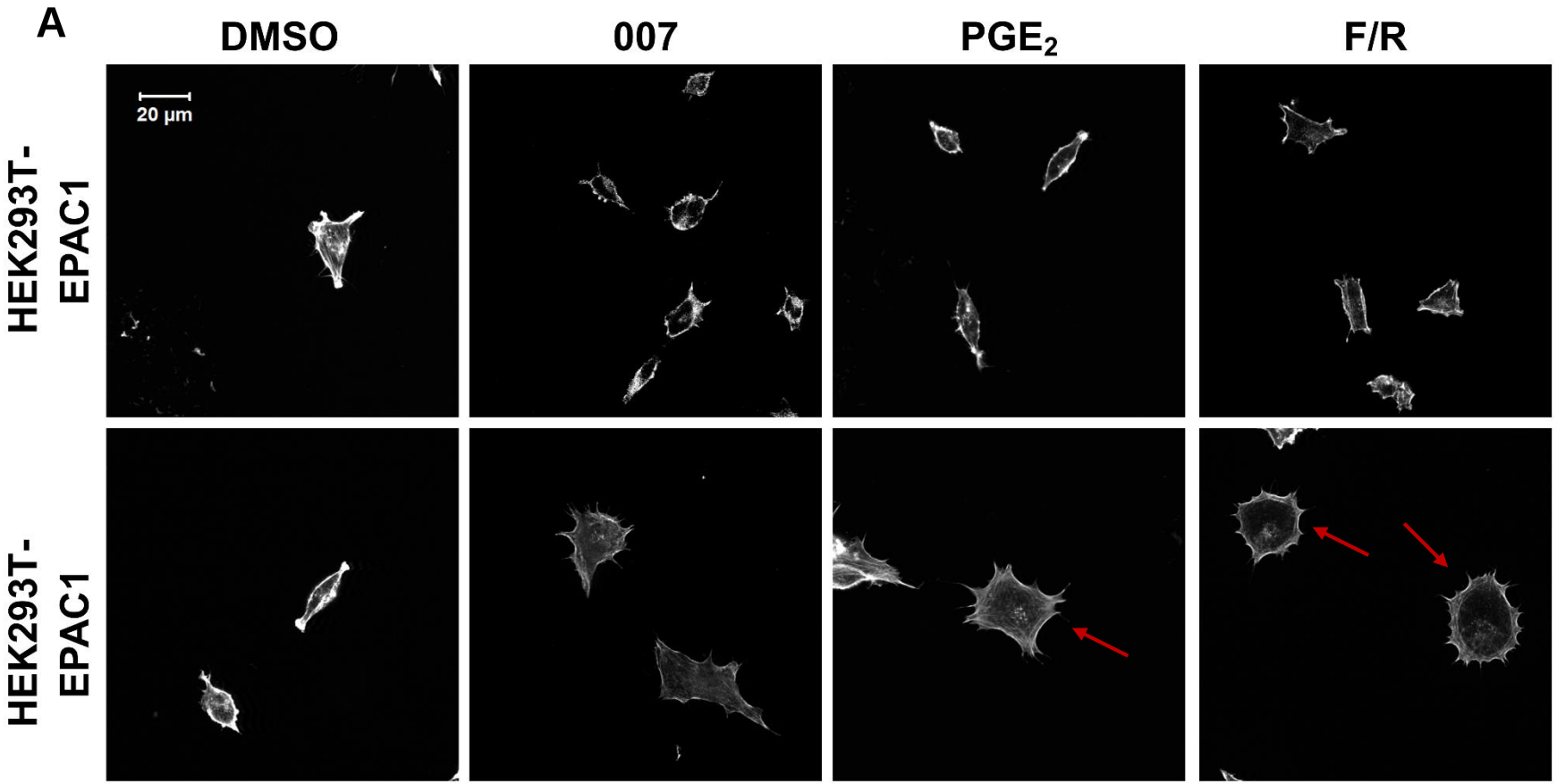

Figure 4-3 : EPAC1 is required but not sufficient for cytoskeletal reorganisation.
A -HEK293T-EPAC1 and -vector cells were grown in the presence of DMSO vehicle control (12.8 mM, 60 minutes), 007 (10 µM, 60 minutes), prostaglandin E_2 (PGE_2, 10 µM, 60 minutes) and forskolin and rolipram in combination (F/R, 10 µM, 60 minutes). Cells were fixed and F-actin was visualised using rhodamine phalloidin. **B** (see overleaf) - Cell areas were calculated from 10 random cell images (displayed as mean of three independent experiments +/- SEM). *** = P<0.001, two way ANOVA using Tukeys post test. Arrows indicate actin polymerisation at the cell periphery.

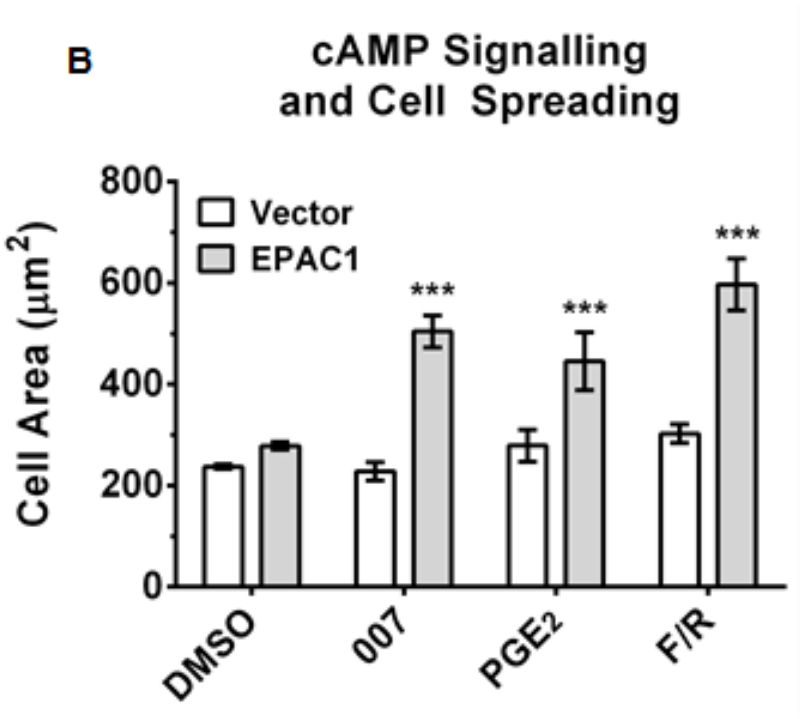

4.2.3 Activation of PKA is required for Maximal Cell Spreading

EPAC1 and PKA have been observed to act synergistically to control a range of cellular processes (Hochbaum et al. 2007; Lorenowicz et al. 2008; Aslam et al. 2010; Birukova et al. 2010; Hewer et al. 2011). Indeed, direct EPAC1 activation is insufficient to produce maximal cell spreading and cortical actin bundling in HEK293T-EPAC1 cells (Figure 4-3-A). However, global cAMP elevation is able to produce these effects suggesting a supplementary role for PKA beyond those of EPAC1 (Figure 4-3). In order to test the involvement of PKA in EPAC1 mediated cell spreading, HEK293T-EPAC1 cells were treated with the PKA inhibitor, H-89. As observed previously, F/R was able to produce maximal spreading above levels obtained by EPAC1 activation alone. H-89 treatment had no effect on basal cell areas, or on cell spreading induced by 007. However, cell spreading in response to F/R was significantly reduced as a result of PKA inhibition with H-89 (Figure 4-4). Interestingly, F/R-induced spreading was reduced by H-89 to levels comparable with 007 stimulation, indicating that PKA is responsible for secondary cell spreading effects that complement EPAC1-mediated cell spreading.

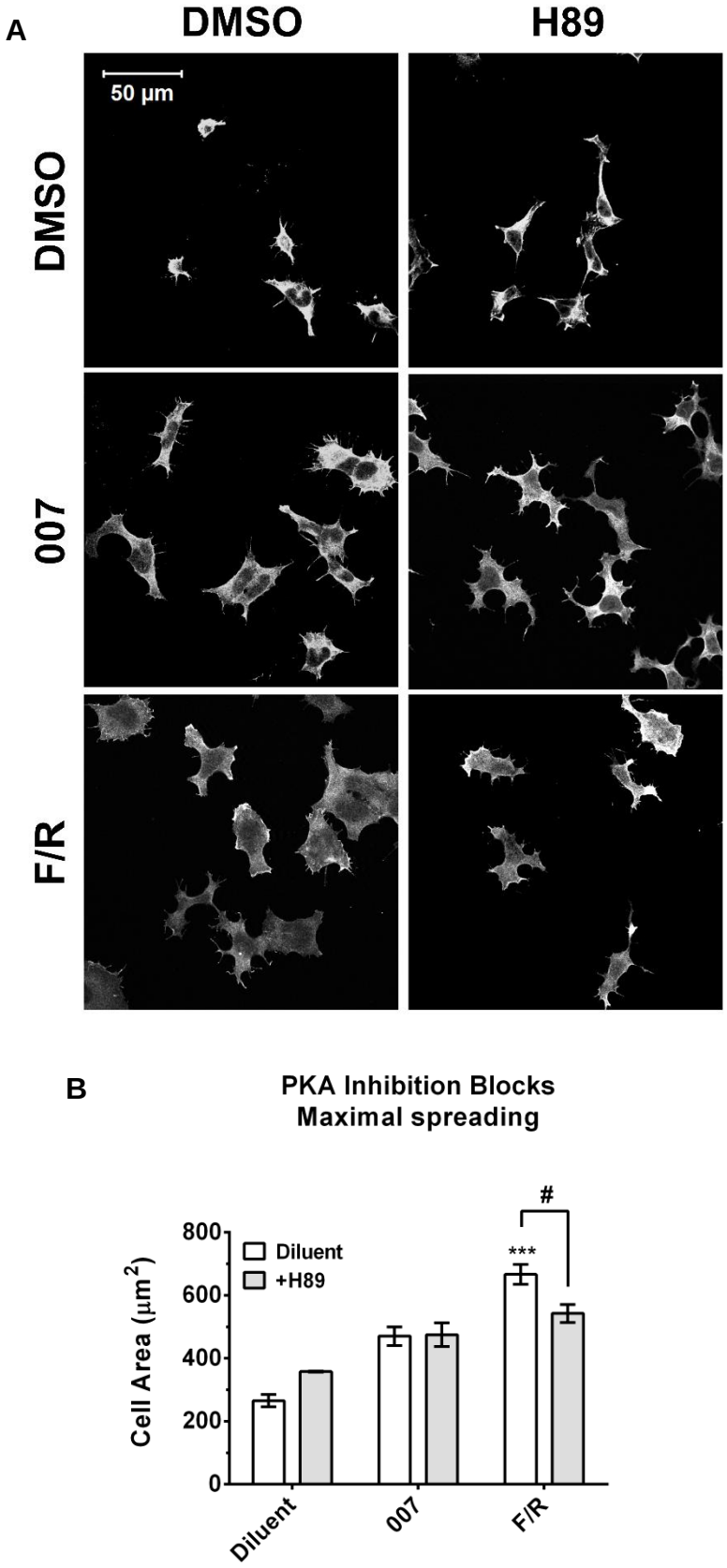

Figure 4-4 : PKA inhibition limits cAMP but not EPAC1-mediated cell spreading.
A -HEK293T cells were preincubated with the PKA inhibitor H-89 (10 µM, 30 minutes) or DMSO vector (12.8 mM, 30 minutes) before stimulation of cAMP pathways with F/R or 007 (10 µM, 60 minutes) or incubation with a DMSO vehicle control (12.8 mM, 60 minutes). Cells were fixed and confocal immunofluorescent microscopy using α-ezrin antibody (white) was employed to detect the cell body. **B** - Cell areas were calculated from 10 randomly acquired images and the mean cell area from three independent experiments are shown (+/-s.e.m.).comparison of F/R treated cell areas to basal cell areas - *** - $p<0.001$. # - $p<0.05$, two way ANOVA with Tukeys post test, n-3.

4.2.4 cAMP Elevation is Coupled to an EPAC1-dependent Redistribution of an ERM protein in HEK293T Cells

Expression of the actin cytoskeletal linker, ezrin, has been observed to be essential for EPAC1-mediated cell spreading (Ross et al. 2011) and also acts as a PKA anchoring protein (AKAP) (Dransfield et al. 1997). As such, ezrin represents a candidate for the coordination of EPAC1 and PKA synergistic effects on cell spreading. Furthermore, the role of ezrin in linking F-actin to the plasma membrane is crucial in regulating the cell cortex and membrane protrusions, processes that contribute to cell morphology (Zhu et al. 2010). We therefore aimed to determine the role of ezrin in cAMP-mediated cell spreading and cytoskeletal reorganisation in HEK293T-EPAC1 cells.

The intracellular distribution of endogenous ERM proteins in stably transfected HEK293T cells was assessed by immunofluorescent staining with an antibody that detects the ERM family members ezrin, radixin and moesin. Immunofluorescent detection demonstrated a stable cytosolic distribution of ERM proteins following cAMP stimulation in vector-transfected cells (Figure 4-5). However, in EPAC1-expressing cells, anti-ERM immunofluorescent detection revealed protein accumulation at the plasma membrane in response to F/R stimulation. Therefore, at least one ERM family member is cAMP responsive and its intracellular localisation is dependent on the presence of EPAC1 within HEK293T cells.

In order to determine which ERM family members respond to cAMP elevation in transfected HEK293T-EPAC1 cells, isoform-specific antibodies were employed to visualise the individual subcellular distributions of ezrin (Figure 4-6), radixin and moesin (Figure 4-5). Radixin and moesin maintained largely diffuse and nuclear distributions respectively, regardless of the cell line or treatment applied (Figure 4-5). Neither protein adopted a membrane distribution consistent with that observed by detection of total ERM protein, suggesting that neither radixin, nor moesin are responsive to cAMP in HEK293T cells.

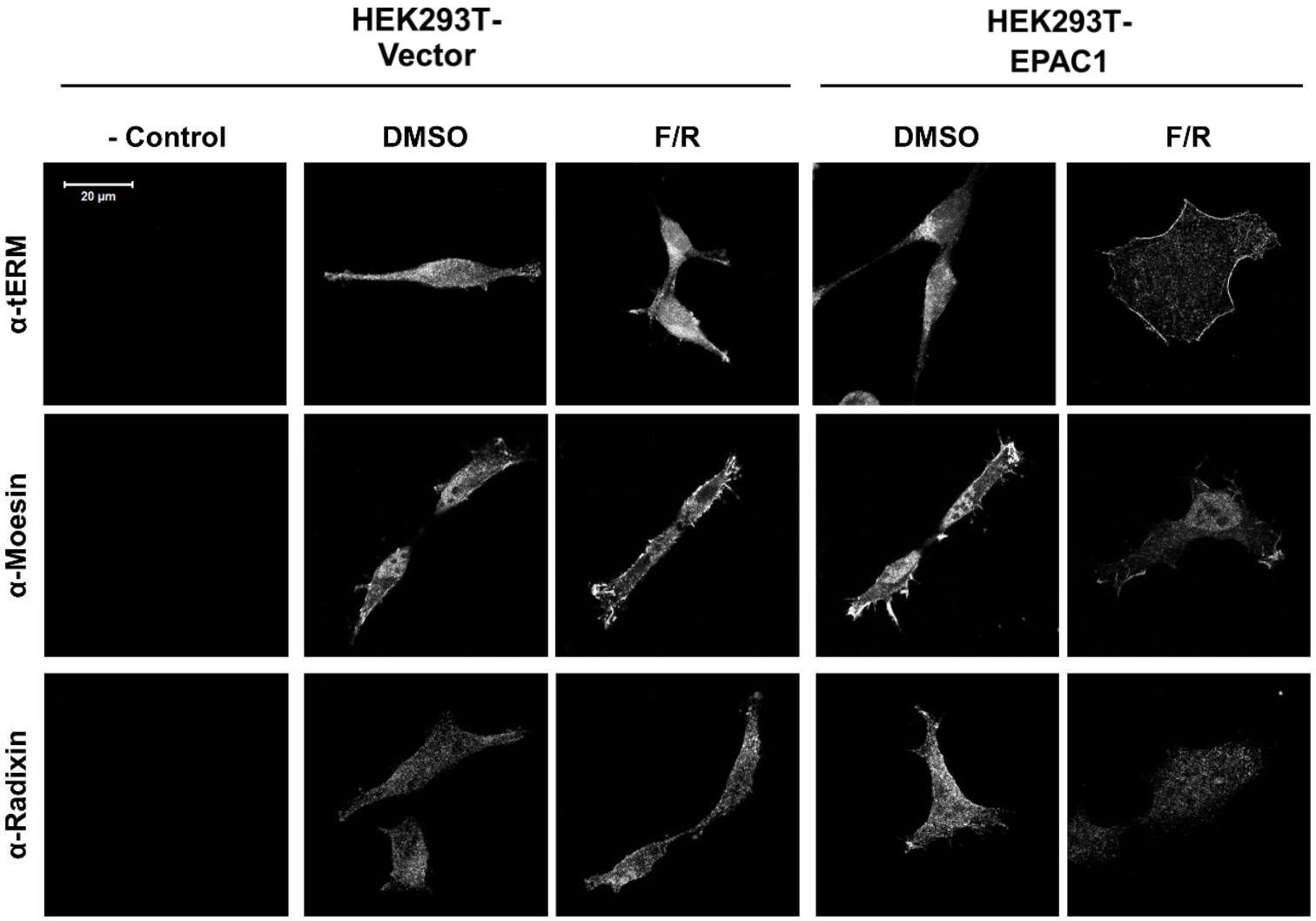

Figure 4-5 : An ERM protein accumulates at the plasma membrane in HEK293T-EPAC1 in response to cAMP elevation. HEK293T-EPAC1 and vector cells were prepared for immunofluorescence by fixation. Cells were stained for ERM proteins with the indicated antibodies (white).“- control” was performed in the absence of primary antibody.

In contrast ezrin was observed to localise to membrane projections in HEK293T-vector cells and EPAC1 expressing cells (Figure 4-6). Following cAMP stimulation and cell spreading, ezrin appeared to become more diffuse within the cytosol, which is probably due to increased cell area and perimeter associated with isotropic cell spreading. However, within EPAC1-expressing cells, the accumulation of ezrin at sites of membrane ruffling and projection (Figure 4-6-Arrows) suggests that ezrin may be involved in, or respond to, cortical actin reorganisation. Furthermore, the distribution of total ERM and ezrin at the plasma membrane suggests that ezrin may represent the cAMP-responsive ERM protein observed in HEK293T-EPAC1 cells (Figure 4-5).

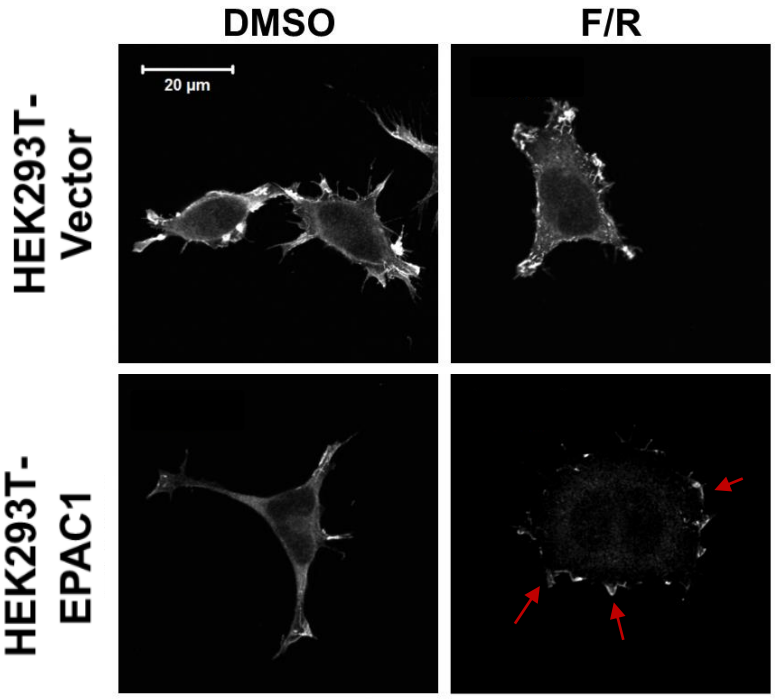

Figure 4-6 : Ezrin is found at the plasma membrane.
Cells were fixed with paraformaldehyde and ezrin was detected by immunofluorescence confocal microscopy (white) using ezrin-specific antibodies. Red arrow indicates ezrin at a point of plasma membrane ruffling.

4.2.5 Ezrin Undergoes Post Translational Modification in Response to PKA activation

Given the role of ezrin in the control of membrane dynamics and cytoskeletal organisation, we decided to test its ability to respond to elevations in intracellular cAMP. HEK293T-vector and HEK293T-EPAC1 cells were treated with F/R (60 minutes), particulate fractions were prepared from cells and then western blotted using anti-ezrin antibodies. Western blot analyses revealed that ezrin exists as two distinct molecular weight isoforms, a low molecular weight form representing around 80% of cellular ezrin and a high molecular weight form representing the remaining ezrin. Interestingly, following cAMP elevation, the heavy molecular weight isoform of ezrin underwent a band-shift, suggesting post-translational modification, yielding a third, high molecular weight form of ezrin (Figure 4-7). In addition to the formation of a third ezrin immunoreactive band, the intermediate molecular weight form of ezrin became weaker, suggesting that only the heavy form of ezrin is subject to post translational modification in response to cAMP. Although ezrin has been linked to EPAC1 cell spreading (Ross et al. 2011), the cAMP induced increase in molecular weight was observed in both EPAC- and vector-expressing cells suggesting that ezrin post translational modification is not specifically linked to EPAC1 activity (Figure 4-7).

PKA has been observed to regulate ezrin, directing its activity and cellular function by phosphorylation of Ser66 (Zhou et al. 2003) and Thr567 (Zhu et al. 2007). We have found that PKA is able to synergise with EPAC1 to produce secondary spreading effects. Therefore, in order to check that PKA is responsible for post translational modification of ezrin, cells were stimulated with 007 or F/R. In agreement with the results shown in Figure 4-7, EPAC1 activation alone was unable to induce post translational modification of ezrin, whereas a high molecular weight form of ezrin was produced in response to F/R stimulation (Figure 4-7). This provides further evidence that EPAC1 is not involved in the post translational modification of ezrin. Importantly, PKA inhibition by H-89 ablated the increase in the molecular weight of ezrin observed, implicating PKA signalling in the post translational modification of ezrin.

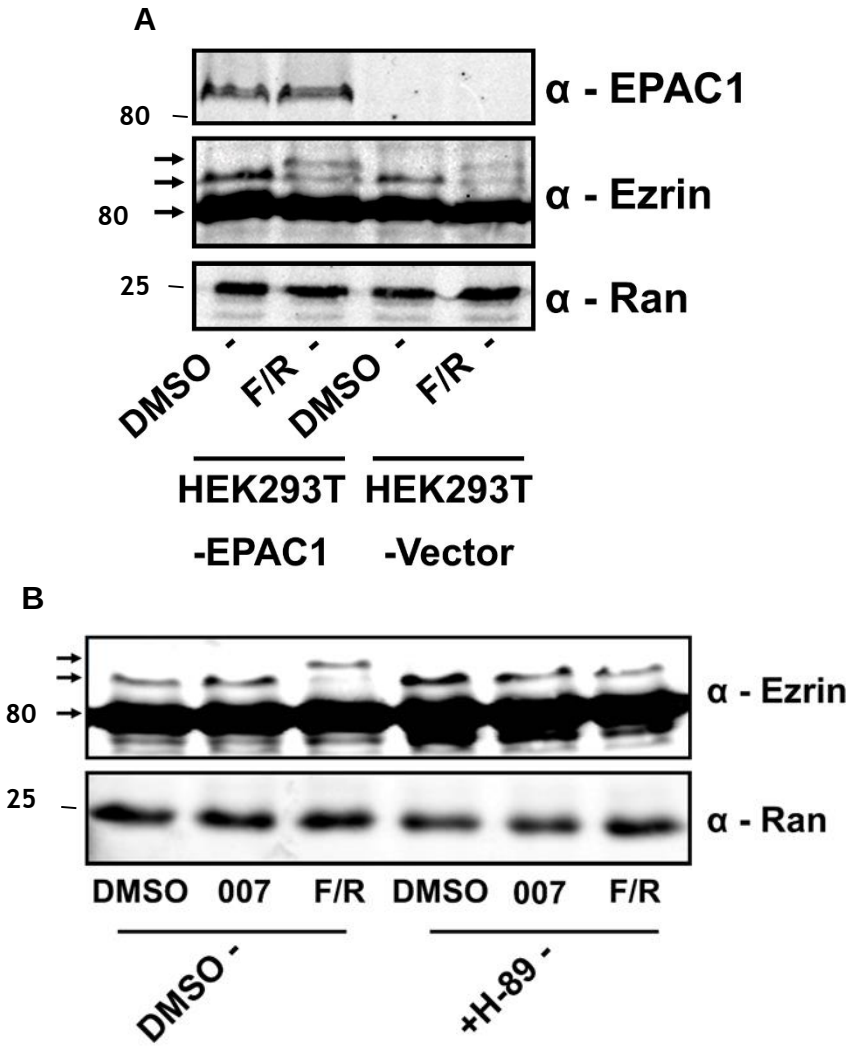

Figure 4-7 : PKA induces post translational modification of ezrin independently of EPAC1. **A** - Cells from -EPAC1 and -vector expressing HEK293T cells were stimulated with a DMSO vehicle control (12.8 mM, 60 minutes), 007 (10 µM, 60 minutes) or F/R (10 µM, 60 minutes). Following fractionation, the particulate fraction was prepared for western blotting of ezrin. **B** – HEK293T-EPAC1 cells were pre-treated with DMSO or H-89 (10 µM, 30 minutes) and stimulated as indicated (10 µM, 60 minutes). Particulate fractions were probed with the indicated antibodies in order to assess EPAC1 expression (α - EPAC1) and equal loading (α - Ran). Arrows indicate the position of each ezrin isoform, and the positions of molecular weight markers are shown (kDa).

4.2.6 Ezrin is not Directly Involved in Cell Spreading

Ezrin is controlled by a wide range of phosphorylation events that regulate its activity and interaction with various binding partners, including actin (Fehon et al. 2010). In order to assess the role of ezrin phosphorylation in EPAC1-mediated cell spreading, HEK293T-EPAC1 cells were transfected with GFP, a WT ezrin-GFP construct and two inactive ezrin mutants. Ezrin activation is promoted by phosphorylation at Thr567 which disrupts the closed, auto-inhibited form of the protein (Matsui et al. 1998; Bosk et al. 2011). A phospho-null T567A mutant is unable to become phosphorylated and the function of this ezrin mutant is attenuated (Ross et al. 2011). In order to correlate the effects of each phospho-mutant to the actin binding properties of ezrin, a mutant deficient in actin binding was introduced into HEK293T-EPAC1 cells. Indeed, ezrin-R579A has been reported to inhibit the interaction of ezrin with actin and limit the functional effects of ezrin within the cell (Saleh et al. 2009). The effects of these mutant forms of ezrin may reveal the importance of ezrin in the control of HEK293T morphology, and in addition may suggest a potential regulatory site, through which cAMP signalling may regulate Ezrin activity.

Transfection of HEK293T-EPAC1 cells with either GFP or WT-ezrin had no effect on cell morphology or the response of HEK293T-EPAC1 cells to 007 or F/R (Figure 4-8). Furthermore, GFP and WT-ezrin transfected cells exhibited cell spreading in response to 007 (Figure 4-8), similar to its effects in untransfected cells (Figure 4-3). Furthermore, the cell perimeter increased linearly with cell area as the borders of the cell extended in a uniform manner with stimulation. However, the introduction of T567A- and R579A-ezrin-GFP constructs produced dramatic changes in cell morphology. Indeed, unstimulated cells displayed significantly higher cell perimeters consistent with the formation of membrane projections (Figure 4-8). Furthermore, basal cell areas were observed to increase in the presence of phospho-null mutants, though this effect was not significant (Figure 4-8-A). Although ezrin-T567A and -R579A altered basal cell morphology, the spreading response to 007 and F/R was unchanged. We have observed ezrin post translational modification in response to PKA (Figure 4-7), however, ezrin-T567A displays no alteration in the cAMP-mediated spreading response despite the loss of this key phosphorylation site (Figure 4-8). Indeed, F/R mediated cell spreading

is unaffected, suggesting that PKA mediated post translational modification occurs at a distinct site within ezrin, or that ezrin post translational modification is not required for cAMP-mediated cell spreading.

A phosphomimetic ezrin mutant (T567D) has been shown to promote ezrin activity (Bosk et al. 2011). In addition to Thr567, Ser66 has been implicated in ezrin activation in response to direct phosphorylation by PKA (Zhou et al. 2003). We therefore transfected HEK293T-EPAC1 cells with GFP-tagged ezrin-T567D and ezrin-S66D in order to assess whether the introduction of phosphomimetic ezrin mutants is able to provoke cell spreading or PKA-mediated supplemental spreading. As previously shown, transfection of either GFP or WT-ezrin had no effect on F/R mediated spreading (Figure 4-8).

Interestingly, the ability of cells to undergo cell spreading was unaffected by the expression of a T567D-phosphomimetic mutant (Figure 4-8-C). These results suggest that either ezrin post translational modification in response to cAMP is not involved in Thr567 phosphorylation, or that ezrin does not contribute to the cell spreading response. Interestingly, cells expressing ezrin-S66D exhibited a trend of reduced spreading potential. This suggests that Ser66 phosphorylation may oppose the effects of PKA-mediated post translational modification. As such, neither Ser66 nor Thr567 phospho-mimetic mutants are able to link the PKA-mediated post translational modification of ezrin to cell spreading.

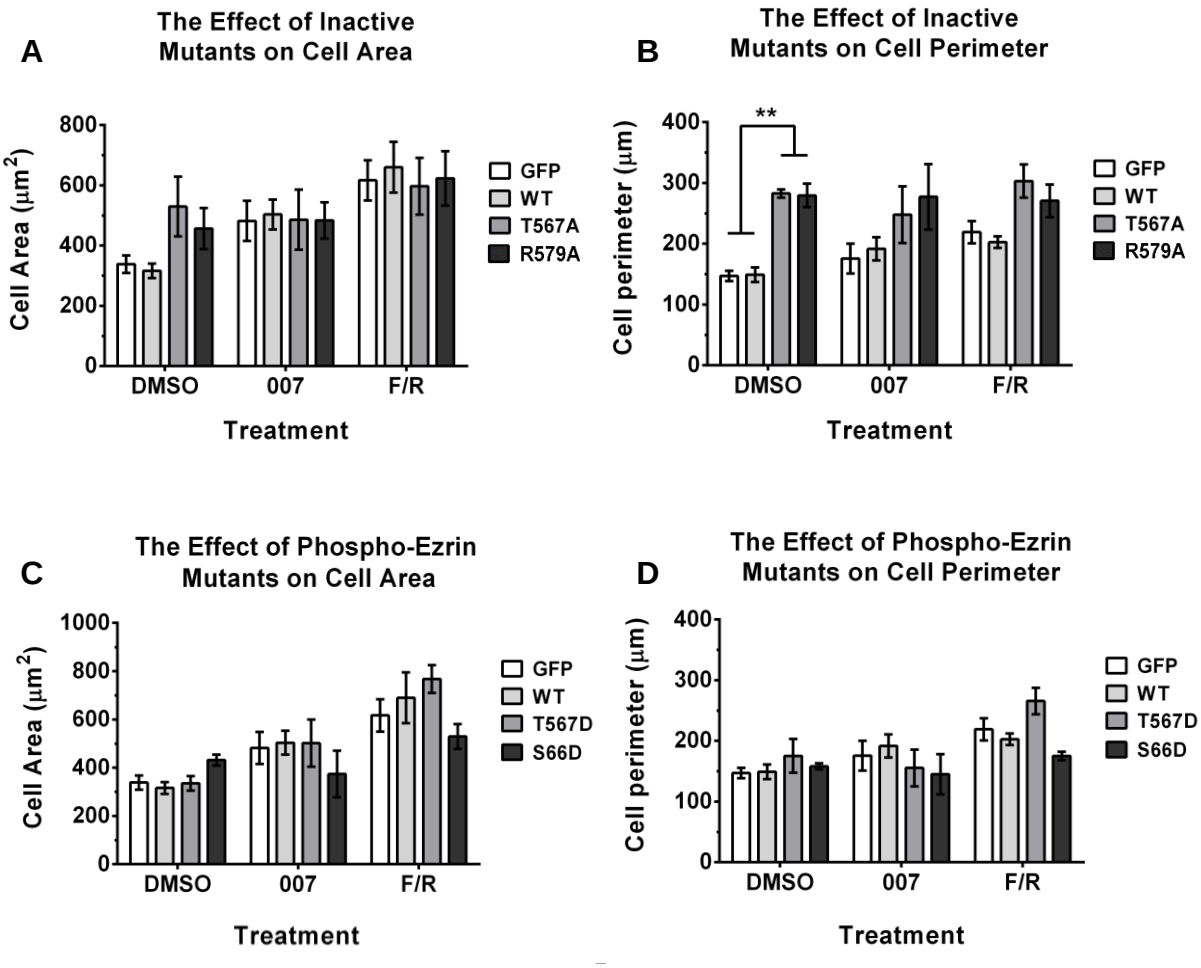

Figure 4-8 : Ezrin is not involved in cAMP-mediated spreading, but is involved in basal cell morphology.
HEK293T were transfected with the GFP-Ezrin constructs indicated, followed by stimulation with a DMSO vector control (12.8 mM, 60 minutes), 007 (10 µM, 60 minutes) or F/R (10 µM, 60 minutes). Ezrin-GFP expressing cells were imaged and cell areas (**A** + **C**) and perimeters (**B** + **D**) were calculated (5 images per experiment, N=3, +/-s.e.m.). Graphs A+B represent inhibitory mutants and graphs C+D represent active mutants, grouped and separated for ease of analysis (GFP and WT represent the same data sets in both graphs. **-p<0.01, two-way ANOVA using Tukeys post test. **E** - Representative images stained for F-actin with rhodamine phalloidin shown on following page. Red arrows indicate extended protrusions.

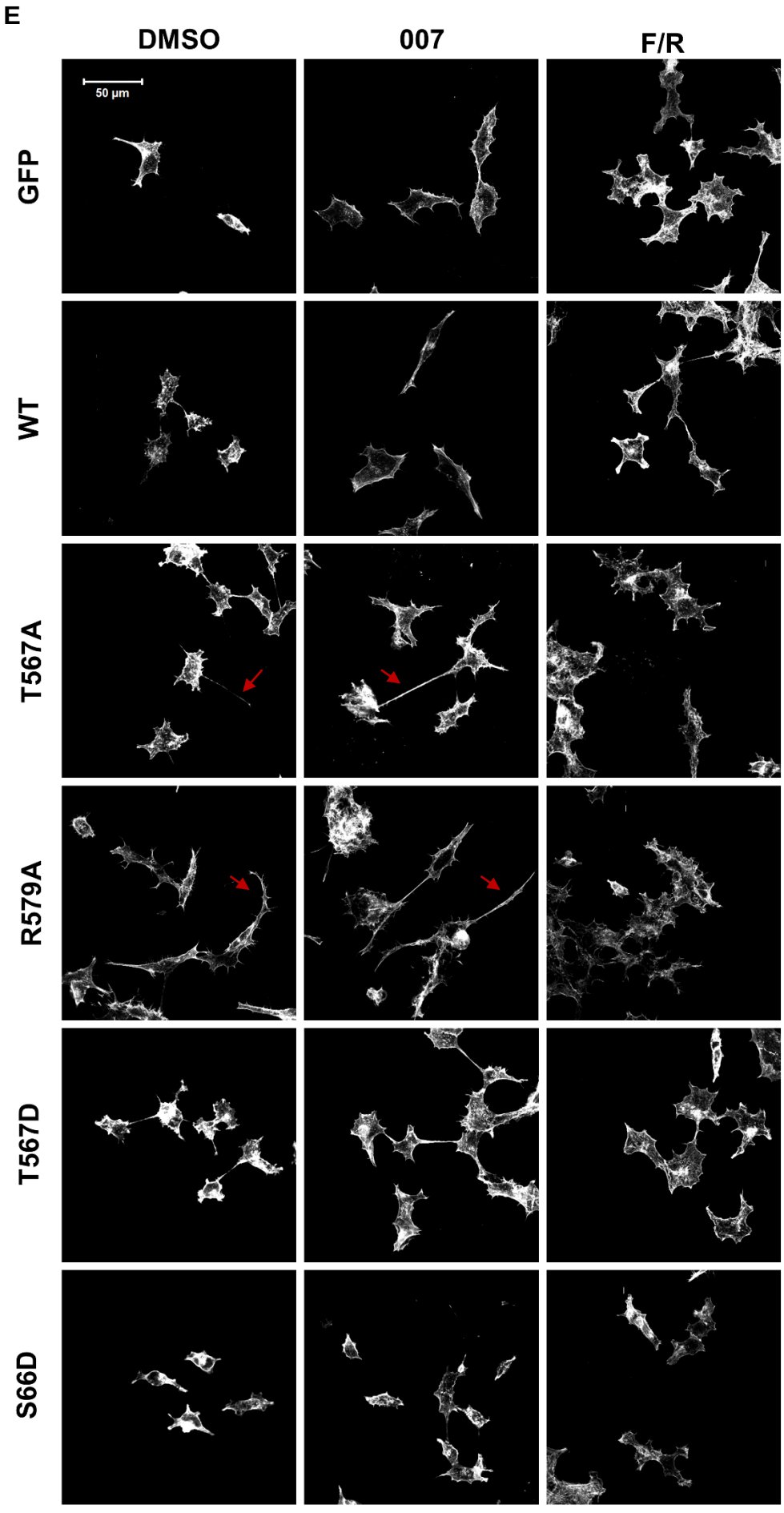
E
DMSO
007
F/R
50 µm
GFP
WT
T567A
R579A
T567D
S66D

4.2.7 ROCK Activation is required for Maximal Cell Spreading

RhoA is a Rho family GTPase that regulates cytoskeletal elements through the activation of RhoA activated protein kinase (ROCK) (Budzyn et al. 2006). PKA has been reported to alter the activity of the RhoA family of cytoskeletal regulators suggesting a potential mechanism through which PKA may promote cell spreading (Cardone et al. 2005). In order to assess whether cell spreading involves ROCK activity, vector- and EPAC1-transfected HEK293T cells were treated with the ROCK inhibitor, Y27632 alongside cAMP elevating agents. Cells were stained with rhodamine phalloidin in order to detect alterations in actin polymerisation and F/R-mediated spreading (Figure 4-9-A). Treatment of both vector- and EPAC1-expressing HEK293T with Y27632 had no effect on cell area (Figure 4-9). Interestingly, cell spreading in response to F/R activation was attenuated by 20% (+-9%) following ROCK inhibition, supporting a role for ROCK in cell spreading (Figure 4-9-B). Interestingly, ROCK inhibition promoted the formation of membrane protrusions similarly to cells transfected with T567A and R579A mutants, suggesting a possible link between ezrin Thr567 phosphorylation/actin binding and ROCK activity.

We propose that ezrin is not directly involved in HEK293T-EPAC1 spreading. Rather, ezrin is able to promote isotropic growth by stabilising the membrane and limiting actin rich projections. However, PKA appears to regulate this function by promoting Thr567 phosphorylation and the accumulation of ezrin at actin rich membrane ruffles subsequent to EPAC1 activation (Figure 4-6, Figure 4-7). Ezrin has been shown to affect Rho GTPase signalling by anchoring it to cell projections, suggesting a possible link between PKA, ezrin distribution, ezrin post translational modification and ROCK. However, ezrin does not appear to affect cell spreading and thus PKA may produce supplemental cell spreading through a distinct mechanism involving ROCK.

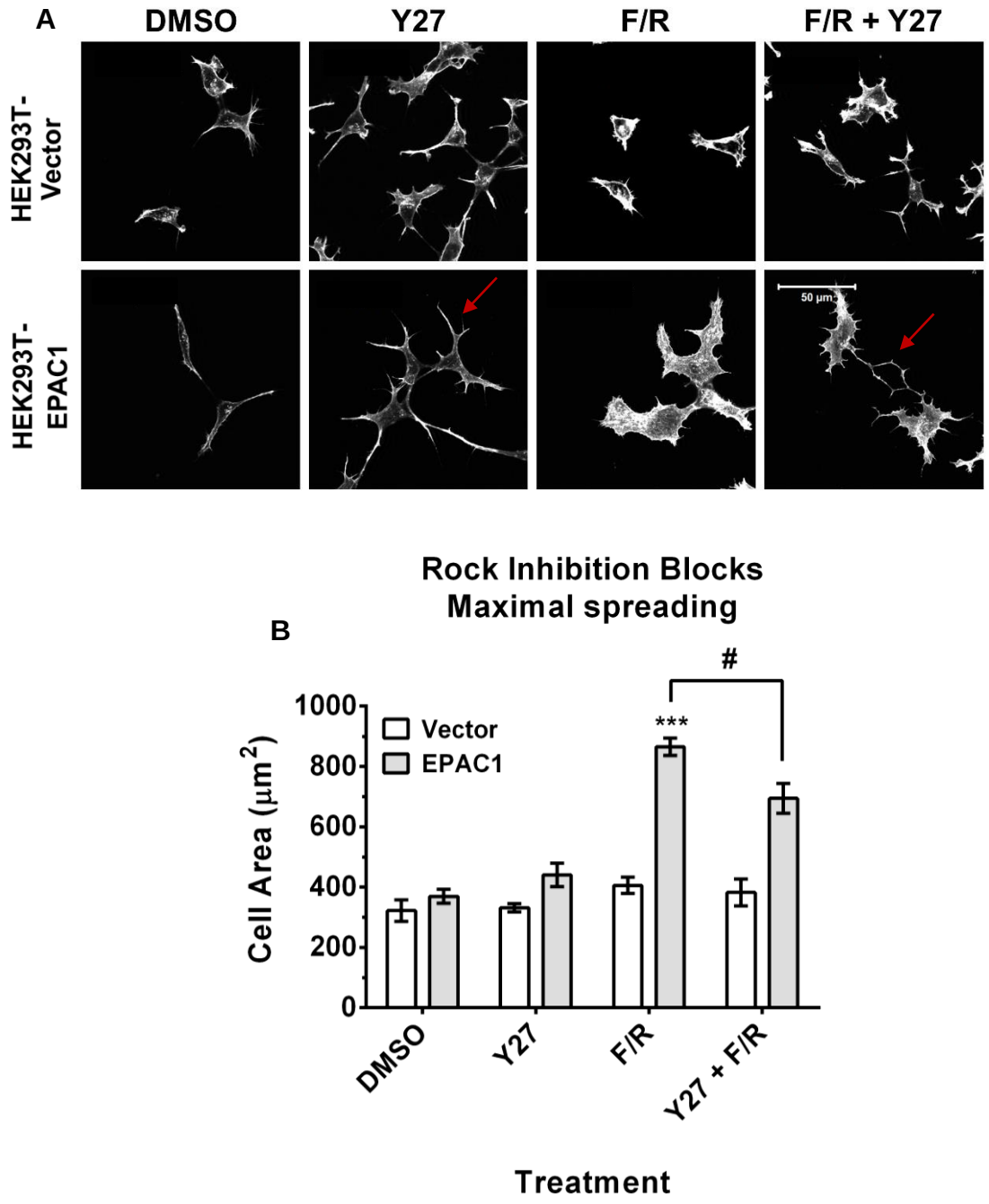

Figure 4-9 : The ROCK inhibitor Y27632 attenuates cell spreading in HEK293T cells. **A** - HEK293T-vector and or EPAC1 cells were stimulated for 60 minutes with forskolin plus rolipram (F/R, 10 µM) in the presence or absence of the ROCK inhibitor, Y27632 (Y27, 10µM), and then actin was visualised by microscopic detection of rhodamine phalloidin. Red arrows indicate the formation of elongated protrusions. **B** - Cell areas were calculated and presented as histograms (mean +/- s.e.m.). Significant differences are indicated; # - $p<0.05$ and *** - $p<0.001$, two way ANOVA using Tukeys post test, n-3.

4.3 DISCUSSION

In this chapter, the role for cAMP in the regulation of cell morphology has been observed to involve both EPAC1 and PKA in HEK293T cells. Importantly, in all cell lines tested, direct activation of EPAC1 is sufficient to induce cell spreading and in cells which do not express EPAC1, cAMP is unable to provoke cell spreading. Thus, EPAC1 appears to play a central role in the cell spreading response and contributes to a growing appreciation of the importance of EPAC1 in the control of cell morphology (Gupta and Yarwood 2005; Sehrawat et al. 2008).

Although EPAC1 is important for cell spreading in HEK293T cells, cAMP elevation consistently produced cell areas greater than EPAC1 activation alone in both HUVEC and HEK293T-EPAC1 cells. One explanation is that higher levels of EPAC activation were produced following F/R stimulation than by 007 stimulation, an effect that may produce distinct cellular signalling, as has been previously reported (Yokoyama et al. 2008). However, in order to confirm the role of PKA in the regulation of these processes the PKA inhibitor H-89 was used to regulate the PKA component of the cAMP signal. Indeed, inhibition of PKA was able to attenuate F/R induced spreading but had no effect on cell spreading induced by 007 stimulation. This suggests a secondary, synergistic effect of PKA on cell spreading. This secondary effect was dubbed supplemental cell spreading, due to the intrinsic requirement of a primary EPAC1 activation event (Figure 4-10). The requirement of EPAC1 for the synergistic effects of PKA on cell spreading may be particularly important in light of novel EPAC1 specific inhibitors recently developed (Courilleau et al. 2012). However, care must be taken when assessing the effects of H-89, as it is a potent inhibitor of a range of kinases in addition to PKA (Lochner and Moolman, 2006). However, the ability of H-89 to reverse the effects of cAMP elevation on the post translational modification of ezrin suggests a specific PKA effect. Future work may require the effects of PKA to be assessed through use of a less promiscuous inhibitor, such as the peptide inhibitor PKI.

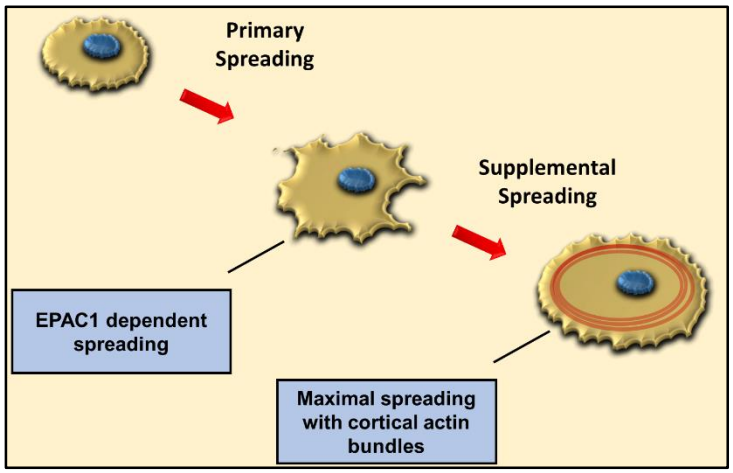

Figure 4-10 : Schematic of EPAC1 spreading
The two stages of cell spreading are outlined. EPAC1 is required for the initial spreading effect, however maximal cell spreading is only observed when both EPAC1 and PKA pathways are activated in concert. This correlates with an increase in cortical actin bundling.

Much work has centred on EPAC1-mediated regulation of the Rho family of GTPases. Indeed, EPAC1-Rap1 signalling through VAV/TIAM has been shown to provoke morphological change primarily through RAC (Arthur et al. 2004; Birukova et al. 2007; Birukova et al. 2010). However, PKA has been shown to produce morphological change by down-regulation of RhoA activity through phosphorylation of RhoGDP dissociation inhibitor, which forms an inactive complex with RhoA when activated (Oishi et al. 2012). As such, the putative role of the RhoA effector, ROCK, in PKA mediated supplemental spreading was tested.

The ROCK inhibitor, Y27632, reduced cell spreading in response to F/R. However, neither PKA inhibition nor ROCK inhibition reduced cell spreading below that of EPAC1-mediated spreading produced by 007. We therefore propose that PKA and ROCK act through a shared mechanism completely independent of EPAC1-mediated spreading. Interestingly, PKA appears to activate the RhoA pathway, rather than inhibiting the effects of RhoA, as has been previously observed (Oishi et al. 2012). However, despite confirming that ROCK inhibition can limit cell spreading, it is important to indicate a direct link between PKA and RhoA/ROCK activation. This could be achieved by RhoA pulldown with either the RhoA-GTP binding protein Rhotekin, or immunoprecipitation with antibodies specific for the active form of RhoA (Birukova et al. 2010; Gozo et al. 2013). Furthermore, the

same protocol is available to measure RAC activity in response to EPAC1 activation, which may confirm the reported activation of RAC in response to EPAC1 (Birukova et al. 2007; Birukova et al. 2010). Further work is required to determine the roles of the RhoA and RAC pathways in cAMP-mediated cell spreading, though the involvement of cAMP in regulating Rho GTPases, cell spreading and vascular endothelial barrier function is particularly compelling considering the emergence of novel regulators of the EPAC pathway.

In addition to cell spreading, the supplementary effects of PKA appear to be responsible for the reorganisation of the actin cytoskeleton. Cortical actin bundling is observed only when both EPAC and PKA pathways are activated in concert, suggesting synergy between cAMP pathways (Figure 4-3). Recently, the ERM protein ezrin has been implicated in EPAC1-mediated cell spreading (Ross et al. 2011). Ezrin is able to regulate cortical actin structures and membrane dynamics (Liu et al. 2012) and, furthermore, both PKA and ROCK are involved in regulating ezrin by direct phosphorylation of key activation sites (Matsui et al. 1998; Zhou et al. 2003; Zhu et al. 2007). We therefore attempted to characterise the role of ezrin in cytoskeletal organisation and morphology.

Interestingly, a direct link between PKA activity and the post translational modification of ezrin supported a potential mechanism underlying supplemental spreading and cortical actin bundling. The F/R stimulated increase in molecular weight is consistent with a phosphorylation event, suggesting that PKA may induce ezrin phosphorylation. Although only a small component of total cellular ezrin is observed to become modified, this is in agreement with previous reports suggesting that rapid turnover prevents the accumulation of phospho-forms (Zhu et al. 2007). It would be useful in future experiments to employ phosphatase inhibitors to limit the turnover of ezrin phosphorylation, facilitating the study of ezrin and its cellular effects.

In order to test the relationship between ezrin and cell morphology, a range of ezrin mutants were introduced into HEK293T cells (Figure 4-8). Notably, inhibiting Thr567 phosphorylation (with mutant T568A), or the interaction between ezrin and actin (with mutant R579A) had a striking effect on cell morphology. However, the effect of these mutants was in sharp contrast to the response to EPAC1

activation (Figure 4-8). Whereas EPAC1 activation produced uniform isotropic growth (Figure 4-3), changes in cell area in ezrin transfected cells was associated with the formation of multiple projections from the cell and a large increase in the basal perimeter. These results suggest that ezrin is involved in maintaining basal cell shape, but is uninvolved in EPAC1-mediated cell spreading.

Despite not being involved in the process of EPAC1-mediated cell spreading, we endeavoured to assess the effects of PKA-mediated post translational modification on ezrin distribution and cytoskeletal regulation. Indeed, the introduction of inactive mutants affected the morphology of transfected cells. The similarity between ezrin-T567A and the actin binding mutant R579A in cell morphology (Figure 4-8) suggests that ezrin-T567A may no longer be able to form stable membrane-actin linkages. Indeed earlier reports have suggested that active ezrin plays a role in stabilising the plasma membrane and regulating the formation of cell projections (Saleh et al. 2009). These results suggest a potential mechanism by which ezrin can regulate cell shape, and a mechanism by which PKA may potentiate the EPAC1-mediated cell spreading effect.

Although we have been unable to identify the site of ezrin post translational modification that is responsive to PKA activation, altering ezrins actin binding activity and limiting Thr567 phosphorylation are able to affect basal cell shape and modelling of the actin cytoskeleton. The ability of PKA to regulate ezrin through post translational modification suggests a pathway involving PKA, ezrin and regulation of the actin cytoskeleton. We conclude that ezrin may therefore play a key role in regulating cell shape, but is not involved in EPAC1- or PKA-mediated cell spreading. Indeed, ezrin may act as a scaffold, maintaining membrane stability, rather than promoting cell spreading. This hypothesis is not incompatible with earlier reports of a requirement for ezrin in cell spreading (Ross et al. 2011), as ezrin knockout may have strikingly different effects compared to the overexpression of phospho-null/mimetic mutant forms performed here. It would therefore be interesting to confirm the reported effects of siRNA mediated knockdown of ezrin and to couple this with reintroduction of the ezrin mutants discussed here. Such an approach may confirm a basic requirement of ezrin in the control of cell morphology and determine the effects of mutant ezrin activity on cell morphology.

In conclusion, we propose that ezrin is involved in the cell spreading response of HEK293T-EPAC1 cells following cAMP stimulation by promoting isotropic growth by stabilising the cell membrane and limiting actin rich projections. We also propose that PKA regulates these functions by promoting Thr567 phosphorylation and the accumulation of ezrin at actin rich membrane ruffles subsequent to EPAC1 activation. In this regard ezrin has been shown to affect Rho GTPase signalling by anchoring it to cell projections (Saleh et al. 2009). In agreement with this we have found that inhibition of ROCK, inhibits cell spreading in response to F/R treatment of HEK293T-EPAC1 cells, suggesting a possible link between EPAC1, PKA-promoted ezrin redistribution and ROCK activity in the promotion of maximal cell spreading by cAMP.

Chapter 5 : Subcellular Distribution and Targeting of EPACs

5.1 Introduction

cAMP signalling is subject to compartmentalisation within the cell (Stangherlin and Zaccolo 2012). Control over the cAMP signal is mediated by the cAMP-specific phosphodiesterase (PDE) families which are able degrade cAMP into 5'-AMP, allowing precise control over signal duration and intensity (Stangherlin and Zaccolo 2012). In addition, the localisation of cAMP-PDEs allows the formation of distinct subcellular compartments rich in cAMP, leading to selective activation of co-distributed EPAC or PKA molecules. Therefore, cAMP signalling is regulated not only by the induction and depletion of the cAMP signal, but also by the localisation of effector molecules to cAMP rich compartments. Indeed, it has been shown that cAMP signalling molecules can produce strikingly different cellular effects as a result of intracellular targeting (Buxton and Brunton 1983).

A growing body of evidence suggests that the subcellular distribution of EPACs has a strong effect on the signalling pathways it activates. The first clues that indicated a role for compartmentalisation in the regulation of EPAC arose during the study of its redistribution during the cell cycle. During interphase EPAC1 was observed to adopt a perinuclear distribution (Qiao et al. 2002). However, as the cell cycle progressed, EPAC underwent redistribution, resulting in colocalisation alongside microtubules, the mitotic spindle and the contractile ring (Qiao et al. 2002). Subsequently, it was shown that interaction of EPAC1 with microtubules (Mei and Cheng 2005) and microtubule accessory proteins (Magiera et al. 2004; Gupta and Yarwood 2005; Yarwood 2005; Borland et al. 2006) is particularly important. In particular, EPAC1 was observed to stabilise microtubule polymerisation (Mei and Cheng 2005) and promote actin stability within vasculature endothelial cells (Gupta and Yarwood 2005; Sehrawat et al. 2008). Thus, the distribution of EPAC within the cell appears to determine the nature of the response to elevations in intracellular cAMP.

Recent studies have focused on the importance of the perinuclear distribution of EPAC1, which is dominant during interphase (Mei et al. 2002; Qiao et al. 2002; Wang et al. 2006; Liu et al. 2010; Gloerich et al. 2011). Nuclear localisation of EPAC1 appears to be mediated through interaction between the zinc finger domain of the nuclear pore component Ran binding protein 2 (RANBP2) and the catalytic

domain of EPAC1 (Gloerich et al. 2011). Interestingly, this interaction appears to limit the GEF activity of EPAC1, suggesting that complex formation may act to negatively regulate EPAC1 activity within the cell (Gloerich et al. 2011). Moreover, the intracellular distribution of EPAC1 has been shown to determine which pool of Rap GTPase is activated. For example, whereas Rap1 has been observed to localise at cell-cell junctions within vascular endothelial cells (Wittchen et al. 2005), Rap2 is located within a perinuclear compartment (Pannekoek et al. 2013). Therefore, the relocalisation of EPAC1 from a perinuclear locale to cell junctions may be required for EPAC1 to activate Rap1, rather than Rap2 activation. Interestingly, Rap1 is linked to beneficial barrier protective effects in vascular endothelial cells, whereas Rap2 appears to opposes these beneficial effects (Pannekoek et al. 2013), which further supports the idea that subcellular targeting of EPAC is vital to its function (Wittchen et al. 2005).

As a result of the growing appreciation of the importance of compartmentalisation for EPAC1 function, it is now important to dissect the mechanisms underlying EPAC targeting. EPAC1 has been shown to play an important role in vascular endothelial barrier function, although no effective therapeutics have yet been developed to regulate EPAC1 activity in this context. It may therefore be possible to regulate EPAC1 activity by altering its subcellular distribution. Determining the mechanisms controlling the intracellular distribution of EPAC1 may therefore yield both insighs into the role of compartmentalisation on cAMP signalling, as well as novel therapeutic approaches to regulate EPAC1 activity within disease states. Given the growing appreciation that compartmentalisation of EPAC proteins controls their function and activity, the aim here is to investigate the structural elements in EPAC isoforms that assist their recruitment to the nuclear membrane. An in depth understanding of EPAC targeting may allow the disruption of protein-protein interactions with disruptor peptides or small molecules, resulting in the redistribution of EPACs within the cell. Since targeting and function of EPAC1 appear to be intricately linked, disrupting the normal distribution of EPAC proteins may alter the effects of EPACs within disease.

In this chapter I aim to;

- Confirm nuclear localisation of EPAC1 within HEK293T cells.
- Identify the structural requirements for EPAC1 localisation.
- Use targeted mutagenesis to disrupt EPAC1 nuclear localisation.

5.2 Results

5.2.1 The Anti-EPAC1 (5D3) Antibody Preferentially Detects Active EPAC1

The subcellular distribution of FLAG-tagged EPAC1 was assessed in transfected HEK293T cells by immunofluorescence staining using the anti-EPAC1 (5D3) antibody purchased from New England Biolabs. Anti-EPAC1 (5D3) has been reported to preferentially interact with EPAC1 in the active, cAMP-bound state as the antibody epitope lies within the CNB of EPAC1 (Zhao 2006). Anti-EPAC1 (5D3) was able to detect EPAC1 protein in cells expressing EPAC1, but not in cells expressing vector alone (Figure 5-1-A). However, elevation of intracellular cAMP following treatment with forskolin and rolipram (F/R), led to increased EPAC1 immunofluorescence within the nuclei of transfected cells. In order to assess the importance of cAMP binding and activation on the nuclear enrichment of EPAC1, cells were transiently transfected with wild type EPAC1 (WT) or an EPAC1 mutant deficient in cAMP-binding (R279E; Figure 5-1-B). Whereas anti-EPAC1 (5D3) immunofluorescence increased within the nuclei of WT transfected cells following F/R treatment, cells expressing EPAC1 R279E were unaffected by elevated cAMP levels. Therefore, it appears that cAMP binding to EPAC1 is crucial to the increase in EPAC1 nuclear staining observed following F/R stimulation.

In order to assess whether EPAC1 accumulates in the nucleus following stimulation, we next compared the subcellular distribution of EPAC1 protein in HEK293T cells using antibodies that detect WT EPAC1 or the epitope tag fused to EPAC1 (Figure 5-2). This was achieved by transfecting HEK293T cells with HA-tagged EPAC1 (EPAC1-HA) and probing the intracellular distribution of EPAC1 with anti-EPAC1 (5D3) and anti-HA antibodies. Detection of intracellular EPAC1 with anti-HA antibodies revealed a distinct perinuclear distribution of EPAC1 (Figure 5-2-A), which is in agreement with published results (Gloerich et al. 2011). Furthermore, there was no more increase in EPAC1 nuclear staining following F/R stimulation in cells probed with an anti-HA antibody. Interestingly, immunoprecipitation (IP) of FLAG-tagged EPAC1 from transfected cells using the anti-EPAC1 (5D3) antibody resulted in greater levels of EPAC1-FLAG protein being precipitated following F/R stimulation (Figure 5-2-B). Given that the anti-EPAC1 (5D3) antibody preferentially detects EPAC1 in F/R-treated cells, these data

suggest that the subcellular distribution of EPAC1 is constant following F/R stimulation, and that differences in EPAC1 detection result from changes in anti-EPAC1 (5D3) antibody selectivity. Together these results demonstrate that EPAC1 is localised to the nucleus in HEK293T cells, where it becomes activated following elevations in intracellular cAMP.

5.2.2 EPAC1 and EPAC2 are localised to Distinct Subcellular Compartments in HEK293T Cells

EPAC1 and EPAC2 have been observed to exist within distinct subcellular compartments; hence whereas EPAC1 maintains a perinuclear distribution during interphase (Mei et al. 2002; Qiao et al. 2002; Wang et al. 2006; Liu et al. 2010; Gloerich et al. 2011), EPAC2 is largely cytoplasmic (Li et al. 2006; Niimura et al. 2009). In order to compare and contrast the subcellular distributions of each EPAC isoform, HEK293T cells were transfected, EPAC1-HA or EPAC2-HA constructs. EPAC protein distribution was then assessed using immunofluorescent confocal microscopy using an anti-HA antibody. In agreement with previous studies, EPAC1 was observed to accumulate at the nuclear membrane, whereas EPAC2 was distributed throughout the cell (Figure 5-3) (Li et al. 2006; Gloerich et al. 2011). Furthermore, co-staining of EPAC1 with the nuclear pore protein, RANBP2, revealed a strong level of colocalisation between EPAC1 and the nuclear pore complex (Figure 5-3-Inset). This colocalisation was not observed in EPAC2-HA transfected cells. It is interesting to note that the distribution of both EPAC1 and EPAC2 remained constant following F/R stimulation, despite previous reports that EPAC1 (Gloerich et al. 2011) and EPAC2 (Li et al. 2006) undergo translocation in following activation.

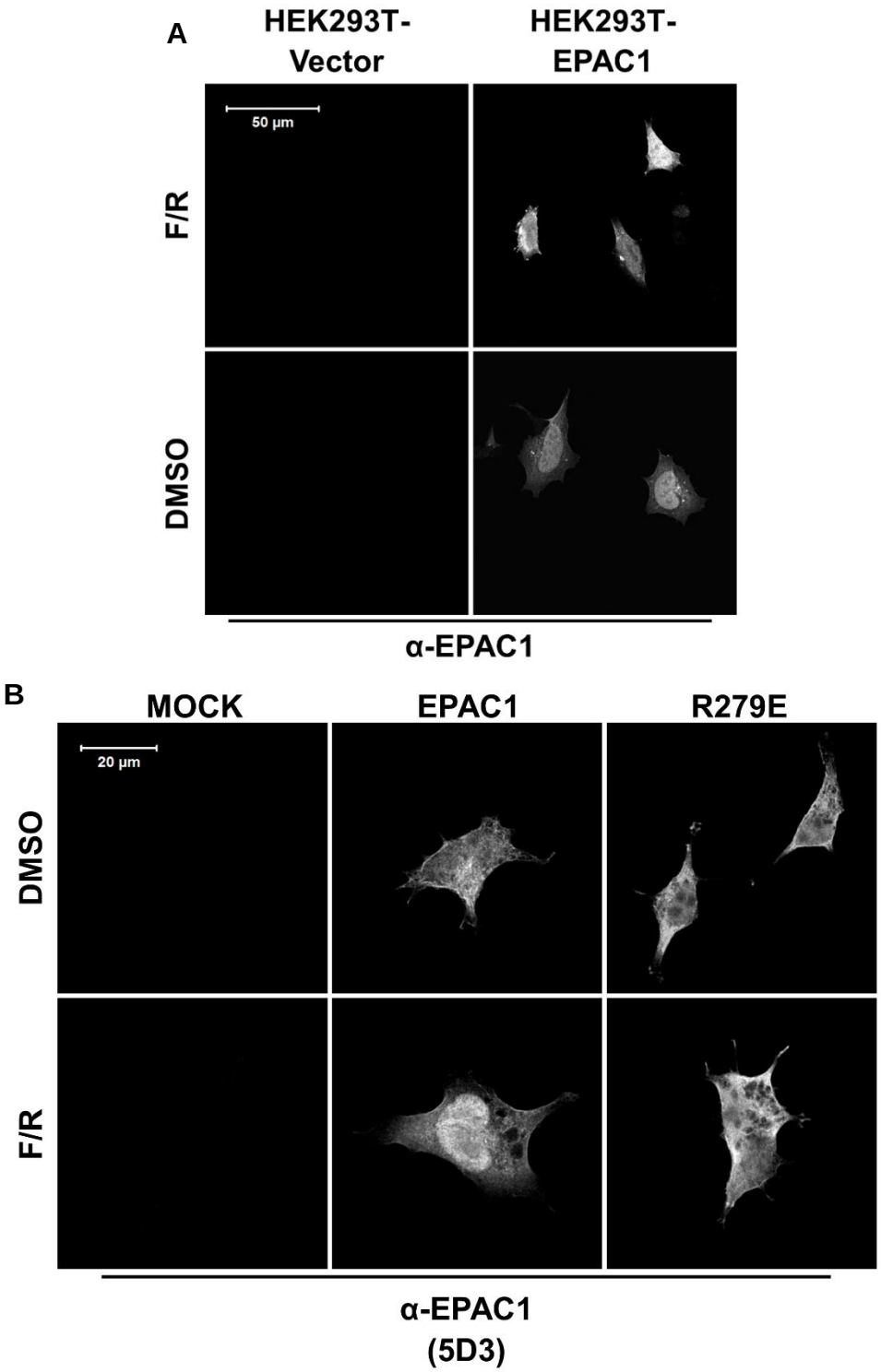

Figure 5-1 : Anti-EPAC1 (5D3) nuclear staining requires EPAC1 activation.
A – Stably transfected HEK293T cells, expressing either a vector or an EPAC1-FLAG construct were treated with a DMSO vehicle control (12.8 mM, 60 minutes) or a combination of forskolin and rolipram (F/R, 10 µM, 60 minutes). Cells were then fixed for immunofluorescent staining using anti-EPAC1 (5D3) antibody. B - HEK293T cells were transiently transfected with either wild type EPAC1 or EPAC1-R279E constructs and then incubated with DMSO vehicle control (12.8 mM, 60 minutes) or F/R (10 µM, 60 minutes), followed by immunostaining with an anti-EPAC1 (5D3) antibody.

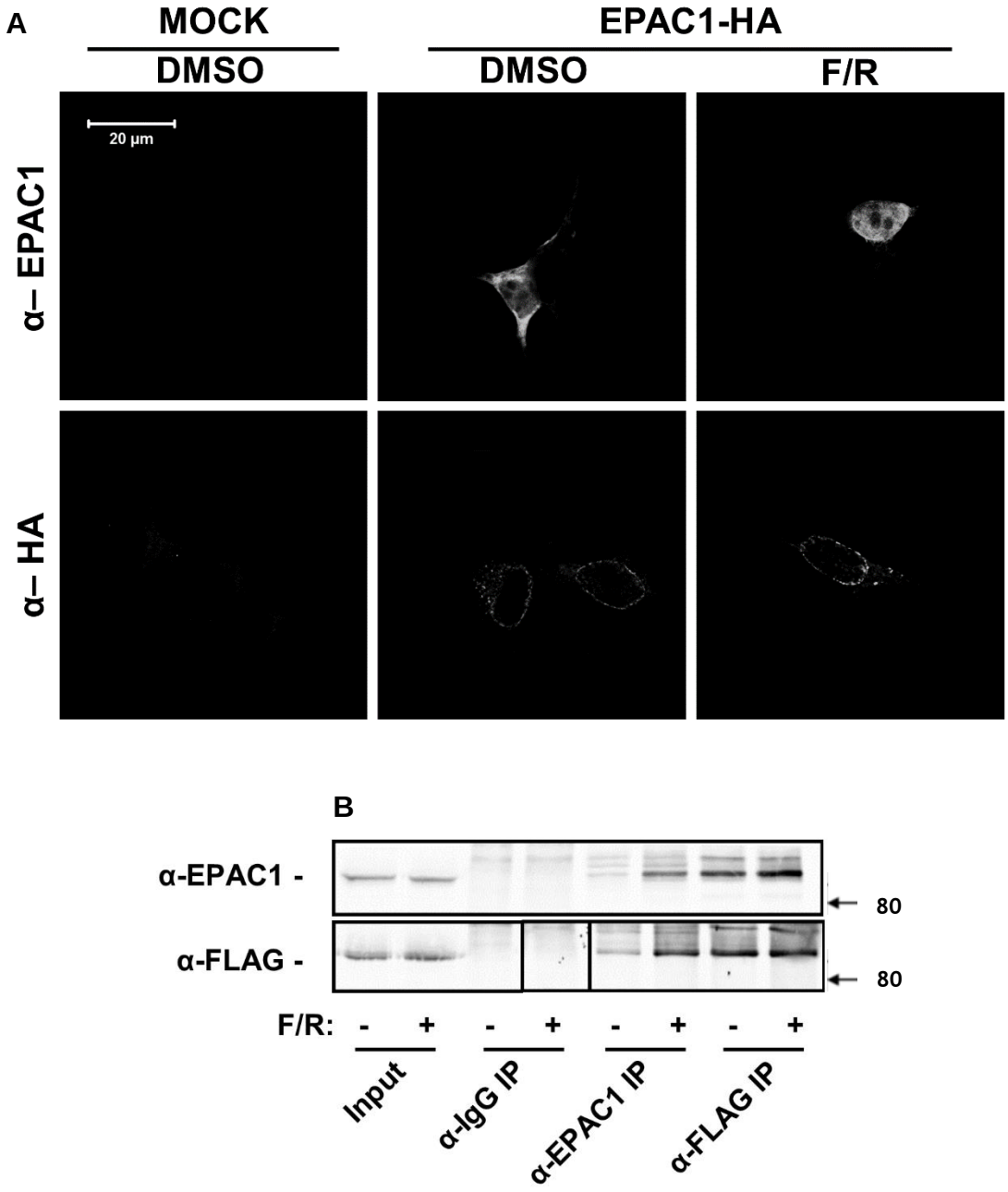

Figure 5-2 : Anti-EPAC1 (5D3) antibody binding is cAMP sensitive.
A - HEK293T cells were transiently transfected with either vector or EPAC1-HA construct. Cells were then treated with DMSO vehicle control (12.8 mM, 60 minutes) or F/R (10 µM, 60 minutes), fixed and then probed using anti-EPAC1 (5D3) or anti-HA antibodies as indicated. **B** - Immunoprecipitation of EPAC1 from stably transfected HEK293T cells. Cell lysates (input) were immunoprecipitated with anti-IgG (mouse), anti-EPAC1 (5D3) or anti-FLAG antibodies (square indicates lane moved for ease of presentation) and immunoprecipitates were then probed by western blotting for anti-EPAC1 and anti-FLAG as indicated. Positions of molecular weight markers are shown (kDa)

In order to confirm the nuclear localisation of EPAC1 (Figure 5-3), transfected cells were fractionated into nuclear and cytoplasmic components. Efficient separation of nuclear and cytosolic fractions was confirmed by the presence of the nuclear pore protein RANBP2 within the nuclear fraction only (Figure 5-4-A). Detection of EPAC1 and EPAC2 within each fraction by western blotting confirmed the distributions revealed by immunofluorescent techniques. Specifically, EPAC1 was enriched within the nuclear fraction alongside the nuclear pore protein RANBP2, whereas EPAC2 was enriched in the cytoplasmic fraction (Figure 5-4-A). Furthermore, densitrometric analysis of the cellular distribution of each isoform demonstrated that 68% (+/-8%) of total cellular EPAC1 but only 40% (+/-8%) of EPAC2 was found within the nuclear fraction (Figure 5-4-B). Indeed, EPAC1 was significantly more abundant within the nuclear fraction compared to EPAC2. Similar to the microscopic distribution observed (Figure 5-3), F/R stimulation had no effect on the distribution of either isoform between fractions. Although F/R stimulation was able to induce CREB phosphorylation, consistent with upregulated PKA activity (Delghandi et al. 2005), it was unable to induce EPAC translocation. This suggests that intracellular translocation of EPAC proteins, as previously reported (Li et al. 2006; Gloerich et al. 2011), may be cell type or condition dependent.

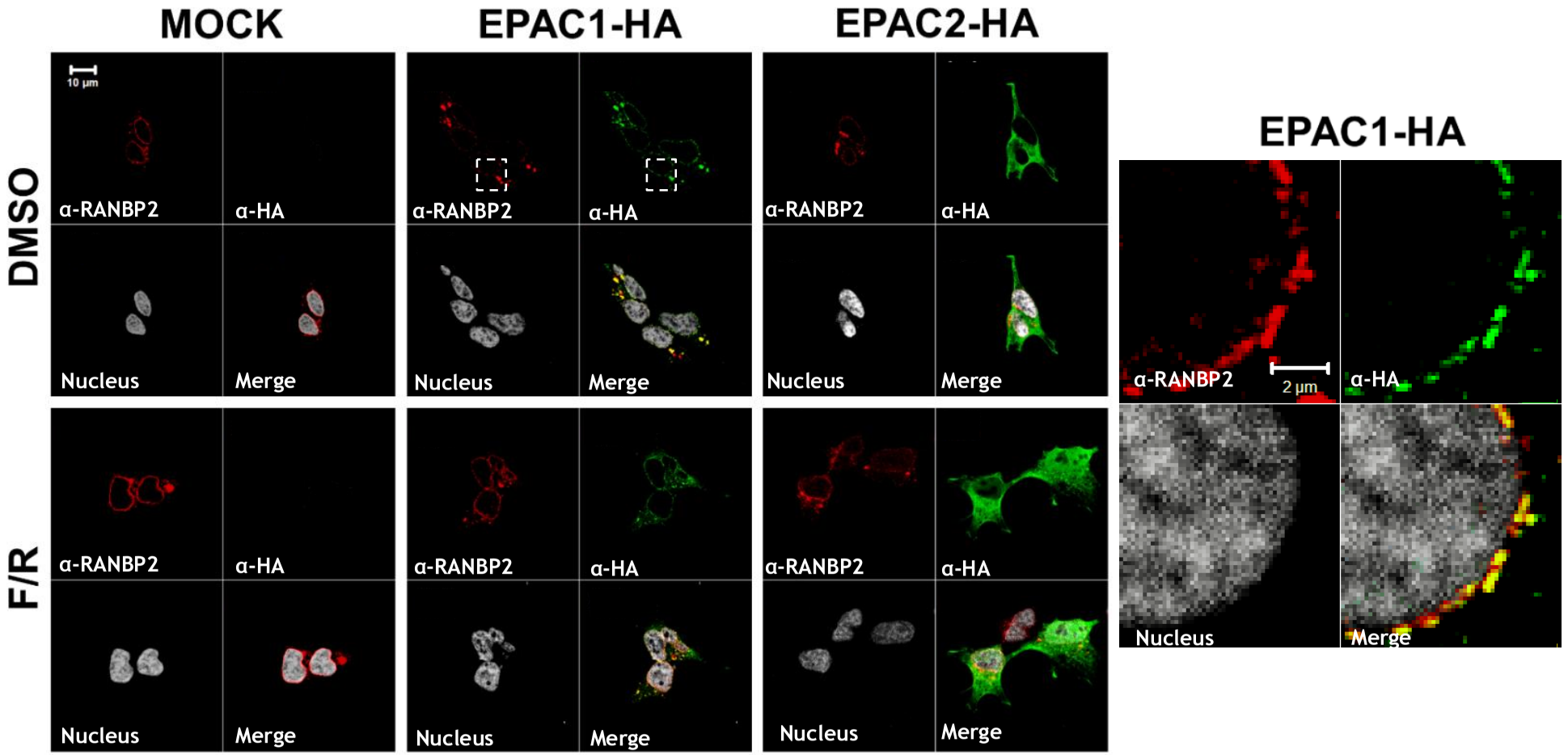

Figure 5-3 : The distribution of EPAC isoforms are different in HEK293T.
The distributions of EPAC1 and EPAC2 within HEK293T cells via detection of the fusion HA-tag with the anti-HA antibody (green). The nuclear pore protein RANBP2 is shown (red). The nucleus has been stained using “Reddot” (white). Inset indicates the strong colocalisation of EPAC1 with RANBP2 at the nuclear membrane under basal conditions (DMSO, 12.8 mM, 60 minutes).

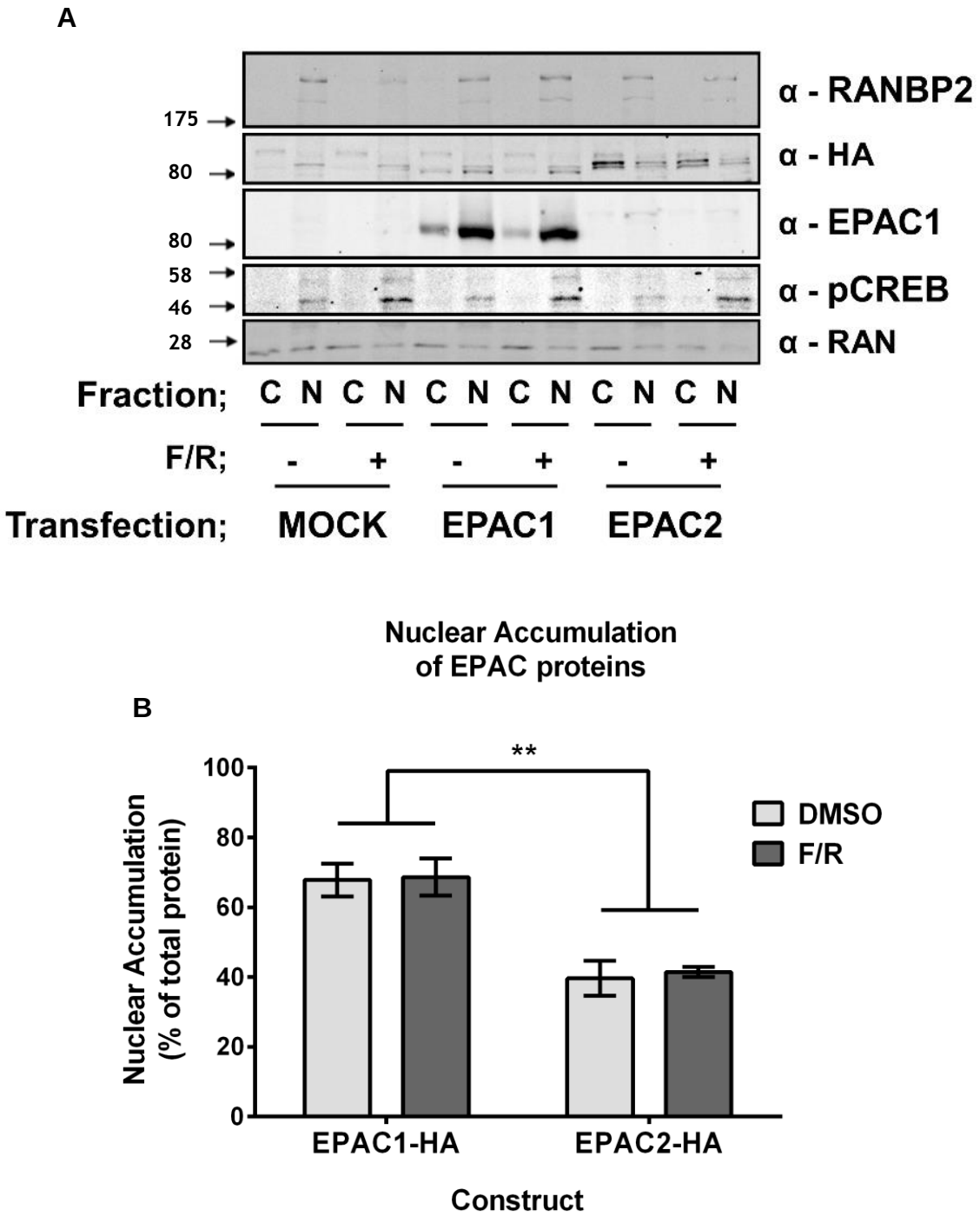

Figure 5-4 : EPAC isoforms fractionate to distinct pools.
HEK293T cells were fractionated following stimulation with DMSO (12.8 mM, 60 minutes) or F/R (10 µM, 60 minutes) into nuclear and cytoplasmic distributions. **A** - Fractions were western with the indicated antibodies. Position of molecular weight markers are shown (kDa). **B** - Accumulation of transfected protein into the nuclear fraction was assessed by densitrometric analysis of low intensity blots (n-3, +/-s.e.m.). ** - P<0.01 two way ANOVA using Dunnets post test.

5.2.3 The C-terminus of EPAC1 is involved in the Localisation of EPAC1 to the Nucleus

EPAC1 is localised to the perinuclear region with RANBP2 in transfected HEK293T cells (Figure 5-3). Indeed, a direct interaction between EPAC1 and RANBP2 has been proposed to control EPAC1 localisation (Gloerich et al. 2011). Both nuclear accumulation (Borland et al. 2006) and RANBP2 interaction (Gloerich et al. 2011) have been attributed to the CDC25 Homology Domain (CDC25-HD) of EPAC1, however the precise region of interaction has not yet been determined. In order to define the region of EPAC1 involved in its nuclear localisation, a range of truncated EPAC1 mutants were introduced into HEK293T cells. As previously reported (Borland et al. 2006; Gloerich et al. 2011) deletion of the N-terminal regulatory domain of EPAC1 up to the CDC25-HD (EPAC1 620-881) had no effect on nuclear accumulation, indicating that the N-terminus of EPAC1 is dispensable for nuclear targeting (Figure 5-5). In order to ascertain the region required for nuclear targeting, the CDC25-HD domain was truncated by 70 amino acid increments yielding EPAC1 691-881, 764-881 and 838-881. When transfected into HEK293T cells, both EPAC1 691-881 and EPAC1 764-881 were observed to show a similar distribution to wild type EPAC1 within the nuclear fraction (Figure 5-5). However, EPAC1 838-881 was observed to accumulate within the cytoplasmic fraction (Figure 5-5), suggesting nuclear localisation of EPAC1 may require amino acids 764-838.

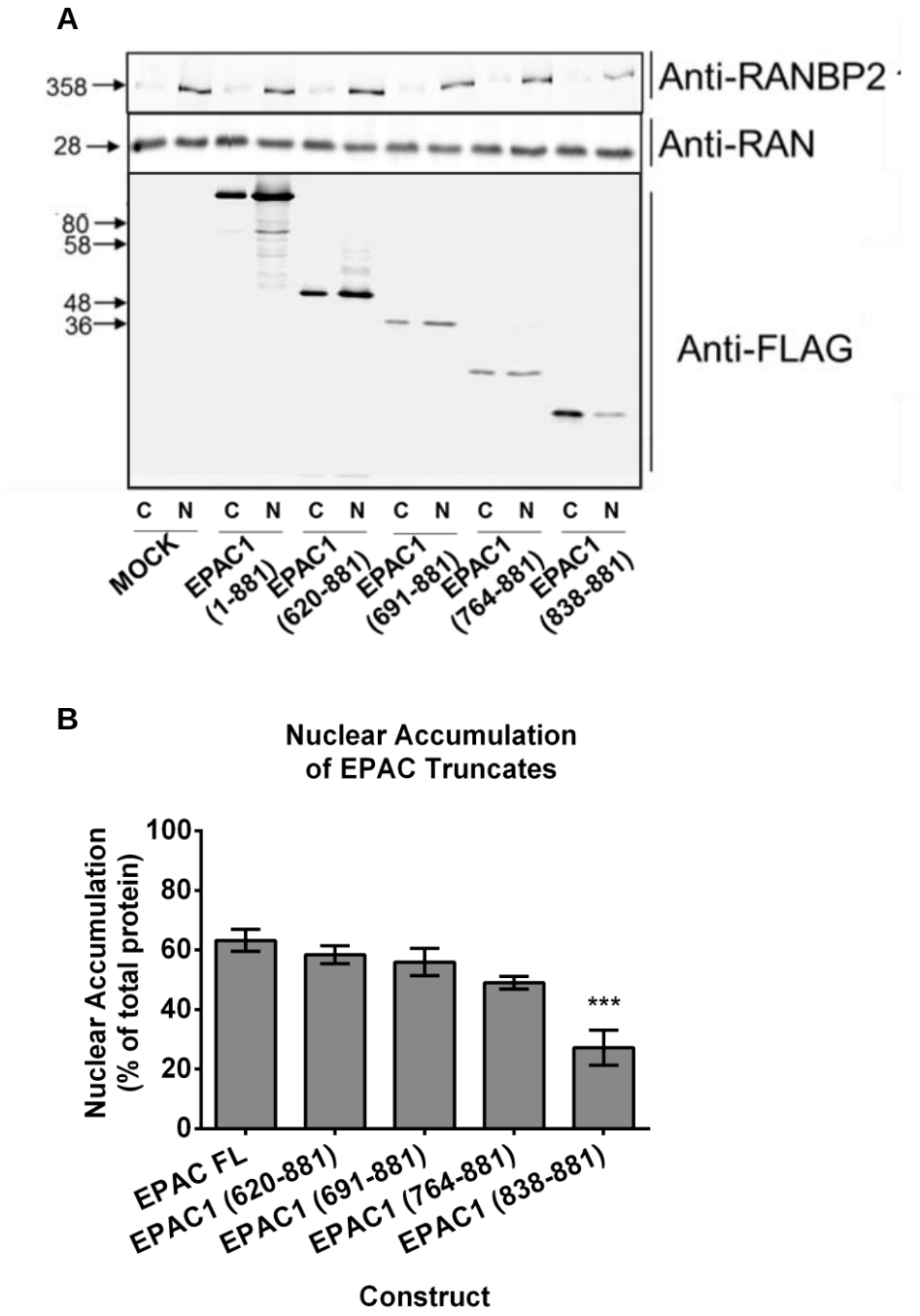

Figure 5-5 : EPAC1 nuclear localisation is reduced by deletion of amino acids 764-838. **A** – HEK293T cells were transiently transfected with truncated EPAC1 mutants, fractionated and cytoplasmic and nuclear fractions were western blotted with the indicated antibodies. **B** - Quantification of the relative distribution of EPAC1 transfected mutants into the nuclear fraction (+/- s.e.m.). ***- P<0.001, ANOVA using Dunnets post test, n-3. EPAC FL- full length EPAC1, 620-881 is the full CDC25-HD and 691-881, 764-881 and 838-881 represent further truncation through the CDC25-HD.

5.2.4 Amino acids 764-838 are involved in Targeting EPAC1 to the Nucleus

In order to confirm the importance of this region in nuclear targeting, amino acids 764-838 were deleted from full-length EPAC1 (EPAC1 Δ764-838) and the resulting mutant was transfected into HEK293T cells. Immunoblots of cell fractions from EPAC1- and EPAC1 Δ764-838 -transfected cells revealed higher levels of cytosolic EPAC1 Δ764-838 compared to wild type protein (Figure 5-6-A). Quantification of the immunoblots revealed that EPAC1 Δ764-838 displayed significantly reduced levels within the nuclear fraction (Figure 5-6-B), suggesting that the deleted residues are involved in nuclear localisation of EPAC1. In order to confirm that a loss in nuclear accumulation of EPAC1 represents a *bona fide* disruption of EPAC1 targeting, wild type and EPAC1 Δ764-838 were transfected into HEK293T cells and their intracellular distribution was analysed using immunofluorescent microscopy (Figure 5-6-C). In agreement with the fractionation data, deletion of amino acids 764-838 resulted in a redistribution of EPAC1 within the cell. Immuno-detection of FLAG tagged wild type EPAC1 demonstrated colocalisation with RANBP2 at the nuclear membrane, whereas EPAC1 Δ764-838 failed to accumulate at the perinuclear domain (Figure 5-6-C). Indeed, EPAC1 Δ764-838 adopted a largely cytosolic distribution demonstrating its reduced association with the nuclear fraction. Together, cell fractionation and immunofluorescent experiments implicate amino acids 764-838 of EPAC1 as being important for the regulation of EPAC1 subcellular distribution and represent a novel nuclear localisation domain (NLD) within EPAC1.

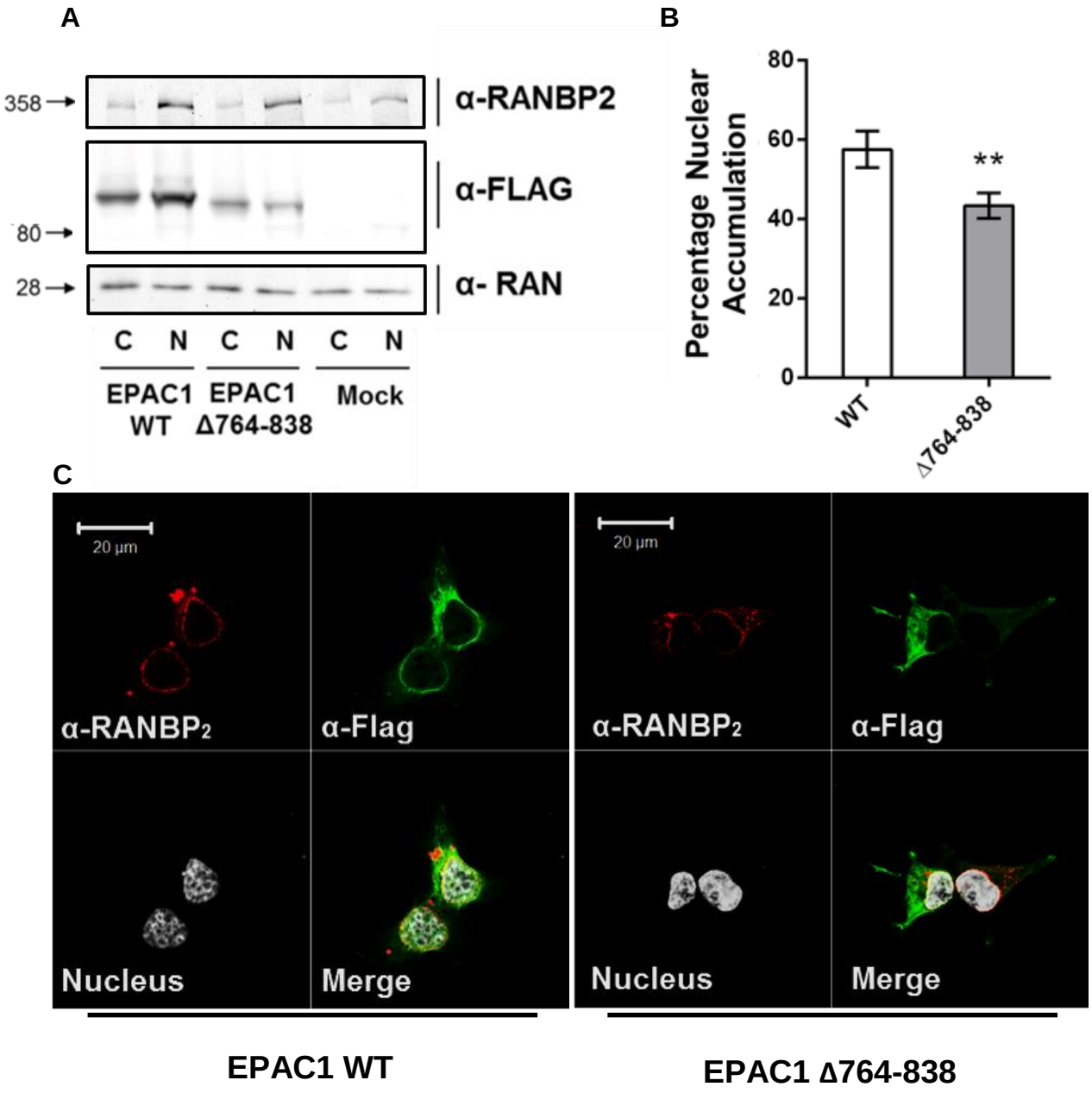

Figure 5-6 : Deletion of amino acids 764-838 limits EPAC1 targeting.
A - Western blot analysis of the cytoplasmic and nuclear components of HEK293T cells transfected with full length EPAC1 (WT) or a mutant lacking amino acids 764-838 (Δ764-838). Positions of molecular weight markers is shown (kDa). **B** – Densitometric intensity of bands from western blots were calculated and the percentage distribution of each mutant within the nuclear fraction is shown (+/-s.e.m.). ** - $p<0.01$, ANOVA using Dunnets post test, n-3. **C** - HEK293T cells transfected with EPAC1-WT (left) or EPAC1 Δ764-838 (right) were probed using anti-FLAG antibodies (green) to detect transfected EPAC mutants. The nuclear membrane is labelled using an anti-RANBP2 antibody (red) and Reddot nuclear stain is shown in white (nucleus). Overlapped images reveal co-localisation (merge).

5.2.5 Amino Acid Sequence Alignment of EPAC1 and EPAC2 Reveals Two Potential Nuclear Localisation Domains.

EPAC1 nuclear targeting has been linked to direct interactions between the EPAC1 CDC25-HD and RANBP2 (Gloerich et al. 2011). It is possible, therefore, that the putative NLD identified here (Figure 5-6) is involved in nuclear targeting through interactions with RANBP2. In addition, whereas EPAC1 accumulates at the nuclear membrane, EPAC2 is mainly cytosolic, suggesting that the targeting mechanisms involved are not shared between the two EPAC isoforms. Indeed, since EPAC1 is targeted to the nucleus by the NLD whereas EPAC2 is not, regions of low homology within this region may reveal structural differences which underlie the distinct subcellular distributions of the two proteins observed here (Figure 5-3).

In order to identify any sequence homology between the two isoforms, the primary sequence of EPAC1, amino acids 764-838, was aligned with the corresponding residues of EPAC2 (amino acids 915-979). Interestingly, the putative NLD overlaps with the EPAC1 CDC25-HD which is intimately involved in Rap-GTPase binding and GEF activity, as such, EPAC1 and EPAC2 share considerable homology within this region (Figure 5-7-A). However, two regions of low homology, dubbed Area1 and Area2, were identified that may underlie the differences in localisation observed between EPAC1 and EPAC2. In addition to low homology, both sites were determined to be available for protein-protein interaction by their solvent exposure (Figure 5-7-B). Area1 (composing residues R805, A806 and M809; EPAC1 nomenclature) sits within a groove between two conserved alpha helices and may form a suitable site for protein interaction. Area2 is a region of 15 amino acids which forms an extended loop, absent in EPAC2, which may be sufficiently long to allow the formation of secondary structure involved in protein-protein interactions. As a result of their low homology and their surface exposure, Area1 and Area2 represent putative regions involved in EPAC1 nuclear targeting.

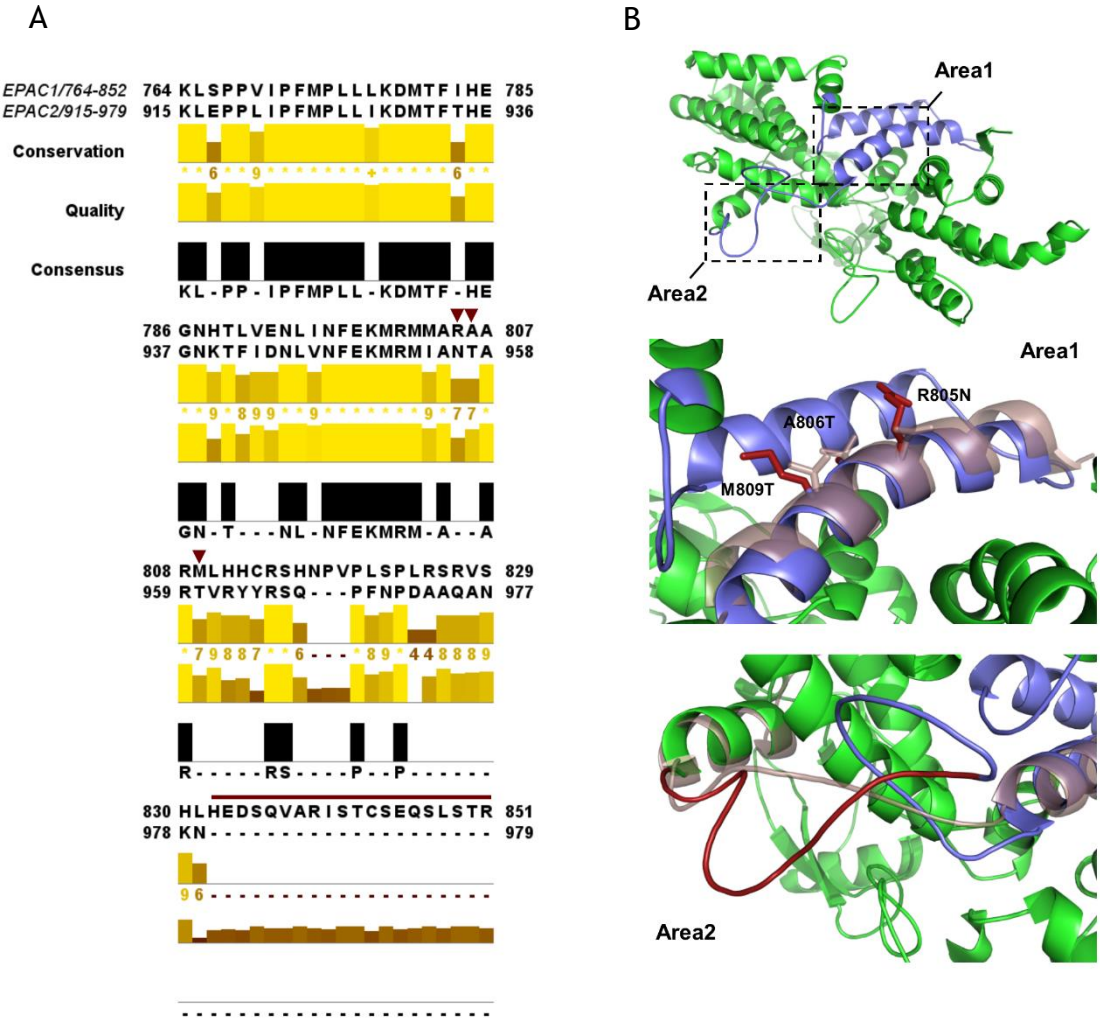

Figure 5-7 : Identifying regions of low homology between EPAC isoforms within the NLD. A - Sequence alignment of EPAC1 (amino acids 764-851) against EPAC2 (amino acids 915-979), incorporating residues 764-838 (NLD) and amino acids 839-851, which are absent in EPAC2, but present in EPAC1. This region is highly conserved with the exception of two regions which are also predicted to be surface exposed when mapped onto EPAC2 (2byv). The positions of Area1 point mutations (R805N, A806T and M809T) are indicated by red arrowheads. The residues deleted by mutagenesis in Area2 (amino acids 832-851) are highlighted (red line). B - Homology modelling of EPAC1 based on EPAC2 crystal structure (2byv) (Rehmann et al. 2006) shows the CDC25-HD (green) and putative NLD (Blue). Insets identify the potential interaction sites in Area1 and Area2, with the specific exposed surface residues of EPAC1 shown (red). The effects of EPAC1 mutagenesis to the corresponding EPAC2A sequences are shown by superimposing the structure of EPAC2A (purple, transparent).

5.2.6 Mutagenesis of either Area1 or Area2 does not affect the Subcellular Localisation of EPAC1

Area1 and Area2 (Figure 5-7) represent regions in EPAC2 that are potentially involved in nuclear targeting. In order to test the roles of Area1 and Area2, specific amino acids were mutagenized to the homologous residues of EPAC2. Since EPAC2 is not targeted to the nucleus and maintains catalytic activity, mimicking the sequence of EPAC2 in EPAC1, namely R806N, A807T and M810T, may disrupt nuclear localisation whilst maintaining catalytic activity. In addition, Area2 was mutated by removing amino acids 824-844 in EPAC1. In addition, a third EPAC1 mutant was designed to alter the secondary structure of the putative NLD and inhibit protein-protein interactions within this region; accordingly P819A, P821A and P824A (3P-A) mutations were designed to release the strict rigidity imparted by proline residues within the region between Area1 and Area2. Transfection of HEK293T cells allowed the nuclear accumulation of each mutant to be analyses by western blotting (Figure 5-8). As shown previously, wild type EPAC1 was found to retain a largely nuclear distribution, whereas EPAC1 Δ764-838 was enriched within the cytoplasmic fraction (Figure 5-8-A). However, the subcellular location of the Area1, Area2 and 3P-A mutants was found to be similar to that of wild type EPAC1. Indeed, quantification of immunoblots demonstrated that there was no significant difference in distribution between wild type EPAC1 and the mutant proteins (Figure 5-8-B). These data suggest that the difference in localisation observed between EPAC1 and EPAC2 is not due protein-protein interactions involving Area1 or Area2 of EPAC1.

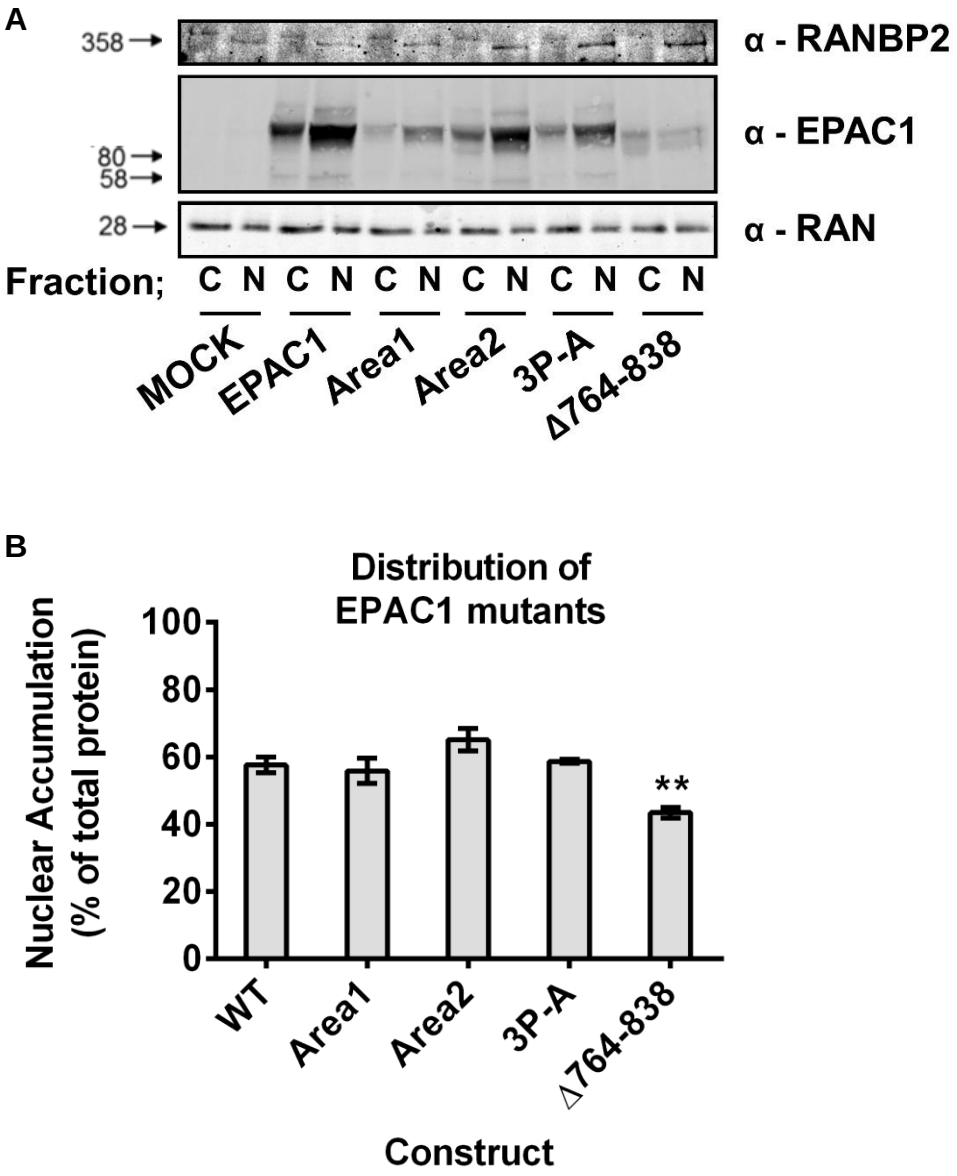

Figure 5-8 : Mutations within the EPAC1 NLD have no effect on the subcellular distribution of EPAC1.

HEK293T cells were transfected with wild type EPAC1 or NLD mutants. **A** – HEK293T cells were fractionated into nuclear and cytoplasmic compartments and transfected proteins were detected by immunoblotting with anti-EPAC1 (5D3) antibodies. The nuclear pore protein, RANBP2, was western blotted to demonstrate the fidelity of the fractionation process. Antibodies to Ran GTPase were used to demonstrate equal protein loading. **B** – Densitrometric analysis of band intensity was carried out and the amount of nuclear EPAC1 was calculated as a percentage of total protein observed (+/-s.e.m.). ** - $p<0.01$, ANOVA using Dunnets post test, n-3.

5.2.7 The CNB1 Domain of EPAC2 Interferes with Nuclear Localisation

The high degree of homology within the putative NLD of EPAC1 and EPAC2, combined with the inability of NLD mutants to affect nuclear localisation of EPAC1, suggests that EPAC2 targeting may be mediated by regions outside of the NLD. If so other structural differences between EPAC1 and EPAC2 may underlie the differences in subcellular localisation observed between the two proteins. One major difference between EPAC isoforms is the presence of a second N-terminal CNB (CNB1) (de Rooij et al. 2000) in EPAC2. Indeed, analysis of the crystal structure of EPAC2 (2BYV) (Rehmann et al. 2006) reveals that the CNB1 comes into close proximity with the N-terminal section of the putative NLD (Figure 5-9-A). It is therefore possible that steric interference from the CNB1 of EPAC2 blocks access of the NLD to potential nuclear localisation partners, such as RANBP2. Indeed, CNB1 has previously been implicated in the subcellular targeting of EPAC2 (Niimura et al. 2009). Interestingly, differential splicing of the EPAC2 gene in the adrenal glands results in the loss of the additional N-terminal CNB, CNB1, yielding a truncated form of EPAC2, namely EPAC2B (full length EPAC2 will henceforth be referred to as EPAC2A) (Niimura et al. 2009). In order to assess the importance of the CNB1 of EPAC2A in nuclear localisation, EPAC2A and EPAC2B were transfected into HEK293T cells and their subcellular distribution was compared with that of EPAC1. Whereas EPAC2B was observed to accumulate within the nuclear fraction, the full length EPAC2A construct was largely cytosolic (Figure 5-9-B). Interestingly, EPAC2B was observed to be present in the nuclear fraction at similar levels to EPAC1, achieving levels significantly higher than EPAC2A (Figure 5-9-C). These data support the CNB1 as an important factor in determining the subcellular distribution of EPAC2A.

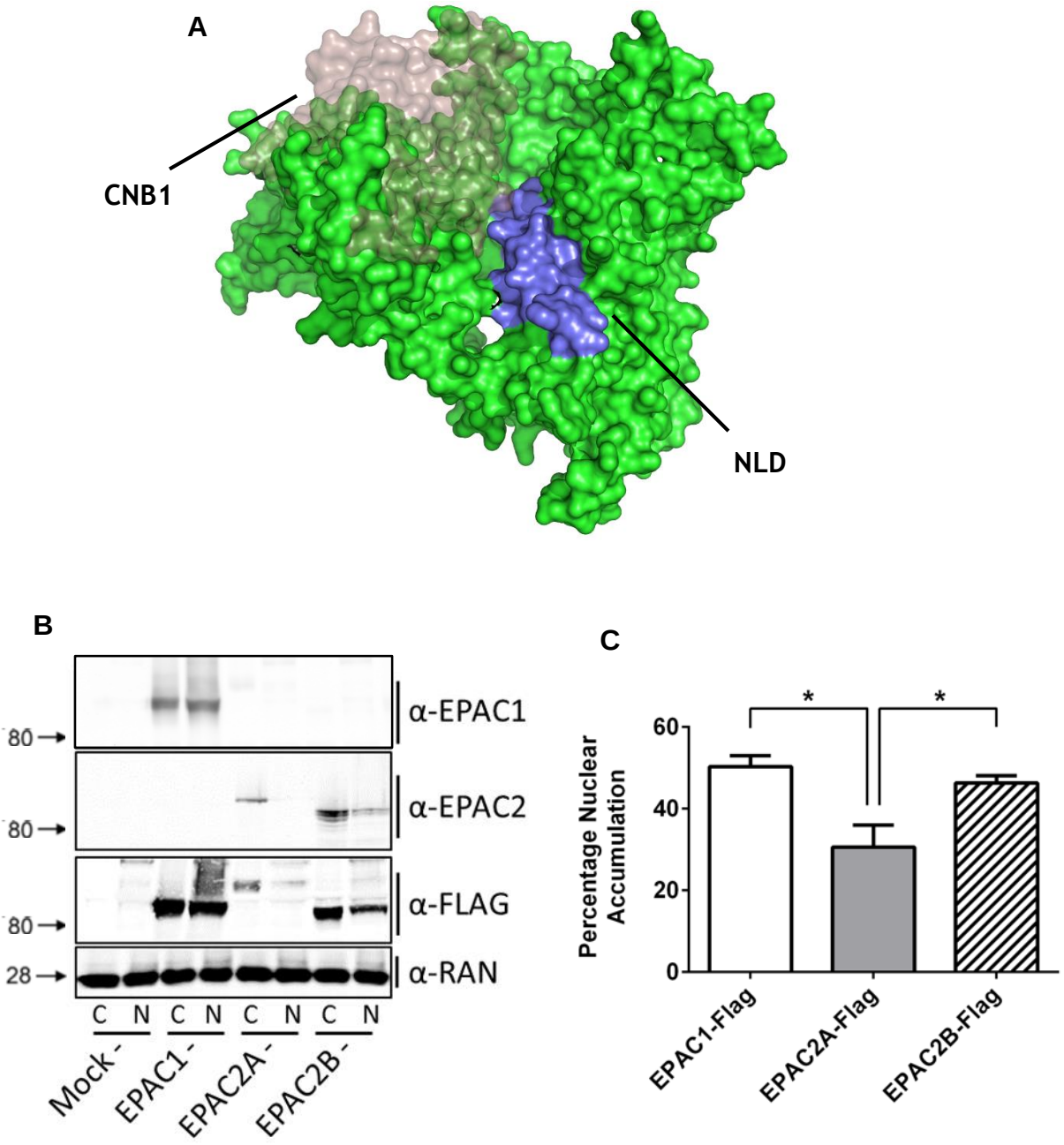

Figure 5-9 : EPAC2B is enriched in the nuclear fraction compared to EPAC2A.
A - A homology model of EPAC2B is shown (based on sequence alignment of EPAC2B with EPAC2A, crystal structure 2BYV, surface representation, green). The additional N-terminal CNB1 of EPAC2A is superimposed (purple, transparent) to highlight its proximity to the NLD. **B** - HEK293T cells were transfected with full length EPAC1, EPAC2A or EPAC2B. Fractionation and western blotting was carried out to reveal the accumulation of each mutant to the cytoplasmic or nuclear fractions. **C** - Quantitative densitometry of low exposure western blots was carried out and the calculation of nuclear EPAC is shown as a percentage of total protein (+/-s.e.m.). * - $p<0.05$, ANOVA using Tukeys post test, n-3.

5.3 Discussion

In order to study the effects of compartmentalisation of EPAC on cAMP signalling it was first necessary to accurately determine the localisation of EPAC within the cell. This was done initially by carrying out immunofluorescence of EPAC1-transfected cells using different antisera. Although the anti-EPAC1 (5D3) antibody from New England Biolabs successfully detected over-expression of HA-tagged EPAC1 (Figure 5-1), the distribution within the cell was strikingly different to that detected using anti-HA antibodies (Figure 5-1). This was due to the fact that the anti-EPAC1 (5D3) displayed selectivity for the active conformation of EPAC1, which was demonstrated by enhanced immunoprecipitation of EPAC1 following cAMP elevation. As a result, anti-EPAC1 (5D3) allowed immunofluorescent detection of the active pool of EPAC1 within the cell. In unstimulated cells this was observed within the cytosol, suggesting EPAC1 activation within this compartment at basal cAMP levels. However, in response to F/R stimulation immunostaining with anti-EPAC1 (5D3) revealed a strong nuclear enrichment in immunoreactivity, suggesting that EPAC1 is either shuttled into or activated within this compartment. This indicates that there is basal EPAC1 activation within the cytosol and cAMP elevation promotes an active pool within the nucleus. The preferential detection of active EPAC1 with the anti-EPAC1 (5D3) antibody may therefore provide a useful tool to investigate the effects of EPAC1 activation and targeting within the cell. However, to our knowledge, the properties of anti-EPAC1 (5D3) have not yet been taken advantage of to assess EPAC1 compartmentalisation.

A number of reports have reported the targeting of EPAC1 and EPAC2A to different subcellular locales (Li et al. 2006; Wang et al. 2006; Niimura et al. 2009; Gloerich et al. 2011). Indeed, we have confirmed here that the majority of cellular EPAC1 adopts a perinuclear distribution within HEK293T cells, whereas EPAC2A is largely distributed throughout the cell (Figure 5-3). Furthermore, a putative NLD was identified by determining the distribution of EPAC1 mutants truncated from the N-terminus. Fractionation experiments revealed that the regulatory domain, and the majority of the catalytic CDC25-HD domain, are dispensable for the nuclear localisation of EPAC1 (Figure 5-5). However, deletion of residues 764-838 within the CDC25-HD was sufficient to significantly reduce the association of EPAC1 with

nuclear fractions, supporting the idea that this region of EPAC1 plays a role in nuclear targeting. Although the EPAC1 Δ764-838 mutant displayed altered subcellular distribution, the region involved in nuclear targeting overlapped with the central catalytic site of EPAC1. As such, any significant alterations in this region are likely to disrupt catalytic GEF activity, and it was therefore not possible to further test the effects of EPAC1 nuclear targeting on downstream signalling pathways.

EPAC1 and EPAC2A display marked differences in their subcellular localisation and the targeting of EPAC1 appears to depend on residues 764-838. As such, areas of low homology between EPAC1 and EPAC2A, within the region spanning amino acids 764-838, were identified that may facilitate nuclear targeting. Three potential sites were identified, Area1, Area2 and 3P-A, which, due to their relative positions on the surface of EPAC1, may be involved in protein-protein interactions and nuclear targeting. Although mutagenesis of these regions failed to affect the subcellular localisation of EPAC1, they were identified as the only sites of low homology available for protein-protein interaction within this region. Since there is a high degree of homology between EPAC1 and EPAC2A in the remainder of the region 764-838, it was concluded that the putative NLD may, in fact, be shared between EPAC1 and EPAC2A. However, the differential localisation of EPAC1 and EPAC2A suggests that structural differences outside of the NLD may be responsible for the reduced nuclear accumulation of EPAC2A.

Recently, the extra, low affinity CNB1 of EPAC2A has been observed to be important in controlling its subcellular distribution (Niimura et al. 2009). Upon inspection of the crystal structure of EPAC2A (2BYV(Rehmann et al. 2006)) it can be seen that CNB1 lies in close proximity to the putative NLD identified within EPAC1. Although crystallisation of EPAC1 has not yet been achieved, homology modelling of EPAC1 suggested that amino acids 764-838 of EPAC1 are more exposed for protein-protein interaction than the homologous region of EPAC2A. In order to test whether the CNB1 of EPAC2A is involved in disrupting nuclear targeting, a novel, tissue-specific EPAC isoform, EPAC2B, was employed. EPAC2B is subject to alternate splicing, which results in the loss of CNB1, though the sequence is identical to EPAC2A outside of this region. Therefore EPAC2B represents an excellent tool in testing the importance of the CNB1 in nuclear

targeting. Indeed, the CNB1 of EPAC2A was observed to be important in promoting accumulation to the cytoplasmic fraction as EPAC2B exhibited significant enrichment within the nuclear fraction, similarly to EPAC1. This effect proves the importance of the EPAC2A CNB1 in promoting a cytoplasmic localisation; however the mechanistic role remains unknown. We propose that the CNB1 of EPAC2A forms intra molecular bonds that are absent in EPAC1 and EPAC2B, which disrupt protein interactions with RANBP2 (Gloerich et al. 2011) and, therefore, nuclear localisation. It would be particularly interesting to mutate the EPAC2B NLD to assess whether this region is responsible for the distribution of EPAC2B to the nuclear fraction (Figure 5-9). This may suggest that the CNB1 of EPAC2A may have developed as a mechanism to sterically block access to the NLD, which is common to all EPAC isoforms. CNB1 has also been reported to act via protein-protein interactions which tether EPAC2A to the plasma membrane (Niimura et al. 2009). As such it is important to test the manner in which EPAC2A localisation is mediated by CNB1.

Here we have further defined the regions involved in EPAC1 nuclear localisation. Nuclear localisation of EPAC1 has previously been attributed to interactions with the nuclear scaffold protein, RANBP2 (Gloerich et al. 2011). We have defined a NLD that exists within the CDC25-HD domain of EPAC1 and results in the co-localisation of EPAC1 with RANBP2 in HEK293T cells. However, further work is required to prove that nuclear localisation of EPAC1 occurs via protein-protein interactions with the NLD. Analysis of the NLD reveals a high degree of homology between EPAC isoforms, which suggests that the factors which control nuclear localisation may be shared between EPAC1 and EPAC2A. However, we propose that the CNB1 of EPAC2A may have developed as a mechanism to block access to the NLD and alter the distribution of EPAC2A relative to EPAC1. Indeed, the distribution of EPAC2A to the cytosol relies on the expression of CNB1. Such a mechanism may inform the development of peptides able to block nuclear targeting and alter the signalling pathways activated by EPAC1 within different cellular systems.

The localisation of EPAC1 is likely to affect its activation and the downstream signalling pathways activated as result of cAMP induction. As such, the study of the factors controlling its distribution may lead to therapeutics which influence

the localisation of EPAC, rather than its catalytic activity. Interestingly, EPAC1-/- mice have no reported abnormalities in vascular endothelial function, whereas EPAC1 activation is reported to produce protective effects in vascular endothelial cells (VECs) (Parnell et al. 2012). This apparent discrepancy may be explained by EPAC1 being under tight negative regulation within VECs. Indeed, nuclear tethering of EPAC1 is coupled to inhibition of its catalytic activity (Gloerich et al. 2011), suggesting that EPAC1 activity may be inhibited by nuclear sequestration. As such, displacement of EPAC1 from the nucleus may have dramatic effects, relieving its inhibition and inducing protective that have been attributed to EPAC1 activation within VECs (Parnell et al. 2012).

Chapter 6 : Discussion

6.1 Discussion

The potential for regulation of EPAC1 activity as a therapeutic avenue may be realised due to the recent discovery of a range of small molecule regulators of EPAC proteins (Table 1-1 and Table 1-2). However, despite the potential benefit of EPAC activation for the treatment of disease, particularly inflammatory diseases, there remains a lack of small molecule EPAC1-selective agonists.

In order to identify novel small molecules that are able to bind to and activate EPAC1, we have devised a novel HTS assay based on an existing fluorescence based competition assay, using the fluorescent cAMP analogue 8-NBD-cAMP. This assay has been shown to be effective in HTS and has been used to identify a number of small molecules capable of interacting with EPAC 1 and 2 (Tsalkova et al. 2012). The basis of the assay relies on an increase in fluorescence intensity associated with the binding of 8-NBD-cAMP to the CNB of EPAC protein. Here we have shown that EPAC1- and EPAC2-CNBs can be purified (Figure 3-1) and are able to bind to cAMP, or 8-NBD-cAMP, facilitating their use in this competition assay (Figure 3-3). Furthermore, we have devised experimental conditions that provide robust and reproducible identification of compounds which are able to compete with 8-NBD-cAMP for binding to the EPAC-CNBs (Figure 3-3 to 3-9). We have shown that screening EPAC1 and EPAC2 simultaneously in HTS allowed the identification of isoform selective small molecules within a pilot screen (Table 3-8). Previous attempts to perform dual EPAC1 and EPAC2 HTS may have been hindered by the requirement of existing assays for the catalytic activity of EPACs and the low solubility of full length recombinant EPAC1. However, the use of the isolated CNBs of EPAC1 and EPAC2 described here overcomes these difficulties. Simultaneous screening of both EPAC1- and EPAC2-CNBs not only increases the potential of discovering an EPAC1 selective compound, but allows greater stringency by allowing the elimination of non-specific agents at the primary screening stage. Indeed, we have described here the successful identification of an EPAC1-selective compound and numerous EPAC2-selective compounds from a small pilot screen. One of these compounds, conjugated oestrogen, is unlikely to be suitable for drug development due to the difficulty in producing and modifying steroid analogues and the likely extensive off target effects associated with using a ligand to endogenous hormone receptors. However, this small pilot screen highlights the

ability of dual EPAC1/EPAC2 HTS to isolate EPAC isoform selective compounds. As such, extensive, large scale HTS can now be carried out to isolate further compounds suitable for the future development of isoform selective EPAC regulators.

The 8-NBD-cAMP displacement assay identifies compounds that interact directly with the CNB of EPACs; however these interactions could either inhibit or promote EPAC activation. In order to discriminate between potential agonists and antagonists isolated in primary HTS, we devised a cell based screening assay which couples EPAC1 activation directly to HEK293T cell morphological change (Figure 3-12). Importantly, these cell shape changes rely on the expression of stably transfected EPAC1 and, as such, facilitate the comparison of rapid, isotropic cell spreading between vector- and EPAC1-expressing HEK293T cells, allowing confirmation of EPAC1 activation by small molecules. Furthermore, activation and inhibition of a variety of cAMP responsive pathways were unable to reproduce the distinct morphological changes associated with EPAC1 activation (Figure 3-12 to 3-15), demonstrating the specificity of this assay to EPAC1 activation. Thus, a cell spreading assay represents a powerful, stringent, in vivo mechanism to confirm the ability of small molecules to promote EPAC1 activation. Changes in cell shape and adherent properties can be measured in real time by measuring dynamic mass redistribution, namely the change in refractive index of a resonant waveguide grating (RWG) according to the mass of molecules, or in this case entire cells, attached to the surface. This approach is amenable to a high throughput plate format using Corning “EPIC” technology, where 96 well plates have incorporated RWG onto the adherent surface. This approach may allow a high number of potential agonists to be tested in a high throughput manner, and thereby facilitate the drug development process. The combination of an EPAC isoform-specific HTS approach and a secondary phenotypic assay, to discriminate between agonists and antagonists, represents a powerful approach to discover EPAC1 agonists (Figure 3-17), although further techniques may be required to adequately define the structure-activity relationship of any hit compounds. However, this screening cascade will facilitate drug discovery by promoting isoform selectivity, reducing the presence of denaturing agents and allowing common features which promote isoform selectivity to be identified prior to compound chemical modification.

The use of HEK293T-EPAC1 cell spreading in a drug screening assay prompted us to assess the mechanisms underlying EPAC1-mediated morphological change. Various studies have linked EPAC1-Rap1 activation to RAC activity and cell spreading (Arthur et al. 2004; Ross et al. 2011; Ross et al. 2012; Post et al. 2013). This pathway has been shown to have beneficial effects for vascular endothelial barrier function through a reorganisation of the actin cytoskeleton (Birukova et al. 2007; Birukova et al. 2008; Birukova et al. 2010). Despite a central role for EPAC in the control of barrier function, PKA appears to synergise with EPAC for maximal barrier protection in response to cAMP (Birukova et al. 2010). We hypothesised that EPAC1 and PKA may also synergise to promote cell spreading effects in response to cAMP and, indeed, both HEK293T-EPAC1 cells (Figure 3-12) and HUVECs (Figure 4-2) exhibited greater cell spreading when global cAMP levels were elevated with F/R than observed when EPAC1 was activated directly with 007. Interestingly, inhibiting PKA was able to reduce the spreading effects of global cAMP elevation, but not EPAC1 activation, supporting the idea that there is synergy between EPAC1 and PKA in cell spreading (Figure 4-4). However, PKA was unable to produce any alteration in cell area in the absence of EPAC1 expression, suggesting that PKA may play a supplementary role in cell spreading, but is unable to produce cell spreading alone. Despite the well characterised EPAC1-mediated activation of RAC (Post et al. 2013), PKA appeared to promote supplemental spreading through regulation of RhoA, as inhibition of the RhoA-activated kinase, ROCK, with Y27632 produced a similar, EPAC1 independent, attenuation of cell spreading (Figure 4-9). EPAC has previously been reported to act through RAC (Birukova et al. 2007); it is therefore possible that EPAC and PKA synergise through the classically antagonistic RAC and RhoA pathways (Ory et al. 2000). However, further work is required to characterise the role of the Rho GTPases in the cell spreading response.

In attempting to identify the mechanisms underlying EPAC1-mediated cell spreading and supplemental spreading, ezrin presented itself as a potential candidate. Ezrin has been implicated in regulating membrane stability (Bretscher 1999; Liu et al. 2012) and Rho GTPase activity (Takahashi et al. 1997) and, as such, may play a role in mediating cAMP-mediated cell spreading. Furthermore, ezrin has been reported to be involved in EPAC1-mediated cell spreading (Ross et

al. 2011). Moreover, both PKA and ROCK are able to directly phosphorylate ezrin and regulate its function (Matsui et al. 1998; Zhou et al. 2003; Haas et al. 2007).

Upon examination, ezrin was found to display a plasma membrane distribution (Figure 4-6) and undergo post translational modification (Figure 4-7) in response to cAMP elevation, which suggests a functional response to cAMP elevation. Indeed, post translational modification of ezrin was reversed by treatment with the PKA inhibitor H-89 (Figure 4-7), suggesting that PKA may directly phosphorylate ezrin, as has been previously reported (Wang et al. 2005). Despite these observations, introducing inactive ezrin mutants, or constitutively active mutants failed to affect either EPAC1-mediated or supplementary cell spreading (Figure 4-8). However, the introduction of inactive mutants (T567A (Ross et al. 2011) and R579A (Saleh et al. 2009)) drastically altered cell morphology promoting cell extensions, rather than the consistent cell spreading displayed in GFP or WT-ezrin transfected cells. It would appear that PKA is able to regulate ezrin and cell shape, but is unable to promote spreading, suggesting that the role of EPAC1 may be to promote cell spreading in response to cAMP, and a PKA-ezrin pathway regulates that manner in which this occurs. It would therefore be interesting to assess the effects of EPAC1, PKA and ezrin on vascular endothelial cell function and whether cell spreading and regulation of cell shape may also contribute to vascular endothelial barrier function. This may be particularly important in light of the development of EPAC1 inhibitors which, in addition to EPAC1 inactivation, may limit the synergistic, isotropic cell growth associated with PKA and EPAC1 activation.

The function of EPAC proteins has been shown to be affected by altered subcellular distribution (Li et al. 2006; Niimura et al. 2009; Consonni et al. 2012). EPAC1 has recently been shown to produce distinct effects within the vascular endothelium depending on the pool of Rap GTPase activated; for example, nuclear Rap2 activation reduced endothelial barrier function, whereas activation of plasma membrane Rap1 promoted it (Pannekoek et al. 2013). In this manner, altering EPAC1 localisation within vascular endothelial cells may shift the balance of Rap1/2 activation, producing a shift from pro-inflammatory to anti-inflammatory signalling. Furthermore, EPAC1 has been reported to be inactivated within a perinuclear complex with RANBP2 (Gloerich et al. 2011). As such,

disrupting this inhibitory complex may promote the anti-inflammatory effects of EPAC1 within vasculature endothelial cells.

EPAC1 and EPAC2 have strikingly different sub-cellular distributions when transfected into HEK293T cells. EPAC1 forms a strong perinuclear ring within the cell, whereas EPAC2 is observed throughout the cell (Figure 5-3). Indeed, this differential targeting may rely on structural differences between EPAC1 and EPAC2 that target each isoform to their respective locale. The nuclear pore protein RANBP2 has been reported to promote a perinuclear distribution and bind to EPAC1 within the catalytic CDC25-HD domain (Gloerich et al. 2011). We have identified a region important in promoting a strong perinuclear localisation within HEK293T cells. Indeed, deletion of amino acids 764-838 limits the distribution of EPAC1 alongside the pore protein within the nuclear compartment (Figure 5-6). Therefore, residues 764-838 within the CDC25-HD represent a potential binding site for the RANBP2 zinc finger domain, which is able to sequester and inhibit EPAC1 (Gloerich et al. 2011). However, we were unable to define the importance of targeting in EPAC1 function as this deletion overlaps the catalytic site of EPAC1, likely ablating its catalytic activity.

In addition to discovering a site important for the nuclear targeting of EPAC1, the role of the CNB1 of EPAC2 was investigated for its role in targeting of EPAC2 to the cytosolic fraction. As has been previously reported, a truncated form of EPAC2A, EPAC2B, which lacks CNB1 displays disrupted sub-cellular targeting (Niimura et al. 2009). In particular, EPAC2B was observed to be present within the nuclear fraction at significantly higher levels than EPAC2A (Figure 5-9). EPAC1 and EPAC2A show considerable homology within the nuclear localisation domain and mutagenesis of regions of low homology failed to disrupt EPAC1 targeting (Figure 5-8). We therefore conclude that the nuclear localisation domain is conserved between isoforms, but that EPAC2 is targeted to the cytosol by the CNB1. Indeed, mimicking the disruptive qualities of the CNB1 through small molecule or peptide intervention may allow EPAC1 to be displaced from the nuclear membrane, prompting both its catalytic activity and activation of an anti-inflammatory pool of Rap1 at the plasma membrane of vascular endothelial cells (Pannekoek et al. 2013). However, further work is required to confirm whether altered subcellular distribution is achieved by disrupting an interaction with RANBP2 or through

another mechanism. Indeed, it is possible that the CNB1 mediates an interaction with a hitherto unidentified cytosolic protein within HEK293T cells. In addition, it will be necessary to assess the functional significance of EPAC targeting within relevant physiologically systems, such as the vascular endothelium and pancreatic ß-cells. Controlling compartmentalisation of cAMP effectors provides a potential mechanism for precise regulation of cAMP signalling within the cell with therapeutic benefit.

6.2 Future Directions

We have shown that a dual EPAC1-CNB/EPAC2-CNB fluorescence based competition assay is effective in HTS for the identification of isoform selective EPAC interacting compounds. However, in order to identify potential small molecule regulators of EPAC1, large scale HTS is required. The joint European compound library provided by the European Lead Factory (www.europeanleadfactory.eu) contains a comprehensive range of over 300,000 drug-like compounds. Screening such a large library is likely to yield many hit compounds, which can be taken forward in further screening and development. In addition to the primary screen outlined, the suitability of HEK293T cell spreading for secondary screening must be assessed. Indeed, a plate based, high throughput approach using dynamic mass redistribution measurement is a strong candidate for discriminating between EPAC1 agonists and antagonists. However, such an approach must be rigorously tested for accuracy and reproducibility, although the requirement for EPAC1 in cAMP mediated morphological change suggests that comparison of EPAC1 expressing cells to null HEK293T is likely to allow reliable assessment of EPAC1 activation.

We have outlined a role for PKA in supplementing the effects of EPAC1 in cell spreading. However, the mechanisms which underlie EPAC1 and PKA-mediated cell spreading in HEK293T-EPAC1 remain unknown. Rho GTPases are strong candidates as downstream effectors of the cAMP signal and the ability of EPAC1 and PKA to regulate Rho GTPases would confirm a potential signalling pathway from cAMP to cell morphological change. Indeed, it would be interesting to test constitutively active or dominant negative Rho GTPases for their ability to promote or block cAMP-mediated cell spreading. The ability of EPAC1 and PKA to regulate Rho GTPases, coupled with their requirement in cell spreading, would provide strong evidence for a novel interplay between RhoA and RAC signalling pathways in the control of cell spreading. As ezrin appears to respond to PKA activation, but not EPAC1 signalling in HEK293T cells, the potential role of ezrin in anchoring PKA to the cell periphery should be tested, as this may be the functional mechanism through which ezrin may act to regulate cell shape. Once the precise signalling pathways involved in cell morphology have been found, their role in regulating vascular endothelial barrier function should be assessed in order

to establish EPAC1-mediated cell spreading as an important regulator of vascular function.

We have isolated a domain within EPACs that is involved in the nuclear localisation of EPAC1. In order to define the role of EPAC1 targeting in its signalling function, it will be necessary to disrupt EPAC1 from its normal distribution within the cell. One approach is to develop a disruptor peptide which may block accumulation of EPAC1 at the nuclear membrane. This would allow the precise role of EPAC1 nuclear targeting to be assessed. Furthermore, if the CNB1 of EPAC2A is indeed involved in blocking nuclear accumulation by an intramolecular interaction with the nuclear localisation domain, then the regions involved may form the basis of a disruptor peptide. To achieve this, a peptide array may be used to confirm both the presence of intramolecular interactions between the CNB1 and the nuclear localisation domain of EPAC2 and identify the residues involved. Finally, it would be interesting to identify the partners involved in nuclear targeting. The RANBP2-zinc finger has been proposed as an interacting partner with EPAC1 (Gloerich et al. 2011). Co-immunoprecipitation and pulldown experiments may provide one route to confirming the interaction between EPAC1 and the zinc finger domain of RANBP2.

List of References

Alcalay, Y., E. Hochhauser, V. Kliminski, J. Dick, M. A. Zahalka, D. Parnes, H. Schlesinger, Z. Abassi, A. Shainberg, R. F. Schindler, T. Brand and G. Kessler-Icekson (2013). "Popeye domain containing 1 (Popdc1/Bves) is a caveolae-associated protein involved in ischemia tolerance." PLoS One **8**(9): e71100.

Almahariq, M., C. Chao, F. C. Mei, M. R. Hellmich, I. Partikeev, M. Motamedi and X. Cheng (2014). "Pharmacological Inhibition and Genetic Knockdown of EPAC1 Reduce Pancreatic Cancer Metastasis in vivo." Molecular Pharmacology 87(2):142-9

Almahariq, M., F. Mei, H. Wang, A. T. Cao, S. Yao, L. Soong, J. Sun, Y. Cong, J. Chen and X. Cheng (2014). "Exchange Protein Directly Activated by cAMP (EPAC1) Modulates Regulatory T Cell-Mediated Immune Suppression." Biochemical Journal 465(2):295-303

Almahariq, M., T. Tsalkova, F. C. Mei, H. Chen, J. Zhou, S. K. Sastry, F. Schwede and X. Cheng (2013). "A novel EPAC-specific inhibitor suppresses pancreatic cancer cell migration and invasion." Molecular Pharmacology **83**(1): 122-128.

Ammon, H. P. and A. B. Muller (1985). "Forskolin: from an ayurvedic remedy to a modern agent." Planta Medica **51**(6): 473-477.

Andree, B., T. Hillemann, G. Kessler-Icekson, T. Schmitt-John, H. Jockusch, H. H. Arnold and T. Brand (2000). "Isolation and characterization of the novel popeye gene family expressed in skeletal muscle and heart." Developmental Biology **223**(2): 371-382.

Arthur, W. T., L. A. Quilliam and J. A. Cooper (2004). "Rap1 promotes cell spreading by localizing Rac guanine nucleotide exchange factors." Journal of Cell Biology. **167**(1): 111-122.

Aslam, M., F. V. Hartel, M. Arshad, D. Gunduz, Y. Abdallah, H. Sauer, H. M. Piper and T. Noll (2010). "cAMP/PKA antagonizes thrombin-induced inactivation of endothelial myosin light chain phosphatase: role of CPI-17." Cardiovascular Journal **87**(2): 375-384. .

Asli, N. G. S., C. ; Taosheng, C. (2013). Chapter 7; Data Analysis Approaches in High Throughput Screening. Drug Discovery.

Babenko, A. P., L. Aguilar-Bryan and J. Bryan (1998). "A view of sur/KIR6.X, KATP channels." Annual Review of Physiology **60**: 667-687.

Baggio, L. L. and D. J. Drucker (2007). "Biology of incretins: GLP-1 and GIP." Gastroenterology **132**(6): 2131-2157.

Baumer, Y., V. Spindler, R. C. Werthmann, M. Bunemann and J. Waschke (2009). "Role of Rac 1 and cAMP in endothelial barrier stabilization and thrombin-induced barrier breakdown." Journal of Cell Physiology. **220**(3): 716-726.

Beavo, J. A. (1995). "Cyclic nucleotide phosphodiesterases: functional implications of multiple isoforms." Physiological Reviews **75**(4): 725-748.

Beckers, C. M., V. W. van Hinsbergh and G. P. van Nieuw Amerongen (2010). "Driving Rho GTPase activity in endothelial cells regulates barrier integrity." Thrombosis and Haemostasis **103**(1): 40-55.

Ben-Aissa, K., G. Patino-Lopez, N. V. Belkina, O. Maniti, T. Rosales, J. J. Hao, M. J. Kruhlak, J. R. Knutson, C. Picart and S. Shaw (2012). "Activation of moesin, a protein that links actin cytoskeleton to the plasma membrane, occurs by phosphatidylinositol 4,5-bisphosphate (PIP2) binding sequentially to two sites and releasing an autoinhibitory linker." Journal of Biological Chemistry **287**(20): 16311-16323.

Berg, J., J. Tymoczko and L. Stryer (2002). Section 21.2, Phosphorylase Is Regulated by Allosteric Interactions and Reversible Phosphorylation. Biochemistry. 5th edition. New York, W H Freeman.

Bernardi, B., G. F. Guidetti, F. Campus, J. R. Crittenden, A. M. Graybiel, C. Balduini and M. Torti (2006). "The small GTPase Rap1b regulates the cross talk between platelet integrin alpha2beta1 and integrin alphaIIbbeta3." Blood **107**(7): 2728-2735.

Berthet, J., T. W. Rall and E. W. Sutherland (1957). "The relationship of epinephrine and glucagon to liver phosphorylase. IV. Effect of epinephrine and glucagon on the reactivation of phosphorylase in liver homogenates." Journal of Biological Chemistry **224**(1): 463-475.

Birukova, A. A., D. Burdette, N. Moldobaeva, J. Xing, P. Fu and K. G. Birukov (2010). "Rac GTPase is a hub for protein kinase A and Epac signaling in endothelial barrier protection by cAMP." Microvascular Research **79**(2): 128-138.

Birukova, A. A., T. Zagranichnaya, E. Alekseeva, G. M. Bokoch and K. G. Birukov (2008). "Epac/Rap and PKA are novel mechanisms of ANP-induced Rac-mediated pulmonary endothelial barrier protection." Journal of Cell Physiology. **215**(3): 715-724.

Birukova, A. A., T. Zagranichnaya, P. Fu, E. Alekseeva, W. Chen, J. R. Jacobson and K. G. Birukov (2007). "Prostaglandins PGE(2) and PGI(2) promote endothelial barrier enhancement via PKA- and Epac1/Rap1-dependent Rac activation." Experimental Cell Research **313**(11): 2504-2520.

Boettner, B. and L. Van Aelst (2009). "Control of cell adhesion dynamics by Rap1 signaling." Current Opinions in Cell Biology. **21**(5): 684-693. .

Bogacheva, A. M., G. N. Rudenskaya, Y. E. Dunaevsky, G. G. Chestuhina and B. N. Golovkin (2001). "New subtilisin-like collagenase from leaves of common plantain." Biochimie **83**(6): 481-486.

Bogatcheva, N. V., J. G. Garcia and A. D. Verin (2002). "Molecular mechanisms of thrombin-induced endothelial cell permeability." Biochemistry **67**(1): 75-84.

Bogatcheva, N. V., J. G. Garcia and A. D. Verin (2002). "Role of tyrosine kinase signaling in endothelial cell barrier regulation." Vascular Pharmacology. **39**(4-5): 201-212.

Bond, M., Y. J. Wu, G. B. Sala-Newby and A. C. Newby (2008). "Rho GTPase, Rac1, regulates Skp2 levels, vascular smooth muscle cell proliferation, and intima formation in vitro and in vivo." Cardiovascular Research **80**(2): 290-298.

Borland, G., R. J. Bird, T. M. Palmer and S. J. Yarwood (2009). "Activation of protein kinase Calpha by EPAC1 is required for the ERK- and CCAAT/enhancer-binding protein beta-dependent induction of the SOCS-3 gene by cyclic AMP in COS1 cells." Journal of Biological Chemistry **284**(26): 17391-17403. .

Borland, G., M. Gupta, M. M. Magiera, C. J. Rundell, S. Fuld and S. J. Yarwood (2006). "Microtubule-associated protein 1B-light chain 1 enhances activation of Rap1 by exchange protein activated by cyclic AMP but not intracellular targeting." Molecular Pharmacology **69**(1): 374-384.

Borland, G., B. O. Smith and S. J. Yarwood (2009). "EPAC proteins transduce diverse cellular actions of cAMP." British Journal of Pharmacology **158**(1): 70-86. .

Bos, J. L. (2005). "Linking Rap to cell adhesion." Current Opinions in Cell Biology **17**(2): 123-128.

Bosk, S., J. A. Braunger, V. Gerke and C. Steinem (2011). "Activation of F-actin binding capacity of ezrin: synergism of PIP(2) interaction and phosphorylation." Biophysical Journal **100**(7): 1708-1717.

Bretscher, A. (1989). "Rapid phosphorylation and reorganization of ezrin and spectrin accompany morphological changes induced in A-431 cells by epidermal growth factor." Journal of Cell Biology **108**(3): 921-930.

Bretscher, A. (1999). "Regulation of cortical structure by the ezrin-radixin-moesin protein family." Current Opinion in Cell Biology **11**(1): 109-116.

Brown, L. M., K. E. Rogers, N. Aroonsakool, J. A. McCammon and P. A. Insel (2014). "Allosteric inhibition of Epac: computational modeling and experimental validation to identify allosteric sites and inhibitors." Journal of Biological Chemistry **289**(42): 29148-29157.

Brown, L. M., K. E. Rogers, J. A. McCammon and P. A. Insel (2014). "Identification and validation of modulators of exchange protein activated by cAMP (Epac) activity: structure-function implications for Epac activation and inhibition." Journal of Biological Chemistry **289**(12): 8217-8230.

Bruunsgaard, H., M. Pedersen and B. K. Pedersen (2001). "Aging and proinflammatory cytokines." Current Opinions in Hematology **8**(3): 131-136.

Budzyn, K., P. D. Marley and C. G. Sobey (2006). "Targeting Rho and Rho-kinase in the treatment of cardiovascular disease." Trends in Pharmacological Sciences **27**(2): 97-104.

Burnouf, C. and M. P. Pruniaux (2002). "Recent advances in PDE4 inhibitors as immunoregulators and anti-inflammatory drugs." Current Pharmaceutical Design **8**(14): 1255-1296.

Buxton, I. L. and L. L. Brunton (1983). "Compartments of cyclic AMP and protein kinase in mammalian cardiomyocytes." Journal of Biological Chemistry **258**(17): 10233-10239.

Calabro, P., G. Limongelli, G. Pacileo, G. Di Salvo, P. Golino and R. Calabro (2008). "The role of adiposity as a determinant of an inflammatory milieu." Journal of Cardiovascular Medicine **9**(5): 450-460.

Cardone, R. A., A. Bagorda, A. Bellizzi, G. Busco, L. Guerra, A. Paradiso, V. Casavola, M. Zaccolo and S. J. Reshkin (2005). "Protein kinase A gating of a pseudopodial-located RhoA/ROCK/p38/NHE1 signal module regulates invasion in breast cancer cell lines." Molecular Biology of the Cell **16**(7): 3117-3127.

Cass, L. A., S. A. Summers, G. V. Prendergast, J. M. Backer, M. J. Birnbaum and J. L. Meinkoth (1999). "Protein kinase A-dependent and -independent signaling pathways contribute to cyclic AMP-stimulated proliferation." Molecular and Cellular Biology **19**(9): 5882-5891.

Chen, H., T. Tsalkova, O. G. Chepurny, F. C. Mei, G. G. Holz, X. Cheng and J. Zhou (2013). "Identification and characterization of small molecules as potent and specific EPAC2 antagonists." Journal of Medical Chemistry **56**(3): 952-962.

Chen, H., T. Tsalkova, F. C. Mei, Y. Hu, X. Cheng and J. Zhou (2012). "5-Cyano-6-oxo-1,6-dihydro-pyrimidines as potent antagonists targeting exchange proteins directly activated by cAMP." Bioorganic and Medicinal Chemistry Letters **22**(12): 4038-4043.

Chen, H., C. Wild, X. Zhou, N. Ye, X. Cheng and J. Zhou (2014). "Recent advances in the discovery of small molecules targeting exchange proteins directly activated by cAMP (EPAC)." Journal of Medicinal Chemistry **57**(9): 3651-3665.

Cheng, X., Z. Ji, T. Tsalkova and F. Mei (2008). "Epac and PKA: a tale of two intracellular cAMP receptors." Acta Biochimica and Biophysical Sinica (Shanghai) **40**(7): 651-662.

Chepurny, O. G., G. G. Kelley, I. Dzhura, C. A. Leech, M. W. Roe, E. Dzhura, X. Li, F. Schwede, H. G. Genieser and G. G. Holz (2010). "PKA-dependent potentiation of glucose-stimulated insulin secretion by Epac activator 8-pCPT-2'-O-Me-cAMP-AM in human islets of Langerhans." American Journal of Physiology, Endocrinology and Metabolism **298**(3): E622-633.

Christensen, A. E., F. Selheim, J. de Rooij, S. Dremier, F. Schwede, K. K. Dao, A. Martinez, C. Maenhaut, J. L. Bos, H. G. Genieser and S. O. Doskeland (2003). "cAMP analog mapping of Epac1 and cAMP kinase. Discriminating analogs demonstrate that Epac and cAMP kinase act synergistically to promote PC-12 cell neurite extension." Journal of Biological Chemistry **278**(37): 35394-35402.

Consonni, S. V., M. Gloerich, E. Spanjaard and J. L. Bos (2012). "cAMP regulates DEP domain-mediated binding of the guanine nucleotide exchange factor Epac1 to phosphatidic acid at the plasma membrane." Proceedings of the National Academy of Sciences of the United States of America **109**(10): 3814-3819.

Courilleau, D., M. Bisserier, J. C. Jullian, A. Lucas, P. Bouyssou, R. Fischmeister, J. P. Blondeau and F. Lezoualc'h (2012). "Identification of a tetrahydroquinoline analog as a pharmacological inhibitor of the cAMP-binding protein Epac." Journal of Biological Chemistry **287**(53): 44192-44202.

Cullere, X., S. K. Shaw, L. Andersson, J. Hirahashi, F. W. Luscinskas and T. N. Mayadas (2005). "Regulation of vascular endothelial barrier function by Epac, a cAMP-activated exchange factor for Rap GTPase." Blood **105**(5): 1950-1955.

Dao, K. K., K. Teigen, R. Kopperud, E. Hodneland, F. Schwede, A. E. Christensen, A. Martinez and S. O. Doskeland (2006). "Epac1 and cAMP-dependent protein kinase holoenzyme have similar cAMP affinity, but their cAMP domains have distinct structural features and cyclic nucleotide recognition." Journal of Biological Chemistry **281**(30): 21500-21511.

de Rooij, J., H. Rehmann, M. van Triest, R. H. Cool, A. Wittinghofer and J. L. Bos (2000). "Mechanism of regulation of the Epac family of cAMP-dependent RapGEFs." Journal of Biological Chemistry **275**(27): 20829-20836.

de Rooij, J., F. J. Zwartkruis, M. H. Verheijen, R. H. Cool, S. M. Nijman, A. Wittinghofer and J. L. Bos (1998). "Epac is a Rap1 guanine-nucleotide-exchange factor directly activated by cyclic AMP." Nature **396**(6710): 474-477.

Delghandi, M. P., M. Johannessen and U. Moens (2005). "The cAMP signalling pathway activates CREB through PKA, p38 and MSK1 in NIH 3T3 cells." Cell Signal **17**(11): 1343-1351.

Ding, W. G. and J. Gromada (1997). "Protein kinase A-dependent stimulation of exocytosis in mouse pancreatic beta-cells by glucose-dependent insulinotropic polypeptide." Diabetes **46**(4): 615-621.

Downey, G. P., C. K. Chan, P. Lea, A. Takai and S. Grinstein (1992). "Phorbol ester-induced actin assembly in neutrophils: role of protein kinase C." Journal of Cell Biology **116**(3): 695-706.

Dransfield, D. T., A. J. Bradford, J. Smith, M. Martin, C. Roy, P. H. Mangeat and J. R. Goldenring (1997). "Ezrin is a cyclic AMP-dependent protein kinase anchoring protein." EMBO Journal **16**(1): 35-43.

Duchniewicz, M., T. Zemojtel, M. Kolanczyk, S. Grossmann, J. S. Scheele and F. J. Zwartkruis (2006). "Rap1A-deficient T and B cells show impaired integrin-mediated cell adhesion." Molecular and Cellular Biology **26**(2): 643-653.

Dzhura, I., O. G. Chepurny, G. G. Kelley, C. A. Leech, M. W. Roe, E. Dzhura, P. Afshari, S. Malik, M. J. Rindler, X. Xu, Y. Lu, A. V. Smrcka and G. G. Holz (2010). "Epac2-dependent mobilization of intracellular Ca(2)+ by glucagon-like peptide-1 receptor agonist exendin-4 is disrupted in beta-cells of phospholipase C-epsilon knockout mice." Journal of Physiology **588**(Pt 24): 4871-4889.

Dzhura, I., O. G. Chepurny, C. A. Leech, M. W. Roe, E. Dzhura, X. Xu, Y. Lu, F. Schwede, H. G. Genieser, A. V. Smrcka and G. G. Holz (2011). "Phospholipase C-epsilon links Epac2 activation to the potentiation of glucose-stimulated insulin secretion from mouse islets of Langerhans." Islets **3**: 3.

Edgar, R. C. (2004). "MUSCLE: multiple sequence alignment with high accuracy and high throughput." Nucleic Acids Research **32**(5): 1792-1797.

Ellson, R., M. Mutz, B. Browning, L. Lee, C. L. Miller and R. Papen (2003). "Transfer of Low Nanoliter Volumes between Microplates Using Focused Acoustics—Automation Considerations." Journal of the Association for Laboratory Automation **9**(5): 28-34.

Enserink, J. M., A. E. Christensen, J. de Rooij, M. van Triest, F. Schwede, H. G. Genieser, S. O. Doskeland, J. L. Blank and J. L. Bos (2002). "A novel Epac-specific cAMP analogue demonstrates independent regulation of Rap1 and ERK." Nature Cell Biology **4**(11): 901-906.

Enserink, J. M., L. S. Price, T. Methi, M. Mahic, A. Sonnenberg, J. L. Bos and K. Tasken (2004). "The cAMP-Epac-Rap1 pathway regulates cell spreading and cell adhesion to laminin-5 through the alpha3beta1 integrin but not the alpha6beta4 integrin." Journal of Biological Chemistry **279**(43): 44889-44896.

Estevez, M., E. Martinez, S. J. Yarwood, M. J. Dalby and J. Samitier (2014). "Adhesion and migration of cells responding to microtopography." Journal of Biomedical Materials Research

Fehon, R. G., A. I. McClatchey and A. Bretscher (2010). "Organizing the cell cortex: the role of ERM proteins." Nature Reviews Molecular Cell Biology **11**(4): 276-287.

Froese, A., S. S. Breher, C. Waldeyer, R. F. Schindler, V. O. Nikolaev, S. Rinne, E. Wischmeyer, J. Schlueter, J. Becher, S. Simrick, F. Vauti, J. Kuhtz, P. Meister, S. Kreissl, A. Torlopp, S. K. Liebig, S. Laakmann, T. D. Muller, J. Neumann, J. Stieber, A. Ludwig, S. K. Maier, N. Decher, H. H. Arnold, P. Kirchhof, L. Fabritz and T. Brand (2012). "Popeye domain containing proteins are essential for stress-mediated modulation of cardiac pacemaking in mice." Journal of Clinical Investigation **122**(3): 1119-1130.

Fujimoto, K., T. Shibasaki, N. Yokoi, Y. Kashima, M. Matsumoto, T. Sasaki, N. Tajima, T. Iwanaga and S. Seino (2002). "Piccolo, a Ca2+ sensor in pancreatic beta-cells. Involvement of cAMP-GEFII.Rim2.Piccolo complex in cAMP-dependent exocytosis." Journal of Biological Chemistry **277**(52): 50497-50502.

Fukuhara, S., A. Sakurai, H. Sano, A. Yamagishi, S. Somekawa, N. Takakura, Y. Saito, K. Kangawa and N. Mochizuki (2005). "Cyclic AMP potentiates vascular endothelial cadherin-mediated cell-cell contact to enhance endothelial barrier function through an Epac-Rap1 signaling pathway." Molecular and Cellular Biology **25**(1): 136-146.

Gabrielli, M., C. N. Martini, J. N. Brandani, L. J. Iustman, D. G. Romero and C. V. M. del (2014). "Exchange protein activated by cyclic AMP is involved in the regulation of adipogenic genes during 3T3-L1 fibroblasts differentiation." Development Growth and Differentiation **56**(2): 143-151.

Gary, R. and A. Bretscher (1995). "Ezrin self-association involves binding of an N-terminal domain to a normally masked C-terminal domain that includes the F-actin binding site." Molecular Biology of the Cell **6**(8): 1061-1075.

Gelinas, J. N., J. L. Banko, M. M. Peters, E. Klann, E. J. Weeber and P. V. Nguyen (2008). "Activation of exchange protein activated by cyclic-AMP enhances long-lasting synaptic potentiation in the hippocampus." Learning and Memory. **15**(6): 403-411. Print 2008.

Gerasimenko, Y. P., I. N. Bogacheva, N. A. Shcherbakova and A. N. Makarovskii (2001). "Bioelectric activity of spinal cord in patients with vertebrospinal pathologies." Bulletin of Experimental Biology and Medicine **132**(5): 1106-1109.

Gerits, N., S. Kostenko, A. Shiryaev, M. Johannessen and U. Moens (2008). "Relations between the mitogen-activated protein kinase and the cAMP-dependent protein kinase pathways: comradeship and hostility." Cellular Signalling **20**(9): 1592-1607.

Gitschier, H. J., A. B. Bergeron and D. H. Randle (2014). "Label-free cell-based dynamic mass redistribution assays." Current Protocols in Chemical Biology **6**(1): 39-51.

Glading, A., J. Han, R. A. Stockton and M. H. Ginsberg (2007). "KRIT-1/CCM1 is a Rap1 effector that regulates endothelial cell cell junctions." Journal of Cell Biology **179**(2): 247-254.

Gloerich, M. and J. L. Bos (2010). "Epac: defining a new mechanism for cAMP action." Annual Review of Pharmacology and Toxicology. **50**: 355-375.

Gloerich, M. and J. L. Bos (2011). "Regulating Rap small G-proteins in time and space." Trends in Cell Biology **21**(10): 615-623.

Gloerich, M., B. Ponsioen, M. J. Vliem, Z. Zhang, J. Zhao, M. R. Kooistra, L. S. Price, L. Ritsma, F. J. Zwartkruis, H. Rehmann, K. Jalink and J. L. Bos (2010). "Spatial regulation of cyclic AMP-Epac1 signaling in cell adhesion by ERM proteins." Molecular and Cellular Biology **30**(22): 5421-5431. .

Gloerich, M., M. J. Vliem, E. Prummel, L. A. Meijer, M. G. Rensen, H. Rehmann and J. L. Bos (2011). "The nucleoporin RanBP2 tethers the cAMP effector Epac1 and inhibits its catalytic activity." Journal of Cell Biology **193**(6): 1009-1020.

Gould, K. L., A. Bretscher, F. S. Esch and T. Hunter (1989). "cDNA cloning and sequencing of the protein-tyrosine kinase substrate, ezrin, reveals homology to band 4.1." EMBO Journal **8**(13): 4133-4142.

Gozo, M. C., P. J. Aspuria, D. J. Cheon, A. E. Walts, D. Berel, N. Miura, B. Y. Karlan and S. Orsulic (2013). "Foxc2 induces Wnt4 and Bmp4 expression during muscle regeneration and osteogenesis." Cell Death and Differentiation **20**(8): 1031-1042.

GraphPad (Software). "San Diego California USA, www.graphpad.com."

Greenfield, N. J. (2006). "Using circular dichroism spectra to estimate protein secondary structure." Nature Protocols **1**(6): 2876-2890.

Gulino, D., E. Delachanal, E. Concord, Y. Genoux, B. Morand, M. O. Valiron, E. Sulpice, R. Scaife, M. Alemany and T. Vernet (1998). "Alteration of endothelial cell monolayer integrity triggers resynthesis of vascular endothelium cadherin." Journal of Biological Chemistry **273**(45): 29786-29793.

Gupta, M. and S. J. Yarwood (2005). "MAP1A light chain 2 interacts with exchange protein activated by cyclic AMP 1 (EPAC1) to enhance Rap1 GTPase activity and cell adhesion." Journal of Biological Chemistry **280**(9): 8109-8116.

Haas, M. A., J. C. Vickers and T. C. Dickson (2007). "Rho kinase activates ezrin-radixin-moesin (ERM) proteins and mediates their function in cortical neuron growth, morphology and motility in vitro." Journal of Neuroscience Research **85**(1): 34-46.

Hall, J., K. L. Thomas and B. J. Everitt (2001). "Cellular imaging of zif268 expression in the hippocampus and amygdala during contextual and cued fear memory retrieval: selective activation of hippocampal CA1 neurons during the recall of contextual memories." Journal of Neuroscience **21**(6): 2186-2193.

Hamada, K., T. Shimizu, T. Matsui, S. Tsukita and T. Hakoshima (2000). "Structural basis of the membrane-targeting and unmasking mechanisms of the radixin FERM domain." EMBO Journal **19**(17): 4449-4462.

Harper, S. M., H. Wienk, R. W. Wechselberger, J. L. Bos, R. Boelens and H. Rehmann (2007). "Structural dynamics in the activation of EPAC." Journal of Biological Chemistry.

Harris, K. P. and J. T. Littleton (2011). "Vesicle trafficking: a Rab family profile." Current Biology **21**(20): R841-843.

Heiska, L. and O. Carpen (2005). "Src phosphorylates ezrin at tyrosine 477 and induces a phosphospecific association between ezrin and a kelch-repeat protein family member." Journal of Biological Chemistry **280**(11): 10244-10252.

Herbst, K. J., C. Coltharp, L. M. Amzel and J. Zhang (2011). "Direct activation of Epac by sulfonylurea is isoform selective." Chemistry and Biology **18**(2): 243-251.

Herfindal, L., G. Nygaard, R. Kopperud, C. Krakstad, S. O. Doskeland and F. Selheim (2013). "Off-target effect of the Epac agonist 8-pCPT-2'-O-Me-cAMP on P2Y12 receptors in blood platelets." Biochemical and Biophysical Research Communications **437**(4): 603-608.

Hewer, R. C., G. B. Sala-Newby, Y. J. Wu, A. C. Newby and M. Bond (2011). "PKA and Epac synergistically inhibit smooth muscle cell proliferation." Journal of Molecular and Cellular Cardiology **50**(1): 87-98.

Hochbaum, D., K. Hong, G. Barila, F. Ribeiro-Neto and D. L. Altschuler (2007). "Epac, in synergy with PKA, is required for cAMP-mediated mitogenesis." Journal of Biological Chemistry.

Holz, G. G. (2004). "Epac: A new cAMP-binding protein in support of glucagon-like peptide-1 receptor-mediated signal transduction in the pancreatic beta-cell." Diabetes **53**(1): 5-13.

Holz, G. G., G. Kang, M. Harbeck, M. W. Roe and O. G. Chepurny (2006). "Cell physiology of cAMP sensor Epac." Journal of Physiology **577**(Pt 1): 5-15.

Hothi, S. S., I. S. Gurung, J. C. Heathcote, Y. Zhang, S. W. Booth, J. N. Skepper, A. A. Grace and C. L. Huang (2008). "Epac activation, altered calcium homeostasis and ventricular arrhythmogenesis in the murine heart." Pflugers Archiv. European Journal of Physiology **457**(2): 253-270.

Hulme, E. C. and M. A. Trevethick (2010). "Ligand binding assays at equilibrium: validation and interpretation." British Journal of Pharmacology **161**(6): 1219-1237.

Iezzi, M., L. Eliasson, M. Fukuda and C. B. Wollheim (2005). "Adenovirus-mediated silencing of synaptotagmin 9 inhibits Ca2+-dependent insulin secretion in islets." FEBS Letters **579**(23): 5241-5246.

Inc, A. C. D. (2014). "ACD/ChemSketch". Toronto, ON, Canada, www.acdlabs.com.

Iversen, P. W., B. Beck, Y. F. Chen, W. Dere, V. Devanarayan, B. J. Eastwood, M. W. Farmen, S. J. Iturria, C. Montrose, R. A. Moore, J. R. Weidner and G. S. Sittampalam (2004). HTS Assay Validation. Assay Guidance Manual, chapter 3.

Kai, A. K., A. K. Lam, Y. Chen, A. C. Tai, X. Zhang, A. K. Lai, P. K. Yeung, S. Tam, J. Wang, K. S. Lam, P. M. Vanhoutte, J. L. Bos, S. S. Chung, A. Xu and S. K. Chung (2013). "Exchange protein activated by cAMP 1 (Epac1)-deficient mice develop beta-cell dysfunction and metabolic syndrome." FASEB Journal **27**(10): 4122-4135.

Kanes, S. J., J. Tokarczyk, S. J. Siegel, W. Bilker, T. Abel and M. P. Kelly (2007). "Rolipram: a specific phosphodiesterase 4 inhibitor with potential antipsychotic activity." Neuroscience **144**(1): 239-246.

Kang, G., O. G. Chepurny, B. Malester, M. J. Rindler, H. Rehmann, J. L. Bos, F. Schwede, W. A. Coetzee and G. G. Holz (2006). "cAMP sensor Epac as a determinant of ATP-sensitive potassium channel activity in human pancreatic beta cells and rat INS-1 cells." Journal of Physiology **573**(Pt 3): 595-609.

Kang, G. and G. G. Holz (2003). "Amplification of exocytosis by Ca2+-induced Ca2+ release in INS-1 pancreatic beta cells." Journal of Physiology **546**(Pt 1): 175-189.

Kang, G., J. W. Joseph, O. G. Chepurny, M. Monaco, M. B. Wheeler, J. L. Bos, F. Schwede, H. G. Genieser and G. G. Holz (2003). "Epac-selective cAMP analog 8-pCPT-2'-O-Me-cAMP as a stimulus for Ca2+-induced Ca2+ release and exocytosis in pancreatic beta-cells." Journal of Biological Chemistry **278**(10): 8279-8285.

Kapur, S. and D. Mamo (2003). "Half a century of antipsychotics and still a central role for dopamine D2 receptors." Progress in Neuro-Psychopharmacology and Biological Psychiatry **27**(7): 1081-1090.

Kasai, K., M. Ohara-Imaizumi, N. Takahashi, S. Mizutani, S. Zhao, T. Kikuta, H. Kasai, S. Nagamatsu, H. Gomi and T. Izumi (2005). "Rab27a mediates the tight docking of insulin granules onto the plasma membrane during glucose stimulation." Journal of Clinical Investigation **115**(2): 388-396.

Kaupp, U. B. and R. Seifert (2002). "Cyclic nucleotide-gated ion channels." Physiology Reviews **82**(3): 769-824.

Kawasaki, H., G. M. Springett, N. Mochizuki, S. Toki, M. Nakaya, M. Matsuda, D. E. Housman and A. M. Graybiel (1998). "A family of cAMP-binding proteins that directly activate Rap1." Science **282**(5397): 2275-2279.

Keely, S. L. (1979). "Prostaglandin E1 activation of heart cAMP-dependent protein kinase: apparent dissociation of protein kinase activation from increases in phosphorylase activity and contractile force." Molecular Pharmacology **15**(2): 235-245.

Keiper, M., M. B. Stope, D. Szatkowski, A. Bohm, K. Tysack, F. Vom Dorp, O. Saur, P. A. Oude Weernink, S. Evellin, K. H. Jakobs and M. Schmidt (2004). "Epac- and Ca2+ -controlled activation of Ras and extracellular signal-regulated kinases by Gs-coupled receptors." Journal of Biological Chemistry **279**(45): 46497-46508.

Kelley, G. G., O. G. Chepurny, F. Schwede, H. G. Genieser, C. A. Leech, M. W. Roe, X. Li, I. Dzhura, E. Dzhura, P. Afshari and G. G. Holz (2009). "Glucose-dependent potentiation of mouse islet insulin secretion by Epac activator 8-pCPT-2'-O-Me-cAMP-AM." Islets. **1**(3): 260-265.

Kida, T., K. Sawada, K. Kobayashi, M. Hori, H. Ozaki and T. Murata (2014). "Diverse effects of prostaglandin E(2) on vascular contractility." Heart and Vessels **29**(3): 390-395.

Kimura, T. E., A. Duggirala, C. C. Hindmarch, R. C. Hewer, M. Z. Cui, A. C. Newby and M. Bond (2014). "Inhibition of Egr1 expression underlies the anti-mitogenic effects of cAMP in vascular smooth muscle cells." Journal of Molecular and Cellular Cardiology **72**: 9-19.

Kooistra, M. R., M. Corada, E. Dejana and J. L. Bos (2005). "Epac1 regulates integrity of endothelial cell junctions through VE-cadherin." FEBS Letters **579**(22): 4966-4972.

Kraemer, A., H. R. Rehmann, R. H. Cool, C. Theiss, J. de Rooij, J. L. Bos and A. Wittinghofer (2001). "Dynamic interaction of cAMP with the Rap guanine-nucleotide exchange factor Epac1." Journal of Molecular Biology **306**(5): 1167-1177.

Krebs, E. G. and J. A. Beavo (1979). "Phosphorylation-dephosphorylation of enzymes." Annual Review of Biochemistry **48**: 923-959.

Krieg, J. and T. Hunter (1992). "Identification of the two major epidermal growth factor-induced tyrosine phosphorylation sites in the microvillar core protein ezrin." Journal of Biological Chemistry **267**(27): 19258-19265.

Kwan, E. P., X. Gao, Y. M. Leung and H. Y. Gaisano (2007). "Activation of exchange protein directly activated by cyclic adenosine monophosphate and protein kinase A regulate common and distinct steps in promoting plasma membrane exocytic and granule-to-granule fusions in rat islet beta cells." Pancreas **35**(3): e45-54.

Lacabaratz-Porret, C., E. Corvazier, T. Kovacs, R. Bobe, R. Bredoux, S. Launay, B. Papp and J. Enouf (1998). "Platelet sarco/endoplasmic reticulum Ca2+ATPase isoform 3b and Rap 1b: interrelation and regulation in physiopathology." Biochemical Journal **332 (Pt 1)**: 173-181.

Laddha, S. S. and S. P. Bhatnagar (2009). "A new therapeutic approach in Parkinson's disease: some novel quinazoline derivatives as dual selective phosphodiesterase 1 inhibitors and anti-inflammatory agents." Bioorganic and Medicinal Chemistry **17**(19): 6796-6802.

Laurent, A. C., M. Bisserier, A. Lucas, F. Tortosa, M. Roumieux, A. De Regibus, A. Swiader, Y. Sainte-Marie, C. Heymes, C. Vindis and F. Lezoualc'h (2014). "Exchange protein directly activated by cAMP 1 promotes autophagy during cardiomyocyte hypertrophy." Cardiovascular Research

Levitzki, A. (1987). "Regulation of adenylate cyclase by hormones and G-proteins." FEBS Letters **211**(2): 113-118.

Li, Y., S. Asuri, J. F. Rebhun, A. F. Castro, N. C. Paranavitana and L. A. Quilliam (2006). "The RAP1 guanine nucleotide exchange factor Epac2 couples cyclic AMP and Ras signals at the plasma membrane." Journal of Biological Chemistry **281**(5): 2506-2514.

Liu, C., M. Takahashi, Y. Li, T. J. Dillon, S. Kaech and P. J. Stork (2010). "The interaction of Epac1 and Ran promotes Rap1 activation at the nuclear envelope." Molecular and Cellular Biology **30**(16): 3956-3969.

Liu, Y., N. V. Belkina, C. Park, R. Nambiar, S. M. Loughhead, G. Patino-Lopez, K. Ben-Aissa, J. J. Hao, M. J. Kruhlak, H. Qi, U. H. von Andrian, J. H. Kehrl, M. J. Tyska and S. Shaw (2012). "Constitutively active ezrin increases membrane tension, slows migration, and impedes endothelial transmigration of lymphocytes in vivo in mice." Blood **119**(2): 445-453.

Lochner, A. and Moolman, J.A. (2006). "The many faces of H89: a review" Cardiovascular drug reviews 24(3-4):261-74

Lorenowicz, M. J., M. Fernandez-Borja, M. R. Kooistra, J. L. Bos and P. L. Hordijk (2008). "PKA and Epac1 regulate endothelial integrity and migration through parallel and independent pathways." European Journal of Cell Biology **87**(10): 779-792. Epub 2008 Jul 2016.

Lorenz, R., T. Aleksic, M. Wagner, G. Adler and C. K. Weber (2008). "The cAMP/Epac1/Rap1 pathway in pancreatic carcinoma." Pancreas. **37**(1): 102-103.

Magiera, M. M., M. Gupta, C. J. Rundell, N. Satish, I. Ernens and S. J. Yarwood (2004). "Exchange protein directly activated by cAMP (EPAC) interacts with the light chain (LC) 2 of MAP1A." Biochemical Journal **382**(Pt 3): 803-810.

Mangeat, P., C. Roy and M. Martin (1999). "ERM proteins in cell adhesion and membrane dynamics: Authors' correction." Trends in Cell Biology **9**(7): 289.

Marion, S., E. Hoffmann, D. Holzer, C. Le Clainche, M. Martin, M. Sachse, I. Ganeva, P. Mangeat and G. Griffiths (2011). "Ezrin promotes actin assembly at the phagosome membrane and regulates phago-lysosomal fusion." Traffic **12**(4): 421-437.

Matsui, T., M. Maeda, Y. Doi, S. Yonemura, M. Amano, K. Kaibuchi and S. Tsukita (1998). "Rho-kinase phosphorylates COOH-terminal threonines of ezrin/radixin/moesin (ERM) proteins and regulates their head-to-tail association." Journal of Cell Biology **140**(3): 647-657.

Matulef, K. and W. N. Zagotta (2003). "Cyclic nucleotide-gated ion channels." Annual Review of Cell and Developmental Biology **19**: 23-44.

Maurice, D. H., H. Ke, F. Ahmad, Y. Wang, J. Chung and V. C. Manganiello (2014). "Advances in targeting cyclic nucleotide phosphodiesterases." Nat Rev Drug Discov **13**(4): 290-314.

Mayr, B. and M. Montminy (2001). "Transcriptional regulation by the phosphorylation-dependent factor CREB." Nature Reviews Molecular and Cellular Biology **2**(8): 599-609.

Mayr, L. M. and D. Bojanic (2009). "Novel trends in high-throughput screening." Current Opinions in Pharmacology **9**(5): 580-588.

McPhee, I., L. C. Gibson, J. Kewney, C. Darroch, P. A. Stevens, D. Spinks, A. Cooreman and S. J. MacKenzie (2005). "Cyclic nucleotide signalling: a molecular approach to drug discovery for Alzheimer's disease." Biochemical Society Transactions **33**(Pt 6): 1330-1332.

Mei, F. C. and X. Cheng (2005). "Interplay between exchange protein directly activated by cAMP (Epac) and microtubule cytoskeleton." Molecular Biosystems **1**(4): 325-331.

Mei, F. C., J. Qiao, O. M. Tsygankova, J. L. Meinkoth, L. A. Quilliam and X. Cheng (2002). "Differential signaling of cyclic AMP: opposing effects of exchange protein directly activated by cyclic AMP and cAMP-dependent protein kinase on protein kinase B activation." Journal of Biological Chemistry **277**(13): 11497-11504.

Metrich, M., M. Berthouze, E. Morel, B. Crozatier, A. M. Gomez and F. Lezoualc'h (2010). "Role of the cAMP-binding protein Epac in cardiovascular physiology and pathophysiology."European Journal of Physiology **459**(4): 535-546.

Metrich, M., A. Lucas, M. Gastineau, J. L. Samuel, C. Heymes, E. Morel and F. Lezoualc'h (2008). "Epac mediates beta-adrenergic receptor-induced cardiomyocyte hypertrophy." Circulation Research **102**(8): 959-965.

Metrich, M., E. Morel, M. Berthouze, L. Pereira, P. Charron, A. M. Gomez and F. Lezoualc'h (2009). "Functional characterization of the cAMP-binding

proteins Epac in cardiac myocytes." Pharmacological Reports **61**(1): 146-153.

Mongillo, M., T. McSorley, S. Evellin, A. Sood, V. Lissandron, A. Terrin, E. Huston, A. Hannawacker, M. J. Lohse, T. Pozzan, M. D. Houslay and M. Zaccolo (2004). "Fluorescence resonance energy transfer-based analysis of cAMP dynamics in live neonatal rat cardiac myocytes reveals distinct functions of compartmentalized phosphodiesterases." Circulation Research **95**(1): 67-75.

Moy, A. B., J. Van Engelenhoven, J. Bodmer, J. Kamath, C. Keese, I. Giaever, S. Shasby and D. M. Shasby (1996). "Histamine and thrombin modulate endothelial focal adhesion through centripetal and centrifugal forces." Journal of Clinical Investigation **97**(4): 1020-1027.

Nelson, D. A., L. Aguilar-Bryan and J. Bryan (1992). "Specificity of photolabeling of beta-cell membrane proteins with an 125I-labeled glyburide analog." Journal of Biological Chemistry **267**(21): 14928-14933.

Newhall, K. J., A. R. Criniti, C. S. Cheah, K. C. Smith, K. E. Kafer, A. D. Burkart and G. S. McKnight (2006). "Dynamic anchoring of PKA is essential during oocyte maturation." Current Biology **16**(3): 321-327.

Niggli, V., C. Andreoli, C. Roy and P. Mangeat (1995). "Identification of a phosphatidylinositol-4,5-bisphosphate-binding domain in the N-terminal region of ezrin." FEBS Letters **376**(3): 172-176.

Niimura, M., T. Miki, T. Shibasaki, W. Fujimoto, T. Iwanaga and S. Seino (2009). "Critical role of the N-terminal cyclic AMP-binding domain of Epac2 in its subcellular localization and function." Journal of Cellular Physiology **219**(3): 652-658.

Oestreich, E. A., H. Wang, S. Malik, K. A. Kaproth-Joslin, B. C. Blaxall, G. G. Kelley, R. T. Dirksen and A. V. Smrcka (2007). "Epac-mediated activation of phospholipase C(epsilon) plays a critical role in beta-adrenergic receptor-dependent enhancement of Ca2+ mobilization in cardiac myocytes." Journal of Biological Chemistry **282**(8): 5488-5495.

Ohba, Y., N. Mochizuki, K. Matsuo, S. Yamashita, M. Nakaya, Y. Hashimoto, M. Hamaguchi, T. Kurata, K. Nagashima and M. Matsuda (2000). "Rap2 as a slowly responding molecular switch in the Rap1 signaling cascade." Molecular and Cellular Biology **20**(16): 6074-6083.

Oishi, A., N. Makita, J. Sato and T. Iiri (2012). "Regulation of RhoA signaling by the cAMP-dependent phosphorylation of RhoGDIalpha." Journal of Biological Chemistry **287**(46): 38705-38715.

Ory, S., Y. Munari-Silem, P. Fort and P. Jurdic (2000). "Rho and Rac exert antagonistic functions on spreading of macrophage-derived multinucleated cells and are not required for actin fiber formation." Journal of Cell Science **113 (Pt 7)**: 1177-1188.

Otmakhov, N. and J. E. Lisman (2002). "Postsynaptic application of a cAMP analogue reverses long-term potentiation in hippocampal CA1 pyramidal neurons." Journal of Neurophysiology **87**(6): 3018-3032.

Ozaki, N., T. Shibasaki, Y. Kashima, T. Miki, K. Takahashi, H. Ueno, Y. Sunaga, H. Yano, Y. Matsuura, T. Iwanaga, Y. Takai and S. Seino (2000). "cAMP-GEFII is a direct target of cAMP in regulated exocytosis." Nature Cell Biology **2**(11): 805-811.

Pannekoek, W. J., J. R. Linnemann, P. M. Brouwer, J. L. Bos and H. Rehmann (2013). "Rap1 and Rap2 antagonistically control endothelial barrier resistance." PLoS One **8**(2): e57903.

Park, J. H., S. J. Kim, S. H. Park, D. G. Son, J. H. Bae, H. K. Kim, J. Han and D. K. Song (2012). "Glucagon-like peptide-1 enhances glucokinase activity in

pancreatic beta-cells through the association of Epac2 with Rim2 and Rab3A." Endocrinology **153**(2): 574-582.

Park, S. J., F. Ahmad, A. Philp, K. Baar, T. Williams, H. Luo, H. Ke, H. Rehmann, R. Taussig, A. L. Brown, M. K. Kim, M. A. Beaven, A. B. Burgin, V. Manganiello and J. H. Chung (2012). "Resveratrol ameliorates aging-related metabolic phenotypes by inhibiting cAMP phosphodiesterases." Cell **148**(3): 421-433.

Parnell, E., B. O. Smith, T. M. Palmer, A. Terrin, M. Zaccolo and S. J. Yarwood (2012). "Regulation of the inflammatory response of vascular endothelial cells by EPAC1." British Journal of Pharmacology **166**(2): 434-446.

Pearson, M. A., D. Reczek, A. Bretscher and P. A. Karplus (2000). "Structure of the ERM protein moesin reveals the FERM domain fold masked by an extended actin binding tail domain." Cell **101**(3): 259-270.

Penzes, P., K. M. Woolfrey and D. P. Srivastava (2011). "Epac2-mediated dendritic spine remodeling: implications for disease." Molecular and Cellular Neurosciences **46**(2): 368-380.

Pereira, L., H. Cheng, D. H. Lao, L. Na, R. J. van Oort, J. H. Brown, X. H. Wehrens, J. Chen and D. M. Bers (2013). "Epac2 mediates cardiac beta1-adrenergic-dependent sarcoplasmic reticulum Ca2+ leak and arrhythmia." Circulation **127**(8): 913-922.

Pereira, L., M. Metrich, M. Fernandez-Velasco, A. Lucas, J. Leroy, R. Perrier, E. Morel, R. Fischmeister, S. Richard, J. P. Benitah, F. Lezoualc'h and A. M. Gomez (2007). "The cAMP binding protein Epac modulates Ca2+ sparks by a Ca2+/calmodulin kinase signalling pathway in rat cardiac myocytes." Journal of Physiology **583**(Pt 2): 685-694.

Pereira, L., G. Ruiz-Hurtado, E. Morel, A. C. Laurent, M. Metrich, A. Dominguez-Rodriguez, S. Lauton-Santos, A. Lucas, J. P. Benitah, D. M. Bers, F. Lezoualc'h and A. M. Gomez (2012). "Epac enhances excitation-transcription coupling in cardiac myocytes." Journal of Molecular and Cellular Cardiology **52**(1): 283-291.

Pidoux, G. and K. Tasken (2010). "Specificity and spatial dynamics of protein kinase A signaling organized by A-kinase-anchoring proteins." Journal of Molecular Endocrinology **44**(5): 271-284.

Ponsioen, B., J. Zhao, J. Riedl, F. Zwartkruis, G. van der Krogt, M. Zaccolo, W. H. Moolenaar, J. L. Bos and K. Jalink (2004). "Detecting cAMP-induced Epac activation by fluorescence resonance energy transfer: Epac as a novel cAMP indicator." EMBO Reports **5**(12): 1176-1180.

Poppe, H., S. D. Rybalkin, H. Rehmann, T. R. Hinds, X. B. Tang, A. E. Christensen, F. Schwede, H. G. Genieser, J. L. Bos, S. O. Doskeland, J. A. Beavo and E. Butt (2008). "Cyclic nucleotide analogs as probes of signaling pathways." Nature Methods. **5**(4): 277-278.

Post, A., W. J. Pannekoek, S. H. Ross, I. Verlaan, P. M. Brouwer and J. L. Bos (2013). "Rasip1 mediates Rap1 regulation of Rho in endothelial barrier function through ArhGAP29." Proceedings of the National Academy of Sciences of the United States of America **110**(28): 11427-11432.

Qiao, J., F. C. Mei, V. L. Popov, L. A. Vergara and X. Cheng (2002). "Cell cycle-dependent subcellular localization of exchange factor directly activated by cAMP." Journal of Biological Chemistry **277**(29): 26581-26586.

Rabe, K. F. (2011). "Update on roflumilast, a phosphodiesterase 4 inhibitor for the treatment of chronic obstructive pulmonary disease." British Journal of Pharmacology **163**(1): 53-67.

Rall, T. W. and E. W. Sutherland (1958). "Formation of a cyclic adenine ribonucleotide by tissue particles." Journal of Biological Chemistry **232**(2): 1065-1076.

Rangarajan, S., J. M. Enserink, H. B. Kuiperij, J. de Rooij, L. S. Price, F. Schwede and J. L. Bos (2003). "Cyclic AMP induces integrin-mediated cell adhesion through Epac and Rap1 upon stimulation of the beta 2-adrenergic receptor." Journal of Cell Biology **160**(4): 487-493.

Reese, D. E., M. Zavaljevski, N. L. Streiff and D. Bader (1999). "bves: A novel gene expressed during coronary blood vessel development." Developmental Biology **209**(1): 159-171.

Rehmann, H. (2005). "Characterization of the activation of the rap-specific exchange factor epac by cyclic nucleotides." Methods in Enzymology **407**: 159-173.

Rehmann, H. (2012). "Epac2: a sulfonylurea receptor?" Biochemical Society Transactions **40**(1): 6-10.

Rehmann, H. (2013). "Epac-inhibitors: facts and artefacts." Scientific Reports **3**: 3032.

Rehmann, H., E. Arias-Palomo, M. A. Hadders, F. Schwede, O. Llorca and J. L. Bos (2008). "Structure of Epac2 in complex with a cyclic AMP analogue and RAP1B." Nature **27**: 27.

Rehmann, H., J. Das, P. Knipscheer, A. Wittinghofer and J. L. Bos (2006). "Structure of the cyclic-AMP-responsive exchange factor Epac2 in its auto-inhibited state." Nature **439**(7076): 625-628.

Rehmann, H., B. Prakash, E. Wolf, A. Rueppel, J. de Rooij, J. L. Bos and A. Wittinghofer (2003). "Structure and regulation of the cAMP-binding domains of Epac2." Nature Structural Biology **10**(1): 26-32.

Rehmann, H., F. Schwede, S. O. Doskeland, A. Wittinghofer and J. L. Bos (2003). "Ligand-mediated activation of the cAMP-responsive guanine nucleotide exchange factor Epac." Journal of Biological Chemistry **278**(40): 38548-38556.

Rehmann, H., A. Wittinghofer and J. L. Bos (2007). "Capturing cyclic nucleotides in action: snapshots from crystallographic studies." Nature Reviews Molecular and Cellular Biology **8**(1): 63-73.

Ross, S. H., A. Post, J. H. Raaijmakers, I. Verlaan, M. Gloerich and J. L. Bos (2011). "Ezrin is required for efficient Rap1-induced cell spreading." Journal of Cell Science **124**(Pt 11): 1808-1818.

Ross, S. H., E. Spanjaard, A. Post, M. J. Vliem, H. Kristyanto, J. L. Bos and J. de Rooij (2012). "Rap1 Can Bypass the FAK-Src-Paxillin Cascade to Induce Cell Spreading and Focal Adhesion Formation." PLoS One **7**(11): e50072.

Saleh, H. S., U. Merkel, K. J. Geissler, T. Sperka, A. Sechi, C. Breithaupt and H. Morrison (2009). "Properties of an ezrin mutant defective in F-actin binding." Journal of Molecular Biology **385**(4): 1015-1031.

Sali, A. and T. L. Blundell (1993). "Comparative protein modelling by satisfaction of spatial restraints." Journal of Molecular Biology **234**(3): 779-815.

Sands, W. A., H. D. Woolson, G. R. Milne, C. Rutherford and T. M. Palmer (2006). "Exchange protein activated by cyclic AMP (Epac)-mediated induction of suppressor of cytokine signaling 3 (SOCS-3) in vascular endothelial cells." Molecular and Cellular Biology **26**(17): 6333-6346.

Schindler, R. F., K. L. Poon, S. Simrick and T. Brand (2012). "The Popeye domain containing genes: essential elements in heart rate control." Cardiovascular Diagnosis and Therapy **2**(4): 308-319.

Schlepper, M., J. Thormann and V. Mitrovic (1989). "Cardiovascular effects of forskolin and phosphodiesterase-III inhibitors." Basic Research in Cardiology **84 Suppl 1**: 197-212.

Schrödinger, L. "The PyMOL Molecular Graphics System, Version 1.5.0.4."

Scott, A. I., A. F. Perini, P. A. Shering and L. J. Whalley (1991). "In-patient major depression: is rolipram as effective as amitriptyline?" European Journal of Clinical Pharmacology **40**(2): 127-129.

Scott, J. D., C. W. Dessauer and K. Tasken (2013). "Creating order from chaos: cellular regulation by kinase anchoring." Annual Review of Pharmacology and Toxicology **53**: 187-210.

Sears, M. R. (2001). "The evolution of beta2-agonists." Respiratory Medicine **95 Suppl B**: S2-6.

Sears, M. R. and J. Lotvall (2005). "Past, present and future--beta2-adrenoceptor agonists in asthma management." Respiratory Medicine **99**(2): 152-170.

Sehrawat, S., X. Cullere, S. Patel, J. Italiano, Jr. and T. N. Mayadas (2008). "Role of Epac1, an Exchange Factor for Rap GTPases, in Endothelial Microtubule Dynamics and Barrier Function." Molecular Biology of the Cell.

Sehrawat, S., T. Ernandez, X. Cullere, M. Takahashi, Y. Ono, Y. Komarova and T. N. Mayadas (2011). "AKAP9 regulation of microtubule dynamics promotes Epac1-induced endothelial barrier properties." Blood. **117**(2): 708-718. .

Seino, S. and T. Shibasaki (2005). "PKA-dependent and PKA-independent pathways for cAMP-regulated exocytosis." Physiological Reviews **85**(4): 1303-1342.

Seino, S., H. Takahashi, W. Fujimoto and T. Shibasaki (2009). "Roles of cAMP signalling in insulin granule exocytosis." Diabetes, Obesity and Metabolism **11 Suppl 4**: 180-188.

Shi, J. and L. Wei (2013). "Rho kinases in cardiovascular physiology and pathophysiology: the effect of fasudil." Journal of Cardiovascular Pharmacology **62**(4): 341-354.

Shibasaki, T., H. Takahashi, T. Miki, Y. Sunaga, K. Matsumura, M. Yamanaka, C. Zhang, A. Tamamoto, T. Satoh, J. Miyazaki and S. Seino (2007). "Essential role of Epac2/Rap1 signaling in regulation of insulin granule dynamics by cAMP." Proceedings of the National Academy of Sciences of the United States of America **104**(49): 19333-19338.

Simons, P. C., S. F. Pietromonaco, D. Reczek, A. Bretscher and L. Elias (1998). "C-terminal threonine phosphorylation activates ERM proteins to link the cell's cortical lipid bilayer to the cytoskeleton." Biochemical and Biophysical Research Communications **253**(3): 561-565.

Sittampalam, G. S., S. D. Kahl and W. P. Janzen (1997). "High-throughput screening: advances in assay technologies." Current Opinion in Chemical Biology **1**(3): 384-391.

Siuciak, J. A. (2008). "The role of phosphodiesterases in schizophrenia : therapeutic implications." CNS Drugs **22**(12): 983-993.

Slater, S. J., J. L. Seiz, B. A. Stagliano and C. D. Stubbs (2001). "Interaction of protein kinase C isozymes with Rho GTPases." Biochemistry **40**(14): 4437-4445.

Smith, P. K., R. I. Krohn, G. T. Hermanson, A. K. Mallia, F. H. Gartner, M. D. Provenzano, E. K. Fujimoto, N. M. Goeke, B. J. Olson and D. C. Klenk (1985). "Measurement of protein using bicinchoninic acid." Analytical Biochemistry **150**(1): 76-85.

Srivastava, D. P., K. A. Jones, K. M. Woolfrey, J. Burgdorf, T. A. Russell, A. Kalmbach, H. Lee, C. Yang, M. M. Bradberry, D. Wokosin, J. R. Moskal, M. F. Casanova, J. Waters and P. Penzes (2012). "Social, communication, and

cortical structural impairments in Epac2-deficient mice." Journal of Neuroscience **32**(34): 11864-11878.
Srivastava, D. P., K. M. Woolfrey, K. A. Jones, C. T. Anderson, K. R. Smith, T. A. Russell, H. Lee, M. V. Yasvoina, D. L. Wokosin, P. H. Ozdinler, G. M. Shepherd and P. Penzes (2012). "An autism-associated variant of Epac2 reveals a role for Ras/Epac2 signaling in controlling basal dendrite maintenance in mice." PLoS Biol **10**(6): e1001350.
Stangherlin, A. and M. Zaccolo (2012). "Phosphodiesterases and subcellular compartmentalized cAMP signaling in the cardiovascular system." American Journal of Physiology: Heart and Circulation Physiology **302**(2): H379-390.
Ster, J., F. de Bock, F. Bertaso, K. Abitbol, H. Daniel, J. Bockaert and L. Fagni (2009). "Epac mediates PACAP-dependent long-term depression in the hippocampus." Journal of Physiology **587**(Pt 1): 101-113.
Stockton, R. A., R. Shenkar, I. A. Awad and M. H. Ginsberg (2010). "Cerebral cavernous malformations proteins inhibit Rho kinase to stabilize vascular integrity." Journal of Experimental Medicine **207**(4): 881-896.
Stork, P. J. and J. M. Schmitt (2002). "Crosstalk between cAMP and MAP kinase signaling in the regulation of cell proliferation." Trends in Cell Biology **12**(6): 258-266.
Su, Y., W. R. Dostmann, F. W. Herberg, K. Durick, N. H. Xuong, L. Ten Eyck, S. S. Taylor and K. I. Varughese (1995). "Regulatory subunit of protein kinase A: structure of deletion mutant with cAMP binding domains." Science **269**(5225): 807-813.
Sutherland, E. W. and T. W. Rall (1958). "Fractionation and characterization of a cyclic adenine ribonucleotide formed by tissue particles." Journal of Biological Chemistry **232**(2): 1077-1091.
Sutherland, E. W. and W. D. Wosilait (1956). "The relationship of epinephrine and glucagon to liver phosphorylase. I. Liver phosphorylase; preparation and properties." Journal of Biological Chemistry **218**(1): 459-468.
Suzuki, S., U. Yokoyama, T. Abe, H. Kiyonari, N. Yamashita, Y. Kato, R. Kurotani, M. Sato, S. Okumura and Y. Ishikawa (2010). "Differential roles of Epac in regulating cell death in neuronal and myocardial cells." J **285**(31): 24248-24259. .
Takahashi, K., T. Sasaki, A. Mammoto, K. Takaishi, T. Kameyama, S. Tsukita and Y. Takai (1997). "Direct interaction of the Rho GDP dissociation inhibitor with ezrin/radixin/moesin initiates the activation of the Rho small G protein." Journal of Biological Chemistry **272**(37): 23371-23375.
Takahashi, T., T. Shibasaki, H. Takahashi, K. Sugawara, A. Ono, N. Inoue, T. Furuya and S. Seino (2013). "Antidiabetic sulfonylureas and cAMP cooperatively activate Epac2A." Science Signalling **6**(298): ra94.
Tamaki, T., C. E. Hura and R. T. Kunau, Jr. (1989). "Dopamine stimulates cAMP production in canine afferent arterioles via DA1 receptors." American Journal of Physiology **256**(3 Pt 2): H626-629.
Tang, Z., D. Shi, B. Jia, J. Chen, C. Zong, D. Shen, Q. Zheng, J. Wang and X. Tong (2012). "Exchange protein activated by cyclic adenosine monophosphate regulates the switch between adipogenesis and osteogenesis of human mesenchymal stem cells through increasing the activation of phosphatidylinositol 3-kinase." International Journal of Biochemistry and Cell Biology **44**(7): 1106-1120.
Tasken, K. and E. M. Aandahl (2004). "Localized effects of cAMP mediated by distinct routes of protein kinase A." Physiological Reviews **84**(1): 137-167.

Taylor, S. S., C. Kim, D. Vigil, N. M. Haste, J. Yang, J. Wu and G. S. Anand (2005). "Dynamics of signaling by PKA." Biochimica et Biophysica Acta **1754**(1-2): 25-37.

Tsalkova, T., A. V. Gribenko and X. Cheng (2011). "Exchange protein directly activated by cyclic AMP isoform 2 is not a direct target of sulfonylurea drugs." Assay and Drug Developent Technology **9**(1): 88-91. .

Tsalkova, T., F. C. Mei and X. Cheng (2012). "A fluorescence-based high-throughput assay for the discovery of exchange protein directly activated by cyclic AMP (EPAC) antagonists." PLoS One **7**(1): e30441.

Tsalkova, T., F. C. Mei, S. Li, O. G. Chepurny, C. A. Leech, T. Liu, G. G. Holz, V. L. Woods, Jr. and X. Cheng (2012). "Isoform-specific antagonists of exchange proteins directly activated by cAMP." Proceedings of the National Academy of Sciences of the United States of America **109**(45): 18613-18618.

Vliem, M. J., B. Ponsioen, F. Schwede, W. J. Pannekoek, J. Riedl, M. R. Kooistra, K. Jalink, H. G. Genieser, J. L. Bos and H. Rehmann (2008). "8-pCPT-2'-O-Me-cAMP-AM: an improved Epac-selective cAMP analogue." Chembiochem **9**(13): 2052-2054.

Vranken, W. F., W. Boucher, T. J. Stevens, R. H. Fogh, A. Pajon, M. Llinas, E. L. Ulrich, J. L. Markley, J. Ionides and E. D. Laue (2005). "The CCPN data model for NMR spectroscopy: development of a software pipeline." Proteins **59**(4): 687-696.

Walsh, D. A., J. P. Perkins and E. G. Krebs (1968). "An adenosine 3',5'-monophosphate-dependant protein kinase from rabbit skeletal muscle." Journal of Biological Chemistry **243**(13): 3763-3765.

Wang, H., Z. Guo, F. Wu, F. Long, X. Cao, B. Liu, Z. Zhu and X. Yao (2005). "PKA-mediated protein phosphorylation protects ezrin from calpain I cleavage." Biochemical and Biophysical Research Communications **333**(2): 496-501.

Wang, Z., T. J. Dillon, V. Pokala, S. Mishra, K. Labudda, B. Hunter and P. J. Stork (2006). "Rap1-mediated activation of extracellular signal-regulated kinases by cyclic AMP is dependent on the mode of Rap1 activation." Molecular and Cellular Biology **26**(6): 2130-2145.

Waterhouse, A. M., J. B. Procter, D. M. Martin, M. Clamp and G. J. Barton (2009). "Jalview Version 2--a multiple sequence alignment editor and analysis workbench." Bioinformatics **25**(9): 1189-1191.

Wiejak, J., J. Dunlop, S. Gao, G. Borland and S. J. Yarwood (2012). "Extracellular signal-regulated kinase mitogen-activated protein kinase-dependent SOCS-3 gene induction requires c-Jun, signal transducer and activator of transcription 3, and specificity protein 3 transcription factors." Molecular Pharmacology **81**(5): 657-668. .

Wiejak, J., J. Dunlop and S. J. Yarwood (2014). "The role of c-Jun in controlling the EPAC1-dependent induction of the SOCS3 gene in HUVECs." FEBS Letters **588**(9): 1556-1561.

Wittchen, E. S., R. A. Worthylake, P. Kelly, P. J. Casey, L. A. Quilliam and K. Burridge (2005). "Rap1 GTPase inhibits leukocyte transmigration by promoting endothelial barrier function." Journal of Biological Chemistry **280**(12): 11675-11682. Epub 12005 Jan 11620.

Wojciak-Stothard, B. and A. J. Ridley (2002). "Rho GTPases and the regulation of endothelial permeability." Vascular Pharmacology **39**(4-5): 187-199.

Woolfrey, K. M., D. P. Srivastava, H. Photowala, M. Yamashita, M. V. Barbolina, M. E. Cahill, Z. Xie, K. A. Jones, L. A. Quilliam, M. Prakriya and P. Penzes (2009). "Epac2 induces synapse remodeling and depression and its disease-associated forms alter spines." Nature Neuroscience **12**(10): 1275-1284.

Woolson, H. D., V. S. Thomson, C. Rutherford, S. J. Yarwood and T. M. Palmer (2009). "Selective inhibition of cytokine-activated extracellular signal-regulated kinase by cyclic AMP via Epac1-dependent induction of suppressor of cytokine signalling-3." Cell Signalling **21**(11): 1706-1715.

XLfit Software, I., Guildford, UK.

Yamamizu, K., T. Matsunaga, S. Katayama, H. Kataoka, N. Takayama, K. Eto, S. Nishikawa and J. K. Yamashita (2012). "PKA/CREB signaling triggers initiation of endothelial and hematopoietic cell differentiation via Etv2 induction." Stem Cells **30**(4): 687-696.

Yan, J., F. C. Mei, H. Cheng, D. H. Lao, Y. Hu, J. Wei, I. Patrikeev, D. Hao, S. J. Stutz, K. T. Dineley, M. Motamedi, J. D. Hommel, K. A. Cunningham, J. Chen and X. Cheng (2013). "Enhanced leptin sensitivity, reduced adiposity, and improved glucose homeostasis in mice lacking exchange protein directly activated by cyclic AMP isoform 1." Molecular and Cellular Biology **33**(5): 918-926.

Yang, Y., X. Shu, D. Liu, Y. Shang, Y. Wu, L. Pei, X. Xu, Q. Tian, J. Zhang, K. Qian, Y. X. Wang, R. S. Petralia, W. Tu, L. Q. Zhu, J. Z. Wang and Y. Lu (2012). "EPAC null mutation impairs learning and social interactions via aberrant regulation of miR-124 and Zif268 translation." Neuron **73**(4): 774-788.

Yarwood, S. J. (2005). "Microtubule-associated proteins (MAPs) regulate cAMP signalling through exchange protein directly activated by cAMP (EPAC)." Biochemical Society Transactions **33**(Pt 6): 1327-1329.

Yarwood, S. J., G. Borland, W. A. Sands and T. M. Palmer (2008). "Identification of CCAAT/enhancer-binding proteins as exchange protein activated by cAMP-activated transcription factors that mediate the induction of the SOCS-3 gene." Journal of Bioloical Chemistry **283**(11): 6843-6853.

Yasuda, T., T. Shibasaki, K. Minami, H. Takahashi, A. Mizoguchi, Y. Uriu, T. Numata, Y. Mori, J. Miyazaki, T. Miki and S. Seino (2010). "Rim2alpha determines docking and priming states in insulin granule exocytosis." Cell Metabolism **12**(2): 117-129.

Yokoyama, U., S. Minamisawa, H. Quan, T. Akaike, M. Jin, K. Otsu, C. Ulucan, X. Wang, E. Baljinnyam, M. Takaoka, M. Sata and Y. Ishikawa (2008). "Epac1 is upregulated during neointima formation and promotes vascular smooth muscle cell migration." American Journal of Physiology: Heart and Circulatory Physiology **295**(4): H1547-1555.

Zaccolo, M. (2006). "Phosphodiesterases and compartmentalized cAMP signalling in the heart." European Journal of Cell Biology **85**(7): 693-697.

Zaccolo, M. and T. Pozzan (2002). "Discrete microdomains with high concentration of cAMP in stimulated rat neonatal cardiac myocytes." Science. **295**(5560): 1711-1715.

Zhadanov, A. B., D. W. Provance, Jr., C. A. Speer, J. D. Coffin, D. Goss, J. A. Blixt, C. M. Reichert and J. A. Mercer (1999). "Absence of the tight junctional protein AF-6 disrupts epithelial cell-cell junctions and cell polarity during mouse development." Current Biology **9**(16): 880-888.

Zhang, C. L., M. Katoh, T. Shibasaki, K. Minami, Y. Sunaga, H. Takahashi, N. Yokoi, M. Iwasaki, T. Miki and S. Seino (2009). "The cAMP sensor Epac2 is a direct target of antidiabetic sulfonylurea drugs." Science **325**(5940): 607-610.

Zhang, J. H., T. D. Chung and K. R. Oldenburg (1999). "A Simple Statistical Parameter for Use in Evaluation and Validation of High Throughput Screening Assays." Journal of Biomolecular Screening **4**(2): 67-73.

Zhao, J. (2006). Subcellular Localisation of Epac. Biologie Proefschriften.

Zhou, R., X. Cao, C. Watson, Y. Miao, Z. Guo, J. G. Forte and X. Yao (2003). "Characterization of protein kinase A-mediated phosphorylation of ezrin in gastric parietal cell activation." Journal of Biological Chemistry **278**(37): 35651-35659.

Zhu, L., J. Crothers, Jr., R. Zhou and J. G. Forte (2010). "A possible mechanism for ezrin to establish epithelial cell polarity." American Journal of Physiology: Cell Physiology **299**(2): C431-443.

Zhu, L., R. Zhou, S. Mettler, T. Wu, A. Abbas, J. Delaney and J. G. Forte (2007). "High turnover of ezrin T567 phosphorylation: conformation, activity, and cellular function." American Journal of Physiology: Cell Physiology **293**(3): C874-884.